Numerical Methods for Random Ordinary Differential Equations and their Applications in Biology and Medicine

Dissertation
zur Erlangung des Doktorgrades
der Naturwissenschaften

vorgelegt beim Fachbereich Informatik und Mathematik
der Johann Wolfgang Goethe-Universität
in Frankfurt am Main

von
Yusuke Asai
aus Tokyo

Frankfurt am Main 2016
(D 30)

vom Fachbereich Informatik und Mathematik der
Johann Wolfgang Goethe-Universität als Dissertation angenommen.

Dekan:	Prof. Dr. Uwe Brinkschulte
Gutachter:	Prof. Dr. Peter E. Kloeden
	Prof. Dr. Andreas Neuenkirch
Datum der Disputation:	04/05/2016

Acknowledgements

First of all, I would like to thank my supervisor Prof. Dr. Peter E. Kloeden for all of his help and suggestions. His lectures on numerical methods on deterministic and stochastic differential equations really fascinated me and I have much fun with my Ph.D. subject, the numerics for random ordinary differential equations. His words encouraged me a lot in writing paper and also doing research itself.
Moreover, I thank Prof. Dr. Eva Herrmann for her constant support and encouragement since my master study. I enjoyed mathematical modeling in medicine, in particular, hepatitis C viral kinetics very much. It was my starting point of my whole study in Frankfurt and it is still one of my favorite topics.
I thank Prof. Dr. Andreas Neunkirch for being the co-referee of this thesis and also for his advice, especially for his help on simulation of fractional Brownian motion and its integrals.
I am greatly indebted to my colleagues in the Institute of Biostatistics and Mathematical Modeling, Dr. Hanns Ackermann, Dimitra Bon, Dr. Natalie Filmann, Annette Lehn, Dr. Julia Rey, Dr. Tje Lin Chung and Marion Bruns, for their general support and fruitful discussion about modeling and biostatistics.
In addition, I want to thank my colleagues in the Institute of Mathematics, Dr. Janosch Rieger, Sebastian Becker, Sergej Spanier and Dr. Marco Noll, and also Prof. Dr. Arnulf Jentzen for their general help and their suggestion in computation.
Furthermore, I thank to my friends in Frankfurt and in Japan for their support in every respect.
Finally, I am grateful to my parents and my brother for their support from Japan. Even though they are far away from Frankfurt, I feel they are with me all the time and it helps me a lot.

Contents

List of publications.

- Asai Y., Herrmann E. and Kloeden P.E., Stable integration of stiff random ordinary differential equations, *Stochastic Analysis and Applications*, **31** (2013) 293–313.

- Asai Y. and Kloeden P.E., Numerical schemes for random ODEs via stochastic differential equations, *Communications in Applied Analysis*, (2013) **17** no.3 & 4, 511–528.

- Asai Y. and Kloeden P.E., Multi-step methods for random ODEs driven by Itô diffusions, *Journal of Computational and Applied Mathematics*, **294** (2016) 210–224.

- Asai Y. and Kloeden P.E., Numerical schemes for random ODEs with affine noise, *Numerical Algorithms*, (2016) 72:155–171.

- Herrmann E. and Asai Y., Viral kinetic modeling of chronic hepatitis C and B infection, in *Nonautonomous Dynamical Systems in the Life Sciences. Lecture Notes in Mathematics*, Springer 2013, 251–268.

- Asai Y., Caraballo T., Han X. and Kloeden P.E., A random model for immune response to virus in fluctuating environments, *Springer*.

Chapter 1

Introduction

Brownian motion is a rapid oscillatory motion of microscopic particles. It is named after the Scottish botanist Robert Brown, who first gave precise description of this phenomenon while he was observing pollen grains in water in 1827 [82]. The phenomenon caught great interest of scientists for decades and Einstein explained that the Brownian motion can be obtained as the result of the motion of molecules in a liquid in 1905 [33]. Smoluchowski also formulated Brownian motion and he estimated that Brownian motion can be described from the expectation of 10^{20} per second times collisions between the particle and water molecules in 1906 [23].

Before the formulation by Einstein and Smoluchowski, Bachelier observed similar movement in stock market and independently developed mathematical model of a stock variation with such fluctuations in 1900 [11]. In his model, the coefficient functions were supposed to be dependent only on time, i.e., homogeneous in space. The model was later reintroduced by Kolmogorov in 1931 [71].

Mathematical formulations of Brownian motion were attempted by many mathematicians. In 1908, Langevin wrote down the motion of particles according to Newton's laws and it was given by

$$m\frac{d^2x(t)}{dt^2} = -\zeta\frac{dx(t)}{dt} + F(t), \tag{1.1}$$

where m is a mass of a particle, $-\zeta dx(t)/dt$ is a systematic force, which describes a dynamical friction experienced by the particle, and $F(t)$ is a force from molecular collisions in the liquid and gives random fluctuations to the particles [4, 24]. The equation (1.1) has a form of ordinary differential equation (ODE), however, $F(t)$ is considered to be Gaussian white noise and there is a difficulty in analyzing its properties.

Kolmogorov circumvented the problem and introduced parabolic partial differential equations (PDEs) which describe the transition probability of Markov process. The PDEs are called as the first and the second PDEs in [71] and later the forward and backward Kolmogorov equations [22, 84, 104].

Since then, the theory of PDEs, the potential theory and semi-group theory started to be applied in the field of probability theory while only measure theory and Fourier analysis were the main analytical tools at that time.

According to the Kolmogorov's theory, a continuous Markov process $\{X(t)\}$ satisfies

$$\begin{cases} \mathbb{E}(X(t+\Delta_t) - X(t)|X(t) = x) & = a(t,x)\Delta_t + o(\Delta_t) \\ \mathbb{V}(X(t+\Delta_t) - X(t)|X(t) = x) & = b(t,x)\Delta_t + o(\Delta_t) \end{cases}, \tag{1.2}$$

where Δ_t is a small time interval, and this was the starting point of Itô's stochastic differential equations (SDEs). Based on (1.2), Itô derived an SDE in the form:

$$dX(t) = a(t, X(t))\, dt + \sqrt{b(t, X(t))}\, dW(t), \tag{1.3}$$

and he tried to find a sample path of continuous Markov process [53].

First of all, Itô wrote (1.3) in the integral form:

$$X(t) = X(t_0) + \int_{t_0}^{t} a(s, X(s))\, ds + \int_{t_0}^{t} \sigma(s, X(s))\, dW(s), \tag{1.4}$$

where $\sigma = \sqrt{b}$. The first integral on the right hand side of (1.4) is pathwise a Riemann-Stieltjes integral. On the other hand, a sample path of Brownian motion $\{W(t)\}$ does not have a bounded variation and the second integral cannot be defined in the same manner. Itô defined a stochastic integral $\int_{t_0}^{t} Y(s)dW(s)$ as

$$\int_{t_0}^{t} Y(s)\, dW(s) = \lim_{|\Delta|\to 0} \sum_{i=1}^{n} Y(s_{i-1})(W(s_i) - W(s_{i-1})),$$

for $t_0 = s_0 < s_1 < \ldots < s_n = t$ and $|\Delta| = \max(s_i - s_{i-1})$ for nonanticipative process $Y(t)$, i.e., independent of the future increments of the Wiener process.

When $\sigma \equiv 0$, the equation (1.4) turns to be deterministic and it can be solved by Picard's approximation method. Itô applied this idea to the case $\sigma \neq 0$ and showed the existence and uniqueness of the solution of (1.4) when the coefficient functions $a(t,x)$ and $\sigma(t,x)$ satisfy global or local Lipschitz conditions (which is briefly introduced in subsection 2.2). Moreover, the solution is Markov process and satisfies Kolmogorov's conditions (1.2).

Itô's theory was developed to understand and describe Markov processes, but now we can find its applications in various kinds of fields such as biology, medicine, physics and finance [2, 35, 85]. In particular, in financial mathematics, the theory of stochastic processes is a fundamental tool to describe the concepts and ideas now [39].

1.1 Random ordinary differential equations

Another modeling approach to include noise terms in differential equations is random ordinary differential equations (RODEs). RODEs are ODEs which have a stochastic process in their vector field functions and can be investigated pathwise as deterministic ODEs. They have been used in a wide range of applications such as biology, medicine, population dynamics and engineering [15, 70, 81, 90, 92] and play an important role in the theory of random dynamical systems (see Arnold [5]), however, they have been long overshadowed by SDEs.

A simple example of a RODE is given by

$$\frac{dx}{dt} = -x + \sin Y(t), \tag{1.5}$$

where $Y(t)$ is a stochastic process [57]. This equation looks similar to the Langevin equation (1.1), in which $F(t)$ is assumed to be Gaussian white noise. The use of Gaussian noise is supported by the Central Limit Theorem and it fits well with various kinds of mathematical models. However, such noise process is sometimes not realistic in applications because it is not bounded [31]. For example, the parameter values are often strictly positive in biology and medicine and models with unbounded noise may lead undesirable results such as negative values or excessively large values. In order to avoid such problems, mathematical models with bounded noise are recently introduced and they are now applied in physics, biology and engineering.

In general, RODEs can be written in the form:

$$\frac{dx}{dt} = f(x, Y(t)), \tag{1.6}$$

where $Y(t)$ is a stochastic process. Here we assume regular noise rather than Gaussian noise and typically we consider continuous noise processes which satisfy Hölder condition, such as Brownian motion or fractional Brownian motion (fBm), but also the noise processes with jumps, e.g., Poisson process or compound Poisson process, can be included in RODEs.

In addition to the property of the noise, sometimes it is much easier to develop models with noise by RODEs than SDEs. Allen built mathematical models with SDEs by including all possible changes within and among compartments [2, 3]. Interactions among compartments can be included in the system and such a method has an advantage in model building especially for small systems, however, it becomes too complicated for large ones.

RODEs may have more advantages from these points and I decide to reinvestigate mathematical modeling with RODEs and the numerical methods for RODEs.

When the noise is regular noise, there is, in fact, a close connection between RODEs and SDEs.

Suppose that a stochastic process $Y(t)$ in (1.5) satisfies an Itô stochastic ordinary differential equation (SODE), i.e.,

$$dY(t) = a(Y(t))\,dt + b(Y(t))\,dW(t), \tag{1.7}$$

with $W(t)$ a scalar Wiener process. Then, the RODE (1.5) can be transformed into the 2-dimensional SODEs:

$$d\begin{pmatrix} X(t) \\ Y(t) \end{pmatrix} = \begin{pmatrix} f(X(t), Y(t)) \\ a(Y(t)) \end{pmatrix} dt + \begin{pmatrix} 0 \\ b(Y(t)) \end{pmatrix} dW(t), \tag{1.8}$$

here $f(X(t), Y(t)) = -X(t) + \sin Y(t)$ for (1.5). When $a \equiv 0$ and $b \equiv 1$, then (1.7) reduces to a Wiener process, i.e., $Y(t) = W(t)$.

On the other hand, Doss and Sussmann proved that any finite dimensional SDE with commutative noise can be transformed to a RODE and it was later generalized to all SDEs by Imkeller, Schmalfuß and Lederer. Suppose that a scalar SDE with additive noise is given as

$$dX(t) = f(X(t))\,dt + dW(t). \tag{1.9}$$

An example of Ornstein-Uhlenbeck (OU) processes $O(t)$ is given by

$$dO(t) = -O(t)\,dt + dW(t). \tag{1.10}$$

By subtracting integral forms of (1.10) from (1.9) and defining $z(t) := X(t) - O(t)$, the corresponding RODE is now obtained:

$$\frac{dz}{dt} = f(z + O(t)) + O(t).$$

Through the Doss-Sussmann transformation and its generalizations, it was shown that RODEs and the corresponding SDEs have the same (transformed) solutions [32, 49, 51, 93].

1.2 Numerical approximation

Most deterministic differential equations cannot be solved explicitly, so they must be simulated in order to visualize the behavior and trajectories of the systems. Numerical methods for deterministic ODEs have long history and arbitrary higher order schemes can be derived by using Taylor expansions. In addition to the Taylor schemes, Runge-Kutta schemes and linear multistep methods (LMMs) were developed and widely used in applications [18, 36, 41, 42, 61]. Stiff systems are often observed in practice, however, explicit schemes are not suitable for such systems because of the stability problem. In

such cases, implicit schemes have important advantages and various implicit schemes were introduced and their stability regions were also investigated [18, 61].

Similar to the deterministic calculus, most of the SDEs and random differential equations (RDEs) do not have explicit analytical solutions and numerical methods are important tools to investigate the systems.

In the case of SDEs, such numerical methods for deterministic calculus are inconsistent or the traditional orders of convergence are not attained even if they are applicable. It is necessary to derive new types of numerical schemes and they were developed by applying stochastic Itô-Taylor expansions iteratively. Typical examples are Euler-Maruyama scheme, which is the stochastic Euler scheme, and Milstein scheme and they satisfy 0.5- and 1.0-order convergence respectively. Stochastic Runge-Kutta schemes and LMMs have also been constructed based on the stochastic Itô-Taylor expansions [16, 66, 76]. Recently Buckwar & Winkler derived stochastic LMMs (SLMMs) with higher order when the diffusion term is small [13, 14] and the third paper [9] is written based on the idea. The stochastic Itô-Taylor expansions are important backbone in this thesis and the details are introduced in chapter 2.

On the other hand, we can apply deterministic calculus pathwise to RODE. Typically the driving stochastic process $Y(t)$ in a RODE (1.6) has at most Hölder continuous sample paths. The resulting vector field $(t, x) \mapsto f(x, y(t))$ is, thus, at most Hölder continuous in time, no matter how smooth the vector field is in its original variables, so the sample paths of the solution of (1.6) are certainly continuously differentiable, but their derivatives are at most Hölder continuous in time. Consequently, although the classical numerical schemes for ODEs can be applied pathwise to RODEs, they do not achieve their traditional orders.

Recently Grüne & Kloeden derived explicit averaged Euler scheme (EAES) by taking the average of the noise within the vector field [37]. In addition, new forms of higher order Taylor-like schemes for RODEs were derived systematically in [56, 64], see also section 2.3. However, it is still important to build higher order numerical schemes and computationally less expensive as well as numerically stable schemes and this is the motivation of this thesis. The schemes in [56, 64] are very general, so RODEs with special structure, i.e., RODEs with Itô noise and RODEs with affine structure, are focused and numerical schemes which exploit these special structures are investigated.

1.3 Outline

This thesis is based on the following four published papers [7, 8, 9, 10].

[7] Asai Y., Herrmann E. and Kloeden P.E., Stable integration of stiff

random ordinary differential equations, *Stochastic Analysis and Applications*, **31** (2013) 293–313.

The paper [7] was based on a note by A. Jentzen and P.E. Kloeden and the schemes, the implicit averaged Euler scheme (IAES) and the implicit averaged midpoint scheme (IAMS), are natural extensions of the EAES introduced in [38]. Since the paper was based on unpublished notes by Jentzen and Kloeden, the details of the paper are not discussed here, but will be briefly introduced in preliminaries and stability sections.

[8] Asai Y. and Kloeden P.E., Numerical schemes for random ODEs via stochastic differential equations, *Communications in Applied Analysis*, (2013) **17** no.3 & 4, 511–528.

The second one [8] is about the derivation of arbitrary higher order Itô-Taylor schemes via RODE-SODE transformation, which we saw in (1.8). When we discuss the convergence order, the coefficient functions and their partial derivatives are assumed to be uniformly bounded. This assumption excludes many interesting examples and we showed the pathwise convergence of the schemes under weaker conditions in this paper.

[9] Asai Y. and Kloeden P.E., Multi-step methods for random ODEs driven by Itô diffusions, *Journal of Computational and Applied Mathematics*, **294** (2016) 210–224.

SLMMs for the coupled RODE-SODE system are discussed in the third paper [9]. Arbitrary higher order SLMMs are constructed via RODE-SODE transformation and the corresponding consistency conditions are obtained. In addition, the pathwise convergence as well as a nonlinear numerical stability property, specifically B-stability, are investigated in the paper.

[10] Asai Y. and Kloeden P.E., Numerical schemes for random ODEs with affine noise, *Numerical Algorithms*, (2016) 72:155–171.

Itô noise is assumed in the second and third paper [8, 9], but general noise and RODEs with affine structure are assumed in the fourth paper [10]. The discussion here is closely related to the numerics of control theory given in [37] and Taylor schemes, derivative free schemes and LMMs are introduced here.

In addition, two examples presented in chapter 7 are taken from the poster:

- Asai Y. and Herrmann E., Mathematical modeling by random ordinary differential equations and their numerical methods (poster), *Population Approach Group in Europe 2015*, 03-05/06/2015, Crete, Greece.

1.3.1 The structure of the thesis

The thesis is structured as follows.

In chapter 2, Taylor expansion for deterministic ODEs are introduced in order to recapture the idea of building numerical schemes and evaluating their convergence order. The stochastic Itô-Taylor expansions are basic backbone to build numerical methods for SDEs and they are given in the following section 2.2. After Taylor-like expansions for RODEs [56] are briefly discussed in 2.3.1, the averaged schemes, namely the EAES, the IAES and the IAMS, are introduced in section 2.3.2. In addition, the notations appearing in this thesis are introduced in 2.4.

The numerical methods for RODEs with Itô noise process are derived for the coupled RODE-SODE in chapter 3. In section 3.1, Itô-Taylor schemes for RODE part in a coupled RODE-SODE are derived using the stochastic Itô-Taylor expansions. Those schemes have derivative terms in general and derivative free schemes are given by replacing the derivatives by finite differences. The pathwise convergence of Itô-Taylor schemes of arbitrary higher order is also discussed in this section.

Based on the stochastic Itô-Taylor expansions, SLMMs are derived in section 3.2. Derivation of the consistency conditions up to order 2.0 are illustrated and the general form of arbitrary higher order SLMMs with corresponding consistency conditions are given here. Moreover, the pathwise convergence of SLMMs is shown.

In chapter 4, RODEs with more general noise, but a more specific structure, are considered. Here we assume that the RODEs have an affine structure in the noise. The numerical methods are built using the hierarchical set notation given in chapter 2. Affine-RODE-Taylor schemes, derivative-free schemes and LMMs are derived in this chapter.

Stiff equations are often observed in practice and stability is a big issue in numerical simulations. After showing the solvabilities and convergence of the IAES and the IAMS, their B-stability are discussed in chapter 5. Then B-stability of 1.5-order SLMM is shown as an illustrative example and the argument is applied to arbitrary higher order SLMMs in the end.

Multiple stochastic integrals appear in the numerical methods when we derive higher order schemes. The integration and approximation of stochastic processes are discussed in chapter 6. Wiener process and OU process are approximated by using probability distribution and exact integration is given for compound Poisson process. In addition, fBm and the Riemann integral of fBm are generated by Cholesky decomposition and the combination of Cholesky decomposition or the fast Fourier transformation (FFT) with the random midpoint displacement (RMD) method. Their calculation costs are compared with different step sizes and number of simulation times.

To illustrate their widespread application and to compare their computational performance, the derived numerical schemes are applied to various

kinds of models in biology and medicine in chapter 7. Different kinds of noisy scenario are assumed in practice and bounded noisy parameters driven by Itô diffusion processes are illustrated here. The error and step size as well as computational costs are compared among previously and newly developed numerical schemes with different step sizes.

Chapter 2

Preliminaries and notation

Most mathematical models are very complicated and we often cannot obtain explicit analytical expressions for their solutions. In such cases, numerical approximations play very important role and they give us insights of the behavior of the solutions. However, the approximations are done in discrete steps in time while the models themselves are continuous in time. In order to have good approximations, i.e. approximations with small numerical errors, it is necessary to choose or develop appropriate numerical methods. Moreover, the accuracy is highly dependent on the step sizes for the simulation and the numerical errors get smaller as the step sizes become smaller. However, the computational costs get larger for such small step sizes and we need to choose suitable step size for each method.

Taylor expansions are the backbone of developing numerical methods. Firstly the deterministic Taylor expansions as well as the derivation of the corresponding Taylor schemes are illustrated in section 2.1 in order to recapture the basic idea of numerical approximation [61]. Such schemes are, in fact, rarely used in practice, but they are used as a tool to derive other numerical methods such as Runge-Kutta schemes and LMMs as well as to estimate the numerical errors and the convergence orders of other schemes.

Similar to the deterministic Taylor expansions, the stochastic Itô-Taylor expansions are the fundamental tools in the derivation of numerical methods for SDEs. As we saw in section 1.1, RODEs with Itô noise can be written in the RODE-SODE form and the stochastic Itô-Taylor expansions are applied in order to build numerical schemes. After a brief introduction of Itô calculus and standard assumptions, Itô-Taylor expansions for SDEs are given in section 2.2. The existence and uniqueness theorem for SDEs and the necessary conditions as well as two kinds of convergence, namely strong convergence and pathwise convergence, are also introduced here. Different from deterministic calculus, we often have more derivative terms in stochastic calculus. The useful notations to describe the set of derivatives were introduced in [66] and the hierarchical set notations and the notations for multiple integrals are

given in this section.

In addition, Jentzen and Kloeden recently introduced Taylor-like expansions for RODEs [56] and developed a new class of numerical methods for RODEs. Some of their schemes are applied to numerical simulations in chapter 7 and the Taylor-like expansions are given in subsection 2.3.1.

The EAES was built by Grüne & Kloeden by averaging the noise terms in the vector fields [37] and later Asai, Herrmann & Kloeden introduced the IAES and the IAMS [7], which were based on the unpublished notes by Jentzen and Kloeden. These averaged schemes are also given in section 2.3.2.

Some more notations, such as the combination of the stochastic integrals and the reduced hierarchical sets, are introduced in the last section and the corresponding examples are illustrated.

Throughout this thesis, we assume that the solution exists on the given time interval $[t_0, T]$. In addition, we assume the cases with $d = 1$ throughout this chapter.

2.1 Taylor expansions for deterministic ODEs

Consider the initial value problem (IVP) of ODEs given by

$$\frac{dx}{dt} = f(t, x), \qquad x(t_0) = x_0,$$

with solution $x(t) = x(t, t_0, x_0)$. Now we suppose that the solution $x(t) : [t_0, T] \to \mathbb{R}$ is $p+1$ times continuously differentiable. Then $x(t)$ has a Taylor expansion around $t_n \in [t_0, T]$ and it is given by

$$\begin{aligned} x(t_n) &= x(t_{n-1}) + \frac{dx}{dt}(t_{n-1})\Delta_n + \cdots + \frac{1}{p!}\frac{d^p x}{dt^p}(t_{n-1})\Delta_n^p \\ &\quad + \frac{1}{(p+1)!}\frac{d^{p+1}x}{dt^{p+1}}(\theta_{n-1})\Delta_n^{p+1}, \end{aligned} \tag{2.1}$$

where $\Delta_n = t_n - t_{n-1}$ and an intermediate value $\theta_{n-1} \in [t_{n-1}, t_n] \subset [t_0, T]$.

Now introduce a differential operator D:

$$Dg(t, x) := \frac{\partial g}{\partial t}(t, x) + f(t, x)\frac{\partial g}{\partial t}(t, x).$$

Applying the chain rule to the function $g(t, x)$ gives

$$\frac{dg}{dt}(t, x(t)) = \frac{\partial g}{\partial t}(t, x(t)) + \frac{\partial g}{\partial x}(t, x(t))f(t, x(t)) = Dg(t, x(t)),$$

since $dx/dt = f(t, x(t))$. With the help of the operator D, the derivatives of $x(t)$ can be written as

$$\frac{d^j x}{dt^j}(t) = D^{j-1} f(t, x(t)), \qquad j = 1, 2, \cdots, \tag{2.2}$$

for sufficiently smooth f. Replacing the derivative terms in (2.1) by (2.2) gives the p-order Taylor expansions:

$$\begin{aligned} x(t_n) &= x(t_{n-1}) + \sum_{j=1}^{p} \frac{1}{j!} D^{j-1} f(t_{n-1}, x(t_{n-1})) \Delta_n^j \\ &\quad + \frac{1}{(j+1)!} D^p f(\theta_{n-1}, x(\theta_{n-1})) \Delta_n^{p+1}. \end{aligned}$$

By disregarding the last term, the p-order Taylor scheme can be derived:

$$x_n = x_{n-1} + \sum_{j=1}^{p} \frac{1}{j!} D^{j-1} f(t_{n-1}, x_{n-1}) \Delta_n^j, \tag{2.3}$$

where x_n is an approximated value of $x(t)$ at $t = t_n$. A typical example of the Taylor scheme is Euler scheme and it has a form:

$$x_n = x_{n-1} + f(t_{n-1}, x_{n-1}) \Delta_n. \tag{2.4}$$

In order to estimate the numerical error, define the local discretization error L_n given by

$$L_n := |x(t_n, t_{n-1}, x(t_{n-1})) - x_n|. \tag{2.5}$$

This is the term disregarded when (2.3) was developed and

$$L_n \leq \frac{1}{(j+1)!} \Delta_n^{p+1} |D^p f(\theta_{n-1}, x(\theta_{n-1}, t_{n-1}, x(t_{n-1})))| \sim \mathcal{O}(\Delta_n^{p+1}).$$

In general, the coefficients $D^{j-1} f(t_{n-1}, x(t_{n-1}))$ in (2.3) is too complicated to be estimated and such Taylor schemes are rarely implemented in practice, but used to establish the convergence order and error of other schemes.

2.1.1 One-step schemes

When we can describe the schemes in the form:

$$x_n = x_{n-1} + \Phi(\Delta_n, t_{n-1}, x_{n-1}, x_n),$$

for some increment function Φ, the schemes are called one-step schemes. The Euler scheme (2.4) is an example of a one-step scheme and Φ is given by

$$\Phi(\Delta_n, t, x, y) = f(t, x).$$

When $\Phi(\Delta_n, t, x, y) = f(t + \Delta_n, y)$, i.e.,

$$x_n = x_{n-1} + f(t_n, x_n) \Delta_n, \tag{2.6}$$

the scheme is called the implicit Euler scheme. x_n is on the right hand side of (2.6) and because of this structure, we need to solve an algebraic equation at each time step. However, such implicit schemes have important advantages such as numerical stability and are often applied to stiff systems.

In addition to the explicit and implicit Euler schemes, there are many of the one-step schemes derived in the literature [18, 41, 42, 61]:

the trapezoidal scheme:

$$\Phi(\Delta_n, t, x, y) = \frac{1}{2}\left(f(t,x) + f(t+\Delta_n, y)\right),$$

the Heun scheme:

$$\Phi(\Delta_n, t, x, y) = \frac{1}{2}\left(f(t,x) + f(t+\Delta_n, x+f(t,x)\Delta_n)\right), \tag{2.7}$$

the p-order Taylor scheme:

$$\Phi(\Delta_n, t, x, y) = \sum_{j=1}^{p} \frac{1}{j!} f(t,x)\Delta_n^{j-1}.$$

The above Heun scheme is a simple example of Runge-Kutta schemes, which is the class of derivative free one-step schemes. As we can see from the form of the increment function Φ given by (2.7), the function f is evaluated at several intermediate points within the discretization subinterval. When we evaluate the function at s intermediate points, we call the scheme s stages Runge-Kutta scheme. Obviously, the Heun scheme is a Runge-Kutta scheme with 2 stages.

In general, Runge-Kutta scheme with s stages has a form:

$$\begin{aligned} x_n &= x_{n-1} + \Delta_n \sum_{i=1}^{s} b_i k_i^{(n-1)}, \\ k_i^{(n-1)} &= f\left(t_{n-1} + c_i\Delta_n, x_{n-1} + \Delta_n \sum_{j=1}^{s} a_{i,j} k_j^{(n-1)}\right), \qquad i = 1, \cdots, s, \end{aligned}$$

where $0 \le c_1 < c_2 < \cdots < c_s \le 1$.

2.1.2 Multi-step methods

Different from one-step schemes, multi-step methods use the information from the past, i.e., they evaluate the value at t_n with the information at current time t_{n-1} as well as the values of $x_{n-2}, \cdots, x_{n-s}$ from the previous time points $t_{n-2}, \cdots, t_{n-s}$.

For example, the family of s-step LMMs have a general form:

$$\sum_{j=0}^{s} \alpha_j x_{n-j} = \Delta_t \sum_{j=0}^{s} \beta_j f_{n-j}, \tag{2.8}$$

where the coefficients α_j and β_j satisfy consistency conditions and f_{n-j} is the approximated value of f at t_{n-j}. In addition, the equidistant step size Δ_t is assumed on the given interval.

The α_j and β_j in (2.8) are obtained by evaluating the local error (2.5) at $t = t_n$. As an illustrative example, we derive them for $s = 2$ here.

The local discretization error L_n is

$$\begin{aligned} L_n &= |x(t_n, t_{n-1}, x(t_{n-1})) - x_n| \\ &= |\sum_{j=0}^{2} \alpha_j x(t_{n-j}) - \Delta_t \sum_{j=0}^{2} \beta_j f(t_{n-j}, x(t_{n-j}))|. \end{aligned} \tag{2.9}$$

The Taylor expansions of $x(t)$ and $f(t, x(t))$ at t_n and t_{n-1} around t_{n-2} are given by

$$\begin{aligned} x(t_n) &= x(t_{n-2}) + f(t_{n-2}, x(t_{n-2}))(2\Delta_t) + \frac{1}{2} Df(\theta_{n-1}, x(\theta_{n-1}))(2\Delta_t)^2, \\ x(t_{n-1}) &= x(t_{n-2}) + f(t_{n-2}, x(t_{n-2}))\Delta_t + \frac{1}{2} Df(\theta_{n-2}, x(\theta_{n-2}))\Delta_t^2, \\ f(t_n, x(t_n)) &= f(t_{n-2}, x(t_{n-2})) + Df(\theta_{n-1}, x(\theta_{n-1}))(2\Delta_t), \\ f(t_{n-1}, x(t_{n-1})) &= f(t_{n-2}, x(t_{n-2})) + Df(\theta_{n-2}, x(\theta_{n-2}))\Delta_t, \end{aligned}$$

for some $\theta_{n-2} \in [t_{n-2}, t_{n-1}]$ and $\theta_{n-1} \in [t_{n-2}, t_n]$. Now substituting the corresponding terms in (2.9) yields

$$\begin{aligned} L_n \leq\ & |(\alpha_0 + \alpha_1 + \alpha_2) x(t_{n-2}) \\ & + (2\alpha_0 + \alpha_1 - (\beta_0 + \beta_1 + \beta_2))\, f(t_{n-2}, x(t_{n-2}))\Delta_t| + |R|, \end{aligned}$$

where R is a remainder term given by

$$\begin{aligned} R = \Big\{ & 2\alpha_0 Df(\theta_{n-1}, x(\theta_{n-1})) + \frac{1}{2} Df(\theta_{n-2}, x(\theta_{n-2})) \\ & - \Big(2\beta_0 Df(\theta_{n-1}, x(\theta_{n-1})) + \beta_1 Df(\theta_{n-2}, x(\theta_{n-2})) \Big) \Big\} \Delta_t^2. \end{aligned} \tag{2.10}$$

Obviously, the remainder term $R \sim \mathcal{O}(\Delta_t^2)$ and if α_j and β_j satisfy the following consistency conditions:

$$\alpha_0 + \alpha_1 + \alpha_2 = 0, \qquad 2\alpha_0 + \alpha_1 = \beta_0 + \beta_1 + \beta_2, \tag{2.11}$$

$L_n \leq C\Delta_t^2$ for some constant $C > 0$. This means the 2-step LMMs (2.8) show 1-order convergence.

Typical examples of 2-step LMMs are Adams-Bashford scheme:

$$x_n = x_{n-1} + \frac{1}{2} (3f_{n-1} - f_{n-2})\, \Delta_t, \tag{2.12}$$

and Adams-Moulton scheme:

$$x_n = x_{n-1} + \frac{1}{12}\left(5f_n + 8f_{n-1} - f_{n-2}\right)\Delta_t, \tag{2.13}$$

which are explicit and implicit schemes, respectively.

The remainder terms are evaluated by Taylor expansions iteratively and higher order LMMs or LMMs with more steps can be generated in the same manner.

2.2 Taylor expansions for SODEs

Stochastic calculus is not as robust as deterministic calculus, so it is better in this case to start with Taylor expansions and Taylor schemes to ensure that we get a consistent schemes. Consider 1-dimensional scalar Itô SODEs given by

$$dX(t) = f(t, X(t))\,dt + g(t, X(t))\,dW(t), \tag{2.14}$$

where the drift and diffusion coefficients f, $g : [t_0, T] \times \mathbb{R} \to \mathbb{R}$ and $W(t)$ is a standard Wiener process. This differential form is rather symbolical and it can be written in the integral form:

$$X(t) = X(t_0) + \int_{t_0}^{t} f(s, X(s))\,ds + \int_{t_0}^{t} g(s, X(s))\,dW(s). \tag{2.15}$$

As we saw in chapter 1, the first integral is pathwise a Riemann integral and the second an Itô stochastic integral.

The existence and uniqueness theorem for the SDEs (2.15) can be obtained under so-called *standard assumptions* by applying Picard type iteration [35, 78, 85].

Assumption 1. ***(Global-Lipschitz and linear growth conditions.)*** *The coefficients f and g are said to satisfy* global Lipschitz condition *and* linear growth condition *when the following inequalities hold respectively*

$$|f(t, X) - f(t, X')| + |g(t, X) - g(t, X')| \leq K|X - X'|, \tag{2.16}$$

$$|f(t, X)|^2 + |g(t, X)|^2 \leq K^2(1 + |X|^2), \tag{2.17}$$

where $t \in [t_0, T]$ and X, $X' \in \mathbb{R}$, for some constant K.

Theorem 1. ***(Existence and uniqueness theorem.)*** *Suppose that f, $g : [t_0, T] \times \mathbb{R} \to \mathbb{R}$ are continuous in both variables and satisfy* (2.16) *and* (2.17) *for all X, $X' \in \mathbb{R}$ and all $t \in [t_0, T]$. In addition, suppose that the initial condition X_0^2 is non-anticipative with respect to the Wiener process $W(t)$ with $\mathbb{E}(X_0^2) < \infty$.*

Then, there exists a solution $X(t)$ of (2.15) defined on $[t_0, T]$ which is continuous with probability 1 and $\sup_{t_0 \le t \le T} \mathbb{E}(X(t)^2) < \infty$. Moreover, a property of pathwise uniqueness holds, i.e.,

$$\mathbb{P}\Big(\sup_{t_0 \le t \le T} |X(t) - X'(t)| = 0 \Big) = 1,$$

for two solutions $X = \{X(t), t \in [t_0, T]\}$ and $X' = \{X'(t), t \in [t_0, T]\}$.

Now let $U : [t_0, T] \times \mathbb{R} \to \mathbb{R}$ be a two times continuously differentiable function and $X(t)$ be a solution of (2.15). Then the following integral equation, which is known as the Itô formula, is obtained:

$$U(t, X(t)) = U(t_0, X(t_0)) + \int_{t_0}^{t} L^0 U(s, X(s))\, ds + \int_{t_0}^{t} L^1 U(s, X(s))\, dW(s) \tag{2.18}$$

with the differential operators:

$$L^0 U = \frac{\partial U}{\partial t} + f \frac{\partial U}{\partial x} + \frac{1}{2} g^2 \frac{\partial^2 U}{\partial x^2}, \qquad L^1 U = g \frac{\partial U}{\partial x}. \tag{2.19}$$

Taking $U = f$ and $U = g$ in (2.18) and putting them into (2.15) yield

$$X(t) = X(t_0) + f(t_0, X(t_0)) \int_{t_0}^{t} ds + g(t_0, X(t_0)) \int_{t_0}^{t} dW(s) + R, \tag{2.20}$$

where the last term R is

$$\begin{aligned} R \;=\; & \int_{t_0}^{t} \int_{t_0}^{s_1} L^0 f(s_2, X(s_2))\, ds_2 ds_1 + \int_{t_0}^{t} \int_{t_0}^{s_1} L^1 f(s_2, X(s_2))\, dW(s_2) ds_1 \\ & + \int_{t_0}^{t} \int_{t_0}^{s_1} L^0 g(s_2, X(s_2))\, ds_2 dW(s_1) \\ & + \int_{t_0}^{t} \int_{t_0}^{s_1} L^1 g(s_2, X(s_2))\, dW(s_2) dW(s_1). \end{aligned} \tag{2.21}$$

Discarding the remainder term R given as (2.21) leads Euler-Maruyama approximation:

$$X_t \approx X_0 + f(t_0, X_0) \int_{t_0}^{t} ds + g(t_0, X_0) \int_{t_0}^{t} dW(s).$$

This leads Euler-Maruyama scheme:

$$X_n = X_{n-1} + f(t_{n-1}, X_{n-1}) \Delta_n + g(t_{n-1}, X_{n-1}) \Delta W_n, \tag{2.22}$$

where

$$\Delta_n = t_n - t_{n-1} = \int_{t_{n-1}}^{t_n} ds, \qquad \Delta W_n = \int_{t_{n-1}}^{t_n} dW(s). \tag{2.23}$$

Applying the chain rule again to $U = L^1 g$ in (2.20) and omitting the remainder terms yield

$$\begin{aligned} X_t &\approx X_0 + f(t_0, X_0)\int_{t_0}^{t} ds + g(t_0, X_0)\int_{t_0}^{t} dW(s) \\ &\quad + L^1 g(t_0, X_0)\int_{t_0}^{t}\int_{t_0}^{s_1} dW(s_2)dW(s_1), \end{aligned}$$

which is called Milstein approximation [66, 76] and the corresponding scheme is given by

$$\begin{aligned} X_n &= X_{n-1} + f(t_{n-1}, X_{n-1})\Delta_n + g(t_{n-1}, X_{n-1})\Delta W_n \\ &\quad + L^1 g(t_{n-1}, X_{n-1})\frac{1}{2}\left((\Delta W_n)^2 - \Delta_n\right), \end{aligned} \tag{2.24}$$

because

$$\int_{t_0}^{t}\int_{t_0}^{s_1} dW(s_2)dW(s_1) = \frac{1}{2}\left((\Delta W_n)^2 - \Delta_n\right).$$

By iterating the same argument, the arbitrary higher order stochastic Itô-Taylor expansions and the corresponding Itô-Taylor schemes are obtained. Moreover, similar to the numerical methods for deterministic ODEs, Runge-Kutta schemes and LMMs have been developed based on the stochastic Itô-Taylor expansions and their numerical errors are evaluated.

Different from convergence in deterministic sense, there are different kinds of convergence in SDEs, such as weak convergence or strong convergence, and numerical methods often show different orders of convergence in the different contexts. In this thesis, mainly strong and pathwise approximations are discussed and they are introduced in the following subsections.

2.2.1 Strong convergence

Now consider a partition $t_0 < t_1 < \cdots < t_n = T$ of the interval $[t_0, T]$ with step sizes $\Delta_i = t_i - t_{i-1}$ and maximum step size $\Delta := \max_{i=1,\cdots,n} \Delta_i$. Suppose that X_i is an approximation by some numerical scheme of $X(t_i)$ for a solution of $X(t)$ of the SDE (2.14). Then the numerical scheme is said to converge strongly of order γ if

$$\left(\mathbb{E}\sup_{i=0,\cdots,n} |X(t_i) - X_i|^p\right)^{1/p} \leq K_{p,T}\Delta^{\gamma}, \tag{2.25}$$

for some constant $K_{p,T}$.

By applying the stochastic Itô-Taylor expansions in the discarded terms and including necessary ones, arbitrary higher order strong Itô-Taylor schemes

are obtained [66]. In general, γ-order strong Itô-Taylor schemes can be written in the form:

$$X_t = \sum_{\alpha \in \Lambda_\gamma} L^\alpha id_X(t_0, X_0) I_{\alpha,t_0,t}, \tag{2.26}$$

where Λ_γ is the hierarchical set of multi-indices given by

$$\Lambda_\gamma = \Big\{\alpha \in \mathcal{M}_m : l(\alpha) + n(\alpha) \leq 2\gamma \quad \text{or} \quad l(\alpha) = n(\alpha) = \gamma + \frac{1}{2}\Big\}, \tag{2.27}$$

where $n(\alpha)$ is the number of components of α that are equal to 0 and $l(\alpha)$ is the length of α. In addition, $\mathcal{M}_m$ is given as

$$\mathcal{M}_m = \Big\{\alpha = (j_1, \cdots, j_l) \in \{0, 1, 2, \cdots, m\}^l : l \in \mathbb{N}\Big\} \cup \{\emptyset\},$$

with $\emptyset$ being the empty index of length $l(\emptyset) = 0$. Moreover, for a multi-index $\alpha = (j_1, \cdots, j_l)$ with $l \geq 1$, the multiple integrals $I_{\alpha,t_0,t}$ and iterated operators L^α are defined by

$$I_{\alpha,t_0,t} := \int_{t_0}^{t} \dots \int_{t_0}^{s_2} dW^{j_1}(s_1) \cdots dW^{j_l}(s_l), \qquad L^\alpha := L^{j_1} \cdots L^{j_l},$$

with $I_{\emptyset,t_0,t} = 1$ and $L^\emptyset = id$.

The hierarchical sets for the Euler-Maruyama scheme (2.22) and Milstein scheme (2.24) are given by $\{\emptyset, (0), (1)\}$ and $\{\emptyset, (0), (1), (1,1)\}$. Obviously they satisfy 0.5-order and 1.0-order strong convergence, respectively, although the Euler scheme (2.4) has order 1.0.

2.2.2 Pathwise convergence

Under the same assumption given in 2.2.1, the numerical scheme is said to converge pathwise if

$$\sup_{i=0,\cdots,n} |X(t_i, \omega) - X_i(\omega)| \to 0 \qquad \text{as} \quad \Delta \to 0 \tag{2.28}$$

for almost all $\omega \in \Omega$, where Ω is the sample space of a given probability space $(\Omega, \mathcal{F}, \mathbb{P})$.

Pathwise convergence has not been much discussed until recently, however, in general, the numerical approximation is carried out path by path and the calculation is done for a fixed $\omega \in \Omega$. Moreover, the theory of random dynamical systems is of pathwise nature.

Gyöngy showed that the explicit Euler-Maruyama scheme with equidistant step size $1/n$ satisfies $(0.5-\epsilon)$-order pathwise convergence for arbitrary $\epsilon > 0$ [40]. Using an idea in his proof, Kloeden & Neuenkirch showed that Itô-Taylor schemes with arbitrary higher order pathwise convergence can be developed [65].

Their result is the backbone for the proof given in subsection 3.2.2. The lemma, which connects the convergence in p-th mean and pathwise convergence, and the theorem are recalled here.

Lemma 1. *Let $\alpha > 0$ and $K(p) \in [0, \infty)$ for $p \geq 1$. In addition, let Z_n, $n \in \mathbb{N}$, be a sequence of random variables such that*

$$(\mathbb{E}|Z_n|^p)^{1/p} \leq K(p) \cdot n^{-\alpha}$$

for all $p \geq 1$ and all $n \in \mathbb{N}$. Then for all $\epsilon > 0$ there exists a random variable η_ϵ such that

$$|Z_n| \leq \eta_\epsilon \cdot n^{-\alpha+\epsilon} \qquad \text{almost surely}$$

for all $n \in \mathbb{N}$. Moreover, $\mathbb{E}|\eta_\epsilon|^p < \infty$ for all $p \geq 1$.

Theorem 2. (Pathwise convergence of the strong Itô-Taylor schemes.) *Under the standard assumptions, the γ-order strong Itô-Taylor scheme converges pathwise with order $(\gamma - \epsilon)$ for all $\epsilon > 0$, i.e.,*

$$\sup_{i=0,\cdots,n} |X(t_i, \omega) - X_i(\omega)| \leq K_\epsilon^{(\gamma)}(\omega)\Delta^{\gamma-\epsilon}$$

for almost all $\omega \in \Omega$.

This result is not restricted to the Itô-Taylor schemes and they applied the same argument to the stochastic Adams-Moulton method and the Euler-Maruyama scheme for stochastic delay equations and determined the rates of their pathwise convergence.

2.3 Numerical schemes for RODEs

2.3.1 Taylor-like expansions for RODEs

Now consider a RODE written in the form:

$$\frac{dx}{dt} = f(x, Y(t)),$$

where $Y(t)$ is the driving stochastic process. Suppose that the function f is infinitely often continuously differentiable in its variables. Then, the IVP:

$$\frac{dx}{dt} = f(x, Y(t)), \qquad x(t_0) = x_0, \tag{2.29}$$

has a unique solution on some finite interval $[t_0, T]$.

The driving sample process $Y(t)$ has at most Hölder continuous sample paths and the sample paths of solutions are continuously differentiable, but

their derivatives are at most Hölder continuous in time. This means that the classical Taylor expansion cannot be applied to the solution $x(t)$ of the IVP (2.29). Nevertheless, due to the special structure of a RODE and the smoothness of f in both variables, Jentzen & Kloeden developed implicit Taylor-like expansions and introduced arbitrary higher order RODE-Taylor schemes [56, 57, 64].

Define

$$\Delta x_s := x(s) - \hat{x}, \qquad \Delta Y_s := Y(s) - \hat{Y},$$

where

$$\hat{x} := x(\hat{t}), \qquad \hat{Y} := Y(\hat{t}),$$

for an arbitrary $\hat{t} \in [t_0, T)$. Taylor expansion of f with respect to x and Y is given by

$$\begin{aligned} f(x(s), Y(s)) &= \sum_{i=0}^{k} \frac{1}{i!} \left(\Delta x_s \frac{\partial}{\partial x} + \Delta Y_s \frac{\partial}{\partial y} \right)^i f(\hat{x}, \hat{Y}) + R_{k+1}(s) \\ &= \sum_{|\alpha| \leq k} \frac{1}{\alpha!} \partial^\alpha f(\hat{x}, \hat{Y}) (\Delta x_s)^{\alpha_1} (\Delta Y_s)^{\alpha_2} + R_{k+1}(s), \end{aligned}$$

for some $k \in \mathbb{N}_0$ where $\mathbb{N}_0$ is a set of non-negative integers. Here, a multi-index $\alpha = (\alpha_1, \alpha_2) \in \mathbb{N}_0^2$ and

$$|\alpha| := \alpha_1 + \alpha_2, \quad \alpha! := \alpha_1! \alpha_2!, \quad \partial^\alpha := (\partial_1)^{\alpha_1} (\partial_2)^{\alpha_2},$$

with $\partial^{(0,0)} f = f$ and $(0,0)! = 1$. In addition, the remainder term $R_{k+1}(s)$ is given by

$$R_{k+1}(s) = \sum_{|\alpha| = k+1} \frac{1}{\alpha!} \partial^\alpha f(\hat{x} + \xi_s \Delta x_s, \hat{Y} + \xi_s \Delta Y_s) (\Delta x_s)^{\alpha_1} (\Delta Y_s)^{\alpha_2},$$

for some $\xi_s \in [0, 1]$.

The IVP (2.29) can be written in the integral form as

$$x(t) = \hat{x} + \int_{\hat{t}}^{t} f(x(s), Y(s))\, ds.$$

Then $\Delta x_t = x(t) - \hat{x}$ is given by

$$\Delta x_t = \sum_{|\alpha| \leq k} \frac{1}{\alpha!} \partial^\alpha f(\hat{x}, \hat{Y}) \int_{\hat{t}}^{t} (\Delta x_s)^{\alpha_1} (\Delta Y_s)^{\alpha_2}\, ds + \int_{\hat{t}}^{t} R_{k+1}(s)\, ds. \quad (2.30)$$

The right hand side of the equation (2.30) contains Δx_s term and it is implicit and thus not a standard Taylor expansion. Nevertheless, this Taylor-like expansion can be used as a basis for deriving new classes of numerical schemes for RODEs.

Similar to the Taylor schemes and Itô-Taylor schemes, RODE-Taylor schemes can be obtained by discarding the remainder term. When $k = 0$, (2.30) reduces to

$$x(t) = \hat{x} + f(\hat{x}, \hat{Y}) \int_{\hat{t}}^{t} ds + \int_{\hat{t}}^{t} R_1(s)\, ds,$$

and this gives

$$X_n = X_{n-1} + f(X_{n-1}, Y_{n-1})\Delta_n, \tag{2.31}$$

which is the Euler scheme (2.4).

For $k \geq 1$, Δx_s remains inside the integral (2.30) and we need to evaluate this term with appropriate numerical schemes of lower order than that of the scheme to be derived. The higher order RODE-Taylor schemes can be built by iterating the procedure enough times. In general, the resulting K-RODE-Taylor scheme has a form

$$X_n^{K,\Delta_n} = X_{n-1}^{K,\Delta_n} + \sum_{\mathcal{A}_K} N_\alpha^K(t_n, t_{n-1}, X_{n-1}^{K,\Delta_n}), \tag{2.32}$$

with the step size $\Delta_n = t_n - t_{n-1}$ and $\mathcal{A}_K$ is a set of multi-indices of the form:

$$\mathcal{A}_K := \{\alpha = (\alpha_1, \alpha_2) \in \mathbb{N}_0^2 | \quad |\alpha|_\theta = \alpha_1 + \theta\alpha_2 < K\},$$

where $K \in \mathbb{R}_0$, a set of non-negative real numbers, and $\theta \in (0, 1]$ is the noise process specific value. Here,

$$N_\alpha^{(K)}(\hat{t} + \Delta_n, \hat{t}, \hat{x}) := \frac{1}{\alpha!}\partial^\alpha f(\hat{x}, \hat{Y}) \int_{\hat{t}}^{\hat{t}+\Delta_n} \left(\Delta x_{\Delta_s}^{(K-|\alpha|_\theta)}(\hat{t}, \hat{x})\right)^{\alpha_1} (\Delta Y_s)^{\alpha_2}\, ds,$$

with $\Delta_s = s - \hat{t}$ and

$$\Delta x_{\Delta_n}^{(K)} := \sum_{|\alpha|_\theta < K} N_\alpha^{(K)}(\hat{t} + \Delta_n, \hat{t}, \hat{x}),$$

with $\Delta x_{\Delta_n}^{(0)} = 0$.

Schemes of arbitrary higher order can be derived in this way (see [55, 56, 64]). In this thesis we investigate RODEs with a special structure, i.e., with Itô noise or affine noise, and take advantage of the structure to derive simpler schemes.

2.3.2 Averaged schemes

In subsection 2.3.1, the Euler scheme for RODEs is given by (2.31) on equidistant discretization subintervals $[t_{n-1}, t_n]$. The order of convergence depends on the Hölder exponents of the stochastic process $Y(t)$ which is given by $\theta \in (0, 1]$ and satisfies

$$\|Y(t, \omega) - Y(s, \omega)\| \leq \Theta(\omega)\, |t - s|^\theta, \qquad \omega \in \Omega, \tag{2.33}$$

for a random variable $\Theta(\omega) : \Omega \to [0, \infty)$ and $s,\ t \in [0, T]$. Here $\|\cdot\|$ is arbitrary, but fixed norm on $\mathbb{R}^m$.

A special case of the RODE with affine structure was considered by Grüne & Kloeden [38], i.e., of the form:

$$\frac{dx}{dt} = f^0(x) + f^1(x)\, Y(t) \tag{2.34}$$

and they showed for the affine RODE that the $\min(2\theta, 1)$-order convergence is attained by the averaged explicit Euler scheme

$$X_n = X_{n-1} + \left(f^0(X_{n-1}) + f^1(X_{n-1}) I_{n-1}\right) \Delta_n,$$

where the integral

$$I_{n-1}(\omega) := \frac{1}{\Delta_n} \int_{t_{n-1}}^{t_n} Y(s, \omega)\, ds$$

provides more information about the noise process within the discretization interval.

The counterpart of the scheme for a general RODE would require us to average the entire vector field, i.e., to use the integral

$$\frac{1}{\Delta_n} \int_{t_{n-1}}^{t_n} f(X_{n-1}, Y(s, \omega))\, ds.$$

This is computationally expensive even for low dimensional systems. An alternative idea, suggested in [59], is to use the averaged noise within the vector field, which leads to the EAES:

$$X_n = X_{n-1} + f(X_{n-1}, I_{n-1})\Delta_n. \tag{2.35}$$

Similarly, we can derive the IAES:

$$X_n = X_{n-1} + f(X_n, I_{n-1})\Delta_n, \tag{2.36}$$

and the IAMS:

$$X_n = X_{n-1} + f\left(\frac{1}{2}(X_{n-1} + X_n), I_{n-1}\right) \Delta_n. \tag{2.37}$$

The following theorems generalize analogous results for deterministic ODEs satisfying a one-sided Lipschitz condition:

Assumption 2. ***(One-sided Lipschitz condition.)***
There exists a constant $L \in \mathbb{R}$ such that

$$\left\langle f(x, \omega) - f(x', \omega), x - x' \right\rangle \leq L \left\| x - x' \right\|^2, \tag{2.38}$$

for all $x,\ x' \in \mathbb{R}^d$ and $\omega \in \mathbb{R}^m$. When $L < 0$, this condition is called dissipative *one-sided Lipschitz condition.*

It follows from Assumption 2 that

$$\begin{aligned}\frac{d}{dt}\|x(t)-x'(t)\| &= 2\left\langle x(t)-x'(t), f(x(t),Y(t))-f(x'(t),Y(t))\right\rangle \\ &\leq 2L\,\|x(t)-x'(t)\|^2,\end{aligned}$$

for any two solution of the RODE (2.29), so

$$\|x(t)-x'(t)\|^2 \leq \exp(2Lt)\,\|x(0)-x'(0)\|^2.$$

In particular, when $L < 0$, the solutions converge to each other pathwise in time. In fact, in this case all solutions converge pathwise to a unique stochastic stationary solution (see e.g., [20]).

Theorem 3. ***(Solvability, convergence and B-stability of the IAES.)*** *The IAES* (2.36) *is uniquely solvable when $L < 0$ without restriction on the step size, whereas it is uniquely solvable for step sizes $\Delta_t \in (0, L^{-1})$ when $L > 0$.*

Moreover, the IAES converges pathwise with order $\min(2\theta, 1)$ *in the following sense: when $L \leq 0$,*

$$\sup_{i=0,1,\cdots,n} \|x(t_i) - X_i\| \leq TC_E \cdot \Delta_t^{\min(2\theta,1)}$$

holds pathwise for all $\Delta_t \leq 1$, and when $L > 0$,

$$\sup_{i=0,1,\cdots,n} \|x(t_i) - X_i\| \leq \frac{C_E}{L}\left(\exp\left(\frac{LT}{1-\alpha}\right) - 1\right) \cdot \Delta_t^{\min(2\theta,1)}$$

for all $\Delta_t \leq \min(1, \alpha L^{-1})$ and each (arbitrary) $\alpha \in (0,1)$.

Furthermore, the IAES is B-stable when $L \leq 0$.

Theorem 4. ***(Solvability, convergence and B-stability of the IAMS.)*** *The IAMS* (2.37) *is uniquely solvable for all step sizes when $L \leq 0$ and for step sizes $\Delta_t \in (0, 4L^{-1})$ when $L > 0$.*

Moreover, the IAMS converges pathwise with order 2θ with the following bounds: when $L \leq 0$,

$$\sup_{i=0,1,\cdots,n} \|x(t_i) - X_i\| \leq TC_M \cdot \Delta_t^{2\theta}$$

holds pathwise for all $\Delta_t \leq 1$, and when $L > 0$,

$$\sup_{i=0,1,\cdots,n} \|x(t_i) - X_i\| \leq \left(\exp\left(\frac{\alpha LT}{1-\alpha}\right) - 1\right)\left(\frac{C_M}{\alpha L}\right) \cdot \Delta_t^{2\theta}$$

for all $\Delta_t \leq \min(1, \alpha L^{-1})$ and each (arbitrary) $\alpha \in (0,1)$.

Furthermore, the IAMS is B-stable when $L \leq 0$.

The proofs of the above theorems are given in section 5.1.

2.4 Additional notations

In addition to the notations appeared in the previous sections, some more notations are introduced here.

The multiple stochastic integrals $I_{\alpha,t_{n-1}}[f(\cdot)]$ is given by

$$I_{\alpha,t_{n-1}}[f(\cdot)] = \int_{t_{n-1}}^{t_n} \cdots \int_{t_{n-1}}^{s_{l-1}} f(s_l)\, dW^{j_l}(s_l) \cdots dW^{j_1}(s_1). \tag{2.39}$$

In the special case with $f \equiv 1$, we denote $I_{\alpha,t_{n-1}}[1] = I_{\alpha,t_{n-1}}$, which appeared in section 2.2.

A combination of stochastic integrals $\hat{I}^{t_n}_{\alpha,t_{n-k}}$ is define by the combination of stochastic integrals I_α between the time points t_{n-k} and t_n. For example, when $\alpha = (1,1,0)$ and $k = 3$, the corresponding stochastic integrals $\hat{I}^{t_n}_{(1,1,0),t_{n-3}}[f(\cdot)]$ is given by

$$\begin{aligned}
\hat{I}^{t_n}_{(1,1,0),t_{n-3}}[f(\cdot)] &= I_{(1,1,0),t_{n-3}}[f(\cdot)] + I_{(1,1),t_{n-3}}[f(\cdot)](I_{(0),t_{n-2}} + I_{(0),t_{n-1}}) \\
&+ I_{(1),t_{n-3}}[f(\cdot)](I_{(1,0),t_{n-2}} + I_{(1),t_{n-2}} I_{(0),t_{n-1}} + I_{(1,0),t_{n-1}}) \\
&+ I_{(1,1,0),t_{n-2}}[f(\cdot)] + I_{(1,1),t_{n-2}}[f(\cdot)] I_{(0),t_{n-1}} \\
&+ I_{(1),t_{n-2}}[f(\cdot)] I_{(1,0),t_{n-1}} + I_{(1,1,0),t_{n-1}}[f(\cdot)].
\end{aligned} \tag{2.40}$$

The reduced hierarchical set Λ_γ^0 is a subset of Λ_γ and it is given by

$$\Lambda_\gamma^0 = \{\alpha \in \Lambda_\gamma : \alpha = \emptyset \text{ or } l(\alpha) \geq 1 \text{ with the last component } j_l = 0\}. \tag{2.41}$$

The remainder set of Λ_γ is given as

$$\mathcal{B}(\Lambda_\gamma) = \{\alpha \in \mathcal{M} \setminus \Lambda_\gamma : -\alpha \in \Lambda_\gamma\}, \tag{2.42}$$

where $-\alpha$ denotes the multi-index in $\mathcal{M}$ obtained by deleting the first component of α. For example, when $\gamma = 3/2$, the hierarchical set Λ_γ, the remainder set $\mathcal{B}(\Lambda_\gamma)$, the reduced hierarchical set Λ_γ^0 and its remainder set $\mathcal{B}(\Lambda_\gamma^0)$ are given by

$$\begin{aligned}
\Lambda_{3/2} &= \{\emptyset, (1), (0), (1,1), (0,1), (1,0), (0,0), (1,1,1)\}, \\
\mathcal{B}(\Lambda_{3/2}) &= \{(0,1,1), (1,0,1), (0,0,1), (1,1,0), (0,1,0), (1,0,0), (0,0,0), \\
&\qquad (1,1,1,1), (0,1,1,1)\},
\end{aligned}$$

and

$$\begin{aligned}
\Lambda_{3/2}^0 &= \{\emptyset, (0), (1,0), (0,0)\}, \\
\mathcal{B}(\Lambda_{3/2}^0) &= \{(1), (1,1,0), (0,1,0), (1,0,0), (0,0,0)\}.
\end{aligned}$$

Chapter 3

RODEs with Itô noise

In this chapter, numerical schemes for RODEs driven by an Itô diffusion, i.e., the solution of an Itô SODE, are investigated. As we saw in section 1.1, RODEs with an Itô noise process can be written in the coupled RODE-SODE form (1.8):

$$d\begin{pmatrix} X(t) \\ Y(t) \end{pmatrix} = \begin{pmatrix} f(X(t), Y(t)) \\ a(Y(t)) \end{pmatrix} dt + \begin{pmatrix} 0 \\ b(Y(t)) \end{pmatrix} dW(t).$$

This means that the numerical schemes for SODEs can be applied to the coupled system. In particular, when the noise process $Y(t)$ is Wiener process or OU process, they can be generated by using probability distribution, so we need to solve only the RODE part in the coupled system.

The diffusion term of $X(t)$ is zero. Because of this special structure, Itô-Taylor schemes for SODEs can be reduced to simpler forms. Moreover, the schemes often attain higher order convergence when they are applied to the RODE part.

Buckwar & Winkler considered SODEs with small diffusion terms and developed SLMMs with higher order convergence [13, 14]. Similar approach can be applied to the X-component of the RODE-SODE pair, but without restricting the intensity of the noise.

Under standard assumptions, specifically, the uniform boundedness of all partial derivatives, the order γ strong Taylor schemes for SODEs are known to converge pathwise with order $(\gamma - \epsilon)$ for arbitrarily small $\epsilon > 0$. The corresponding scheme applied to X-component thus also converges pathwise with order $(\gamma - \epsilon)$. Using a localization argument, this is extended to RODEs for which the vector field functions do not have uniformly bounded derivatives in the solution variable. Modifications of the Itô-Taylor schemes to derivative-free, implicit and multi-step methods are also considered.

3.1 Taylor schemes

3.1.1 Derivation of strong Taylor schemes

Scalar case

First of all, we consider a scalar case. The scalar RODE driven by a scalar Itô diffusion $Y(t)$:

$$\begin{aligned} \frac{dx}{dt} &= f(x, Y(t)) \\ dY(t) &= a(Y(t))\,dt + b(Y(t))\,dW(t), \end{aligned} \tag{3.1}$$

where $W(t)$ is scalar Wiener process, can be written in a system of Itô SODEs:

$$d\begin{pmatrix} X(t) \\ Y(t) \end{pmatrix} = \begin{pmatrix} f(X(t), Y(t)) \\ a(Y(t)) \end{pmatrix} dt + \begin{pmatrix} 0 \\ b(Y(t)) \end{pmatrix} dW(t),$$

or, in vector notation:

$$d\mathbf{X}(t) = \mathbf{F}(\mathbf{X}(t))\,dt + \mathbf{G}(\mathbf{X}(t))\,dW(t), \tag{3.2}$$

with

$$\mathbf{X} = \begin{pmatrix} x \\ y \end{pmatrix}, \quad \mathbf{F}(\mathbf{X}) = \begin{pmatrix} f(x,y) \\ a(y) \end{pmatrix}, \quad \mathbf{G}(\mathbf{X}) = \begin{pmatrix} 0 \\ b(y) \end{pmatrix}. \tag{3.3}$$

In this case the differential operators L^0 and L^1 reduce to

$$\begin{aligned} L^0 U &= \frac{\partial U}{\partial t} + f(x,y)\frac{\partial U}{\partial x} + a(y)\frac{\partial U}{\partial y} + \frac{1}{2}b(y)^2\frac{\partial^2 U}{\partial y^2}, \\ L^1 U &= b(y)\frac{\partial U}{\partial y}. \end{aligned}$$

Now $\mathbf{X}^1 = x$ and $\mathbf{X}^2 = y$, so

$$L^0 id_{\mathbf{X}^1} = f(x,y), \;\; L^0 id_{\mathbf{X}^2} = a(y), \;\; L^1 id_{\mathbf{X}^1} = 0, \;\; L^1 id_{\mathbf{X}^2} = b(y).$$

Since the $Y(t)$ equation is an SODE in its own right, its order γ strong Taylor scheme is just a scalar version of the usual one, namely,

$$Y_n = \sum_{\alpha \in \Lambda_\gamma} L^\alpha id_{\mathbf{X}^2}(Y_{n-1})\, I_{\alpha, t_{n-1}}, \tag{3.4}$$

which is equivalent to (2.26).

For the X-component, the strong Taylor scheme can be simplified. The integral form of X-component is given by

$$X(t) = X(t_0) + \int_{t_0}^{t} f(X(s), Y(s))\, ds + \int_{t_0}^{t} 0\, dW(s). \tag{3.5}$$

Taking $U = f$ in (2.18) and substituting $f(X(s), Y(s))$ yields

$$X(t) = X(t_0) + f(X(t_0), Y(t_0)) \int_{t_0}^{t} ds + R_1, \tag{3.6}$$

where R_1 is a remainder term and it is given by

$$\begin{aligned} R_1 &= \int_{t_0}^{t} \int_{t_0}^{s_1} L^0 f(X(s_2), Y(s_2))\, ds_2 ds_1 \\ &\quad + \int_{t_0}^{t} \int_{t_0}^{s_1} L^1 f(X(s_2), Y(s_2))\, dW(s_2) ds_1. \end{aligned} \tag{3.7}$$

Discarding the remainder term R_1 in (3.6) gives Euler-Maruyama approximation which now has a form:

$$X_t = X_{t_0} + f(X_{t_0}, Y_{t_0}) \int_{t_0}^{t} ds,$$

and thus the Euler-Maruyama scheme:

$$X_n = X_{n-1} + f(X_{n-1}, Y_{n-1})\Delta_n, \tag{3.8}$$

with $\Delta_n = t_n - t_{n-1} = \int_{t_{n-1}}^{t_n} ds$. This is the same form as (2.4) which is derived for deterministic ODEs. In order to build higher order schemes, we need to deal with the remainder term R_1. Now we consider the cases $U = L^0 f$, $U = L^1 f$ and $U = L^1 L^1 f$. Then, the corresponding Itô formula are given as

$$\begin{aligned} L^0 f(X(t), Y(t)) &= L^0 f(X(t_0), Y(t_0)) + \int_{t_0}^{t} L^0 L^0 f(X(s), Y(s))\, ds \\ &\quad + \int_{t_0}^{t} L^1 L^0 f(X(s), Y(s))\, dW(s) \\ L^1 f(X(t), Y(t)) &= L^1 f(X(t_0), Y(t_0)) + \int_{t_0}^{t} L^0 L^1 f(X(s), Y(s))\, ds \\ &\quad + \int_{t_0}^{t} L^1 L^1 f(X(s), Y(s))\, dW(s) \\ L^1 L^1 f(X(t), Y(t)) &= L^1 L^1 f(X(t_0), Y(t_0)) \\ &\quad + \int_{t_0}^{t} L^0 L^1 L^1 f(X(s), Y(s))\, ds + \int_{t_0}^{t} L^1 L^1 L^1 f(X(s), Y(s))\, dW(s). \end{aligned}$$

Substituting $L^0 f(X(t), Y(t))$ and $L^1 f(X(t), Y(t))$ in R_1 as well as $L^1 L^1 f(X(t), Y(t))$ in $L^1 f(X(t), Y(t))$ leads

$$\begin{aligned} X(t) &= X(t_0) + f(X(t_0), Y(t_0)) \int_{t_0}^{t} ds + L^0 f(X(t_0), Y(t_0)) \int_{t_0}^{t} \int_{t_0}^{s_1} ds_2 ds_1 \\ &\quad + L^1 f(X(t_0), Y(t_0)) \int_{t_0}^{t} \int_{t_0}^{s_1} dW(s_2) ds_1 \qquad (3.9) \\ &\quad + L^1 L^1 f(X(t_0), Y(t_0)) \int_{t_0}^{t} \int_{t_0}^{s_1} \int_{t_0}^{s_2} dW(s_3) dW(s_2) ds_1 + R_{1.5}, \end{aligned}$$

where $R_{1.5}$ is

$$\begin{aligned} R_{1.5} &= \int_{t_0}^{t} \int_{t_0}^{s_1} \int_{t_0}^{s_2} L^0 L^0 f(X(s_3), Y(s_3))\, ds_3 ds_2 ds_1 \\ &\quad + \int_{t_0}^{t} \int_{t_0}^{s_1} \int_{t_0}^{s_2} L^1 L^0 f(X(s_3), Y(s_3))\, dW(s_3) ds_2 ds_1 \\ &\quad + \int_{t_0}^{t} \int_{t_0}^{s_1} \int_{t_0}^{s_2} L^0 L^1 f(X(s_3), Y(s_3))\, ds_3 dW(s_2) ds_1 \\ &\quad + \int_{t_0}^{t} \int_{t_0}^{s_1} \int_{t_0}^{s_2} \int_{t_0}^{s_3} L^0 L^1 L^1 f(X(s_4), Y(s_4))\, ds_4 dW(s_3) dW(s_2) ds_1 \\ &\quad + \int_{t_0}^{t} \int_{t_0}^{s_1} \int_{t_0}^{s_2} \int_{t_0}^{s_3} L^1 L^1 L^1 f(X(s_4), Y(s_4))\, dW(s_4) dW(s_3) dW(s_2) ds_1. \end{aligned}$$

Discarding the remainder term $R_{1.5}$ in (3.9) yields 1.5-order strong Itô-Taylor approximation:

$$\begin{aligned} X_t &= X_{t_0} + f(X_{t_0}, Y_{t_0}) I_{(0),t_0,t} + L^0 f(X_{t_0}, Y_{t_0}) I_{(0,0),t_0,t} \qquad (3.10) \\ &\quad + L^1 f(X_{t_0}, Y_{t_0}) I_{(1,0),t_0,t} + L^1 L^1 f(X_{t_0}, Y_{t_0}) I_{(1,1,0),t_0,t}, \end{aligned}$$

with the multiple stochastic integrals notation introduced in section 2.4.

Since $L^1 id_{\mathbf{X}^1} \equiv 0$, for any index α with $j_l = 1$,

$$L^\alpha id_{\mathbf{X}^1} = L^{\alpha-} L^{j_l} id_{\mathbf{X}^1} = L^{\alpha-} L^1 id_{\mathbf{X}^1} = L^{\alpha-} 0 \equiv 0.$$

Here $\alpha-$ denotes the multi-index in $\mathcal{M}$ obtained by deleting the last component of α. On the other hand, terms like

$$L^1 L^0 id_{\mathbf{X}^1} = L^1 f(x, y) = b(y) \frac{\partial f}{\partial y}(x, y)$$

do not vanish automatically. This gives the general form of the strong Taylor scheme for the X-component:

$$X_n = \sum_{\alpha \in \Lambda_\gamma^0} L^\alpha id_{\mathbf{X}^1}(X_{n-1}, Y_{n-1})\, I_{\alpha, t_{n-1}}, \qquad (3.11)$$

for the reduced hierarchical set given as (2.41).

Vector case

Consider the general vector case with $X \in \mathbb{R}^{d_1}$, $Y \in \mathbb{R}^{d_2}$, i.e., a RODE on $\mathbb{R}^{d_1}$:

$$\frac{dx}{dt} = f(x, Y(t)), \tag{3.12}$$

where $Y(t)$ is the solution of an Itô SODE in $\mathbb{R}^{d_2}$:

$$dY(t) = a(Y(t))\,dt + \sum_{j=1}^{m} b_j(Y(t))\,dW^j(t) \tag{3.13}$$

with m independent scalar Wiener processes $W^1(t), \cdots, W^m(t)$. This forms a system of SODE in $\mathbb{R}^{d_1+d_2}$:

$$d\begin{pmatrix} X(t) \\ Y(t) \end{pmatrix} = \begin{pmatrix} f(X(t), Y(t)) \\ a(Y(t)) \end{pmatrix} dt + \sum_{j=1}^{m} \begin{pmatrix} 0 \\ b_j(Y(t)) \end{pmatrix} dW^j(t). \tag{3.14}$$

Denote $\mathbf{X} = (x, y)^T \in \mathbb{R}^d$, where $d = d_1 + d_2$. Now (3.14) can be written as

$$d\mathbf{X}(t) = \mathbf{F}(\mathbf{X}(t))\,dt + \sum_{j=1}^{m} \mathbf{G}_j(\mathbf{X}(t))\,dW^j(t), \tag{3.15}$$

with coefficient functions:

$$\mathbf{F}(\mathbf{X}) = \begin{pmatrix} f(x, y) \\ a(y) \end{pmatrix}, \quad \mathbf{G}_j(\mathbf{X}) = \begin{pmatrix} 0 \\ b_j(y) \end{pmatrix}.$$

Then, the order γ strong Taylor scheme is

$$\mathbf{X}_n = \sum_{\alpha \in \Lambda_\gamma} L^\alpha id_{\mathbf{X}}(\mathbf{X}_{n-1}) I_{\alpha, t_{n-1}}, \tag{3.16}$$

with the hierarchical set $\Lambda_\gamma \subset \mathcal{M}_m$, $\mathbf{X}_n = (X_n, Y_n)^T$ and differential operators:

$$\begin{aligned} L^0 U &= \frac{\partial U}{\partial t} + \sum_{k=1}^{d_1} f^k(x, y) \frac{\partial U}{\partial x_k} + \sum_{k=1}^{d_2} a^k(y) \frac{\partial U}{\partial y_k} \\ &\qquad + \sum_{k,l=1}^{d_1+d_2} \sum_{j=1}^{m} \frac{1}{2} b_j^k(y) b_j^l(y) \frac{\partial^2 U}{\partial y_k \partial y_l}, \\ L^j U &= \sum_{k=1}^{d_2} b_j^k(y) \frac{\partial U}{\partial y_k}, \qquad j = 1, \ldots, m, \end{aligned}$$

for smooth enough functions $U : [0,T] \times \mathbb{R}^{d_1} \times \mathbb{R}^{d_2} \to \mathbb{R}$. The k-th X-component of the order γ strong Taylor scheme gives the order γ strong RODE-Taylor scheme in componentwise form:

$$X_n^k = \sum_{\alpha \in \Lambda_\gamma^0} L^\alpha id_{\mathbf{X}^k}(X_{n-1}, Y_{n-1}) I_{\alpha, t_{n-1}}, \qquad k = 1, \ldots, d_1, \tag{3.17}$$

where $\Lambda_\gamma^0 \subset \Lambda_\gamma$ is defined as (2.41) as a subset of $\mathcal{M}_m$.

Examples

Some examples of the RODE-Taylor schemes for the scalar system (3.2) with $d_1 = d_2 = 1$ and $m = 1$ are illustrated here. For notational compactness partial derivatives are denoted by subscripts.

If $\gamma = 1/2$, the hierarchical set $\Lambda_{1/2}$ and the reduced set $\Lambda_{1/2}^0$ are given by $\{\emptyset, (0), (1)\}$ and $\{\emptyset, (0)\}$, respectively. The corresponding RODE-Taylor scheme is the Euler-Maruyama scheme which reduces to

$$X_n = X_{n-1} + f(X_{n-1}, Y_{n-1})\Delta_n, \tag{3.18}$$

where $\Delta_n = t_n - t_{n-1} = I_{(0),t_{n-1}}$. Obviously this is equivalent to (3.8). This is also the RODE-Taylor scheme obtainable from the Milstein scheme with $\gamma = 1$ since $\Lambda_1 = \{\emptyset, (0), (1), (1,1)\}$ and $\Lambda_1^0 = \{\emptyset, (0)\}$.

For $\gamma = 3/2$, the situation is more complicated. Here

$$\Lambda_{3/2} = \{\emptyset, (0), (1), (1,1), (0,1), (1,0), (0,0), (1,1,1)\}$$

and $\Lambda_{3/2}^0 = \{\emptyset, (0), (1,0), (0,0)\}$, so the order 1.5 RODE-Taylor scheme is given by

$$\begin{aligned} X_n \;=\; & X_{n-1} + f(X_{n-1}, Y_{n-1})\Delta_n + b(Y_{n-1}) f_y(X_{n_1}, Y_{n-1})\; I_{(1,0),t_{n-1}} \\ & + \Big(f(X_{n-1}, Y_{n-1}) f_x(X_{n-1}, Y_{n-1}) \\ & \quad + a(Y_{n-1}) f_y(X_{n-1}, Y_{n-1}) + \frac{1}{2} b(Y_{n-1})^2 f_{yy}(X_{n-1}, Y_{n-1}) \Big)\; \frac{1}{2}\Delta_n^2. \end{aligned} \tag{3.19}$$

This scheme includes the multiple stochastic integral

$$I_{(1,0),t_{n-1}} = \int_{t_{n-1}}^{t_n} \int_{t_{n-1}}^{s_1} dW(s_2) ds_1,$$

which is correlated to the simple integral $\Delta W_n = I_{(1),t_{n-1}} = \int_{t_{n-1}}^{t_n} dW(s_1)$. They can be generated using two independent $N(0,1)$-distributed random variables (see section 6.1, [7, 66]) G_1 and G_2 as

$$I_{(1),t_{n-1}} = \sqrt{\Delta_n} G_1, \qquad I_{(1,0),t_{n-1}} = \frac{1}{2}\Delta_n^{3/2}\Big(G_1 + \frac{1}{\sqrt{3}} G_2\Big).$$

Similarly, for $\gamma = 2$,

$$\Lambda_2 = \Lambda_{3/2} \cup \{(1,1,0),(1,0,1),(0,1,1),(1,1,1,1)\}$$

and $\Lambda_2^0 = \{\emptyset,(0),(1,0),(0,0),(1,1,0)\}$, which gives the order 2.0 RODE-Taylor scheme

$$\begin{aligned} X_n &= X_{n-1} + f(X_{n-1},Y_{n-1})\Delta_n + b(Y_{n-1})f_y(X_{n-1},Y_{n-1})\, I_{(1,0),t_{n-1}} \\ &\quad + \Big(f(X_{n-1},Y_{n-1})f_x(X_{n-1},Y_{n-1}) + a(Y_{n-1})f_y(X_{n-1},Y_{n-1}) \\ &\qquad + \frac{1}{2}b(Y_{n-1})^2 f_{yy}(X_{n-1},Y_{n-1}) \Big)\, \frac{1}{2}\Delta_n^2 \qquad (3.20) \\ &\quad + \Big(b(Y_{n-1})b_y(Y_{n-1})f_y(X_{n-1},Y_{n-1}) \\ &\qquad + b(Y_{n-1})^2 f_{yy}(X_{n-1},Y_{n-1}) \Big)\, I_{(1,1,0),t_{n-1}}. \end{aligned}$$

This scheme now includes coefficients of the SODE of the driving noise as well as an additional multiple stochastic integral.

3.1.2 Implicit Taylor scheme

Stiff differential equations arise frequently in practice and explicit schemes often perform poorly, while implicit schemes offer better numerical stability properties. The order 1.0 implicit strong Taylor scheme in Kloeden & Platen [67] is a drift-implicit version of the Milstein scheme. For the vector SODE (3.15) with single Wiener process it is

$$\begin{aligned} \mathbf{X}_n^k &= \mathbf{X}_{n-1}^k + \Big(\theta \mathbf{F}^k(\mathbf{X}_n) + (1-\theta)\mathbf{F}^k(\mathbf{X}_{n-1}) \Big)\, \Delta_n \qquad (3.21) \\ &\quad + \mathbf{G}^k(\mathbf{X}_{n-1})\Delta W_n + L^1\mathbf{G}^k(\mathbf{X}_{n-1})\, I_{(1,1),t_{n-1}}, \qquad k = 1,\ldots,d, \end{aligned}$$

where the parameter $\theta \in [0,1]$ characterizes the degree of implicitness. When $\theta = 0$, the equation (3.21) reduces to usual explicit Milstein scheme.

For the scalar SODE (3.2) its X-component gives the order 1.0 implicit strong RODE-Taylor scheme

$$X_n = X_{n-1} + (\theta f(X_n,Y_n) + (1-\theta)f(X_{n-1},Y_{n-1}))\,\Delta_n, \qquad (3.22)$$

which is often called the θ-scheme [44]. It is essentially the Euler scheme.

Similarly, the family of 1.5-order implicit strong Taylor scheme in [67] is,

componentwise,

$$\begin{aligned}
\mathbf{X}_n^k &= \mathbf{X}_{n-1}^k + \Big(\theta_1 \mathbf{F}^k(\mathbf{X}_n) + (1-\theta_1)\mathbf{F}^k(\mathbf{X}_{n-1})\Big)\,\Delta_n \\
&\quad + \left(\frac{1}{2} - \theta_1\right)\Big(\theta_2 L^0\mathbf{F}^k(\mathbf{X}_n) + (1-\theta_2)L^0\mathbf{F}^k(\mathbf{X}_{n-1})\Big)\,\Delta_n^2 \\
&\quad + L^1\mathbf{F}^k\left(\mathbf{X}_{n-1}\right)(I_{(1,0),t_{n-1}} - \theta_1 \Delta W_n \Delta_n\big) \\
&\quad + \mathbf{G}^k(\mathbf{X}_{n-1})\Delta W_n + L^0\mathbf{G}^k(\mathbf{X}_{n-1})I_{(0,1),t_{n-1}} \\
&\quad + L^1\mathbf{G}^k(\mathbf{X}_{n-1})I_{(1,1),t_{n-1}} + L^1L^1\mathbf{G}^k(\mathbf{X}_{n-1})I_{(1,1,1),t_{n-1}},
\end{aligned}$$

where the parameters θ_1, $\theta_2 \in [0,1]$ indicate the extent of implicitness. The corresponding implicit RODE-Taylor scheme is

$$\begin{aligned}
X_n &= X_{n-1} + (\theta_1 f(X_n, Y_n) + (1-\theta_1) f(X_{n-1}, Y_{n-1}))\,\Delta_n \\
&\quad + \left(\frac{1}{2} - \theta_1\right)\big(\theta_2 L^0 f(X_n, Y_n) + (1-\theta_2)L^0 f(X_{n-1}, Y_{n-1})\big)\,\Delta_n^2 \\
&\quad + L^1 f(X_{n-1}, Y_{n-1})\left(I_{(1,0),t_{n-1}} - \theta_1 \Delta W_n \Delta_n\right). \qquad (3.23)
\end{aligned}$$

3.1.3 Derivative-free scheme

The order γ strong Taylor schemes involve derivatives of the coefficient functions of the SODE (3.15), that may be difficult to determine in higher dimensional examples. The derivative-free explicit strong schemes in Kloeden & Platen [67] are Runge-Kutta-like schemes that replace such derivatives by appropriate finite difference quotients to ensure the same order γ strong convergence.

For a single Wiener process, i.e., $m = 1$, the k-th component of the explicit order 1.0 strong scheme for SODEs has the form:

$$\begin{aligned}
\mathbf{X}_n^k &= \mathbf{X}_{n-1}^k + \mathbf{F}^k(\mathbf{X}_{n-1})\Delta_n + \mathbf{G}^k(\mathbf{X}_{n-1})\Delta W_n \\
&\quad + \frac{1}{2\sqrt{\Delta_n}}\Big(\mathbf{G}^k(\tilde{\mathbf{X}}_{n-1}) - \mathbf{G}^k(\mathbf{X}_{n-1})\Big)\left((\Delta W_n)^2 - \Delta_n\right),
\end{aligned}$$

with the support function:

$$\tilde{\mathbf{X}}_{n-1} = \mathbf{X}_{n-1} + \mathbf{F}(\mathbf{X}_{n-1})\Delta_n + \mathbf{G}(\mathbf{X}_{n-1})\sqrt{\Delta_n}.$$

The corresponding RODE scheme is given by (3.18), which does not contain derivative terms, and is the same as for the Euler-Maruyama and Milstein schemes.

Similarly, the order 1.5 explicit strong scheme for SODEs is, componentwise,

$$\begin{aligned}
\mathbf{X}_n^k &= \mathbf{X}_{n-1}^k + \mathbf{F}^k(\mathbf{X}_{n-1})\Delta_n + \frac{1}{2\sqrt{\Delta_n}}\left(\mathbf{F}^k(\tilde{\mathbf{X}}_+) - \mathbf{F}^k(\tilde{\mathbf{X}}_-)\right) I_{(1,0),t_{n-1}} \\
&\quad + \frac{1}{2\Delta_n}\left(\mathbf{F}^k(\tilde{\mathbf{X}}_+) - 2\mathbf{F}^k(\mathbf{X}_{n-1}) + \mathbf{F}^k(\tilde{\mathbf{X}}_-)\right) I_{(0,0),t_{n-1}} \\
&\quad + \mathbf{G}^k(\mathbf{X}_{n-1})\Delta W_n + \frac{1}{2\sqrt{\Delta_n}}\left(\mathbf{G}^k(\tilde{\mathbf{X}}_+) - \mathbf{G}^k(\tilde{\mathbf{X}}_-)\right) I_{(1,1),t_{n-1}} \\
&\quad + \frac{1}{2\Delta_n}\left(\mathbf{G}^k(\tilde{\mathbf{X}}_+) - 2\mathbf{G}^k(\mathbf{X}_{n-1}) + \mathbf{G}^k(\tilde{\mathbf{X}}_-)\right) I_{(0,1),t_{n-1}} \\
&\quad + \frac{1}{2\Delta_n}\left(\mathbf{G}^k(\tilde{\mathbf{\Phi}}_+) - \mathbf{G}^k(\tilde{\mathbf{\Phi}}_-) - \mathbf{G}^k(\tilde{\mathbf{X}}_+) + \mathbf{G}^k(\tilde{\mathbf{X}}_-)\right) I_{(1,1,1),t_{n-1}},
\end{aligned}$$

where

$$\begin{aligned}
\tilde{\mathbf{X}}_\pm &= \mathbf{X}_{n-1} + \mathbf{F}(\mathbf{X}_{n-1})\Delta_n \pm \mathbf{G}(\mathbf{X}_{n-1})\sqrt{\Delta_n}, \\
\tilde{\mathbf{\Phi}}_\pm &= \tilde{\mathbf{X}}_+ \pm \mathbf{G}(\tilde{\mathbf{X}}_+)\sqrt{\Delta_n}.
\end{aligned}$$

$\mathbf{G}^1 \equiv 0$ for $k = 1$ and the X-component gives the RODE-Taylor scheme:

$$\begin{aligned}
X_n &= X_n + f(X_{n-1}, Y_{n-1})\Delta_n \\
&\quad + \frac{1}{2\sqrt{\Delta_n}}\left(f(\tilde{X}, \tilde{Y}_+) - f(\tilde{X}, \tilde{Y}_-)\right) I_{(1,0),t_{n-1}} \qquad (3.24) \\
&\quad + \frac{1}{4}\left(f(\tilde{X}, \tilde{Y}_+) - 2f(X_{n-1}, Y_{n-1}) + f(\tilde{X}, \tilde{Y}_-)\right)\Delta_n
\end{aligned}$$

with

$$\begin{aligned}
\tilde{X} &= X_{n-1} + f(X_{n-1}, Y_{n-1})\Delta_n, \\
\tilde{Y}_\pm &= Y_{n-1} + a(Y_{n-1})\Delta_n \pm b(Y_{n-1})\sqrt{\Delta_n},
\end{aligned}$$

since $\tilde{X} = \tilde{X}_\pm$ here and $I_{(0,0),t_{n-1}} = \frac{1}{2}\Delta_n^2$.

Derivative-free implicit RODE-Taylor schemes can be built in the same manner. When $\theta_1 = 1/2$, the implicit RODE-Taylor scheme (3.23) reduces to

$$\begin{aligned}
X_n &= X_{n-1} + \frac{1}{2}\left(f(X_n, Y_n) + f(X_{n-1}, Y_{n-1})\right)\Delta_n \\
&\quad + L^1 f(X_{n-1}, Y_{n-1})\left(I_{(1,0),t_{n-1}} - \frac{1}{2}\Delta W_n \Delta_n\right). \qquad (3.25)
\end{aligned}$$

Replacing the derivative $L^1 f(X_{n-1}, Y_{n-1})$ in (3.25) by a finite difference quotient gives the derivative-free implicit scheme with $\gamma = 1.5$:

$$\begin{aligned} X_n &= X_{n-1} + \frac{1}{2}\left(f(X_n, Y_n) + f(X_{n-1}, Y_{n-1})\right)\Delta_n \\ &\quad + \frac{1}{2\sqrt{\Delta_n}}\left(f(\tilde{X}, \tilde{Y}_+) - f(\tilde{X}, \tilde{Y}_-)\right)\left(I_{(1,0),t_{n-1}} - \frac{1}{2}\Delta W_n \Delta_n\right) \end{aligned} \tag{3.26}$$

with

$$\begin{aligned} \tilde{X} &= X_{n-1} + f(X_{n-1}, Y_{n-1})\Delta_n, \\ \tilde{Y}_\pm &= Y_{n-1} + a(Y_{n-1})\Delta_n \pm b(Y_{n-1})\sqrt{\Delta_n}. \end{aligned}$$

3.1.4 Pathwise convergence

Kloeden & Neuenkirch showed the pathwise convergence of Itô-Taylor schemes under standard assumptions (Theorem 2 in section 2.2.2 and [65]). The assumptions here are, in fact, too strong just for the pathwise convergence of the RODE-Taylor scheme (3.11) and for many applications. They ensure the strong convergence of the full Taylor scheme (3.4) and (3.11), but the X-component scheme (3.11) can still converge pathwise even when the full scheme does not converge in the strong sense, provided the noise is approximated to the required order. This is possible directly or through the Y-component scheme (3.4) when the noise is a simple process such as a Wiener process or an OU process.

We are interested in the situation where the X-derivatives of the vector field f of the RODE are not uniformly bounded on $\mathbb{R}^d$, but are uniformly bounded in the Y-variable. This corresponds to the noise acting boundedly in the RODE (although the inputed noise $Y(t)$ need not itself be bounded).

Assume now that the coefficients a, b_1, ..., b_m satisfy the standard assumptions, i.e., a, b_1, ..., $b_m \in C_b^{2\gamma+1}$, but $f \in C^{2\gamma+1}$ does not. Since the Y-SODE does not depend on $X(t)$ and satisfies the standard assumptions, the strong order γ Taylor scheme applied to it converges strongly with order γ and pathwise with order $(\gamma - \epsilon)$. However, these schemes applied to the system (3.15) need not converge in strong sense when the standard assumptions do not hold [47, 48], although they may still converge in the pathwise sense.

Based on these ideas, we prove the following theorem:

Theorem 5. (Pathwise convergence of RODE-Taylor scheme.) *Suppose that a, b_1, ..., b_m, $f(X, \cdot) \in C_b^{2\gamma+1}$ and $f(\cdot, Y) \in C^{2\gamma+1}$. Then the solution (X_n, Y_n) of the order γ strong Taylor scheme* (3.11) *converges pathwise to the solution $(X(t), Y(t))$ of* (3.15) *with order $(\gamma - \epsilon)$ on $[0, T]$.*

The proof is based on a localization argument similar to that of Theorem 1 in [58] in a different context, which in turn uses ideas from [40]. It does not depend on the specific structure of the strong Taylor schemes, just the fact that they converge pathwise under the standard assumptions, which follows by a Borel-Cantelli argument as in Lemma 1 of section 2.2.2 when all of the error moments converge with the same order γ. This moment property was established in [65] for the order γ strong Taylor schemes as well as for the two-step Adams-Moulton scheme.

Proof. Let N be some sufficiently large number and define the stopping times:

$$\begin{aligned} \tau^{(N)}(\omega) &= \inf\{t \geq 0 : |X(t,\omega)| > N\} \wedge 2T, \\ \tau_n^{(N)}(\omega) &= \inf\{t \geq 0 : |X_n(t,\omega)| > N\} \wedge 2T. \end{aligned}$$

(The interval $[0, 2T]$ is used here to handle stopping times and other technical issues, but the result will be restricted later to the smaller interval $[0, T]$).

Fix a function $\varphi_N \in C_b^\infty(\mathbb{R}^d; [0,1])$ such that

$$\varphi_N(X) = \begin{cases} 1 & \text{for} \quad |X| \leq N, \\ 0 & \text{for} \quad |X| > N+1 \end{cases}$$

and define the truncated function $f_{\varphi_N} \in C_b^{2\gamma+1}$ by the product $f_\varphi(X,Y) = f(X,Y) \cdot \varphi_N(X)$. Then consider the truncated SODE:

$$dX^{(\varphi_N)}(t) = f_{\varphi_N}\left(X^{(\varphi_N)}(t), Y(t)\right) dt + 0\, dW(t),$$

which we couple with the driving SODE (3.13) for $Y(t)$ to form the modified system of SODEs in $\mathbb{R}^{d+m}$:

$$d\begin{pmatrix} X^{(\varphi_N)}(t) \\ Y(t) \end{pmatrix} = \begin{pmatrix} f_{\varphi_N}\left(X^{(\varphi_N)}(t), Y(t)\right) \\ a(Y(t)) \end{pmatrix} dt + \begin{pmatrix} 0 \\ b(Y(t)) \end{pmatrix} dW(t). \quad (3.27)$$

Clearly

$$\begin{aligned} \tau_n^{(N)}(\omega) &= \inf\{t \geq 0 : X_n(t,\omega) > N\} \wedge 2T \\ &= \inf\left\{t \geq 0 : X_n^{(\varphi_N)}(t,\omega) > N\right\} \wedge 2T \end{aligned}$$

and, as shown in the appendix of [58],

$$X(t \wedge \tau^{(N)})\mathbf{1}_{\{\tau^{(N)}>0\}} = X^{(\varphi_N)}(t \wedge \tau^{(N)})\mathbf{1}_{\{\tau^{(N)}>0\}}$$

for $t \geq 0$, so

$$\begin{aligned} \tau^{(N)}(\omega) &= \inf\{t \geq 0 : |X(t,\omega)| > N\} \wedge 2T \\ &\leq \inf\left\{t \geq 0 : \left|X^{(\varphi_N)}(t,\omega)\right| > N\right\} \wedge 2T. \end{aligned}$$

The coefficients of the modified system of SODEs (3.27) satisfy the standard assumptions, so by Proposition 2 on the pathwise convergence rates of the Itô-Taylor scheme in [58], the interpolated (as above) order γ strong Taylor scheme $\left(X_n^{(\varphi_N)}(t), Y_n(t)\right)$ applied to (3.27) converges strongly with order γ and pathwise with order $(\gamma - \epsilon)$ to its solution $\left(X^{(\varphi_N)}(t), Y(t)\right)$ on the time interval. Thus, for every $\epsilon > 0$, there exists a finite non-negative random variable $\zeta_{\epsilon,2T}^{(N)}$ such that

$$\sup_{t\in[0,2T]} \left| X^{(\varphi_N)}(t,\omega) - X_n^{(\varphi_N)}(t,\omega) \right| \leq \zeta_{\epsilon,2T}^{(N)}(\omega) \cdot n^{-\gamma+\epsilon}, \quad \text{a.s.} \tag{3.28}$$

for all $n \in \mathbb{N}$.

Since

$$X_n^{(\varphi_N)}(t \wedge \tau_n^{(N)})\mathbf{1}_{\{\tau_n^{(N)}>0\}} = X_n(t \wedge \tau_n^{(N)})\mathbf{1}_{\{\tau_n^{(N)}>0\}}, \quad t \in [0, 2T], \quad \text{a.s.},$$

and

$$X(t \wedge \tau^{(N)})\mathbf{1}_{\{\tau^{(N)}>0\}} = X^{(\varphi_N)}(t \wedge \tau^{(N)})\mathbf{1}_{\{\tau^{(N)}>0\}}, \quad t \in [0, 2T], \quad \text{a.s.},$$

it follows that $X_n(t)$ converges pathwise to $X(t)$ with order $(\gamma - \epsilon)$ on $[0, \tau_n^{(N)} \wedge \tau^{(N)})$, i.e.,

$$\sup_{t\in[0,\tau_n^{(N)}\wedge\tau^{(N)})} |X(t,\omega) - X_n(t,\omega)| \leq \zeta_{\epsilon,2T}^{(N)}(\omega) \cdot n^{-\gamma+\epsilon} \tag{3.29}$$

for all $n \in \mathbb{N}$.

Similarly

$$\begin{aligned} \bar{\tau}_n^{(N)}(\omega) &= \inf\{t \geq 0 : |X_n(t,\omega)| > N\} \wedge 2T \\ &= \inf\left\{t \geq 0 : \left|X_n^{(\varphi_N)}(t,\omega)\right| > N\right\} \wedge 2T \end{aligned}$$

and

$$X_n^{(\varphi_N)}(t \wedge \bar{\tau}_n^{(N)})\mathbf{1}_{\{\bar{\tau}_n^{(N)}>0\}} = X_n(t \wedge \bar{\tau}_n^{(N)})\mathbf{1}_{\{\bar{\tau}_n^{(N)}>0\}}, \quad t \in [0, 2T], \quad \text{a.s.}$$

Applying the same argument as above gives

$$\sup_{t\in[0,\tau^{(N)}\wedge\bar{\tau}_n^{(N)})} |X(t,\omega) - X_n^{(\varphi_N)}(t,\omega)| \leq \zeta_{\epsilon,2T}^{(N)}(\omega) \cdot n^{-\gamma+\epsilon}. \tag{3.30}$$

From equations (3.29) and (3.30),

$$\begin{aligned} \sup_{t\in[0,\tau^{(N)}\wedge\tau_n^{(N)})} |X(t,\omega) - X_n(t,\omega)| \quad &+ \quad \sup_{t\in[0,\tau^{(N)}\wedge\bar{\tau}_n^{(N)})} \left|X(t,\omega) - X_n^{(\varphi_N)}(t,\omega)\right| \\ &\leq \quad 2\,\zeta_{\epsilon,2T}^{(N)}(\omega) \cdot n^{-\gamma+\epsilon} \end{aligned}$$

and hence

$$\sup_{t\in[0,\tau')}\left|X_n(t,\omega)-X_n^{(\varphi_N)}(t,\omega)\right|\le 2\,\zeta_{\epsilon,2T}^{(N)}(\omega)\cdot n^{-\gamma+\epsilon} \tag{3.31}$$

for all $n\in\mathbb{N}$, where $\tau'=\tau^{(N)}\wedge\tau_n^{(N)}\wedge\bar\tau_n^{(N)}$. This means that the approximation of the original SODE by original strong Taylor scheme and that for the modified SODE coincide.

Inequality (3.28) implies that

$$\lim_{n\to\infty}\sup_{t\in[0,2T]}|X^{(\varphi_N)}(t,\omega)-X_n^{(\varphi_N)}(t,\omega)|=0$$

for almost all $\omega\in\Omega$, which means that

$$\liminf_{n\to\infty}\tau_n^{(N)}\ge\inf\{t\ge 0:|X^{(\varphi_N)}(t)|>N\}\wedge 2T\quad\text{a.s.}$$

As

$$\tau^{(N)}(\omega)\le\inf\{t\ge 0:|X^{(\varphi_N)}(t,\omega)|>N\}\wedge 2T\quad\text{a.s.},$$

we obtain

$$\liminf_{n\to\infty}\tau_n^{(N)}\ge\tau^{(N)}\quad\text{a.s.} \tag{3.32}$$

By (3.31) and (3.32),

$$\limsup_{n\to\infty}\sup_{t\in[0,\tau^{(N)}(\omega)-T/2]}n^{\gamma-\epsilon}\,|X_n(t,\omega)-X(t,\omega)|\le\zeta_{\epsilon,2T}^{(N)}(\omega)$$

for almost all $\omega\in\Omega$.

Finally, we restrict ourselves to the sample paths with

$$\omega\in\Omega_{N,T}:=\{\omega\in\Omega\ :\ |X(t,\omega)|\le N,\quad t\in[0,2T]\}$$

for appropriate N and T. Then, for such ω, the numerical scheme converges pathwise with order $(\gamma-\epsilon)$ to the solution of the original SODE on the interval $[0,T]$. □

Remark 1. *Note that under the standard assumptions the Euler-Maruyama scheme for additive noise has, in fact, strong order* 1.0 *and hence order* $(1-\epsilon)$ *pathwise convergence. If the* Y *process above can be approximated to strong order* 1.0 *(e.g., through the Milstein scheme), then the Euler-Maruyama scheme for the* X*-component above will have strong order* 1.0 *and hence converge pathwise with order* $(1-\epsilon)$.

3.2 Linear multi-step methods

3.2.1 Derivation of linear multi-step methods

For simplicity, set $d_1 = d_2 = 1$ and $m = 1$ and the equidistant step size Δ_t is assumed on the given time interval in what follows. In addition, it is assumed initially that the stochastic process $Y(t)$ can be generated exactly and its value at t_n is given by $Y(t_n)$. Consider the coupled RODE-SODE in $\mathbb{R}^2$:

$$d\mathbf{X}(t) = \mathbf{F}(\mathbf{X}(t))\,dt + \mathbf{G}(\mathbf{X}(t))\,dW(t), \tag{3.33}$$

with

$$\mathbf{X} = \begin{pmatrix} x \\ y \end{pmatrix}, \quad \mathbf{F}(\mathbf{X}) = \begin{pmatrix} f(x,y) \\ a(y) \end{pmatrix}, \quad \mathbf{G}(\mathbf{X}) = \begin{pmatrix} 0 \\ b(y) \end{pmatrix}.$$

An Euler-Maruyama type linear s-step method for (3.33) is given by

$$\sum_{j=0}^{s} \alpha_j \mathbf{X}_{n-j} = \Delta_t \sum_{j=0}^{s} \beta_j \mathbf{F}(\mathbf{X}_{n-j}) + \sum_{j=1}^{s} \gamma_j \mathbf{G}(\mathbf{X}_{n-j}) I_{(1),t_{n-j}},$$

where $\mathbf{X}_{n-j}$ is an approximated value at t_{n-j}. Since $\mathbf{G}^1 \equiv 0$ its X-component reduces to

$$\sum_{j=0}^{s} \alpha_j X_{n-j} = \Delta_t \sum_{j=0}^{s} \beta_j f(X_{n-j}, Y(t_{n-j})). \tag{3.34}$$

The local error of (3.34) will now be analyzed in order to develop higher order schemes. When $s = 2$, the local error L_n of (3.34) is given by

$$L_n := \left| \sum_{j=0}^{2} \alpha_j X(t_{n-j}) - \Delta_t \sum_{j=0}^{2} \beta_j f(X(t_{n-j}), Y(t_{n-j})) \right|. \tag{3.35}$$

The hierarchical and remainder sets for $\gamma = 1$ are $\Lambda_1^0 = \{\emptyset, (0)\}$ and $\mathcal{B}(\Lambda_1^0) = \{(1), (0,0), (1,0)\}$. The corresponding stochastic Itô-Taylor expansions are

$$X(t_n) = X(t_{n-1}) + f(X(t_{n-1}), Y(t_{n-1})) I_{(0),t_{n-1}} + \sum_{\alpha \in \mathcal{B}(\Lambda_1^0)} I_{\alpha,t_{n-1}}[L^\alpha id_{\mathbf{X}}^1]$$

$$X(t_{n-1}) = X(t_{n-2}) + f(X(t_{n-2}), Y(t_{n-2})) I_{(0),t_{n-2}} + \sum_{\alpha \in \mathcal{B}(\Lambda_1^0)} I_{\alpha,t_{n-2}}[L^\alpha id_{\mathbf{X}}^1].$$

Since the f terms in the local error are already multiplied by Δ_t, they need only be expanded to a lower order, i.e., for the hierarchical and remainder sets $\Lambda_0 = \{\emptyset\}$ and $\mathcal{B}(\Lambda_0) = \{(0), (1)\}$, so

$$f(X(t_n), Y(t_n)) = f(X(t_{n-1}), Y(t_{n-1})) + \sum_{\alpha \in \mathcal{B}(\Lambda_0)} I_{\alpha,t_{n-1}}[L^\alpha f]$$

$$f(X(t_{n-1}), Y(t_{n-1})) = f(X(t_{n-2}), Y(t_{n-2})) + \sum_{\alpha \in \mathcal{B}(\Lambda_0)} I_{\alpha,t_{n-2}}[L^\alpha f].$$

In order to simplify the notation in later expressions, this is the same as

$$\begin{aligned} f(X(t_n),Y(t_n)) &= f(X(t_{n-1}),Y(t_{n-1})) + \sum_{\alpha\in\mathcal{B}(\Lambda_1^0)} I_{\alpha_{[1]},t_{n-1}}[L^\alpha id_{\mathbf{X}}^1] \\ f(X(t_{n-1}),Y(t_{n-1})) &= f(X(t_{n-2}),Y(t_{n-2})) + \sum_{\alpha\in\mathcal{B}(\Lambda_1^0)} I_{\alpha_{[1]},t_{n-2}}[L^\alpha id_{\mathbf{X}}^1], \end{aligned}$$

where $\alpha_{[1]}$ is the first component of α, since the $L^1 id_{\mathbf{X}}^1$ is zero, so the term for $\alpha = (1)$ vanishes.

Substitution of $X(t_n)$, $X(t_{n-1})$, $f(X(t_n),Y(t_n))$ and $f(X(t_{n-1}),Y(t_{n-1}))$ in (3.35) gives

$$\begin{aligned} L_n &= |(\alpha_0+\alpha_1+\alpha_2)X(t_{n-2}) \\ &\quad + (2\alpha_0+\alpha_1-(\beta_0+\beta_1+\beta_2))\,\Delta_t f(X(t_{n-2}),Y(t_{n-2})) + R_1|, \end{aligned}$$

where the remainder term R_1 is

$$\begin{aligned} R_1 &= \sum_{\alpha\in\mathcal{B}(\Lambda_1^0)} \Big(\alpha_0 \hat{I}_{\alpha,t_{n-2}}^{t_n}[L^\alpha id_{\mathbf{X}}^1] + \alpha_1 I_{\alpha,t_{n-2}}[L^\alpha id_{\mathbf{X}}^1] \\ &\qquad -\Delta_t(\beta_0 \hat{I}_{\alpha_{[1]},t_{n-2}}^{t_n}[L^\alpha id_{\mathbf{X}}^1] + \beta_1 I_{\alpha_{[1]},t_{n-2}}[L^\alpha id_{\mathbf{X}}^1])\Big), \end{aligned}$$

where $\hat{I}_{\alpha,t_{n-2}}^{t_n}$ is a combination of stochastic integrals given in section 2.4. When

$$\alpha_0+\alpha_1+\alpha_2 = 0, \quad 2\alpha_0+\alpha_1-(\beta_0+\beta_1+\beta_2) = 0, \tag{3.36}$$

the local error $L_n \le C\Delta_t^{3/2}$ for some constant $C > 0$ and the SLMMs (3.34) with the consistency conditions (3.36) satisfy 1.0-order convergence. Typical examples are the Adams-Bashforth scheme:

$$X_n = X_{n-1} + \frac{1}{2}(3f_{n-1} - f_{n-2})\Delta_t, \tag{3.37}$$

and Adams-Moulton scheme:

$$X_n = X_{n-1} + \frac{1}{12}(5f_n + 8f_{n-1} - f_{n-2})\Delta_t, \tag{3.38}$$

which satisfy 1.0-order convergence and coincide with their deterministic counterparts (2.12) and (2.13).

Order 1.5 scheme

In order to achieve the same order as the 1.5-order strong Itô-Taylor scheme, one has to deal with the remainder term R_1. In this case $\mathcal{B}(\Lambda_1^0) \setminus \{(1)\} = \{(1,0),(0,0)\}$ and $L^1 f$ and $L^0 f$ terms appear in R_1.

Consider the SLMMs in the following form:

$$\begin{aligned}\sum_{j=0}^{2}\alpha_j X_{n-j} &= \Delta_t\sum_{j=0}^{2}\beta_j f(X_{n-j},Y(t_{n-j})) \\ &+\sum_{j=1}^{2}L^1 f(X_{n-j},Y(t_{n-j}))\left(\gamma_j I_{(1,0),t_{n-j}}+\gamma_j^* I_{(1),t_{n-j}}\Delta_t\right) \\ &+\sum_{j=1}^{2}L^0 f(X_{n-j},Y(t_{n-j}))\left(\delta_j I_{(0,0),t_{n-j}}+\delta_j^* I_{(0),t_{n-j}}\Delta_t\right).\end{aligned} \tag{3.39}$$

Then, the local error L_n of (3.39) is given by

$$\begin{aligned}L_n &:= \Big|\sum_{j=0}^{2}\alpha_j X(t_{n-j})-\Delta_t\sum_{j=0}^{2}\beta_j f(X(t_{n-j}),Y(t_{n-j})) \\ &-\sum_{j=1}^{2}L^1 f(X(t_{n-j}),Y(t_{n-j}))\left(\gamma_j I_{(1,0),t_{n-j}}+\gamma_j^* I_{(1),t_{n-j}}\Delta_t\right) \\ &-\sum_{j=1}^{2}L^0 f(X(t_{n-j}),Y(t_{n-j}))\left(\delta_j I_{(0,0),t_{n-j}}+\delta_j^* I_{(0),t_{n-j}}\Delta_t\right)\Big|.\end{aligned} \tag{3.40}$$

The hierarchical set for $\gamma = 1.5$ is now given by $\Lambda_{3/2}^0 = \{\emptyset,(0),(1,0),(0,0)\}$ and the corresponding stochastic Itô-Taylor expansions are

$$X(t_n) = \sum_{\alpha\in\Lambda_{3/2}^0} L^\alpha id_{\mathbf{X}}^1(X(t_{n-1}),Y(t_{n-1}))I_{\alpha,t_{n-1}}] + \sum_{\alpha\in\mathcal{B}(\Lambda_{3/2}^0)\setminus\{(1)\}} I_{\alpha,t_{n-1}}[L^\alpha id_{\mathbf{X}}^1]$$

$$X(t_{n-1}) = \sum_{\alpha\in\Lambda_{3/2}^0} L^\alpha id_{\mathbf{X}}^1(X(t_{n-2}),Y(t_{n-2}))I_{\alpha,t_{n-2}} + \sum_{\alpha\in\mathcal{B}(\Lambda_{3/2}^0)\setminus\{(1)\}} I_{\alpha,t_{n-2}}[L^\alpha id_{\mathbf{X}}^1]$$

and with $\Lambda_{1/2} = \{\emptyset,(0),(1)\}$, so $\mathcal{B}\left(\Lambda_{1/2}\right) = \{(0,0),(1,0),(0,1),(1,1)\}$,

$$\begin{aligned}f(X(t_n),Y(t_n)) &= f(X(t_{n-1}),Y(t_{n-1}))+L^1 f(X(t_{n-1}),Y(t_{n-1}))I_{(1),t_{n-1}} \\ &+L^0 f(X(t_{n-1}),Y(t_{n-1}))I_{(0),t_{n-1}}+\sum_{\alpha\in\mathcal{B}(\Lambda_{1/2})} I_{\alpha,t_{n-1}}[L^\alpha f]\end{aligned}$$

$$\begin{aligned}&f(X(t_{n-1}),Y(t_{n-1})) \\ &\quad= f(X(t_{n-2}),Y(t_{n-2}))+L^1 f(X(t_{n-2}),Y(t_{n-2}))I_{(1),t_{n-2}} \\ &\qquad+L^0 f(X(t_{n-2}),Y(t_{n-2}))I_{(0),t_{n-2}}+\sum_{\alpha\in\mathcal{B}(\Lambda_{1/2})} I_{\alpha,t_{n-2}}[L^\alpha f]\end{aligned}$$

as well as

$$\begin{aligned} L^1 f(X(t_{n-1}), Y(t_{n-1})) &= L^1 f(X(t_{n-2}), Y(t_{n-2})) \\ &\quad + I_{(1),t_{n-2}}[L^1 L^1 f] + I_{(0),t_{n-2}}[L^0 L^1 f] \\ L^0 f(X(t_{n-1}), Y(t_{n-1})) &= L^0 f(X(t_{n-2}), Y(t_{n-2})) \\ &\quad + I_{(1),t_{n-2}}[L^1 L^0 f] + I_{(0),t_{n-2}}[L^0 L^0 f]. \end{aligned}$$

The expansions $X(t_n)$, $X(t_{n-1})$, $f(X(t_n), Y(t_n))$, $f(X(t_{n-1}), Y(t_{n-1}))$, $L^1 f(X(t_{n-1}), Y(t_{n-1}))$ and $L^0 f(X(t_{n-1}), Y(t_{n-1}))$ in (3.40) are replaced by these expansions. The local error is

$$\begin{aligned} L_n &= \Big| (\alpha_0 + \alpha_1 + \alpha_2) X(t_{n-2}) \\ &\quad + (2\alpha_0 + \alpha_1 - (\beta_0 + \beta_1 + \beta_2))\, \Delta_t f(X(t_{n-2}), Y(t_{n-2})) \\ &\quad + \Big(\alpha_0 \hat{I}^{t_n}_{(1,0),t_{n-2}} + \alpha_1 I_{(1,0),t_{n-2}} - \beta_0 \hat{I}^{t_n}_{(1),t_{n-2}} \Delta_t - \beta_1 I_{(1),t_{n-2}} \Delta_t - \gamma_1 I_{(1,0),t_{n-1}} \\ &\qquad - \gamma_2 I_{(1,0),t_{n-2}} - \gamma_1^* I_{(1),t_{n-1}} \Delta_t - \gamma_2^* I_{(1),t_{n-2}} \Delta_t \Big) L^1 f(X(t_{n-2}), Y(t_{n-2})) \\ &\quad + \Big(\alpha_0 \hat{I}^{t_n}_{(0,0),t_{n-2}} + \alpha_1 I_{(0,0),t_{n-2}} - \beta_0 \hat{I}^{t_n}_{(0),t_{n-2}} \Delta_t - \beta_1 I_{(0),t_{n-2}} \Delta_t - \delta_1 I_{(0,0),t_{n-1}} \\ &\qquad - \delta_2 I_{(0,0),t_{n-2}} - \delta_1^* I_{(0),t_{n-1}} \Delta_t - \delta_2^* I_{(0),t_{n-2}} \Delta_t \Big) L^0 f(X(t_{n-2}), Y(t_{n-2})) \\ &\quad + R_{1.5} \Big|. \end{aligned}$$

The remainder term $R_{1.5}$ can be written as

$$\begin{aligned} R_{1.5} &= \sum_{\alpha \in \mathcal{B}(\Lambda^0_{3/2}) \setminus \{(1)\}} \Big\{ \alpha_0 \hat{I}^{t_n}_{\alpha,t_{n-2}}[L^\alpha id^1_{\mathbf{X}}] + \alpha_1 I_{\alpha,t_{n-2}}[L^\alpha id^1_{\mathbf{X}}] \\ &\qquad - \beta_0 \hat{I}^{t_n}_{\alpha_{[1,2]},t_{n-2}}[L^\alpha id^1_{\mathbf{X}}] \Delta_t - \beta_1 I_{\alpha_{[1,2]},t_{n-2}}[L^\alpha id^1_{\mathbf{X}}] \Delta_t \\ &\qquad - \gamma_1 I_{\alpha_{[1]},t_{n-2}}[L^\alpha id^1_{\mathbf{X}}] I_{\alpha_{[2,3]},t_{n-1}} - \gamma_1^* I_{\alpha_{[1]},t_{n-2}}[L^\alpha id^1_{\mathbf{X}}] I_{\alpha_{[2]},t_{n-1}} \Delta_t \\ &\qquad - \delta_1 I_{\alpha_{[1]},t_{n-2}}[L^\alpha id^1_{\mathbf{X}}] I_{\alpha_{[2,3]},t_{n-1}} - \delta_1^* I_{\alpha_{[1]},t_{n-2}}[L^\alpha id^1_{\mathbf{X}}] I_{\alpha_{[2]},t_{n-1}} \Delta_t \Big\}, \end{aligned}$$

where $\alpha_{[1,2]}$ consists of the first and second components of α and $\alpha_{[2,3]}$ are the second and third components of α, since

$$\mathcal{B}(\Lambda_{1/2}) = \Big\{ \alpha : (\alpha, 0) \in \mathcal{B}(\Lambda^0_{3/2}) \setminus \{(1)\} \Big\}$$

and $L^{(\alpha,0)} id^1_{\mathbf{X}} = L^\alpha L^0 id^1_{\mathbf{X}} = L^\alpha f$ while $L^1 id^1_{\mathbf{X}} = 0$. In addition, the terms γ_1 and γ_1^* appear when $\alpha = (1,1,0)$ or $(0,1,0)$ and δ_1 and δ_1^* when $\alpha = (1,0,0)$ or $(0,0,0)$.

The coefficients of $L^1 f(X(t_{n-2}), Y(t_{n-2}))$ can be transformed into

$$(\alpha_0+\alpha_1-\gamma_2)I_{(1,0),t_{n-2}}+(\alpha_0-\gamma_1)I_{(1,0),t_{n-1}} \\ +(\alpha_0-\beta_0-\beta_1-\gamma_2^*)I_{(1),t_{n-2}}\Delta_t-(\beta_0+\gamma_1^*)I_{(1),t_{n-1}}\Delta_t.$$

Similarly the coefficients of $L^0 f(X(t_{n-2}), Y(t_{n-2}))$ can be written as

$$(\alpha_0+\alpha_1-\delta_2)I_{(0,0),t_{n-2}}+(\alpha_0-\delta_1)I_{(0,0),t_{n-1}} \\ +(\alpha_0-\beta_0-\beta_1-\delta_2^*)I_{(0),t_{n-2}}\Delta_t-(\beta_0+\delta_1^*)I_{(0),t_{n-1}}\Delta_t.$$

If the following consistency conditions:

$$\begin{cases}\gamma_1=\delta_1=\alpha_0, \quad \gamma_2=\delta_2=\alpha_0+\alpha_1, \\ \gamma_1^*=\delta_1^*=-\beta_0, \quad \gamma_2^*=\delta_2^*=\alpha_0-\beta_0-\beta_1,\end{cases} \tag{3.41}$$

are satisfied, the SLMMs (3.39) satisfy 1.5-order convergence since both of the coefficients terms of $L^1 f(X(t_{n-2}), Y(t_{n-2}))$ and $L^0 f(X(t_{n-2}), Y(t_{n-2}))$ are 0.

Order 2.0 scheme

Similarly, $\Lambda_2^0=\{\emptyset,(0),(1,0),(0,0),(1,1,0)\}$ and a 2-step SLMM of 2.0-order is given by

$$\begin{aligned}\sum_{j=0}^{2}\alpha_j X_{n-j} &= \Delta_t\sum_{j=0}^{2}\beta_j f(X_{n-j},Y(t_{n-j})) \\ &+\sum_{j=1}^{2}L^1 f(X_{n-j},Y(t_{n-j}))\Big(\gamma_j I_{(1,0),t_{n-j}}+\gamma_j^* I_{(1),t_{n-j}}\Delta_t\Big) \\ &+\sum_{j=1}^{2}L^0 f(X_{n-j},Y(t_{n-j}))\Big(\delta_j I_{(0,0),t_{n-j}}+\delta_j^* I_{(0),t_{n-j}}\Delta_t\Big) \\ &+\sum_{j=1}^{2}L^1L^1 f(X_{n-j},Y(t_{n-j}))\Big(\epsilon_j I_{(1,1,0),t_{n-j}}+\epsilon_j^* I_{(1,1),t_{n-j}}\Delta_t\Big).\end{aligned} \tag{3.42}$$

It requires the additional consistency conditions:

$$\begin{cases}\epsilon_1=\alpha_0, \quad \epsilon_2=\alpha_0+\alpha_1, \\ \epsilon_1^*=-\beta_0, \quad \epsilon_2^*=\alpha_0-\beta_0-\beta_1.\end{cases} \tag{3.43}$$

3-step scheme

SLMMs with more steps can be generated in the same manner. Now we consider 3-step SLMMs in the following form:

$$\begin{aligned}\sum_{j=0}^{3}\alpha_j X_{n-j} &= \Delta_t\sum_{j=0}^{3}\beta_j f(X_{n-j},Y(t_{n-j})) \\ &\quad+\sum_{j=1}^{3}L^1f(X_{n-j},Y(t_{n-j}))\left(\gamma_j I_{(1,0),t_{n-j}}+\gamma_j^* I_{(1),t_{n-j}}\Delta_t\right) \\ &\quad+\sum_{j=1}^{3}L^0f(X_{n-j},Y(t_{n-j}))\left(\delta_j I_{(0,0),t_{n-j}}+\delta_j^* I_{(0),t_{n-j}}\Delta_t\right).\end{aligned} \tag{3.44}$$

Then the local error of (3.44) is given by

$$\begin{aligned}L_n &:= \Big|\sum_{j=0}^{3}\alpha_j X(t_{n-j})-\Delta_t\sum_{j=0}^{3}\beta_j f(X(t_{n-j}),Y(t_{n-j})) \\ &\quad-\sum_{j=1}^{3}L^1f(X(t_{n-j}),Y(t_{n-j}))\left(\gamma_j I_{(1,0),t_{n-j}}+\gamma_j^* I_{(1),t_{n-j}}\Delta_t\right) \\ &\quad-\sum_{j=1}^{3}L^0f(X(t_{n-j}),Y(t_{n-j}))\left(\delta_j I_{(0,0),t_{n-j}}+\delta_j^* I_{(0),t_{n-j}}\Delta_t\right)\Big|.\end{aligned} \tag{3.45}$$

The terms $X(t_n)$, $X(t_{n-1})$, $X(t_{n-2})$, $f(X(t_n),Y(t_n))$, $f(X(t_{n-1}),Y(t_{n-1}))$, $f(X(t_{n-2}),Y(t_{n-2}))$, $L^1f(X(t_{n-1}),Y(t_{n-1}))$, $L^1f(X(t_{n-2}),Y(t_{n-2}))$, $L^0f(X(t_{n-1}),Y(t_{n-1}))$ and $L^0f(X(t_{n-2}),Y(t_{n-2}))$ in (3.45) are replaced by the corresponding stochastic Itô-Taylor expansions. The local error is

$$\begin{aligned}L_n &= \Big|(\alpha_0+\alpha_1+\alpha_2+\alpha_3)X(t_{n-3}) \\ &\quad+(3\alpha_0+2\alpha_1+\alpha_2-(\beta_0+\beta_1+\beta_2+\beta_3))\,\Delta_t f(X(t_{n-3}),Y(t_{n-3})) \\ &\quad+\Big(\alpha_0\hat{I}^{t_n}_{(1,0),t_{n-3}}+\alpha_1\hat{I}^{t_{n-1}}_{(1,0),t_{n-3}}+\alpha_2 I_{(1,0),t_{n-3}} \\ &\qquad-\beta_0\hat{I}^{t_n}_{(1),t_{n-3}}\Delta_t-\beta_1\hat{I}^{t_{n-1}}_{(1),t_{n-3}}\Delta_t-\beta_2 I_{(1),t_{n-3}}\Delta_t \\ &\qquad-\gamma_1 I_{(1,0),t_{n-1}}-\gamma_2 I_{(1,0),t_{n-2}}-\gamma_3 I_{(1,0),t_{n-3}} \\ &\qquad-\gamma_1^* I_{(1),t_{n-1}}\Delta_t-\gamma_2^* I_{(1),t_{n-2}}\Delta_t-\gamma_3^* I_{(1),t_{n-3}}\Delta_t\Big)L^1f(X(t_{n-3}),Y(t_{n-3}))\end{aligned}$$

$$
\begin{aligned}
&+\Big(\alpha_0\hat{I}^{t_n}_{(0,0),t_{n-3}}+\alpha_1\hat{I}^{t_{n-1}}_{(0,0),t_{n-3}}+\alpha_2 I_{(0,0),t_{n-3}}\\
&\quad-\beta_0\hat{I}^{t_n}_{(0),t_{n-3}}\Delta_t-\beta_1\hat{I}^{t_{n-1}}_{(0),t_{n-3}}\Delta_t-\beta_2 I_{(0),t_{n-3}}\Delta_t\\
&\quad-\delta_1 I_{(0,0),t_{n-1}}-\delta_2 I_{(0,0),t_{n-2}}-\delta_3 I_{(0,0),t_{n-3}}\\
&\quad-\delta_1^* I_{(0),t_{n-1}}\Delta_t-\delta_2^* I_{(0),t_{n-2}}\Delta_t-\delta_3^* I_{(0),t_{n-3}}\Delta_t\Big)L^0 f(X(t_{n-3}),Y(t_{n-3}))\\
&\qquad\qquad+R_{1.5}\Big|.
\end{aligned}
$$

The remainder term $R_{1.5}$ here can be written as

$$
\begin{aligned}
R_{1.5}\;=\;&\sum_{\alpha\in\mathcal{B}(\Lambda^0_{3/2})\setminus\{(1)\}}\Big\{\alpha_0\hat{I}^{t_n}_{\alpha,t_{n-3}}[L^\alpha id^1_{\mathbf{X}}]+\alpha_1\hat{I}^{t_{n-1}}_{\alpha,t_{n-3}}[L^\alpha id^1_{\mathbf{X}}]+\alpha_2 I_{\alpha,t_{n-3}}[L^\alpha id^1_{\mathbf{X}}]\\
&\quad-\beta_0\hat{I}^{t_n}_{\alpha_{[1,2]},t_{n-3}}[L^\alpha id^1_{\mathbf{X}}]\Delta_t-\beta_1\hat{I}^{t_{n-1}}_{\alpha_{[1,2]},t_{n-3}}[L^\alpha id^1_{\mathbf{X}}]\Delta_t\\
&\qquad\qquad-\beta_2 I_{\alpha_{[1,2]},t_{n-3}}[L^\alpha id^1_{\mathbf{X}}]\Delta_t\\
&\quad-\gamma_1\hat{I}^{t_{n-1}}_{\alpha_{[1]},t_{n-3}}[L^\alpha id^1_{\mathbf{X}}]I_{\alpha_{[2,3]},t_{n-1}}-\gamma_2 I_{\alpha_{[1]},t_{n-3}}[L^\alpha id^1_{\mathbf{X}}]I_{\alpha_{[2,3]},t_{n-2}}\\
&\quad-\gamma_1^*\hat{I}^{t_{n-1}}_{\alpha_{[1]},t_{n-3}}[L^\alpha id^1_{\mathbf{X}}]I_{\alpha_{[2]},t_{n-1}}\Delta_t-\gamma_2^* I_{\alpha_{[1]},t_{n-3}}[L^\alpha id^1_{\mathbf{X}}]I_{\alpha_{[2]},t_{n-2}}\Delta_t\\
&\quad-\delta_1\hat{I}^{t_{n-1}}_{\alpha_{[1]},t_{n-3}}[L^\alpha id^1_{\mathbf{X}}]I_{\alpha_{[2,3]},t_{n-1}}-\delta_2 I_{\alpha_{[1]},t_{n-3}}[L^\alpha id^1_{\mathbf{X}}]I_{\alpha_{[2,3]},t_{n-2}}\\
&\quad-\delta_1^*\hat{I}^{t_{n-1}}_{\alpha_{[1]},t_{n-3}}[L^\alpha id^1_{\mathbf{X}}]I_{\alpha_{[2]},t_{n-1}}\Delta_t-\delta_2^* I_{\alpha_{[1]},t_{n-3}}[L^\alpha id^1_{\mathbf{X}}]I_{\alpha_{[2]},t_{n-2}}\Delta_t\Big\}.
\end{aligned}
$$

The coefficients of $L^1 f(X(t_{n-3}),Y(t_{n-3}))$ can be transformed into

$$
\begin{aligned}
&(\alpha_0+\alpha_1+\alpha_2-\gamma_3)I_{(1,0),t_{n-3}}+(\alpha_0+\alpha_1-\gamma_2)I_{(1,0),t_{n-2}}\\
&\quad+(\alpha_0-\gamma_1)I_{(1,0),t_{n-1}}+(2\alpha_0+\alpha_1-\beta_0-\beta_1-\beta_2-\gamma_3^*)I_{(1),t_{n-3}}\Delta_t\\
&\quad+(\alpha_0-\beta_0-\beta_1-\gamma_2^*)I_{(1),t_{n-2}}\Delta_t-(\beta_0+\gamma_1^*)I_{(1),t_{n-1}}\Delta_t.
\end{aligned}
$$

Similarly, the coefficient of $L^0 f(X(t_{n-3}),Y(t_{n-3}))$ can be written as

$$
\begin{aligned}
&(\alpha_0+\alpha_1+\alpha_2-\delta_3)I_{(0,0),t_{n-3}}+(\alpha_0+\alpha_1-\delta_2)I_{(0,0),t_{n-2}}\\
&\quad+(\alpha_0-\delta_1)I_{(0,0),t_{n-1}}+(2\alpha_0+\alpha_1-\beta_0-\beta_1-\beta_2-\delta_3^*)I_{(0),t_{n-3}}\Delta_t\\
&\quad+(\alpha_0-\beta_0-\beta_1-\delta_2^*)I_{(0),t_{n-2}}\Delta_t-(\beta_0+\delta_1^*)I_{(0),t_{n-1}}\Delta_t.
\end{aligned}
$$

If the following consistency conditions:

$$
\begin{cases}
\gamma_1=\delta_1=\alpha_0,\quad \gamma_2=\delta_2=\alpha_0+\alpha_1,\quad \gamma_3=\delta_3=\alpha_0+\alpha_1+\alpha_2\\
\gamma_1^*=\delta_1^*=-\beta_0,\quad \gamma_2^*=\delta_2^*=\alpha_0-\beta_0-\beta_1,\\
\gamma_3^*=\delta_3^*=2\alpha_0+\alpha_1-\beta_0-\beta_1-\beta_2,
\end{cases}
\tag{3.46}
$$

are satisfied, the SLMMs (3.44) satisfy 1.5-order convergence since the coefficient of $L^1 f(X(t_{n-3}), Y(t_{n-3}))$ and $L^0 f(X(t_{n-3}), Y(t_{n-3}))$ terms are both 0.

Similarly, $\Lambda_2^0 = \{\emptyset, (0), (1,0), (0,0), (1,1,0)\}$ and a 3-step SLMM of 2.0-order is given by

$$\begin{aligned}\sum_{j=0}^{3} \alpha_j X_{n-j} &= \Delta_t \sum_{j=0}^{3} \beta_j f(X_{n-j}, Y(t_{n-j})) \\ &+ \sum_{j=1}^{3} L^1 f(X_{n-j}, Y(t_{n-j})) \left(\gamma_j I_{(1,0),t_{n-j}} + \gamma_j^* I_{(1),t_{n-j}} \Delta_t\right) \\ &+ \sum_{j=1}^{3} L^0 f(X_{n-j}, Y(t_{n-j})) \left(\delta_j I_{(0,0),t_{n-j}} + \delta_j^* I_{(0),t_{n-j}} \Delta_t\right) \\ &+ \sum_{j=1}^{3} L^1 L^1 f(X_{n-j}, Y(t_{n-j})) \left(\epsilon_j I_{(1,1,0),t_{n-j}} + \epsilon_j^* I_{(1,1),t_{n-j}} \Delta_t\right),\end{aligned} \tag{3.47}$$

which requires the additional consistency conditions:

$$\begin{cases} \epsilon_1 = \alpha_0, \quad \epsilon_2 = \alpha_0 + \alpha_1, \quad \epsilon_3 = \alpha_0 + \alpha_1 + \alpha_2 \\ \epsilon_1^* = -\beta_0, \quad \epsilon_2^* = \alpha_0 - \beta_0 - \beta_1, \quad \epsilon_3^* = 2\alpha_0 + \alpha_1 - \beta_0 - \beta_1 - \beta_2. \end{cases} \tag{3.48}$$

General form

Higher order SLMMs or methods with more steps can be generated in the same manner. In general, the γ-order s-step SLMM, written with the help of the reduced hierarchical set Λ_γ^0, has the form:

$$\begin{aligned}\sum_{j=0}^{s} C_{\emptyset,j} X_{n-j} &= \Delta_t \sum_{j=0}^{s} C_{(0),j} f(X_{n-j}, \bar{Y}_{n-j}) \\ &+ \sum_{j=1}^{s} \sum_{\alpha \in \Lambda_\gamma^0 \setminus \{\emptyset,(0)\}} L^\alpha id_{\mathbf{X}}^1(X_{n-j}, \bar{Y}_{n-j}) \left(C_{\alpha,j} I_{\alpha,t_{n-j}} + C_{\alpha,j}^* I_{\alpha-,t_{n-j}} \Delta_t\right),\end{aligned} \tag{3.49}$$

where the consistency conditions are given as

$$\begin{cases} \sum_{j=0}^{s} C_{\emptyset,j} = 0, \qquad \sum_{j=0}^{s} (s-j) C_{\emptyset,j} = \sum_{j=0}^{s} C_{(0),j}, \\ C_{\alpha,i} = \sum_{j=0}^{i-1} C_{\emptyset,j} \quad \text{for} \quad i = 1, \ldots, s, \\ C_{\alpha,i}^* = \sum_{j=0}^{i-1} \left((i-1-j) C_{\emptyset,j} - C_{(0),j}\right) \quad \text{for} \quad i = 1, \ldots, s, \end{cases} \tag{3.50}$$

for $\alpha \in \Lambda_\gamma^0 \setminus \{\emptyset, (0)\}$. $\bar{Y}_{n-j}$ here is an approximation of $Y(t)$ at t_{n-j} by enough higher order schemes or $Y(t_{n-j})$ itself when $Y(t)$ can be generated exactly.

The method reduces to an explicit scheme when $C_{(0),0} = 0$ (by the order conditions this happens when, e.g., the $C^*_{\alpha,1} = 0$ for all $\alpha \in \Lambda^0_\gamma \backslash \{\emptyset, (0)\}$). Note that these methods now involve partial derivatives of the vector field function.

3.2.2 Pathwise convergence

The pathwise convergence result for X-component of the RODE-SODE pair also holds for the SLMMs derived in subsection 3.2.1. The SLMMs were derived assuming that the process $Y(t)$ can be generated exactly, however, the following theorem is shown also for Y_n, the approximated value by enough higher order schemes.

Theorem 6. (Pathwise convergence of SLMMs.)
Suppose that γ-order s-step SLMM (3.49) *is consistent and that the initial condition X_0 is given and the second initial conditions X_l for $l = 1, \ldots, s-1$ are provided by a 1-step scheme of the same order. In addition, it is supposed that the stochastic process $Y(t)$ can be generated exactly or obtained by γ'-order schemes.*
Then, under the standard assumptions, the approximation X_i converges pathwise with order $(\gamma - \epsilon)$ for all $\epsilon > 0$ and $\gamma' \geq \gamma - 1$, i.e.,

$$\sup_{i=0,\cdots,n} |X(t_i, \omega) - X_i(\omega)| \leq C^{(\gamma)}_\epsilon(\omega) \Delta_t^{\gamma-\epsilon}$$

for almost all $\omega \in \Omega$.

Proof. First of all, assume that the stochastic process $Y(t)$ can be generated exactly, i.e., $\bar{Y}_{n-j} = Y(t_{n-j})$. In addition, we denote $X(t_n) = X(t_n, \omega)$ and $X_n = X_n(\omega)$ in what follows.
The error of the γ-order s-step SLMM is given by

$$\begin{aligned} L_n &= |X(t_n) - X_n| \\ &= \Big| \sum_{j=0}^{s} C_{\emptyset,j} X(t_{n-j}) - \Delta_t \sum_{j=0}^{s} C_{(0),j} f(X(t_{n-j}), Y(t_{n-j})) \qquad (3.51) \\ &\quad - \sum_{j=1}^{s} \sum_{\alpha \in \Lambda^0_\gamma \backslash \{\emptyset,(0)\}} L^\alpha id^1_{\mathbf{X}}(X(t_{n-j}), Y(t_{n-j})) \left(C_{\alpha,j} I_{\alpha,t_{n-j}} + C^*_{\alpha,j} I_{\alpha-,t_{n-j}} \Delta_t \right) \Big|. \end{aligned}$$

Applying the Itô-Taylor expansions to $X(t_{n-j})$ and $f(X(t_{n-j}), Y(t_{n-j}))$ for $j = 0, \ldots, s-1$ and $L^\alpha id^1_{\mathbf{X}}(X(t_{n-j}), Y(t_{n-j}))$ for $j = 1, \ldots, s-1$ yields

$$
\begin{aligned}
L_n \;=\; & \Big| \sum_{j=0}^{s} C_{\emptyset,j} X(t_{n-s}) \\
& + \left(\sum_{j=0}^{s} (s-j) C_{\emptyset,j} - \sum_{j=0}^{s} C_{(0),j} \right) \Delta_t \, f(X(t_{n-s}), Y(t_{n-s})) \\
& \qquad \vdots \\
& + \left(\sum_{j=0}^{s-1} C_{\emptyset,j} \hat{I}^{t_{n-j}}_{\alpha,t_{n-s}} - \sum_{j=0}^{s-1} C_{(0),j} \hat{I}^{t_{n-j}}_{\alpha-,t_{n-s}} \Delta_t - \dots \right. \\
& \left. \cdots - \sum_{j=1}^{s} (C_{\alpha,j} I_{\alpha,t_{n-j}} + C^*_{\alpha,j} I_{\alpha-,t_{n-j}} \Delta_t) \right) L^{\alpha} id^1_{\mathbf{X}}(X(t_{n-s}), Y(t_{n-s})) \\
& \qquad\qquad + R \;\Big|,
\end{aligned}
$$

where the term R is

$$
\begin{aligned}
R \;=\; & \sum_{\alpha \in \mathcal{B}(\Lambda^0_\gamma) \setminus \{(1)\}} \left(\sum_{j=0}^{s-1} C_{\emptyset,j} \hat{I}^{t_{n-j}}_{\alpha,t_{n-s}} [L^{\alpha} id^1_{\mathbf{X}}] - \sum_{j=0}^{s-1} C_{(0),j} \hat{I}^{t_{n-j}}_{\alpha-,t_{n-s}} [L^{\alpha-} f] \Delta_t \right. \\
& \left. - \sum_{j=1}^{s-1} \sum_{\alpha' \in \Lambda^0_\gamma \setminus \{\emptyset,(0)\}} \hat{I}^{t_{n-j}}_{\alpha_{[1]},t_{n-s}} [L^{\alpha} id^1_{\mathbf{X}}] \left(C_{\alpha',j} I_{-\alpha,t_{n-j}} + C^*_{\alpha',j} I_{-\alpha-,t_{n-j}} \Delta_t \right) \right),
\end{aligned}
$$

where $-\alpha-$ is α without the first and the last element.

The consistency conditions are taken to satisfy, e.g.,

$$
\sum_{j=0}^{s} C_{\emptyset,j} = 0, \qquad \sum_{j=0}^{s} (s-j) C_{\emptyset,j} = \sum_{j=0}^{s} C_{(0),j},
$$

which correspond to the 1-order consistency conditions, and the coefficients of $X(t_{n-s})$, $f(X(t_{n-s}), Y(t_{n-s}))$, $\dots$ $L^{\alpha} id^1_{\mathbf{X}}(X(t_{n-s}), Y(t_{n-s}))$ are all 0. It means that the local error depends only on the remainder term R.

Define

$$
C_{L^{\alpha} id^1_{\mathbf{X}}} := \sup_{i=0,\dots,n} \left| L^{\alpha} id^1_{\mathbf{X}}(X(t_i), Y(t_i)) \right|.
$$

Then, the multiple stochastic integrals appearing in R can be evaluated as

$$
\begin{aligned}
\left| \hat{I}^{t_{n-i}}_{\alpha,t_{n-s}} [L^{\alpha} id^1_{\mathbf{X}}] \right| \;\le\; & C_{L^{\alpha} id^1_{\mathbf{X}}} \left| \hat{I}^{t_{n-i}}_{\alpha,t_{n-s}} \right| + \left| \hat{I}^{t_{n-i}}_{(0),t_{n-s}} [\hat{I}^{s_1}_{\alpha,t_{n-s}} [L^0 L^{\alpha} id^1_{\mathbf{X}}]] \right| \\
& + \left| \hat{I}^{t_{n-i}}_{(1),t_{n-s}} [\hat{I}^{s_1}_{\alpha,t_{n-s}} [L^1 L^{\alpha} id^1_{\mathbf{X}}]] \right|
\end{aligned}
$$

for $i = 0, \ldots, s-1$. $\alpha \in \mathcal{B}(\Lambda_\gamma^0)$ and $\hat{I}_{\alpha,t_{n-s}}^{t_{n-i}}$ is at least $\Delta_t^{\gamma+1/2}$ order. In addition,

$$\begin{aligned}\left|\hat{I}_{(0),t_{n-s}}^{t_{n-i}}[\hat{I}_{\alpha,t_{n-s}}^{s_1}[L^0L^\alpha id_{\mathbf{X}}^1]]\right| &\leq C_0\Delta_t^{\gamma+3/2}\\ \left|\hat{I}_{(1),t_{n-s}}^{t_{n-i}}[\hat{I}_{\alpha,t_{n-s}}^{s_1}[L^1L^\alpha id_{\mathbf{X}}^1]]\right| &\leq C_1\Delta_t^{\gamma+1},\end{aligned}$$

for some C_0, $C_1 \geq 0$. Hence,

$$\left|\hat{I}_{\alpha,t_{n-s}}^{t_{n-i}}[L^\alpha id_{\mathbf{X}}^1]\right| \leq C_{L^\alpha id_{\mathbf{X}}^1}\Delta_t^{\gamma+1/2}.$$

The other terms in R can be evaluated in the same manner and, for instance,

$$\begin{aligned}\left|\hat{I}_{\alpha-,t_{n-s}}^{t_{n-i}}[L^{\alpha-}f]\Delta_t\right| &\leq C_{L^\alpha id_{\mathbf{X}}^1}\left|\hat{I}_{\alpha-,t_{n-s}}^{t_{n-i}}\Delta_t\right| + \left|\hat{I}_{(0),t_{n-s}}^{t_{n-i}}[\hat{I}_{\alpha-,t_{n-s}}^{s_1}[L^0L^{\alpha-}f]]\Delta_t\right|\\ &\quad + \left|\hat{I}_{(1),t_{n-s}}^{t_{n-i}}[\hat{I}_{\alpha-,t_{n-s}}^{s_1}[L^1L^{\alpha-}f]]\Delta_t\right|\\ &\leq C_{L^\alpha id_{\mathbf{X}}^1}\Delta_t^{\gamma+1/2}.\end{aligned}$$

Now R can be estimated as

$$R \leq C_R C_{L^\alpha id_{\mathbf{X}}^1}\Delta_t^{\gamma+1/2},$$

for some $C_R > 0$. This leads

$$\sup_{i=0,\ldots,n}|X(t_i) - X_i| = \sup_{i=0,\ldots,n}|R| \leq CC_{L^\alpha id_{\mathbf{X}}^1}\Delta_t^{\gamma+1/2}, \tag{3.52}$$

where the constant C depends on the sample paths (and the time interval) under consideration.

Suppose now that the driving stochastic process $Y(t)$ is approximated by γ'-order scheme. Then the local error $\bar{L}_n$ is given by

$$\begin{aligned}\bar{L}_n &= \left|\sum_{j=0}^{s} C_{\emptyset,j}X(t_{n-j}) - \Delta_t\sum_{j=0}^{s} C_{(0),j}f(X(t_{n-j}),\bar{Y}_{n-j})\right. \qquad (3.53)\\ &\quad \left. -\sum_{j=1}^{s}\sum_{\alpha\in\Lambda_\gamma^0\setminus\{\emptyset,(0)\}} L^\alpha id_{\mathbf{X}}^1(X(t_{n-j}),\bar{Y}_{n-j})\left(C_{\alpha,j}I_{\alpha,t_{n-j}} + C_{\alpha,j}^*I_{\alpha-,t_{n-j}}\Delta_t\right)\right|.\end{aligned}$$

The value $\bar{Y}_{n-j}$ is obtained by γ'-order scheme and

$$|Y(t_{n-j}) - \bar{Y}_{n-j}| \leq \bar{C}\Delta_t^{\gamma'+1/2},$$

for some constant $\bar{C} > 0$. Choose the constant $\bar{C} = \bar{C}_{n-j}$ to satisfy

$$\bar{Y}_{n-j} = Y(t_{n-j}) + \bar{C}_{n-j}\Delta_t^{\gamma'+1/2}. \tag{3.54}$$

Replacing $\bar{Y}_{n-j}$ in (3.53) by (3.54) gives

$$\begin{aligned}\bar{L}_n = \Bigg| & \sum_{j=0}^{s} C_{\emptyset,j} X(t_{n-j}) - \Delta_t \sum_{j=0}^{s} C_{(0),j} f\left(X(t_{n-j}), Y(t_{n-j}) + \bar{C}_{n-j}\Delta_t^{\gamma'+1/2}\right) \\ & - \sum_{j=1}^{s} \sum_{\alpha \in \Lambda_\gamma^0 \setminus \{\emptyset,(0)\}} L^\alpha id_{\mathbf{X}}^1 \left(X(t_{n-j}), Y(t_{n-j}) + \bar{C}_{n-j}\Delta_t^{\gamma'+1/2}\right) \\ & \qquad \left(C_{\alpha,j} I_{\alpha,t_{n-j}} + C^*_{\alpha,j} I_{\alpha-,t_{n-j}} \Delta_t\right) \Bigg|.\end{aligned}$$

By the Lipschitz condition,

$$\begin{aligned}\left| L^\alpha id_{\mathbf{X}}^1 \left(X(t_{n-j}), Y(t_{n-j}) + \bar{C}_{n-j}\Delta_t^{\gamma'+1/2}\right) - L^\alpha id_{\mathbf{X}}^1 (X(t_{n-j}), Y(t_{n-j}))\right| \\ \leq K \bar{C}_{n-j} \Delta_t^{\gamma'+1/2},\end{aligned}$$

for some $K > 0$. Choose $K = K_{\alpha,n-j}$ to satisfy

$$\begin{aligned}L^\alpha id_{\mathbf{X}}^1 \left(X(t_{n-j}), Y(t_{n-j}) + \bar{C}_{n-j}\Delta_t^{\gamma'+1/2}\right) \\ = L^\alpha id_{\mathbf{X}}^1 (X(t_{n-j}), Y(t_{n-j})) + K_{\alpha,n-j} \bar{C}_{n-j} \Delta_t^{\gamma'+1/2}.\end{aligned}$$

This leads the following estimate of $\bar{L}_n$:

$$\begin{aligned}\bar{L}_n \leq \Bigg| & \sum_{j=0}^{s} C_{\emptyset,j} X(t_{n-j}) - \Delta_t \sum_{j=0}^{s} C_{(0),j} f(X(t_{n-j}), Y(t_{n-j})) \\ & - \sum_{j=1}^{s} \sum_{\alpha \in \Lambda_\gamma^0 \setminus \{\emptyset,(0)\}} L^\alpha id_{\mathbf{X}}^1 (X(t_{n-j}), Y(t_{n-j})) \\ & \qquad \left(C_{\alpha,j} I_{\alpha,t_{n-j}} + C^*_{\alpha,j} I_{\alpha-,t_{n-j}} \Delta_t\right) \Bigg| + |\bar{R}|,\end{aligned} \tag{3.55}$$

where the term $\bar{R}$ is given by

$$\begin{aligned}\bar{R} = & \sum_{j=0}^{s} C_{(0),j} \Delta_t K_{(0),n-j} \bar{C}_{n-j} \Delta_t^{\gamma'+1/2} \\ & + \sum_{j=1}^{s} \sum_{\alpha \in \Lambda_\gamma^0 \setminus \{\emptyset,(0)\}} \left(C_{\alpha,j} I_{\alpha,t_{n-j}} + C^*_{\alpha,j} I_{\alpha-,t_{n-j}} \Delta_t\right) K_{\alpha,n-j} \bar{C}_{n-j} \Delta_t^{\gamma'+1/2}.\end{aligned}$$

The first term of the right hand side of (3.55) is the same with L_n and it can be evaluated as (3.52). If $\bar{R}$ is $\Delta_t^{\gamma+1/2}$-order, $\bar{L}_n$ is also the same order. Obviously $(\gamma' + 3/2)$ is the lowest power with respect to Δ_t in $\bar{R}$ and

$$\gamma' + \frac{3}{2} \geq \gamma + \frac{1}{2},$$

i.e., $\gamma' \geq \gamma - 1$, so

$$\bar{L}_n \leq (CC_{L^\alpha id^1_{\mathbf{X}}} + C_{\bar{R}})\Delta_t^{\gamma+1/2},$$

for $\gamma' \geq \gamma - 1$ and some constant $C_{\bar{R}} > 0$. This means that the inequality (3.52) holds also for $\bar{Y}_{n-j}$ obtained by $\gamma' \geq \gamma - 1$ order schemes.

□

Chapter 4

RODEs with affine structure

In chapter 3, we investigate RODE with Itô diffusion and their numerical schemes are developed via RODE-SODE transformation. In this chapter, we include more general noise, but now RODEs with affine structure are considered.

A d-dimensional RODE with m-dimensional affine noise has the form:

$$\frac{dx}{dt} = f^0(t,x) + \sum_{j=1}^{m} f^j(t,x)\,\zeta_t^j, \tag{4.1}$$

where $x = (x^1, \ldots, x^d) \in \mathbb{R}^d$ and the noise process $\zeta_t = (\zeta_t^1, \ldots, \zeta_t^m)$ takes values in $\mathbb{R}^m$. The sample paths of ζ_t are assumed to be at least Lebesgue measurable and almost surely bounded, so the differential equation must be interpreted in the sense of Carathéodory. Typical noise processes are Wiener processes and fBms, which have Hölder continuous sample paths, and compound Poisson processes, which have piecewise constant sample paths.

Numerical schemes for RODEs with affine structure can be constructed with a similar approach that used by Grüne & Kloeden [37] to systematically derive higher order numerical schemes for deterministic affine control systems. These are based on stochastic Stratonovich-Taylor expansion and the hierarchical sets in section 2.4 and [66], which is possible since the chain rules of deterministic and Stratonovich calculi are analogous. After a brief introduction of affine-RODE-Taylor expansions in section 4.1, affine-RODE-Taylor schemes, derivative-free schemes and schemes for affine-RODEs with additive and commutative noises as well as LMMs are developed in sections 4.2 and 4.3, respectively.

4.1 Affine-RODE-Taylor expansions

The RODE (4.1) can be written equivalently in the integral form:

$$x(t) = x(t_0) + \int_{t_0}^{t} f^0(s, x(s))\, ds + \sum_{j=1}^{m} \int_{t_0}^{t} f^j(s, x(s))\, \zeta_s^j\, ds. \tag{4.2}$$

The chain rule:

$$U(t, x(t)) = U(t_0, x(t_0)) + \int_{t_0}^{t} L^0 U(s, x(s))\, ds + \sum_{j=1}^{m} \int_{t_0}^{t} L^j U(s, x(s))\, \zeta_s^j\, ds \tag{4.3}$$

for any continuously differentiable function $U : [t_0, T] \times \mathbb{R}^d \to \mathbb{R}$ can be applied to each function under integral in (4.2). The idea is similar to the derivation of Stratonovich-Taylor expansions that for Stratonovich SDEs in [66], which was later applied to deterministic affine-control systems in [37].

Here the partial differential operators L^0 and L^j are given by

$$L^0 = \frac{\partial}{\partial t} + \sum_{k=1}^{d} f^{0,k} \frac{\partial}{\partial x_k}, \qquad L^j = \sum_{k=1}^{d} f^{j,k} \frac{\partial}{\partial x_k}, \qquad j = 1, \ldots, m, \tag{4.4}$$

where $f^{j,k}$ is the k-th component of the vector valued function f^j for $k = 1$, $\ldots$, d and $j = 1$, $\ldots$, m.

Assume that the coefficients f^0 and f^j in (4.1) are sufficiently smooth real-valued functions. We apply the chain rule (4.3) to the functions $U = f^0$ and $U = f^j$ in (4.2), respectively.

$$\begin{aligned} x(t) \;=\; & x(t_0) + \int_{t_0}^{t} \Big(f^0(t_0, x(t_0)) + \int_{t_0}^{s} L^0 f^0(s_1, x(s_1))\, ds_1 \\ & \qquad + \sum_{j=1}^{m} \int_{t_0}^{s} L^j f^0(s_1, x(s_1))\, \zeta_{s_1}^j\, ds_1 \Big)\, ds \\ & + \sum_{j=1}^{m} \int_{t_0}^{t} \Big(f^j(t_0, x(t_0)) + \int_{t_0}^{s} L^0 f^j(s_1, x(s_1))\, ds_1 \\ & \qquad + \sum_{j_1=1}^{m} \int_{t_0}^{s} L^{j_1} f^j(s_1, x(s_1))\, \zeta_{s_1}^{j_1}\, ds_1 \Big)\, \zeta_s^j\, ds \end{aligned} \tag{4.5}$$

$$= x(t_0) + f^0(t_0, x(t_0)) \int_{t_0}^{t} ds + \sum_{j=1}^{m} f^j(t_0, x(t_0)) \int_{t_0}^{t} \zeta_s^j\, ds + R_1 \tag{4.6}$$

where R_1 is the remainder term given by

$$\begin{aligned} R_1 = & \int_{t_0}^{t}\int_{t_0}^{s_1} L^0 f^0(s_2, x(s_2))\, ds_2 ds_1 + \sum_{j=1}^{m}\int_{t_0}^{t}\int_{t_0}^{s_1} L^j f^0(s_2, x(s_2))\, \zeta_{s_2}^j\, ds_2 ds_1 \\ & + \sum_{j=1}^{m}\int_{t_0}^{t}\int_{t_0}^{s_1} L^0 f^j(s_2, x(s_2))\, \zeta_{s_1}^j\, ds_2 ds_1 \\ & + \sum_{j_1,j_2=1}^{m}\int_{t_0}^{t}\int_{t_0}^{s_1} L^{j_2} f^{j_1}(s_2, x(s_2))\, \zeta_{s_2}^{j_2}\zeta_{s_1}^{j_1}\, ds_2 ds_1. \end{aligned} \tag{4.7}$$

Applying the chain rule again to, e.g., $L^{j_2} f^{j_1}$ in R_1 yields

$$\begin{aligned} x(t) = & \; x(t_0) + f^0(t_0, x(t_0)) \int_{t_0}^{t} ds + \sum_{j=1}^{m} f^j(t_0, x(t_0)) \int_{t_0}^{t} \zeta_s^j\, ds \\ & + \sum_{j_1,j_2=1}^{m} L^{j_2} f^{j_1}(t_0, x(t_0)) \int_{t_0}^{t}\int_{t_0}^{s_1} \zeta_{s_2}^{j_2}\zeta_{s_1}^{j_1}\, ds_2 ds_1 + R_2, \end{aligned}$$

where the remainder term is now

$$\begin{aligned} R_2 = & \int_{t_0}^{t}\int_{t_0}^{s_1} L^0 f^0(s_2, x(s_2))\, ds_2 ds_1 + \sum_{j=1}^{m}\int_{t_0}^{t}\int_{t_0}^{s_1} L^j f^0(s_2, x(s_2))\, \zeta_{s_2}^j\, ds_2 ds_1 \\ & + \sum_{j=1}^{m}\int_{t_0}^{t}\int_{t_0}^{s_1} L^0 f^j(s_2, x(s_2))\, \zeta_{s_1}^j\, ds_2 ds_1 \\ & + \sum_{j_1,j_2=1}^{m}\int_{t_0}^{t}\int_{t_0}^{s_1} L^{j_2} f^{j_1}(s_2, x(s_2))\, \zeta_{s_2}^{j_2}\zeta_{s_1}^{j_1}\, ds_2 ds_1 \\ & + \sum_{j_1,j_2=1}^{m}\int_{t_0}^{t}\int_{t_0}^{s_1}\int_{t_0}^{s_2} L^0 L^{j_2} f^{j_1}(s_2, x(s_2))\, \zeta_{s_2}^{j_2}\zeta_{s_1}^{j_1}\, ds_3 ds_2 ds_1 \\ & + \sum_{j_1,j_2,j_3=1}^{m}\int_{t_0}^{t}\int_{t_0}^{s_1}\int_{t_0}^{s_2} L^{j_3} L^{j_2} f^{j_1}(s_3, x(s_3))\, \zeta_{s_3}^{j_3}\zeta_{s_2}^{j_2}\zeta_{s_1}^{j_1}\, ds_3 ds_2 ds_1. \end{aligned} \tag{4.8}$$

By iterating the same argument, affine-RODE-Taylor expansions of arbitrary higher order can be obtained. This is greatly facilitated by the notation of multi-indices and hierarchical sets.

Define a hierarchical set $\mathcal{A}_N$ and the remainder set $\mathcal{B}(\mathcal{A}_N)$ as

$$\begin{aligned} \mathcal{A}_N &:= \{\alpha \in \mathcal{M}_m \,:\, l(\alpha) \le N\}, \\ \mathcal{B}(\mathcal{A}_N) &:= \{\alpha \in \mathcal{M}_m \setminus \mathcal{A}_N \,:\, -\alpha \in \mathcal{A}_N\}, \end{aligned}$$

where

$$\mathcal{M}_m = \{\alpha = (j_1, \ldots, j_m) \in \{0, 1, 2, \ldots, m\}^l \,:\, l \in \mathbb{N}\} \cup \{\emptyset\}.$$

Now for the hierarchical set $\mathcal{A}_N$ with remainder set $\mathcal{B}(\mathcal{A}_N)$ and a sufficiently smooth function $F : [t_0, T] \times \mathbb{R}^d \to \mathbb{R}$, the $\mathcal{A}_N$-affine-RODE-Taylor expansion of $F(t, x(t))$ for a solution $x(t)$ of the RODE (4.1) is written compactly in the form

$$F(t, x(t)) = \sum_{\alpha \in \mathcal{A}_N} L^\alpha F(t_0, x(t_0)) I_{\alpha,t_0,t} + \sum_{\alpha \in \mathcal{B}(\mathcal{A}_N)} I_{\alpha,t_0,t}[L^\alpha F(\cdot, x(\cdot))], \quad (4.9)$$

where the coefficient functions F_α is given by

$$L^\alpha F := \begin{cases} F & : l = 0 \\ L^{j_1} L^{-\alpha} F & : l \geq 1, \end{cases}$$

with the differential operator L^{j_1} defined by (4.4). Moreover, the following theorem holds.

Theorem 7. (Affine-RODE-expansion.)
Let $F : \mathbb{R}^+ \times \mathbb{R}^d \to \mathbb{R}$ and let $\mathcal{A}_N \in \mathcal{M}_m$ be a hierarchical set with remainder set $\mathcal{B}(\mathcal{A}_N)$. Then the affine-RODE-Taylor expansion corresponding to the hierarchical set $\mathcal{A}_N$ given by (4.9) *holds, provided all of the derivatives of F, f^0, f^1, ..., f^m and all of the multiple integrals of stochastic processes appearing here exist.*

The proof follows that of the stochastic Itô-Taylor expansion for SODE [66] (Theorem 5.5.1).

Proof. The theorem is proved by mathematical induction.

For $N = 0$, the hierarchical set $\mathcal{A}_0 = \{\emptyset\}$ and the equation (4.9) is directly derived from the chain rule (4.3). In addition, the corresponding affine-RODE-Taylor expansion is given by (4.2).

Suppose that (4.9) holds for some k, i.e.,

$$F(t, x(t)) = \sum_{\alpha \in \mathcal{A}_k} L^\alpha F(t_0, x(t_0)) I_{\alpha,t_0,t} + \sum_{\alpha \in \mathcal{B}(\mathcal{A}_k)} I_{\alpha,t_0,t}[L^\alpha F(\cdot, x(\cdot))] \quad (4.10)$$

for the hierarchical set $\mathcal{A}_k = \{\alpha \in \mathcal{M}_m \ : \ l(\alpha) \leq k\}$. Applying the chain rule (4.3) to the second term on the right hand side of (4.10) yields

$$\begin{aligned} &\sum_{\alpha \in \mathcal{B}(\mathcal{A}_k)} I_{\alpha,t_0,t}[L^\alpha F(\cdot, x(\cdot))] \quad (4.11) \\ &\quad = \sum_{\alpha \in \mathcal{B}(\mathcal{A}_k)} L^\alpha F(t_0, x(t_0)) I_{\alpha,t_0,t} + \sum_{\alpha \in \mathcal{B}(\mathcal{B}(\mathcal{A}_k))} I_{\alpha,t_0,t}[L^\alpha F(\cdot, x(\cdot))] \\ &\quad = \sum_{\alpha \in \mathcal{A}_{k+1} \setminus \mathcal{A}_k} L^\alpha F(t_0, x(t_0)) I_{\alpha,t_0,t} + \sum_{\alpha \in \mathcal{B}(\mathcal{A}_{k+1})} I_{\alpha,t_0,t}[L^\alpha F(\cdot, x(\cdot))], \end{aligned}$$

since $\mathcal{B}(\mathcal{A}_k) = \mathcal{A}_{k+1} \setminus \mathcal{A}_k$ and $\mathcal{B}(\mathcal{B}(\mathcal{A}_k)) = \mathcal{B}(\mathcal{A}_{k+1} \setminus \mathcal{A}_k) = \mathcal{B}(\mathcal{A}_{k+1})$. Now substitute (4.11) in (4.10) and we have

$$F(t, x(t)) = \sum_{\alpha \in \mathcal{A}_{k+1}} L^\alpha F(t_0, x(t_0)) I_{\alpha,t_0,t} + \sum_{\alpha \in \mathcal{B}(\mathcal{A}_{k+1})} I_{\alpha,t_0,t}[L^\alpha F(\cdot, x(\cdot))].$$

This means that the equation (4.9) holds for $N = k + 1$ and the Theorem holds for all N. □

4.2 Taylor schemes

4.2.1 Derivation of affine-RODE-Taylor schemes

Affine-RODE-Taylor expansions (4.9) are used with the identity function $F(t, x) \equiv x$, i.e., $F = id$, to construct numerical schemes for RODEs with an affine structure such as (4.1). Thus, componentwise, $k = 1, \ldots, d$,

$$x^k(t) = \sum_{\alpha \in \mathcal{A}_N} L^\alpha id^k(t_0, x(t_0)) I_{\alpha,t_0,t} + \sum_{\alpha \in \mathcal{B}(\mathcal{A}_N)} I_{\alpha,t_0,t}[L^\alpha id^k(\cdot, x(\cdot))]. \tag{4.12}$$

Note that

$$L^0 id^k(t, x) = f^{0,k}(t, x), \qquad L^j id^k(t, x) = f^{j,k}(t, x),$$

for $j = 1, \ldots, m$, componentwise with $k = 1, \ldots, d$.

Higher order affine-RODE-Taylor schemes can be constructed systematically using the affine-RODE-Taylor expansions (4.12) on a finite subintervals $[t_{n-1}, t_n]$ of $[t_0, T]$, renaming and deleting the remainder term of the right hand side of the equation (4.12). In general, the k-th component of the affine-RODE-Taylor scheme of order N for (4.1) has a form:

$$X_n^k = X_{n-1}^k + \sum_{\alpha \in \mathcal{A}_N \setminus \{\emptyset\}} L^\alpha id^k(t_{n-1}, X_{n-1}) I_{\alpha,t_{n-1}}, \tag{4.13}$$

where X_n is an approximated value at t_n. This scheme is indeed of order N if the noise sample paths are continuous or essentially bounded on bounded time intervals.

Theorem 8. (Pathwise convergence.)
Suppose that noise sample paths are continuous or essentially bounded on bounded time intervals. Then, under the assumptions in Theorem 7, the affine-RODE-Taylor scheme (4.13) *has pathwise order of convergence N.*

Proof. The pathwise local discretization error of order N of the affine-RODE-Taylor scheme is given by

$$L_N := \left| \sum_{\alpha \in \mathcal{B}(\mathcal{A}_N)} I_{\alpha,t_{n-1}} \left[L^\alpha id^k(\cdot, x(\cdot, \omega)) \right] \right|.$$

Under the standard assumptions, the RODE (4.1) has a unique solution on a finite time interval $[t_0, T]$. Since the sample paths of its solution are continuous, there is a finite $R(T,\omega)$ such that $|x(t,\omega)| < R(T,\omega)$ for all $t \in [t_0, T]$.

Since the sample paths of the stochastic process ζ_t are assumed to be almost everywhere bounded,

$$C(\alpha, T, \omega) := \text{ess sup}_{t\in[t_0,T]}|\zeta_t^j(\omega)| < \infty,$$

so

$$|I_{\alpha,t_n}| \leq C(\alpha, T, \omega)^{l(\alpha)-n(\alpha)}\Delta_n^{l(\alpha)},$$

where $n(\alpha)$ is the number of zero elements in α, $l(\alpha)$ is the length of α and $\Delta_n = t_n - t_{n-1}$. Define

$$C_{L^\alpha id}(T,\omega) := \sup_{\substack{t\in[t_0,T]\\ |x(t,\omega)|<R(T,\omega)}} \left|L^\alpha id^k(t, x(t,\omega))\right| < \infty.$$

Then the pathwise local discretization error L_N can be estimated as

$$\begin{aligned} L_N &= \sum_{|\alpha|=N+1} \left|I_{\alpha,t_{n-1}}[L^\alpha id^k(\cdot, x(\cdot))]\right| \\ &\leq \sum_{|\alpha|=N+1} C_{L^\alpha id}(T,\omega)\left|I_{\alpha,t_{n-1}}\right| \\ &\leq \sum_{|\alpha|=N+1} C_{L^\alpha id}(T,\omega)C(\alpha,T,\omega)^{N+1-n(\alpha)}\Delta_n^{N+1}, \end{aligned}$$

since all $\alpha \in \mathcal{B}(\mathcal{A}_N)$ have length $l(\alpha) = N+1$. Obviously $L_N \sim \mathcal{O}\left(\Delta_n^{N+1}\right)$, which means that the affine-RODE-Taylor scheme (4.13) has global order of convergence N. □

The Euler approximation is the simplest affine-RODE-Taylor scheme and it has order $N = 1$ pathwise convergence. The corresponding hierarchical set $\mathcal{A}_1$ is $\{\emptyset, (0), (j)\}$ and its k-th component is given by

$$X_n^k = X_{n-1}^k + f^{0,k}(t_{n-1}, X_{n-1})\Delta_n + \sum_{j=1}^m f^{j,k}(t_{n-1}, X_{n-1})I_{(j),t_{n-1}}, \quad (4.14)$$

where

$$\Delta_n = I_{(0),t_{n-1}} = \int_{t_{n-1}}^{t_n} ds \quad \text{and} \quad I_{(j),t_{n-1}} = \int_{t_{n-1}}^{t_n} \zeta_s^j\, ds.$$

The 2-order affine-RODE-Taylor scheme has k-th component given by

$$\begin{aligned} X_n^k = {} & X_{n-1}^k + f^{0,k}(t_{n-1}, X_{n-1})\Delta_n + \sum_{j=1}^m f^{j,k}(t_{n-1}, X_{n-1})I_{(j),t_{n-1}} \quad (4.15)\\ & + \frac{1}{2}L^0 f^{0,k}(t_{n-1}, X_{n-1})\Delta_n^2 + \sum_{\substack{j_1,j_2=0\\ j_1+j_2\neq 0}}^m L^{j_1} f^{j_2,k}(t_{n-1}, X_{n-1})I_{(j_1,j_2),t_{n-1}}, \end{aligned}$$

while the 3-order affine-RODE-Taylor has k-th component given by

$$\begin{aligned} X_n^k &= X_{n-1}^k + f^{0,k}(t_{n-1}, X_{n-1})\Delta_n + \sum_{j=1}^{m} f^{j,k}(t_{n-1}, X_{n-1}) I_{(j),t_{n-1}} \\ &+ \frac{1}{2} L^0 f^{0,k}(t_{n-1}, X_{n-1})\Delta_n^2 + \sum_{\substack{j_1,j_2=0 \\ j_1+j_2\neq 0}}^{m} L^{j_1} f^{j_2,k}(t_{n-1}, X_{n-1}) I_{(j_1,j_2),t_{n-1}} \\ &+ \frac{1}{6} L^0 L^0 f^{0,k}(t_{n-1}, X_{n-1})\Delta_n^3 \\ &+ \sum_{\substack{j_1,j_2,j_3=0 \\ j_1+j_2+j_3\neq 0}}^{m} L^{j_1} L^{j_2} f^{j_3,k}(t_{n-1}, X_{n-1}) I_{(j_1,j_2,j_3),t_{n-1}}, \end{aligned} \tag{4.16}$$

since

$$\begin{aligned} I_{(0,0),t_{n-1}} &= \int_{t_{n-1}}^{t_n} \int_{t_{n-1}}^{s_1} ds_2 ds_1 = \frac{1}{2}\Delta_n^2, \\ I_{(0,0,0),t_{n-1}} &= \int_{t_{n-1}}^{t_n} \int_{t_{n-1}}^{s_1} \int_{t_{n-1}}^{s_2} ds_3 ds_2 ds_1 = \frac{1}{6}\Delta_n^3. \end{aligned}$$

4.2.2 Derivative-free schemes

The above affine-RODE-Taylor schemes involve partial derivatives of the coefficients functions, which may be inconvenient, especially in high dimensions. It is possible to derive derivative-free schemes from them as in section 3.1.3 and [7, 8, 37, 66] by approximating the partial derivatives by suitable finite difference quotients. To illustrate this, consider the scalar RODE with a single noise integral, i.e., $d = m = 1$, and the affine-RODE is given by

$$\frac{dx}{dt} = f^0(t,x) + f^1(t,x)\,\zeta_t^1,$$

for which the affine-RODE-Taylor scheme of order 2 is

$$\begin{aligned} X_n &= X_{n-1} + f^0(X_{n-1})\Delta_n + f^1(t_{n-1}, X_{n-1}) I_{(1),t_{n-1}} \\ &+ \frac{1}{2} L^0 f^0(t_{n-1}, X_{n-1})\Delta_n^2 + \sum_{\substack{j_1,j_2=0 \\ j_1+j_2\neq 0}}^{1} L^{j_1} f^{j_2}(t_{n-1}, X_{n-1}) I_{(j_1,j_2),t_{n-1}}. \end{aligned}$$

The Taylor approximation yields

$$\begin{aligned} L^{j_1} f^{j_2}(t,x) &= f^{j_1}(t,x)\frac{\partial f^{j_2}(t,x)}{\partial x} \\ &= \frac{1}{\Delta_n}\left(f^{j_2}(t, x + f^{j_1}(t,x)\Delta_n) - f^{j_2}(t,x)\right) + \mathcal{O}(\Delta_n), \end{aligned}$$

and the corresponding error introduced in the scheme has order Δ_n^3, which can be included in the local discretization error without reducing the convergence order of the scheme. This gives the 2-order derivative-free scheme:

$$\begin{aligned} X_n &= X_{n-1} + f^0(t_{n-1}, X_{n-1})\Delta_n + f^1(t_{n-1}, X_{n-1})I_{(1),t_{n-1}} \\ &\quad + \frac{1}{2}\left(f^0(t_{n-1}, X_{n-1} + f^0(t_{n-1}, X_{n-1})\Delta_n) - f^0(t_{n-1}, X_{n-1})\right)\Delta_n^2 \\ &\quad + \frac{1}{\Delta_n}\sum_{\substack{j_1,j_2=0 \\ j_1+j_2\neq 0}}^{1}\Big(f^{j_2}(t_{n-1}, X_{n-1} + f^{j_1}(t_{n-1}, X_{n-1})\Delta_n) \\ &\qquad\qquad - f^{j_2}(t_{n-1}, X_{n-1})\Big)I_{(j_1,j_2),t_{n-1}}. \end{aligned} \tag{4.17}$$

4.2.3 Affine-RODEs with special structure

Affine-RODE-Taylor schemes introduced above can be simplified when the coefficients in (4.13) have special structures such as additive noise or commutative noise.

Additive noise

The noise in a RODE is said to be *additive* when the noise coefficients f^1, f^2, ..., f^m are constants or functions of t only, so their derivatives in x are identically zero. Then, all of the "spatial" derivatives of these noise coefficients as well as corresponding higher order terms in the affine-RODE-Taylor schemes vanish. For example, the affine-RODE-Taylor scheme of order 2 (4.15) with additive noise reduces to

$$\begin{aligned} X_n^k &= X_{n-1}^k + f^{0,k}(t_{n-1}, X_{n-1})\Delta_n + \sum_{j=1}^{m} f^{j,k}(t_{n-1}, X_{n-1})I_{(j),t_{n-1}} \\ &\quad + \sum_{j=0}^{m} L^j f^{0,k}(t_{n-1}, X_{n-1})I_{(j,0),t_{n-1}}. \end{aligned}$$

Commutative noise

A noise process is said to be *commutative* if the drift and noise coefficients satisfy

$$L^i f^{j,k}(t,x) = L^j f^{i,k}(t,x) \quad \text{for all } i,j = 0,1,\ldots,m.$$

This then allows

$$\begin{aligned} &L^i f^{j,k}(t_{n-1}, x(t_{n-1}))I_{(i),t_{n-1}}I_{(j),t_{n-1}} \\ &\quad = L^i f^{j,k}(t_{n-1}, x(t_{n-1}))I_{(i,j),t_{n-1}} + L^j f^{i,k}(t_{n-1}, x(t_{n-1}))I_{(j,i),t_{n-1}} \end{aligned}$$

by the integration by parts, i.e.,

$$I_{(i),t_{n-1}} I_{(j),t_{n-1}} = I_{(i,j),t_{n-1}} + I_{(j,i),t_{n-1}} \quad \text{for } i,j = 0,1,\ldots,m.$$

This allows stochastic integrals with lower multiplicity to be used instead of higher ones. In fact, the order 2 affine-RODE-Taylor scheme (4.15) then reduces to

$$\begin{aligned} X_n^k &= X_{n-1}^k + f^{0,k}(t_{n-1},X_{n-1})\Delta_n + \sum_{j=1}^m f^{j,k}(t_{n-1},X_{n-1}) I_{(j),t_{n-1}} \\ &\quad + \frac{1}{2} L^0 f^{0,k}(t_{n-1},X_{n-1})\Delta_n^2 + \sum_{0\le i<j\le m} L^i f^{j,k}(t_{n-1},X_{n-1}) I_{(i),t_{n-1}} I_{(j),t_{n-1}}. \end{aligned}$$

It contains no multiple stochastic integrals.

4.3 Linear multi-step methods

LMMs were derived for RODEs driven by an Itô diffusion, i.e., solution of an Itô SODE, in section 3.2 and [9], using the stochastic Itô-Taylor expansions. Since the driving noise needs not be an Itô diffusion, a similar approach, but now using affine-RODE-Taylor approximations will be outlined here. The resulting multi-step methods are then, in particular, directly applicable to the affine-RODE (4.1). For notational simplicity, denote $I_{(j),t_n}[L^j f(\cdot,x(\cdot))]$ by $I_{(j),t_n}[L^j f]$ in this section. In addition, we assume the equidistant step size Δ_t in this section.

Euler-type s-step LMMs for the RODE (4.1) with m-dimensional affine noise have the general form, componentwise,

$$\sum_{l=0}^s \alpha_l X_{n-l}^k = \sum_{l=0}^s \beta_l f^{0,k}(t_{n-l},X_{n-l})\Delta_t + \sum_{l=1}^s \gamma_l \sum_{j=1}^m f^{j,k}(t_{n-l},X_{n-l}) I_{(j),t_{n-l}}, \tag{4.18}$$

for $k = 1, \ldots, d$. The coefficients in (4.18) need to satisfy certain consistency conditions for the LMMs (4.18) to have order 1. First of all, we derive the consistency conditions for the case $s = 2$.

The pathwise local discretization error L_n of the LMMs (4.18) is given by

$$\begin{aligned} L_n &:= \Big| \sum_{l=0}^2 \alpha_l x^k(t_{n-l}) - \sum_{l=0}^2 \beta_l f^{0,k}(t_{n-l},x(t_{n-l}))\Delta_t \\ &\qquad - \sum_{l=1}^2 \gamma_l \sum_{j=1}^m f^{j,k}(t_{n-l},x(t_{n-l})) I_{(j),t_{n-l}} \Big|. \end{aligned} \tag{4.19}$$

The affine-RODE-Taylor expansions:

$$\begin{aligned} x^k(t_n) &= x^k(t_{n-1}) + f^{0,k}(t_{n-1}, x(t_{n-1}))I_{(0),t_{n-1}} \\ &\quad + \sum_{j=1}^{m} f^{j,k}(t_{n-1}, x(t_{n-1}))I_{(j),t_{n-1}} + \sum_{j_1,j_2=0}^{m} I_{(j_1,j_2),t_{n-1}}[L^{j_1} f^{j_2,k}] \\ x^k(t_{n-1}) &= x^k(t_{n-2}) + f^{0,k}(t_{n-2}, x(t_{n-2}))I_{(0),t_{n-2}} \\ &\quad + \sum_{j=1}^{m} f^{j,k}(t_{n-2}, x(t_{n-2}))I_{(j),t_{n-2}} + \sum_{j_1,j_2=0}^{m} I_{(j_1,j_2),t_{n-2}}[L^{j_1} f^{j_2,k}] \end{aligned}$$

and classical chain rule expansions:

$$\begin{aligned} f^{0,k}(t_n, x(t_n)) &= f^{0,k}(t_{n-1}, x(t_{n-1})) + \sum_{j=0}^{m} I_{(j),t_{n-1}}[L^j f^{0,k}] \\ f^{0,k}(t_{n-1}, x(t_{n-1})) &= f^{0,k}(t_{n-2}, x(t_{n-2})) + \sum_{j=0}^{m} I_{(j),t_{n-2}}[L^j f^{0,k}] \\ f^{j,k}(t_{n-1}, x(t_{n-1})) &= f^{j,k}(t_{n-2}, x(t_{n-2})) + \sum_{j_1=0}^{m} I_{(j_1),t_{n-2}}[L^{j_1} f^{j,k}] \end{aligned}$$

are substituted into the local discretization error (4.19) to yield

$$\begin{aligned} L_n &= \Big| (\alpha_0 + \alpha_1 + \alpha_2) x^k(t_{n-2}) \\ &\quad + (2\alpha_0 + \alpha_1 - (\beta_0 + \beta_1 + \beta_2))\, f^{0,k}(t_{n-2}, x(t_{n-2}))\Delta_t \\ &\quad + \sum_{j=1}^{m} \Big(\alpha_0 I_{(j),t_{n-1}} + (\alpha_0 + \alpha_1) I_{(j),t_{n-2}} \\ &\qquad\qquad - \gamma_1 I_{(j),t_{n-1}} - \gamma_2 I_{(j),t_{n-2}} \Big) f^{j,k}(t_{n-2}, x(t_{n-2})) + R_1 \Big|, \end{aligned}$$

where R_1 is a remainder term given by

$$\begin{aligned} R_1 &= \sum_{j_1,j_2=0}^{m} \Big(\alpha_0 \hat{I}^{t_n}_{(j_1,j_2),t_{n-2}}[L^{j_1} f^{j_2,k}] + \alpha_1 I_{(j_1,j_2),t_{n-2}}[L^{j_1} f^{j_2,k}] \Big) \\ &\quad - \sum_{j=0}^{m} \Big(\beta_0 \hat{I}^{t_n}_{(j),t_{n-2}}[L^j f^{0,k}] + \beta_1 I_{(j),t_{n-2}}[L^j f^{0,k}] \Big) \Delta_t \\ &\quad - \sum_{j_1=0}^{m} \sum_{j_2=1}^{m} \gamma_1 I_{(j_1),t_{n-2}}[L^{j_1} f^{j_2,k}] I_{(j_2),t_{n-1}}. \end{aligned}$$

Now R_1 is Δ_t^2-order and when the coefficients of the LMMs (4.18) satisfy the following consistency conditions:

$$\begin{cases} \alpha_0 + \alpha_1 + \alpha_2 = 0 \\ \beta_0 + \beta_1 + \beta_2 = 2\alpha_0 + \alpha_1 \\ \gamma_1 = \alpha_0, \quad \gamma_2 = \alpha_0 + \alpha_1, \end{cases} \tag{4.20}$$

the LMMs (4.18) have 1.0-order convergence.

In order to construct higher order schemes, the integrands in the remainder term R_1 are expanded in the same manner. Its terms with constant coefficients are now included in the numerical scheme and a new remainder term R_2 with threefold noise integrals is obtained. The corresponding LMMs, which now contain terms with the derivatives $L^0 f^{0,k}$, $L^j f^{0,k}$, $L^0 f^{j,k}$ and $L^{j_1} f^{j_2,k}$, have the form, componentwise,

$$\begin{aligned} \sum_{l=0}^{2} \alpha_l X_{n-l}^k &= \sum_{l=0}^{2} \beta_l f^{0,k}(t_{n-l}, X_{n-l})\Delta_t + \sum_{l=1}^{2} \gamma_l \sum_{j=1}^{m} f^{j,k}(t_{n-l}, X_{n-l}) I_{(j),t_{n-l}} \\ &\quad + \sum_{l=1}^{2} \delta_l \sum_{j=0}^{m} L^j f^{0,k}(t_{n-l}, X_{n-l}) I_{(j),t_{n-l}} \Delta_t \\ &\quad + \sum_{l=1}^{2} \epsilon_l \sum_{j_1,j_2=0}^{m} L^{j_1} f^{j_2,k}(t_{n-l}, X_{n-l}) I_{(j_1,j_2),t_{n-l}}, \end{aligned} \tag{4.21}$$

for $k = 1, \ldots, d$. The corresponding local discretization error is given by

$$\begin{aligned} L_n := \Big| &\sum_{l=0}^{2} \alpha_l x^k(t_{n-l}) - \sum_{l=0}^{2} \beta_l f^{0,k}(t_{n-l}, x(t_{n-l}))\Delta_t \\ &- \sum_{l=1}^{2} \gamma_l \sum_{j=1}^{m} f^{j,k}(t_{n-l}, x(t_{n-l})) I_{(j),t_{n-l}} \\ &- \sum_{l=1}^{2} \delta_l \sum_{j=0}^{m} L^j f^{0,k}(t_{n-l}, x(t_{n-l})) I_{(j),t_{n-l}} \Delta_t \\ &- \sum_{l=1}^{2} \epsilon_l \sum_{j_1,j_2=0}^{m} L^{j_1} f^{j_2,k}(t_{n-l}, x(t_{n-l})) I_{(j_1,j_2),t_{n-l}} \Big|, \end{aligned}$$

and this reduces to

$$
\begin{aligned}
L_n = \Big| & \sum_{j_1,j_2=0}^{m} \Big(\alpha_0 \hat{I}^{t_n}_{(j_1,j_2),t_{n-2}}[L^{j_1} f^{j_2,k}] + \alpha_1 I_{(j_1,j_2),t_{n-2}}[L^{j_1} f^{j_2,k}]\Big) \\
& - \sum_{j=0}^{m} \Big(\beta_0 \hat{I}^{t_n}_{(j),t_{n-2}}[L^{j} f^{0,k}] + \beta_1 I_{(j),t_{n-2}}[L^{j} f^{0,k}]\Big) \Delta_t \\
& - \sum_{j_1=0}^{m} \sum_{j_2=1}^{m} \gamma_1 I_{(j_1),t_{n-2}}[L^{j_1} f^{j_2,k}] I_{(j_2),t_{n-1}} \qquad (4.22) \\
& - \sum_{l=1}^{2} \delta_l \sum_{j=0}^{m} L^j f^{0,k}(t_{n-l}, x(t_{n-l})) I_{(j),t_{n-l}} \Delta_t \\
& - \sum_{l=1}^{2} \epsilon_l \sum_{j_1,j_2=0}^{m} L^{j_1} f^{j_2,k}(t_{n-l}, x(t_{n-l})) I_{(j_1,j_2),t_{n-l}} \Big|
\end{aligned}
$$

from the consistency conditions of order 1. Applying Taylor expansions and chain rules yields

$$
\begin{aligned}
L_n = \Big| & \sum_{j_1,j_2=0}^{m} \Big(\alpha_0 \hat{I}^{t_n}_{(j_1,j_2),t_{n-2}} + \alpha_1 I_{(j_1,j_2),t_{n-2}}\Big) L^{j_1} f^{j_2,k}(t_{n-2}, x(t_{n-2})) \\
& - \sum_{j=0}^{m} \Big(\beta_0 \hat{I}^{t_n}_{(j),t_{n-2}} + \beta_1\Big) \Delta_t L^{j} f^{0,k}(t_{n-2}, x(t_{n-2})) \\
& - \sum_{j_1=0}^{m} \sum_{j_2=1}^{m} \gamma_1 I_{(j_1),t_{n-2}} I_{(j_2),t_{n-1}} L^{j_1} f^{j_2,k}(t_{n-2}, x(t_{n-2})) \\
& - \sum_{j=0}^{m} (\delta_1 I_{(j),t_{n-1}} + \delta_2 I_{(j),t_{n-2}}) \Delta_t L^{j} f^{0,k}(t_{n-2}, x(t_{n-2})) \\
& - \sum_{j_1,j_2=0}^{m} (\epsilon_1 I_{(j_1,j_2),t_{n-1}} + \epsilon_2 I_{(j_1,j_2),t_{n-2}}) L^{j_1} f^{j_2,k}(t_{n-2}, x(t_{n-2})) + R_2 \Big|,
\end{aligned}
$$

where R_2 is the remainder term given by

$$
\begin{aligned}
R_2 = & \sum_{j_1,j_2,j_3=0}^{m} \Big(\alpha_0 \hat{I}^{t_n}_{(j_1,j_2,j_3),t_{n-2}}[L^{j_1} L^{j_2} f^{j_3,k}] + \alpha_1 I_{(j_1,j_2,j_3),t_{n-2}}[L^{j_1} L^{j_2} f^{j_3,k}]\Big) \\
& - \sum_{j_1,j_2=0}^{m} \Big(\beta_0 \hat{I}^{t_n}_{(j_1,j_2),t_{n-2}}[L^{j_1} L^{j_2} f^{0,k}] + \beta_1 I_{(j_1,j_2),t_{n-2}}[L^{j_1} L^{j_2} f^{0,k}]\Big) \Delta_t
\end{aligned}
$$

$$- \sum_{j_1,j_2=0}^{m} \sum_{j_3=1}^{m} \gamma_1 I_{(j_1,j_2),t_{n-2}}[L^{j_1} L^{j_2} f^{j_3,k}] I_{(j_3),t_{n-1}}$$

$$- \sum_{j_1,j_2=0}^{m} \delta_1 I_{(j_1),t_{n-2}}[L^{j_1} L^{j_2} f^{0,k}] I_{(j_2),t_{n-1}} \Delta_t$$

$$- \sum_{j_1,j_2,j_3=0}^{m} \epsilon_1 I_{(j_1),t_{n-2}}[L^{j_1} L^{j_2} f^{j_3,k}] I_{(j_2,j_3),t_{n-1}}.$$

Now $\alpha_0 = \gamma_1$ from the 1.0-order consistency conditions (4.20),

$$\sum_{j_1,j_2=0}^{m} \alpha_0 I_{(j_1),t_{n-2}} I_{(j_2),t_{n-1}} L^{j_1} f^{j_2,k}(t_{n-2}, x(t_{n-2}))$$

$$- \sum_{j_1=0}^{m} \sum_{j_2=1}^{m} \gamma_1 I_{(j_1),t_{n-2}} I_{(j_2),t_{n-1}} L^{j_1} f^{j_2,k}(t_{n-2}, x(t_{n-2}))$$

$$= \sum_{j_1=0}^{m} \alpha_0 I_{(j_1),t_{n-2}} I_{(0),t_{n-1}} L^{j_1} f^{0,k}(t_{n-2}, x(t_{n-2})).$$

The formula (4.21) has 2.0-order convergence if the following consistency conditions:

$$\begin{cases} \delta_1 = -\beta_0, \quad \delta_2 = \alpha_0 - \beta_0 - \beta_1, \\ \epsilon_1 = \alpha_0, \quad \epsilon_2 = \alpha_0 + \alpha_1, \end{cases} \tag{4.23}$$

are satisfied.

3-step schemes

When $s = 3$, the local error L_n of the scheme (4.18) is given by

$$\begin{aligned} L_n \quad := \quad \Big| \sum_{l=0}^{3} \alpha_l x^k(t_{n-l}) - \sum_{l=0}^{3} \beta_l f^{0,k}(t_{n-l}, x(t_{n-l})) \Delta_t \\ - \sum_{l=1}^{3} \gamma_l \sum_{j=1}^{m} f^{j,k}(t_{n-l}, x(t_{n-l})) I_{(j),t_{n-l}} \Big|. \end{aligned} \tag{4.24}$$

In addition to the the affine-RODE-Taylor expansions and classical chain rules for $s = 2$, we have to include terms up to t_{n-3}, i.e.,

$$\begin{aligned} x^k(t_{n-2}) \quad = \quad & x^k(t_{n-3}) + f^{0,k}(t_{n-3}, x(t_{n-3})) I_{(0),t_{n-3}} \\ & + \sum_{j=1}^{m} f^{j,k}(t_{n-3}, x(t_{n-3})) I_{(j),t_{n-3}} + \sum_{j_1,j_2=0}^{m} I_{(j_1,j_2),t_{n-3}}[L^{j_1} f^{j_2,k}] \end{aligned}$$

$$
\begin{aligned}
f^{0,k}(t_{n-2}, x(t_{n-2})) &= f^{0,k}(t_{n-3}, x(t_{n-3})) + \sum_{j=0}^{m} I_{(j),t_{n-3}}[L^j f^{0,k}] \\
f^{j,k}(t_{n-2}, x(t_{n-2})) &= f^{j,k}(t_{n-3}, x(t_{n-3})) + \sum_{j_1=0}^{m} I_{(j_1),t_{n-3}}[L^{j_1} f^{j,k}].
\end{aligned}
$$

The corresponding terms in the local error (4.24) are substituted. It is given by

$$
\begin{aligned}
L_n = \Big| & (\alpha_0+\alpha_1+\alpha_2+\alpha_3)x^k(t_{n-3}) \\
& + (3\alpha_0+2\alpha_1+\alpha_2-(\beta_0+\beta_1+\beta_2+\beta_3))\, f^{0,k}(t_{n-3}, x(t_{n-3}))\Delta_t \\
& + \sum_{j=1}^{m} \Big(\alpha_0 I_{(j),t_{n-1}} + (\alpha_0+\alpha_1) I_{(j),t_{n-2}} + (\alpha_0+\alpha_1+\alpha_2) I_{(j),t_{n-3}} \\
& \qquad -\gamma_1 I_{(j),t_{n-1}} - \gamma_2 I_{(j),t_{n-2}} - \gamma_3 I_{(j),t_{n-3}} \Big) f^{j,k}(t_{n-3}, x(t_{n-3})) + R_1 \Big|,
\end{aligned}
$$

where the remainder term R_1 is now

$$
\begin{aligned}
R_1 = & \sum_{j_1,j_2=0}^{m} \Big(\alpha_0 \hat{I}^{t_n}_{(j_1,j_2),t_{n-3}}[L^{j_1} f^{j_2,k}] + \alpha_1 \hat{I}^{t_{n-1}}_{(j_1,j_2),t_{n-3}}[L^{j_1} f^{j_2,k}] \\
& \qquad + \alpha_2 I_{(j_1,j_2),t_{n-3}}[L^{j_1} f^{j_2,k}] \Big) \\
& - \sum_{j=0}^{m} \Big(\beta_0 \hat{I}^{t_n}_{(j),t_{n-3}}[L^j f^{0,k}] + \beta_1 \hat{I}^{t_{n-1}}_{(j),t_{n-3}}[L^j f^{0,k}] + \beta_2 I_{(j),t_{n-3}}[L^j f^{0,k}] \Big) \Delta_t \\
& - \sum_{j_1=0}^{m} \sum_{j_2=1}^{m} \Big(\gamma_1 \hat{I}^{t_{n-2}}_{(j_1),t_{n-3}}[L^{j_1} f^{j_2,k}] I_{(j_2),t_{n-1}} + \gamma_2 I_{(j_1),t_{n-3}}[L^{j_1} f^{j_2,k}] I_{(j_2),t_{n-2}} \Big).
\end{aligned}
$$

R_1 is Δ_t^2-order and when the coefficients of the LMMs (4.18) satisfy the following consistency conditions:

$$
\begin{cases}
\alpha_0+\alpha_1+\alpha_2+\alpha_3 = 0, \\
\beta_0+\beta_1+\beta_2+\beta_3 = 3\alpha_0+2\alpha_1+\alpha_2, \\
\gamma_1 = \alpha_0, \quad \gamma_2 = \alpha_0+\alpha_1, \quad \gamma_3 = \alpha_0+\alpha_1+\alpha_2,
\end{cases}
$$

the LMMs (4.18) have 1.0-order convergence.

Order 2.0 schemes

Similar to $s = 2$ case, a general form of 2.0-order LMMs is given by

$$\begin{aligned}\sum_{l=0}^{3}\alpha_l X_{n-l}^k = &\sum_{l=0}^{3}\beta_l f^{0,k}(t_{n-l},X_{n-l})\Delta_t + \sum_{l=1}^{3}\gamma_l\sum_{j=1}^{m} f^{j,k}(t_{n-l},X_{n-l})I_{(j),t_{n-l}}\\ &+\sum_{l=1}^{3}\delta_l\sum_{j=0}^{m} L^j f^{0,k}(t_{n-l},X_{n-l})I_{(j),t_{n-l}}\Delta_t\\ &+\sum_{l=1}^{3}\epsilon_l\sum_{j_1,j_2=0}^{m} L^{j_1}f^{j_2,k}(t_{n-l},X_{n-l})I_{(j_1,j_2),t_{n-l}},\end{aligned}$$

and the local discretization error is defined by

$$\begin{aligned}L_n \;:=\; \Big|&\sum_{l=0}^{3}\alpha_l x^k(t_{n-l}) - \sum_{l=0}^{3}\beta_l f^{0,k}(t_{n-l},x(t_{n-l}))\Delta_t\\ &-\sum_{l=1}^{3}\gamma_l\sum_{j=1}^{m} f^{j,k}(t_{n-l},x(t_{n-l}))I_{(j),t_{n-l}}\\ &-\sum_{l=1}^{3}\delta_l\sum_{j=0}^{m} L^j f^{0,k}(t_{n-l},x(t_{n-l}))I_{(j),t_{n-l}}\Delta_t\\ &-\sum_{l=1}^{3}\epsilon_l\sum_{j_1,j_2=0}^{m} L^{j_1}f^{j_2,k}(t_{n-l},x(t_{n-l}))I_{(j_1,j_2),t_{n-l}}\Big|,\end{aligned}$$

The same argument with $s = 2$ yields

$$\begin{aligned}L_n = \Big|&\sum_{j_1,j_2=0}^{m}\Big(\alpha_0\hat{I}^{t_n}_{(j_1,j_2),t_{n-3}} + \alpha_1\hat{I}^{t_{n-1}}_{(j_1,j_2),t_{n-3}}\\ &\qquad+\alpha_2 I_{(j_1,j_2),t_{n-3}}\Big)L^{j_1}f^{j_2,k}(t_{n-3},x(t_{n-3}))\\ &-\sum_{j=0}^{m}\Big(\beta_0\hat{I}^{t_n}_{(j),t_{n-3}} + \beta_1\hat{I}^{t_{n-1}}_{(j),t_{n-3}} + \beta_2 I_{(j),t_{n-3}}\Big)\Delta_t L^j f^{0,k}(t_{n-3},x(t_{n-3}))\\ &-\sum_{j_1=0}^{m}\sum_{j_2=1}^{m}\Big(\gamma_1\hat{I}^{t_{n-1}}_{(j_1),t_{n-3}}I_{(j_2),t_{n-1}}\\ &\qquad+\gamma_2 I_{(j_1),t_{n-3}}I_{(j_1),t_{n-2}}\Big)L^{j_1}f^{j_2,k}(t_{n-3},x(t_{n-3}))\end{aligned}\tag{4.25}$$

$$-\sum_{j=0}^{m}(\delta_1 I_{(j),t_{n-1}}+\delta_2 I_{(j),t_{n-2}}+\delta_3 I_{(j),t_{n-3}})\Delta_t L^j f^{0,k}(t_{n-3},x(t_{n-3}))$$

$$-\sum_{j_1,j_2=0}^{m}(\epsilon_1 I_{(j_1,j_2),t_{n-1}}+\epsilon_2 I_{(j_1,j_2),t_{n-2}}+\epsilon_3 I_{(j_1,j_2),t_{n-3}})$$

$$L^{j_1} f^{j_2,k}(t_{n-3},x(t_{n-3}))+R_2\Big|,$$

where R_2 is a remainder term. The equation (4.25) yields the following consistency conditions of order 2:

$$\begin{cases}\delta_1=-\beta_0, \quad \delta_2=\alpha_0-\beta_0-\beta_1, \quad \delta_3=2\alpha_0+\alpha_1-\beta_0-\beta_1-\beta_2\\ \epsilon_1=\alpha_0, \quad \epsilon_2=\alpha_0+\alpha_1, \quad \epsilon_3=\alpha_0+\alpha_1+\alpha_2.\end{cases}$$

General form

Higher order LMMs as well as LMMs with more steps for the affine-RODEs (4.1) can be generated systematically in the same manner. In general, an s-step LMM for an affine-RODE (4.1) with order N has the form:

$$\begin{aligned}\sum_{l=0}^{s} C_{\emptyset,l}X_{n-l}^k &= \sum_{l=0}^{s} C_{(0),l}f^{0,k}(t_{n-l},X_{n-l})\Delta_t \\ &+\sum_{l=1}^{s}\sum_{j=1}^{m} C_{(j),l}f^{j,k}(t_{n-l},X_{n-l})I_{(j),t_{n-l}} \\ &+\sum_{l=1}^{s}\sum_{\alpha\in\mathcal{A}_N^0\setminus\{(0)\}} C^*_{\alpha,l}L^{\alpha-}f^{0,k}(t_{n-l},X_{n-l})I_{\alpha-,t_{n-l}}\Delta_t \\ &+\sum_{l=1}^{s}\sum_{\alpha\in\mathcal{A}_N\setminus\{\emptyset,(0),(j)\}} C_{\alpha,l}L^{\alpha}id^k(t_{n-l},X_{n-l})I_{\alpha,t_{n-l}},\end{aligned} \tag{4.26}$$

where $\mathcal{A}_N^0$ is given by

$$\mathcal{A}_N^0=\{\alpha\in\mathcal{A}_N \ : \text{the last component } j_l=0\}$$

and the coefficients $C_{\cdot,l}$ satisfy consistency conditions up to N-order.

Chapter 5

Stability

We often encounter stiff systems in practice and the stability property of numerical schemes is a crucial issue when we solve such systems numerically. It is well known from the theory of classical Runge-Kutta schemes for ODEs that an implicit scheme is required for the stable integration of a stiff ODE.

In case of RODEs, we need to take into account of the effects of nonlinearity in the equations, which play a much more significant role in RODEs than deterministic ones. It is also not clear in RODEs or SODEs what class of linear test functions is suitable. In addition, even a simple linear RODE contains a noise term in its matrix and it makes the system pathwise nonautonomous, so it is not easy to generalize the Dahlquist theory since it involves Lyapunov exponents instead of eigenvalues and they are very hard to calculate. In order to circumvent these problems, we focus on the B-stability.

In fact, implicit schemes which are B-stable are even better [28, 42], i.e., preserve the non-expansive structure of trajectories of ODEs with a dissipative one-sided Lipschitz condition, i.e.,

$$\|X_i - X_i'\| \leq \|X_{i-1} - X_{i-1}'\|,$$

for $i = 1, 2, \ldots, n$ where X_i and X_i' are two solutions of the scheme. Recall that no explicit or linear implicit Runge-Kutta scheme is ever B-stable. Since RODEs are generalizations of ODEs, this applies equally well to RODEs.

5.1 B-stability of averaged schemes

Before showing the B-stability of the IAES (2.36) and IAMS (2.37), we prove the solvability and convergence in the Theorems 3 and 4 introduced in subsection 2.3.2.

5.1.1 Solvability of the averaged schemes

The IAES (2.36) and IAMS (2.37) are implicit schemes involving an algebraic equation that needs to be solved for each iterative step. Each one has a

unique solution when the step size Δ_t is small enough when $L > 0$ and arbitrary otherwise.

The proof is based on that of Theorem 6.54 in [28]. Suppose that X_{n-1} is known.

Solvability of the IAES

We start with the IAES (2.36) and consider the mapping $g : \mathbb{R}^d \to \mathbb{R}^d$ defined by

$$y \mapsto X_{n-1} + f\left(y, I_{n-1}\right) \Delta_t - y.$$

It follows from the one-sided Lipschitz condition (2.38) for the vector field f that g satisfies

$$\begin{aligned} \langle g(a) - g(b), a - b\rangle &= \Delta_t \left\langle f(a, I_{n-1}(\omega)) - f(b, I_{n-1}(\omega)), a - b\right\rangle - \|a - b\|^2 \\ &\leq L\Delta_t \|a - b\|^2 - \|a - b\|^2 = (L\Delta_t - 1)\|a - b\|^2, \end{aligned}$$

for all a, $b \in \mathbb{R}^d$, which is a one-sided Lipschitz condition with constant $L\Delta_t - 1$. By assumption we have $L\Delta_t - 1 < 0$, so we can apply the Contractive Dynamics Theorem in [91] to the mapping g to conclude that g has a unique zero, which we denote by X_n. Hence, X_n is the unique fixed point in $\mathbb{R}^d$ of the equation:

$$y = X_{n-1} + f\left(y, I_{n-1}\right) \Delta_t, \qquad y \in \mathbb{R}^d,$$

which proves the unique solvability of the IAES (2.36).

Solvability of the IAMS

A similar argument holds for the IAMS (2.37). We now consider the mapping $g : \mathbb{R}^d \to \mathbb{R}^d$ defined by

$$y \mapsto X_{n-1} + f\left(\frac{1}{2}\left(X_{n-1} + y\right), I_{n-1}\right) \Delta_t - y.$$

From the one-sided Lipschitz condition (2.38) for the vector field f, it follows that

$$\begin{aligned} &\langle g(a) - g(b), a - b\rangle \\ &= \Delta_t \Bigg\langle f\left(\frac{1}{2}\left(X_{n-1}(\omega) + a\right), I_{n-1}(\omega)\right) \\ &\qquad\qquad - f\left(\frac{1}{2}\left(X_{n-1}(\omega) + b\right), I_{n-1}(\omega)\right), a - b\Bigg\rangle - \|a - b\|^2 \\ &\leq (L\Delta_t)\left\|\frac{1}{2}\left(X_{n-1}(\omega) + a\right) - \frac{1}{2}\left(X_{n-1}(\omega) + b\right)\right\|^2 - \|a - b\|^2 \\ &= \frac{1}{4}L\Delta_t \|a - b\|^2 - \|a - b\|^2 = \left(\frac{1}{4}L\Delta_t - 1\right)\|a - b\|^2, \end{aligned}$$

for all a, $b \in \mathbb{R}^d$, i.e., the mapping g satisfies a one-sided Lipschitz condition with constant $L\Delta_t/4 - 1$. Since $L\Delta_t/4 - 1 < 0$, we can also apply Theorem 2.8.4 of [91] to g to conclude that g has a unique zero, which we denote by X_n. Thus, X_n is the unique fixed point in $\mathbb{R}^d$ of the equation:

$$y = X_{n-1} + f\left(\frac{1}{2}\left(X_{n-1} + y\right), I_{n-1}\right)\Delta_t, \qquad y \in \mathbb{R}^d,$$

which proves the unique solvability for the IAMS (2.37).

5.1.2 Convergence of the averaged schemes

Convergence of the IAES

We show by induction over n for the IAES (2.36) that

$$\|x(t_n) - X_n\| \leq \Delta_t^{\min(2\theta,1)} \begin{cases} C_E(n\Delta_t) & : L \leq 0 \\ \dfrac{C_E}{L}\left(\exp\left(\dfrac{Ln\Delta_t}{1-\alpha}\right) - 1\right) & : L > 0 \end{cases} \tag{5.1}$$

holds for every $n = 0, 1, \ldots, N$, which implies the assertion. (We recall that $\alpha \in (0, 1)$ is arbitrary, but fixed here).

For $n = 0$ the assertion is clear. Therefore, suppose that the inequality (5.1) is true for $n \in \{0, 1, \ldots, N-1\}$. We will show that it is then true for $n + 1$. From subsection 5.1.1, the equation

$$z = x(t_n) + f(z, I_n)\,\Delta_t$$

has a unique solution, which we denote by Z. Then, by the one-sided Lipschitz condition (2.38) for f and the Cauchy-Schwarz inequality, we obtain

$$\begin{aligned} \|X_{n+1} - Z\|^2 &= \langle X_{n+1} - Z, X_n - x(t_n)\rangle \\ &\quad + \Delta_t \langle X_{n+1} - Z, f(X_{n+1}, I_n) - f(Z, I_n)\rangle \\ &\leq \|X_{n+1} - Z\| \cdot \|X_n - x(t_n)\| + L\Delta_t \|X_{n+1} - Z\|^2, \end{aligned}$$

from which it follows that

$$\|X_{n+1} - Z\| \leq \left(\frac{1}{1 - L\Delta_t}\right)\|X_n - x(t_n)\|. \tag{5.2}$$

We also have

$$\left\|\int_{t_n}^{t_{n+1}} f(x(s), Y(s))\,ds - \int_{t_n}^{t_{n+1}} f(x(t_{n+1}), Y(s))\,ds\right\| \tag{5.3}$$

$$\leq \frac{1}{2}\left(\sup_{0\leq s,u\leq T} \|f_x\left(x(u), Y(s)\right) f\left(x(u), Y(u)\right)\|\right)\Delta_t^2.$$

By the Mean Value Theorem,

$$\begin{aligned} f(x(t_{n+1}), I_n)\,\Delta_t &= f(x(t_{n+1}), Y(t_n))\,\Delta_t \\ &\quad + \int_{t_n}^{t_{n+1}} \int_0^1 f_y \left(x(t_n), Y(t_n) + \frac{u}{\Delta_t} \int_{t_n}^{t_{n+1}} (Y(v) - Y(t_n))\, dv \right) \\ &\qquad \cdot (Y(s) - Y(t_n))\, du\, ds \end{aligned} \tag{5.4}$$

and

$$\begin{aligned} \int_{t_n}^{t_{n+1}} f(x(t_{n+1}), Y(s))\, ds &= f(x(t_{n+1}), Y(t_n))\,\Delta_t \\ &\quad + \int_{t_n}^{t_{n+1}} \int_0^1 f_y \left(x(t_{n+1}), Y(t_n) + u\,(Y(s) - Y(t_n)) \right) \cdot (Y(s) - Y(t_n))\, du\, ds. \end{aligned} \tag{5.5}$$

Hence, by (5.4) and (5.5), we obtain

$$\begin{aligned} &\left\| f(x(t_{n+1}), I_n)\,\Delta_t - \int_{t_n}^{t_{n+1}} f(x(t_{n+1}), Y(s))\, ds \right\| \\ &\quad \le \left(\sup_{\substack{\|w\| \le \|Y\|_\infty \\ 0 \le s \le T}} \| f_{yy}(x(s), w) \| \right) \\ &\qquad \times \int_{t_n}^{t_{n+1}} \int_0^1 u \left\| \Delta_t^{-1} \int_{t_n}^{t_{n+1}} (Y(v) - Y(t_n))\, dv - (Y(s) - Y(t_n)) \right\| \\ &\qquad\qquad \| Y(s) - Y(t_n) \|\, du\, ds \\ &\quad \le \frac{1}{2} \left(\sup_{\substack{\|w\| \le \|Y\|_\infty \\ 0 \le s \le T}} \| f_{yy}(x(s), w) \| \right) \Theta^2 \cdot \Delta_t^{1+2\theta}, \end{aligned} \tag{5.6}$$

where Θ is the random variable in the Hölder estimate (2.33).

Equations (5.3) and (5.6) give

$$\left\| f(x(t_{n+1}), I_n)\,\Delta_t - \int_{t_n}^{t_{n+1}} f(x(s), Y(s))\, ds \right\| \le C_E \cdot \Delta_t^{1+\min(2\theta, 1)}$$

and we thus obtain

$$
\begin{aligned}
&\|x(t_{n+1}) - Z\|^2 \\
&\quad = \langle x(t_{n+1}) - Z, x(t_{n+1}) - (x(t_n) + f(Z, I_n))\ \Delta_t \rangle \\
&\quad = \left\langle x(t_{n+1}) - Z, \int_{t_n}^{t_{n+1}} f(x(s), Y(s))\, ds - f(Z, I_n)\, \Delta_t \right\rangle \\
&\quad = \left\langle x(t_{n+1}) - Z, \int_{t_n}^{t_{n+1}} f(x(s), Y(s))\, ds - f(x(t_{n+1}), I_n)\, \Delta_t \right\rangle \\
&\qquad\qquad + \Delta_t \left\langle x(t_{n+1}) - Z, f(x(t_{n+1}), I_n) - f(Z, I_n) \right\rangle \\
&\quad \leq \|x(t_{n+1}) - Z\| \cdot \left\| \int_{t_n}^{t_{n+1}} f(x(s), Y(s))\, ds - f(x(t_{n+1}), I_n)\, \Delta_t \right\| \\
&\qquad\qquad + L\Delta_t\ \|x(t_{n+1}) - Z\|^2 \\
&\quad \leq \|x(t_{n+1}) - Z\| \cdot \left(\frac{C_E}{1 - L\Delta_t} \right) \cdot \Delta_t^{1+\min(2\theta,1)}
\end{aligned}
$$

by the one-sided Lipschitz condition (2.38) and the Cauchy-Schwarz inequality. This and equation (5.2) then imply that

$$
\begin{aligned}
\|x(t_{n+1}) - X_{n+1}\| &\leq \|x(t_{n+1}) - Z\| + \|Z - X_{n+1}\| \\
&\leq \left(\frac{C_E}{1 - L\Delta_t} \right) \Delta_t^{1+\min(2\theta,1)} + \left(\frac{1}{1 - L\Delta_t} \right) \|X_n - x(t_n)\| .
\end{aligned}
$$

Finally, the induction assumption (5.1) gives

$$
\begin{aligned}
\|x(t_{n+1}) - X_{n+1}\| &\leq C_E \Delta_t^{1+\min(2\theta,1)} + C_E \cdot n\Delta_t \cdot \Delta_t^{\min(2\theta,1)} \\
&\leq C_E \cdot \Delta_t^{\min(2\theta,1)} (\Delta_t + n\Delta_t) = C_E \cdot (n+1)\Delta_t \cdot \Delta_t^{\min(2\theta,1)}
\end{aligned}
$$

in the case $L \leq 0$ and

$$
\begin{aligned}
&\|x(t_{n+1}) - X_{n+1}\| \\
&\quad \leq \left(\frac{C_E}{1 - \alpha} \right) \Delta_t^{1+\min(2\theta,1)} + \left(1 + \left(\frac{1}{1 - \alpha} \right) L\Delta_t \right) \|X_n - x(t_n)\| \\
&\quad \leq \left(\frac{C_E}{1 - \alpha} \right) \Delta_t^{1+\min(2\theta,1)} \\
&\qquad\qquad + \left(1 + \left(\frac{L}{1 - \alpha} \right) \Delta_t \right) \left(e^{\left(\frac{Ln\Delta_t}{1-\alpha} \right)} - 1 \right) \left(\frac{C_E}{L} \right) \cdot \Delta_t^{\min(2\theta,1)} \\
&\quad \leq \left(\frac{C_E}{1 - \alpha} \right) \Delta_t^{\min(2\theta,1)} \left(\Delta_t + (1 + \beta\Delta_t) \frac{\left(e^{\beta n \Delta_t} - 1 \right)}{\beta} \right)
\end{aligned}
$$

$$
\begin{aligned}
&= \left(\frac{C_E}{1-\alpha}\right) \Delta_t^{\min(2\theta,1)} \cdot \frac{1}{\beta} \left(\beta\Delta_t + (1+\beta\Delta_t)\left(e^{\beta n\Delta_t} - 1\right)\right) \\
&= \left(\frac{C_E}{1-\alpha}\right) \Delta_t^{\min(2\theta,1)} \cdot \frac{1}{\beta} \left(\beta\Delta_t + e^{\beta n\Delta_t} - 1 + \beta\Delta e^{\beta n\Delta_t} - \beta\Delta_t\right) \\
&\leq \left(\frac{C_E}{1-\alpha}\right) \left(\frac{e^{\beta(n+1)\Delta_t} - 1}{\beta}\right) \Delta_t^{\min(2\theta,1)} \\
&= \left(\frac{C_E}{L}\right) \left(e^{\left(\frac{L(n+1)\Delta_t}{1-\alpha}\right)} - 1\right) \cdot \Delta_t^{\min(2\theta,1)}
\end{aligned}
$$

in the case $L > 0$ with $\beta = L/(1-\alpha)$. Here we used the inequality

$$\frac{1}{1-r} \leq 1 + \left(\frac{1}{1-\alpha}\right) r, \qquad r \in [0, \alpha].$$

Convergence of the IAMS

We now show by induction over n for the IAMS (2.37) that

$$\|x(t_n) - X_n\| \leq \Delta_t^{2\theta} \begin{cases} C_M(n\Delta_t) & : L \leq 0 \\ \dfrac{C_M}{L}\left(\exp\left(\dfrac{Ln\Delta_t}{1-\alpha}\right) - 1\right) & : L > 0 \end{cases} \tag{5.7}$$

holds for every $n = 0, 1, \ldots, N$.

This is obvious for $n = 0$. We suppose that inequality (5.7) is true for $n \in \{0, 1, \ldots, N-1\}$ and show that it is then true for $n+1$. Let Z denote the unique solution of the equation

$$z = x(t_n) + f\left(\frac{1}{2}\left(x(t_n) + z\right), I_n\right) \Delta_t,$$

which we know exists from subsection 5.1.1.

Now, we have

$$
\begin{aligned}
&\underbrace{(X_{n+1} - Z)}_{=:E_{n+1}} - \underbrace{(X_n - x(t_n))}_{=:E_n} \\
&\qquad = \underbrace{\left(f\left(\frac{1}{2}\left(X_n + X_{n+1}\right), I_n\right) - f\left(\frac{1}{2}\left(x(t_n) + Z\right), I_n\right)\right)}_{=:A} \Delta_t
\end{aligned}
$$

or

$$E_{n+1} = E_n + A\,\Delta_t.$$

Define

$$e := \frac{1}{2}\left(E_n + E_{n+1}\right) = E_n + \frac{1}{2} A\,\Delta_t.$$

Then

$$\begin{aligned}
\|E_{n+1}\|^2 &= \|E_n + A\Delta_t\|^2 \\
&= \|E_n\|^2 + 2\langle E_n, A\Delta\rangle + \|A\Delta_t\|^2 \\
&= \|E_n\|^2 + 2\left\langle e - \frac{1}{2}A\Delta, A\Delta_t \right\rangle + \|A\Delta_t\|^2 \\
&= \|E_n\|^2 + 2\Delta_t \langle e, A\rangle \\
&= \|E_n\|^2 + 2\Delta_t \left\langle \frac{1}{2}(X_n + X_{n+1}) - \frac{1}{2}(x(t_n) + Z), A \right\rangle \\
&\leq \|E_n\|^2 + 2L\Delta_t \left\| \frac{1}{2}(X_n + X_{n+1}) - \frac{1}{2}(x(t_n) + Z) \right\|^2 \\
&= \|E_n\|^2 + 2L\Delta_t \|e\|^2 .
\end{aligned}$$

Now

$$\begin{aligned}
\|e\|^2 &= \langle e, E_n\rangle + \left\langle e, \frac{1}{2}A\Delta_t \right\rangle \\
&\leq \|e\|\,\|E_n\| + \frac{1}{2}L\Delta_t \|e\|^2 ,
\end{aligned}$$

which implies that

$$\|e\| \leq \left(\frac{1}{1 - \frac{1}{2}L\Delta_t}\right)\|E_n\|.$$

When $L > 0$, we obtain

$$\begin{aligned}
\|E_{n+1}\|^2 &\leq \|E_n\|^2 + \frac{8L\Delta_t}{(2 - L\Delta_t)^2}\|E_n\|^2 \\
&= \left(\frac{(2 - L\Delta_t)^2 + 8L\Delta_t}{(2 - L\Delta_t)^2}\right)\|E_n\|^2 \\
&= \frac{(2 + L\Delta_t)^2}{(2 - L\Delta_t)^2}\|E_n\|^2.
\end{aligned}$$

Finally, in both cases,

$$\|X_{n+1} - Z\| \leq \|X_n - x(t_n)\| \cdot \begin{cases} \dfrac{2 + L\Delta_t}{2 - L\Delta_t} & : L > 0 \\ 1 & : L \leq 0. \end{cases} \tag{5.8}$$

We also have

$$\int_{t_n}^{t_{n+1}} f(x(s), Y(s))\, ds$$
$$= \int_{t_n}^{t_{n+1}} f(x(t_n), Y(s))\, ds + \int_{t_n}^{t_{n+1}} \int_{t_n}^{s} f_x(x(u), Y(s)) f(x(u), Y(u))\, du\, ds$$

and

$$f\left(\frac{1}{2}\left(x(t_n) + x(t_{n+1})\right), I_n\right) \Delta_t - f\left(x(t_n), I_n\right) \Delta_t$$
$$= \frac{1}{2}\Delta_t \int_0^1 f_x\left(x(t_n) + \frac{u}{2}\left(x(t_{n+1}) - x(t_n)\right), I_n\right) du \cdot \left(x(t_{n+1}) - x(t_n)\right),$$

from which we obtain

$$\left\| f\left(\frac{1}{2}\left(x(t_{n+1}) - x(t_n)\right)\Delta_t, I_n\right) - \int_{t_n}^{t_{n+1}} f(x(s), Y(s))\, ds \right\| \le C_M\, \Delta_t^{1+2\theta}.$$

Therefore,

$$\|x(t_{n+1}) - Z\|^2$$
$$= \left\langle x(t_{n+1}) - Z, x(t_{n+1}) - x(t_n) - f\left(\frac{1}{2}\left(x(t_n) + Z\right), I_n\right)\Delta_t \right\rangle$$
$$= \left\langle x(t_{n+1}) - Z, \int_{t_n}^{t_{n+1}} f(x(s), Y(s))\, ds - f\left(\frac{1}{2}\left(x(t_n) + Z\right), I_n\right)\Delta_t \right\rangle$$
$$= \left\langle x(t_{n+1}) - Z, \int_{t_n}^{t_{n+1}} f(x(s), Y(s))\, ds - f\left(\frac{1}{2}\left(x(t_n) + x(t_{n+1})\right), I_n\right)\Delta_t \right\rangle$$
$$+\Delta_t \left\langle x(t_{n+1}) - Z, f\left(\frac{1}{2}\left(x(t_n) + x(t_{n+1})\right), I_n\right) - f\big(\frac{1}{2}\left(x(t_n) + Z\right), I_n\big) \right\rangle$$
$$\le \big\|x(t_{n+1}) - Z\big\| \cdot \left\| \int_{t_n}^{t_{n+1}} f(x(s), Y(s))\, ds - f\big(\frac{1}{2}\left(x(t_n) + x(t_{n+1})\right), I_n\big)\Delta_t \right\|$$
$$+\frac{1}{2} L \Delta_t \|x(t_{n+1}) - Z\|^2$$
$$\le \|x(t_{n+1}) - Z\| \cdot \left(\frac{C_M}{1 - \frac{1}{2}L\Delta_t}\right) \cdot \Delta_t^{1+2\theta},$$

where we have used the one-sided Lipschitz condition (2.38) and the Cauchy-Schwarz inequality.

The last estimate, the estimate (5.2) and the induction assumption (5.1) imply that

$$\begin{aligned}\|x(t_{n+1}) - X_{n+1}\| &\leq \|x(t_{n+1}) - Z\| + \|Z - X_{n+1}\| \\ &\leq C_M \Delta_t^{1+2\theta} + \|X_n - x(t_n)\| \\ &\leq C_M \Delta_t^{1+2\theta} + C_M\, n\Delta_t\, \Delta_t^{2\theta} \\ &\leq C_M\, \Delta_t^{2\theta}\, (\Delta_t + n\Delta_t) = C_M \cdot (n+1)\Delta_t\, \Delta_t^{2\theta}\end{aligned}$$

in the case $L \leq 0$ and

$$\begin{aligned}&\|x(t_{n+1}) - X_{n+1}\| \\ &\quad \leq \|x(t_{n+1}) - Z\| + \|Z - X_{n+1}\| \\ &\quad \leq \left(\frac{2C_M}{2 - L\Delta_t}\right) \Delta_t^{1+2\theta} + \left(\frac{2 + L\Delta_t}{2 - L\Delta_t}\right) \|X_n - x(t_n)\| \\ &\quad \leq \left(\frac{2C_M}{2-\alpha}\right) \Delta_t^{1+2\theta} + \left(1 + \left(\frac{2}{2-\alpha}\right) L\Delta_t\right) \|X_n - x(t_n)\| \\ &\quad \leq \left(\frac{2C_M}{2-\alpha}\right) \Delta_t^{1+2\theta} + \left(1 + \left(\frac{2}{2-\alpha}\right) L\Delta_t\right) \left(e^{\left(\frac{2Ln\Delta_t}{2-\alpha}\right)} - 1\right) \left(\frac{C_M}{L}\right) \Delta_t^{2\theta} \\ &\quad \leq \left(\frac{2C_M}{2-\alpha}\right) \Delta_t^{2\theta} \left(\Delta_t + (1 + \beta\Delta_t)\, \frac{\left(e^{\beta n\Delta_t} - 1\right)}{\beta}\right) \\ &\quad = \left(\frac{2C_M}{2-\alpha}\right) \frac{\Delta_t^{2\theta}}{\beta} \left(\beta\Delta_t + (1 + \beta\Delta_t) \left(e^{\beta n\Delta_t} - 1\right)\right) \\ &\quad = \left(\frac{2C_M}{2-\alpha}\right) \frac{\Delta_t^{2\theta}}{\beta} \left(\beta\Delta_t + e^{\beta n\Delta_t} - 1 + \beta\Delta_t e^{\beta n\Delta_t} - \beta\Delta_t\right) \\ &\quad \leq \left(\frac{2C_M}{2-\alpha}\right) \left(\frac{e^{\beta(n+1)\Delta_t} - 1}{\beta}\right) \Delta_t^{2\theta} \\ &\quad = \left(\frac{C_M}{L}\right) \left(e^{\left(\frac{2L(n+1)\Delta_t}{2-\alpha}\right)} - 1\right) \Delta_t^{2\theta}\end{aligned}$$

in the case $L > 0$ with $\beta = 2L/(2-\alpha)$, where we have used the inequality

$$\frac{2+r}{2-r} \leq 1 + \left(\frac{2}{2-\alpha}\right) r, \qquad r \in [0, \alpha].$$

5.1.3 B-stability of the averaged schemes

B-stability of the IAES

We consider two solutions X_n and X'_n of the IAES (2.36) and denote

$$D := f\left(X_{n+1}, I_n\right)\Delta_t - f\left(X'_{n+1}, I_n\right)\Delta_t.$$

Then, we have

$$\left(X_{n+1} - X'_{n+1}\right) = \left(X_n - X'_n\right) + D$$

and hence

$$\begin{aligned}
\left\|X_{n+1} - X'_{n+1}\right\|^2 &= \left\|\left(X_n - X'_n\right) + D\right\|^2 \\
&= \left\|X_n - X'_n\right\|^2 + 2\left\langle X_n - X'_n, D\right\rangle + \|D\|^2 \\
&= \left\|X_n - X'_n\right\|^2 + 2\left\langle \left(X_{n+1} - X'_{n+1} - D\right), D\right\rangle + \|D\|^2 \\
&= \left\|X_n - X'_n\right\|^2 + 2\left\langle X_{n+1} - X'_{n+1}, D\right\rangle - \|D\|^2 \\
&\leq \left\|X_n - X'_n\right\|^2 + 2\left\langle X_{n+1} - X'_{n+1}, D\right\rangle.
\end{aligned}$$

Now,

$$\left\langle X_{n+1} - X'_{n+1}, D\right\rangle \;\leq\; L\Delta_t \left\|X_{n+1} - X'_{n+1}\right\|^2 \leq 0$$

by the one-sided Lipschitz condition (2.38) and the assumption that $L \leq 0$, so we obtain

$$\left\|X_{n+1} - X'_{n+1}\right\|^2 \leq \left\|X_n - X'_n\right\|^2,$$

which proves the B-stability of the IAES (2.36).

B-stability of the IAMS

For the IAMS (2.37) we also have

$$\left(X_{n+1} - X'_{n+1}\right) = \left(X_n - X'_n\right) + D,$$

but now with

$$D := f\left(\frac{1}{2}\left(X_n + X_{n+1}\right), I_n\right)\Delta_t - f\left(\frac{1}{2}\left(X'_n + X'_{n+1}\right), I_n\right)\Delta_t,$$

which is equivalent to

$$\frac{1}{2}\left(X_n + X_{n+1}\right) - \frac{1}{2}\left(X'_n + X'_{n+1}\right) = \left(X_n - X'_n\right) + \frac{1}{2}D.$$

Hence,

$$\begin{aligned}
&\left\|X_{n+1} - X'_{n+1}\right\|^2 \\
&\quad = \left\|\left(X_n - X'_n\right) + D\right\|^2 \\
&\quad = \left\|X_n - X'_n\right\|^2 + 2\left\langle X_n - X'_n, D\right\rangle + \|D\|^2 \\
&\quad = \left\|X_n - X'_n\right\|^2 + 2\left\langle \frac{1}{2}\left(X_n + X_{n+1}\right) - \frac{1}{2}\left(Y_n + X'_{n+1}\right) - \frac{1}{2}D, D\right\rangle + \|D\|^2 \\
&\quad = \left\|X_n - X'_n\right\|^2 + 2\left\langle \frac{1}{2}\left(X_{n+1} + X_n\right) - \frac{1}{2}\left(X'_{n+1} + X'_n\right), D\right\rangle.
\end{aligned}$$

Finally, by the one-sided Lipschitz condition (2.38) on f and the assumption that $L \leq 0$, we obtain

$$\left\|X_{n+1} - X'_{n+1}\right\|^2 \leq \left\|X_n - X'_n\right\|^2,$$

which means that the IAMS (2.37) is B-stable.

5.2 B-stability of linear multi-step methods

5.2.1 Illustrative example

The essential idea of the proof of B-stability is clear when applied to the 1.5-order implicit SLMM:

$$\begin{aligned}
X_n \;=\; & \frac{1}{2}X_{n-1} + \frac{1}{2}X_{n-2} \\
& + \frac{1}{2}\Delta_t\left(f(X_n, \bar{Y}_n) + f(X_{n-1}, \bar{Y}_{n-1}) + f(X_{n-2}, \bar{Y}_{n-2})\right) \\
& + L^1 f(X_{n-1}, \bar{Y}_{n-1})\left(I_{(1,0),t_{n-1}} - \frac{1}{2}I_{(1),t_{n-1}}\Delta_t\right) \\
& + L^0 f(X_{n-1}, \bar{Y}_{n-1})\left(I_{(0,0),t_{n-1}} - \frac{1}{2}I_{(0),t_{n-1}}\Delta_t\right) \\
& + \frac{1}{2}L^1 f(X_{n-2}, \bar{Y}_{n-2})I_{(1,0),t_{n-2}} + \frac{1}{2}L^0 f(X_{n-2}, \bar{Y}_{n-2})I_{(0,0),t_{n-2}}.
\end{aligned} \tag{5.9}$$

The difference of two solutions X_n and X'_n is given by

$$\begin{aligned}
X_n - X'_n \;=\; & \frac{1}{2}(X_{n-1} - X'_{n-1}) + \frac{1}{2}(X_{n-2} - X'_{n-2}) \\
& + \frac{1}{2}\Delta_t\{(f(X_n, \bar{Y}_n) - f(X'_n, \bar{Y}_n)) + (f(X_{n-1}, \bar{Y}_{n-1}) - f(X'_{n-1}, \bar{Y}_{n-1})) \\
& \qquad + (f(X_{n-2}, \bar{Y}_{n-2}) - f(X'_{n-2}, \bar{Y}_{n-2}))\}
\end{aligned}$$

$$
\begin{aligned}
&+\left(I_{(1,0),t_{n-1}}-\frac{1}{2}I_{(1),t_{n-1}}\Delta_t\right)\left(L^1f(X_{n-1},\bar{Y}_{n-1})-L^1f(X'_{n-1},\bar{Y}_{n-1})\right)\\
&+\frac{1}{2}I_{(1,0),t_{n-2}}(L^1f(X_{n-2},\bar{Y}_{n-2})-L^1f(X'_{n-2},\bar{Y}_{n-2}))\\
&+\left(I_{(0,0),t_{n-1}}-\frac{1}{2}I_{(0),t_{n-1}}\Delta_t\right)\left(L^0f(X_{n-1},\bar{Y}_{n-1})-L^0f(X'_{n-1},\bar{Y}_{n-1})\right)\\
&+\frac{1}{2}I_{(0,0),t_{n-2}}(L^0f(X_{n-2},\bar{Y}_{n-2})-L^0f(X'_{n-2},\bar{Y}_{n-2})).
\end{aligned}
$$

Multiplying both sides by $X_n - X'_n$ yields

$$
\begin{aligned}
\|X_n-X'_n\|^2 &= \frac{1}{2}\Delta_t\left\langle f(X_n,\bar{Y}_n)-f(X'_n,\bar{Y}_n),X_n-X'_n\right\rangle\\
&+\frac{1}{2}\left\langle X_{n-1}-X'_{n-1},X_n-X'_n\right\rangle\\
&+\frac{1}{2}\Delta_t\left\langle f(X_{n-1},\bar{Y}_{n-1})-f(X'_{n-1},\bar{Y}_{n-1}),X_n-X'_n\right\rangle\\
&+\left(I_{(1,0),t_{n-1}}-\frac{1}{2}\Delta_tI_{(1),t_{n-1}}\right)\\
&\qquad\cdot\left\langle L^1f(X_{n-1},\bar{Y}_{n-1})-L^1f(X'_{n-1},\bar{Y}_{n-1}),X_n-X'_n\right\rangle\\
&+\left(I_{(0,0),t_{n-1}}-\frac{1}{2}\Delta_tI_{(0),t_{n-1}}\right)\\
&\qquad\cdot\left\langle L^0f(X_{n-1},\bar{Y}_{n-1})-L^0f(X'_{n-1},\bar{Y}_{n-1}),X_n-X'_n\right\rangle\\
&+\frac{1}{2}\left\langle X_{n-2}-X'_{n-2},X_n-X'_n\right\rangle\\
&+\frac{1}{2}\Delta_t\left\langle f(X_{n-2},\bar{Y}_{n-2})-f(X'_{n-2},\bar{Y}_{n-2}),X_n-X'_n\right\rangle\\
&+\frac{1}{2}I_{(1,0),t_{n-2}}\left\langle L^1f(X_{n-2},\bar{Y}_{n-2})-L^1f(X'_{n-2},\bar{Y}_{n-2}),X_n-X'_n\right\rangle\\
&+\frac{1}{2}I_{(0,0),t_{n-2}}\left\langle L^0f(X_{n-2},\bar{Y}_{n-2})-L^0f(X'_{n-2},\bar{Y}_{n-2}),X_n-X'_n\right\rangle.
\end{aligned}
$$

Lipschitz condition $\|L^\alpha id^1_{\mathbf{X}}(X,\bar{Y})-L^\alpha id^1_{\mathbf{X}}(X',\bar{Y})\|\le K\|X-X'\|$ and the one-sided Lipschitz condition (2.38) give

$$
\begin{aligned}
&\left(1-\frac{1}{2}L\Delta_t\right)\|X_n-X'_n\|^2\\
&\quad\le\ \frac{1}{2}\|X_{n-1}-X'_{n-1}\|\,\|X_n-X'_n\|+\frac{1}{2}K\Delta_t\|X_{n-1}-X'_{n-1}\|\,\|X_n-X'_n\|
\end{aligned}
$$

$$
\begin{aligned}
&+\left|I_{(1,0),t_{n-1}}-\frac{1}{2}\Delta_t I_{(1),t_{n-1}}\right| K\,\|X_{n-1}-X'_{n-1}\|\,\|X_n-X'_n\| \\
&+\left|I_{(0,0),t_{n-1}}-\frac{1}{2}\Delta_t I_{(0),t_{n-1}}\right| K\,\|X_{n-1}-X'_{n-1}\|\,\|X_n-X'_n\| \\
&+\frac{1}{2}\|X_{n-2}-X'_{n-2}\|\,\|X_n-X'_n\|+\frac{1}{2}K\Delta_t\|X_{n-2}-X'_{n-2}\|\,\|X_n-X'_n\| \\
&+\frac{1}{2}|I_{(1,0),t_{n-2}}|\,K\,\|X_{n-2}-X'_{n-2}\|\,\|X_n-X'_n\| \\
&+\frac{1}{2}|I_{(0,0),t_{n-2}}|\,K\,\|X_{n-2}-X'_{n-2}\|\,\|X_n-X'_n\|.
\end{aligned}
$$

Thus,

$$
\|X_n-X'_n\|\le\frac{1}{(1-\frac{1}{2}L\Delta_t)}\left(K_{n-1}\|X_{n-1}-X'_{n-1}\|+K_{n-2}\|X_{n-2}-X'_{n-2}\|\right), \tag{5.10}
$$

where

$$
\begin{aligned}
K_{n-1} &= \frac{1}{2}(1+K\Delta_t) \\
&\quad +K\left(|I_{(1,0),t_{n-1}}|+\frac{1}{2}\Delta_t|I_{(1),t_{n-1}}|+I_{(0,0),t_{n-1}}+\frac{1}{2}\Delta_t I_{(0),t_{n-1}}\right) \\
&\sim \frac{1}{2}(1+K\Delta_t)+\mathcal{O}(\Delta_t^{3/2}) \\
K_{n-2} &= \frac{1}{2}(1+K\Delta_t)+K\left(\frac{1}{2}|I_{(1,0),t_{n-2}}|+\frac{1}{2}I_{(0,0),t_{n-2}}\right) \\
&\sim \frac{1}{2}(1+K\Delta_t)+\mathcal{O}(\Delta_t^{3/2}).
\end{aligned}
$$

Subtracting $\|X_{n-2}-X'_{n-2}\|$ from both sides of equation (5.10) then yields

$$
\begin{aligned}
\|X_n-X'_n\|-\|X_{n-2}-X'_{n-2}\| \le \frac{1}{(1-\frac{1}{2}L\Delta_t)}\Big(&K_{n-1}\|X_{n-1}-X'_{n-1}\| \\
&-\left(1-\frac{1}{2}\Delta_t L-K_{n-2}\right)\|X_{n-2}-X'_{n-2}\|\Big),
\end{aligned}
$$

hence,

$$
\begin{aligned}
&\|X_n-X'_n\|-\|X_{n-2}-X'_{n-2}\| \\
&\qquad\le\frac{K_{n-1}}{(1-\frac{1}{2}L\Delta_t)}\left(\|X_{n-1}-X'_{n-1}\|-\|X_{n-2}-X'_{n-2}\|\right)
\end{aligned}
$$

when $K_{n-1} \leq 1 - \frac{1}{2}L\Delta_t - K_{n-2}$. It follows that

$$\|X_n - X'_n\| \leq \|X_{n-1} - X'_{n-1}\|$$

when $L \leq -2K + \mathcal{O}(\Delta_t^{1/2})$. The SLMM (5.9) is thus B-stable for all step sizes $\Delta_t > 0$, provided the dissipativity (given by L) is large enough for the nonlinearities (given by K).

5.2.2 General case

The above argument can be applied to arbitrary higher order s-step SLMMs. For simplicity, take $C_{\emptyset,0} = 1$. Then, the difference of two solutions of the γ-order s-step SLMMs (3.49) is

$$\begin{aligned}
X_n - X'_n &= C_{(0),0}\Delta_t(f(X_n, \bar{Y}_n) - f(X'_n, \bar{Y}_n)) \\
&+ \sum_{j=1}^{s} \Big\{ C_{\emptyset,j}(X_{n-j} - X'_{n-j}) + C_{(0),j}\Delta_t(f(X_{n-j}, \bar{Y}_{n-j}) - f(X'_{n-j}, \bar{Y}_{n-j})) \\
&\quad + \sum_{\alpha \in \Lambda^0_\gamma \setminus \{\emptyset,(0)\}} (C_{\alpha,j} I_{\alpha,t_{n-j}} + C^*_{\alpha,j} I_{\alpha-,t_{n-j}}\Delta_t) \\
&\qquad (L^\alpha id^1_{\mathbf{X}}(X_{n-j}, \bar{Y}_{n-j}) - L^\alpha id^1_{\mathbf{X}}(X'_{n-j}, \bar{Y}_{n-j})) \Big\}.
\end{aligned}$$

This can be estimated in the same manner as above to yield

$$\|X_n - X'_n\| \leq \frac{1}{(1 - C_{(0),0}L\Delta_t)} \sum_{j=1}^{s} K_{n-j}\|X_{n-j} - X'_{n-j}\|, \tag{5.11}$$

where

$$K_{n-j} = C_{\emptyset,j} + C_{(0),j}K\Delta_t + \sum_{\alpha \in \Lambda^0_\gamma \setminus \{\emptyset,(0)\}} K(C_{\alpha,j}|I_{\alpha,t_{n-j}}| + C^*_{\alpha,j}|I_{\alpha-,t_{n-j}}|\Delta_t).$$

Now subtracting $\sum_{j=2}^{s} \|X_{n-j} - X'_{n-j}\|$ from both sides of (5.11) yields

$$\begin{aligned}
&\|X_n - X'_n\| - \sum_{j=2}^{s} \|X_{n-j} - X'_{n-j}\| \\
&\quad \leq \frac{1}{(1 - C_{(0),0}L\Delta_t)} \Bigg(K_{n-1}\|X_{n-1} - X'_{n-1}\| \\
&\qquad\qquad - \sum_{j=2}^{s} (1 - C_{(0),0}L\Delta_t - K_{n-j})\|X_{n-j} - X'_{n-j}\| \Bigg) \\
&\quad \leq \frac{K_{n-1}}{(1 - C_{(0),0}L\Delta_t)} \Bigg(\|X_{n-1} - X'_{n-1}\| - \sum_{j=2}^{s} \|X_{n-j} - X'_{n-j}\| \Bigg),
\end{aligned}$$

provided $K_{n-1} \leq 1 - C_{(0),0} L\Delta_t - K_{n-j}$.

This gives

$$\|X_n - X'_n\| \leq \|X_{n-1} - X'_{n-1}\|,$$

that is, the B-stability of the γ-order s-step SLMM (3.49) when the constant L satisfies

$$L \leq \frac{(1 - K_{n-1} - K_{n-j})}{C_{(0),0}} \Delta_t \leq -\frac{K}{C_{(0),0}} + \mathcal{O}(\Delta_t^{\frac{1}{2}}).$$

Remark 2. *The constants L and K may depend on the sample path as well as the length of the time interval under consideration. The global nature of the one-sided Lipschitz condition and the standard assumptions are not essential for the proof, just convenient.*

Chapter 6

Integrals of stochastic processes

The numerical schemes derived in the previous chapters require the simulation of noise process ζ_t and their integral:

$$I_{(j_1,\ldots,j_l),t_{n-1}} = \int_{t_{n-1}}^{t_n} \cdots \int_{t_{n-1}}^{s_{l-1}} \zeta_{s_l}^{j_l} \cdots \zeta_{s_1}^{j_1} \, ds_l \cdots ds_1$$

on each discretized subinterval $[t_{n-1}, t_n]$. The components ζ_t^j of the driving noise process are assumed to be at least Lebesgue integrable in time, in particular with essentially bounded sample paths.

In general, for processes with continuous or piecewise continuous sample paths, the integrals can be calculated using Riemann sums on much finer partition of the discretization subinterval so that the error is dominated by local discretization error of the scheme itself. For example, the averaged numerical schemes discussed in subsection 2.3.2 require the averaged noise integral:

$$I_{n-1}(\omega) := \frac{1}{\Delta_n} \int_{t_{n-1}}^{t_n} \zeta_s(\omega) \, ds$$

on each discretization subinterval $[t_{n-1}, t_n]$ with step size Δ_n.

On the other hand, some integrals can be simulated directly if the distributions of ζ_t^j are known. For example, if the noise process ζ_t is a Wiener process or an OU process, then sample paths of the integrals can be calculated directly.

In this chapter, four kinds of noise processes, namely a Wiener process, an OU process, a compound Poisson process and an fBm, are introduced and the processes and their integrals are evaluated.

6.1 Wiener process

Denote a Wiener process by $W(t)$ and define the sample path of the integral as

$$I_{t_{n-1}}(W) := \int_{t_{n-1}}^{t_n} W(s)\, ds.$$

For notational clarity the integral will be derived for the time interval $[0, \Delta]$ in this section and define $\Delta W := W_\Delta - W_0$.

The integral $I_{t_{n-1}}(W)$ is an $\mathcal{N}\left(0, \frac{1}{3}\Delta_n^3\right)$-distributed random variable, so the integral $I_n = \frac{1}{\Delta_n} I_{t_{n-1}}(W)$ in the averaged numerical schemes for RODEs can be simulated directly as

$$I_n = \frac{1}{\sqrt{3}} \Delta_n^{1/2}\, G \tag{6.1}$$

where G is an $\mathcal{N}(0,1)$-distributed random variable.

The integral $I_{t_{n-1}}(W)$ arises in the order $\gamma = 1.5$ strong Taylor scheme for Itô stochastic differential equations (see Chapter 10 in [66]). Essentially, $I(W) := \int_0^\Delta W(s)\, ds$ and ΔW are correlated Gaussian random variables with distributions and correlation:

$$\Delta W \sim \mathcal{N}(0, \Delta), \quad I(W) \sim \mathcal{N}\left(0, \frac{1}{3}\Delta^3\right), \quad \mathbb{E}\left(I(W)\Delta W\right) = \frac{1}{2}\Delta^2.$$

The proof follows from the Itô formula to give the identity:

$$d\left(t\, W(t)\right) = t\, dW(t) + W(t)\, dt$$

and the fact that the Itô integral $\int_0^\Delta t\, dW(s)$ is $\mathcal{N}\left(0, \frac{1}{3}\Delta^3\right)$-distributed, since

$$\mathbb{E}\left(\int_0^\Delta t\, dW(t)\right) = 0, \qquad \mathbb{E}\left(\int_0^\Delta t\, dW(t)\right)^2 = \int_0^\Delta t^2\, dt = \frac{1}{3}\Delta^3$$

by basic properties of the Itô integral.

Common sample paths of $I(W)$ and ΔW can be simulated using two independent $\mathcal{N}(0,1)$-distributed random variables G_1 and G_2 via the linear relationship:

$$\Delta W = \Delta^{1/2} G_1, \qquad I(W) = \frac{1}{2}\Delta^{3/2}\left(G_1 + \frac{1}{\sqrt{3}} G_2\right).$$

This is useful for comparing the numerical schemes with the averaged integral simulated directly or approximated as a Riemann sum.

6.2 Ornstein-Uhlenbeck process

Denote an OU process by $O(t)$ and define the sample path of the integral as

$$I_{t_{n-1}}(O) := \int_{t_{n-1}}^{t_n} O(s)\, ds.$$

We assume again that the integral will be derived for the time interval $[0, \Delta]$ and define $\Delta O := O_\Delta - O_0$.

The integral $I_{t_{n-1}}(O)$ is an $\mathcal{N}(0, \mathfrak{s}^2)$-distributed random variable, where the variance $\mathfrak{s}^2$ is given by

$$\mathfrak{s}^2 := \frac{\sigma^2}{\gamma^3}\left(2\gamma\Delta_n - 1 + e^{-\gamma\Delta_n}\right),$$

where γ is a parameter of OU process. The desired integral $I_n = \frac{1}{\Delta_n} I_{t_{n-1}}(O)$ in the averaged numerical schemes for RODEs can thus be simulated directly as

$$I_n = \frac{\mathfrak{s}}{\Delta_n} G \tag{6.2}$$

using an $\mathcal{N}(0, 1)$-distributed random variable G.

To see this, first note that the OU stochastic stationary process $O(t)$ with positive parameters γ and σ, is a solution of the scalar Itô SODE:

$$dX(t) = -\gamma X(t)\, dt + \sigma\, dW(t), \tag{6.3}$$

which has the explicit solution:

$$X(t) = X_0 e^{-\gamma t} + \sigma e^{-\gamma t} \int_0^t e^{\gamma s}\, dW(s). \tag{6.4}$$

Moreover, by (6.4),

$$\Delta Z := O_\Delta - O_0 e^{-\gamma\Delta} = \sigma e^{-\gamma\Delta} \int_0^\Delta e^{\gamma s}\, dW(s),$$

is Gaussian distributed with mean $\mathbb{E}(\Delta Z) = 0$ and, by the Ito isometry, variance:

$$\begin{aligned}
\mathbb{E}(\Delta Z)^2 &= \mathbb{E}\left(\sigma e^{-\gamma\Delta} \int_0^\Delta e^{\gamma s}\, dW(s),\right)^2 \\
&= \sigma^2 e^{-2\gamma\Delta} \int_0^\Delta e^{2\gamma s}\, ds = \frac{\sigma^2}{2\gamma}\left(1 - e^{-2\gamma\Delta}\right).
\end{aligned}$$

Furthermore, by the generalized Itô isometry,

$$\begin{aligned}
\mathbb{E}(\Delta Z \cdot \Delta W) &= \mathbb{E}\left(\sigma e^{-\gamma\Delta} \int_0^\Delta e^{\gamma s}\, dW(s), \int_0^\Delta dW(s),\right) \\
&= \sigma e^{-\gamma\Delta} \int_0^\Delta e^{\gamma s}\, ds = \frac{\sigma}{\gamma}\left(1 - e^{-\gamma\Delta}\right).
\end{aligned}$$

On the other hand, integrating the SODE (6.3) directly for the solution $O(t)$ over the interval $[0, \Delta]$ gives

$$\begin{aligned} I(O) := \int_0^\Delta O(s)\, ds &= \frac{1}{\gamma}\left(\sigma \int_0^\Delta dW(s) - \int_0^\Delta dO(s)\right) \\ &= \frac{\sigma}{\gamma}\Delta W - \frac{1}{\gamma}\left(O_\Delta - O_0\right) \\ &= \frac{\sigma}{\gamma}\Delta W - \frac{1}{\gamma}\Delta Z + \frac{1}{\gamma}\left(1 - e^{-\gamma\Delta}\right) O_0, \end{aligned}$$

so $I(O)$ is Gaussian distributed with mean $\mathbb{E}\left(I(O)\right) = 0$.

Now it is known that, $O(t)$ is given explicitly by

$$O(t) = \sigma e^{-\gamma t} \int_{-\infty}^t e^{\gamma s}\, dW(s),$$

which requires $W(t)$ to be a two-sided Wiener process, i.e., defined for all $t \in \mathbb{R}$, see [5, 20]. Hence

$$O_0 = \sigma \int_{-\infty}^0 e^{\gamma s}\, dW(s),$$

is $\mathcal{N}(0, \sigma^2/(2\gamma))$-distributed by the properties of the Itô integral, in particular by the Itô isometry,

$$\begin{aligned} \mathbb{E}\left(O_0\right) &= \sigma\mathbb{E}\left(\int_{-\infty}^0 e^{\gamma s}\, dW(s)\right) = 0 \\ \mathbb{E}\left(O_0\right)^2 &= \sigma^2\mathbb{E}\left(\int_{-\infty}^0 e^{\gamma s}\, dW(s)\right)^2 = \sigma^2 \int_{-\infty}^0 e^{2\gamma s}\, ds = \frac{\sigma^2}{2\gamma}. \end{aligned}$$

Since O_0 depends on the Wiener process only up to time $t = 0$, it is clearly independent of ΔW and ΔZ. Hence the variance of $I(O)$ is given by

$$\begin{aligned} \mathbb{E}\left(I(O)^2\right) &= \frac{1}{\gamma^2}\Big[\sigma^2\mathbb{E}\left(\Delta W\right)^2 - 2\sigma\mathbb{E}\left(\Delta W, \Delta Z\right) + \mathbb{E}\left(\Delta Z\right)^2 \\ &\qquad + \left(1 - e^{-\gamma\Delta}\right)^2 \mathbb{E}\left(O_0\right)^2\Big] \\ &= \frac{\sigma^2\Delta}{\gamma^2} - \frac{2\sigma^2}{\gamma^3}\left(1 - e^{-\gamma\Delta}\right) + \frac{\sigma^2}{2\gamma^3}\left(1 - e^{-2\gamma\Delta}\right) + \frac{\sigma^2}{2\gamma^3}\left(1 - e^{-\gamma\Delta}\right)^2 \\ &= \frac{\sigma^2}{\gamma^3}\left(\gamma\Delta - 1 + e^{-\gamma\Delta}\right) =: \mathfrak{s}^2. \end{aligned}$$

6.3 Compound Poisson process

A representative example of a noise process with piecewise continuous sample path is the Poisson process, and, more generally, the compound Poisson process, see [25, 43]. A Poisson process $X(t)$ counts the number of events, which are independent of each other, that occur during a given time interval $[0, t]$. It has the probabilities

$$\mathbb{P}\{X(t) = k\} = (\lambda t)^k \frac{e^{-\lambda t}}{k!}, \qquad k = 0, 1, 2, \ldots, \tag{6.5}$$

where λ is a positive real number.

Let T_1 be the time when the first event occurs and let $N(t)$ the number of events occurred until time t. The distribution function of T_1 is

$$F_1(t) = \mathbb{P}\{T_1 \leq t\} = \mathbb{P}\{N(t) \geq 1\} = \sum_{i=1}^{\infty} (\lambda t)^k \frac{e^{-\lambda t}}{k!} = 1 - e^{-\lambda t},$$

which is continuous and monotonically increasing, hence invertible. Thus T_1 can be simulated as $T_1 = F_1^{-1}(t) = \log(1 - U)/\lambda = \log(V)/\lambda$, where U and $V = 1 - U$ are uniformly distributed on $[0, 1]$.

The compound Poisson process is a Poisson process with jumps of random magnitude, which satisfy a distribution function f, for example uniformly distributed on some bounded interval. It is defined by

$$\zeta_t^j = \sum_{i=1}^{N_t} Y_i, \tag{6.6}$$

where Y_i is the jump magnitude at i-th jump. When the jump magnitude $Y_i \equiv 1$ for all i, the compound Poisson process is just a Poisson process.

Typical trajectories of the compound Poisson processes are shown in Figure 6.1.

The compound Poisson process (6.6) is a left-continuous step function. Let $\zeta_t^j = S_i^j$ for $T_i \leq t < T_{i+1}$. If there is no jump in the interval $[t_{n-1}, t_n)$, then the integration of (6.6) can be given as direct integration gives

$$I_{(j),t_{n-1}} = \int_{t_{n-1}}^{t_n} \zeta_s^j \, ds = \int_{t_{n-1}}^{t_n} S_i^j \, ds = S_i^j \Delta_n.$$

On the other hand if $t_{n-1} < T_i < t_n$ and there are no other jumps in this interval, then

$$\begin{aligned} I_{(j),t_{n-1}} = \int_{t_{n-1}}^{t_n} \zeta_s^j \, ds &= \int_{t_{n-1}}^{T_i} S_{i-1}^j ds + \int_{T_i}^{t_n} S_i^j \, ds \\ &= S_{i-1}^j (T_i - t_{n-1}) + S_i^j (t_n - T_i). \end{aligned}$$

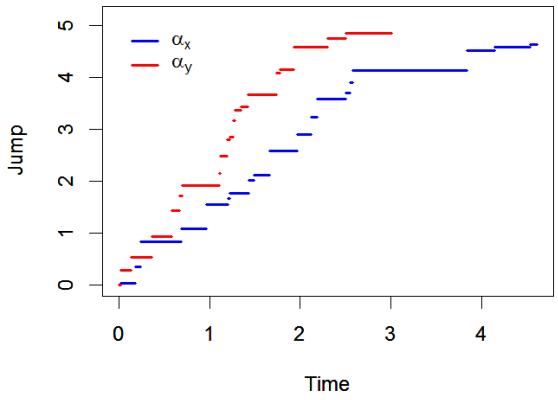

Figure 6.1: Typical trajectories of the compound Poisson processes with $\lambda = 5$ and jumps uniformly distributed on $[0, 0.5]$.

In case there are more jumps on $[t_{n-1}, t_n)$, the given interval is divided into an appropriate number of subintervals and the result summed.

Higher order integrals can be derived in the same manner. Assume that two independent compound Poisson processes $\zeta_t^{j_1}$ and $\zeta_t^{j_2}$ have jumps (only) at T_{i_1} and T_{i_2} on $[t_{n-1}, t_n)$ and their values at the i_1-th and i_2-th jumps are given by $S_{i_1}^{j_1}$ and $S_{i_2}^{j_2}$, respectively. For simplicity, suppose that $t_{n-1} < T_{i_1} < T_{i_2} < t_n$. Then

$$\begin{aligned} I_{(j_1,j_2),t_{n-1}} &= \int_{t_{n-1}}^{t_n}\int_{t_{n-1}}^{s_1} \zeta_{s_1}^{j_1}\zeta_{s_2}^{j_2}\, ds_2 ds_1 \\ &= \int_{t_{n-1}}^{T_{i_1}}\int_{t_{n-1}}^{s_1} S_{i_1-1}^{j_1} S_{i_2-1}^{j_2}\, ds_2 ds_1 + \int_{T_{i_1}}^{T_{i_2}}\int_{T_{i_1}}^{s_1} S_{i_1}^{j_1} S_{i_2-1}^{j_2}\, ds_2 ds_1 \\ &\quad + \int_{T_{i_2}}^{t_n}\int_{T_{i_2}}^{s_1} S_{i_1}^{j_1} S_{i_2}^{j_2}\, ds_2 ds_1 \\ &= \frac{1}{2} S_{i_1-1}^{j_1} S_{i_2-1}^{j_2}(T_{i_1} - t_{n-1})^2 + \frac{1}{2} S_{i_1}^{j_1} S_{i_2-1}^{j_2}(T_{i_2} - T_{i_1})^2 \\ &\quad + \frac{1}{2} S_{i_1}^{j_1} S_{i_2}^{j_2}(t_n - T_{i_2})^2. \end{aligned}$$

On the other hand, if $\zeta_t^{j_1}$ is a stochastic process with continuous sample paths such as a Wiener process $W(t)$ and $\zeta_t^{j_2}$ is an independent compound Poisson process $P(t)$ which has a single jump at time T_{i_2} on $[t_{n-1}, t_n)$ with

value S_{i_2}, then

$$I_{(j_1,j_2),t_{n-1}} = \int_{t_{n-1}}^{t_n}\int_{t_{n-1}}^{s_1} W(s_1)P(s_2)\,ds_2 ds_1$$
$$= S_{i_2-1}\int_{t_{n-1}}^{T_{i_2}} W(s_1)(s_1 - t_{n-1})\,ds_1 + S_{i_2}\int_{T_{i_2}}^{t_n} W(s_1)(s_1 - T_{i_2})\,ds_1.$$

6.4 Fractional Brownian motion

A self-similar process with long range dependence appears in a wide range of applications such as hydrology, geophysics, biology and economy [26]. The idea of such process was first suggested by Kolmogorov and later Mandelbrot & Van Ness introduced the fBm, a family of Gaussian random functions defined by

$$B_H(t) := \frac{1}{\Gamma(H+1/2)}\Big(\int_{-\infty}^{0}\Big[(t-s)^{H-1/2} - (-s)^{H-1/2}\Big]\,dB(s) + \int_0^t (t-s)^{H-1/2} dB(s)\Big), \tag{6.7}$$

where H is a Hurst parameter satisfying $0 < H < 1$ and Γ represents the Gamma function, i.e., $\Gamma(\alpha) := \int_0^\infty x^{\alpha-1}\exp(-x)dx$ [74]. The integrator B is an ordinary Brownian motion and the fBm (6.7) reduces to B when $H = 1/2$.

The fBm is a Gaussian process. It has stationary increments satisfying $\mathbb{E}[B_H(t) - B_H(s)] = 0$ and the variance is given as $\mathbb{E}[(B_H(t) - B_H(s))^2] = |t-s|^{2H}\sigma^2$, where we take $\sigma = 1$ in what follows. In addition, from the self-similar property, the covariance function is given as

$$\mathbb{E}[B_H(t)\,B_H(s)] = \frac{1}{2}(t^{2H} + s^{2H} - |t-s|^{2H}).$$

In literature, a couple of exact and approximate methods have been used to generate fBm [26, 29, 102]. Among them, the Cholesky method, the FFT method and the RMD method [83] are introduced in this section. After generating random Gaussian increments by the above three methods, $B_H(t)$ is obtained by summing up the increments appropriately.

The Riemann integral of the fBm is defined as

$$I_{t_{i-1}}(B_H) := \int_{t_{i-1}}^{t_i} B_H(s)\,ds, \tag{6.8}$$

and we can approximate (6.8) by the Riemann sums as

$$I_{t_{i-1}}(B_H) \approx \Delta_I \sum_{k=1}^{m} B_H(t_{i-1} + k\Delta_I), \tag{6.9}$$

where $\Delta_I = \Delta_t/m$ for $\Delta_t = t_i - t_{i-1}$ and m sufficiently large to achieve the desired accuracy.

For example, in order to achieve Δ_t^2-order convergence, the difference between $I_{t_{i-1}}(B_H)$ and the Riemann sum should be Δ_t^3-order, i.e.,

$$\left| \int_{t_{i-1}}^{t_i} B_H(s)\, ds - \Delta_I \sum_{k=1}^{m} B_H(t_{i-1} + k\Delta_I) \right| \leq C\Delta_t^3, \tag{6.10}$$

for some constant $C > 0$. By Hölder condition, the left hand side of the equation (6.10) can be evaluated as follows:

$$\begin{aligned}
&\left| \int_{t_{i-1}}^{t_i} B_H(s)\, ds - \Delta_I \sum_{k=1}^{m} B_H(t_{i-1} + k\Delta_I) \right| \\
&\leq \sum_{k=1}^{m} \int_{t_{i-1}+(k-1)\Delta_I}^{t_{i-1}+k\Delta_I} \left| B_H(s) - B_H(t_{i-1} + k\Delta_I) \right| ds \\
&\leq \sum_{k=1}^{m} \int_{t_{i-1}+(k-1)\Delta_I}^{t_{i-1}+k\Delta_I} C_\epsilon \left| s - (t_{i-1} + k\Delta_I) \right|^{H-\epsilon} ds \\
&= -\frac{C_\epsilon}{H+1-\epsilon} \sum_{k=1}^{m} [((t_{i-1} + k\Delta_I) - s)^{H+1-\epsilon}]_{t_{i-1}+(k-1)\Delta_I}^{t_{i-1}+k\Delta_I} \\
&= \frac{C_\epsilon}{H+1-\epsilon} \sum_{k=1}^{m} \left((t_{i-1} + k\Delta_I) - (t_{i-1} + (k-1)\Delta_I)\right)^{H+1-\epsilon} \\
&= \frac{C_\epsilon}{H+1-\epsilon} \sum_{k=1}^{m} \Delta_I^{H+1-\epsilon} = \frac{C_\epsilon}{H+1-\epsilon} (m\Delta_I)\Delta_I^{H-\epsilon} = \frac{C_\epsilon}{H+1-\epsilon} \Delta_t \Delta_I^{H-\epsilon},
\end{aligned}$$

where $C_\epsilon \geq 0$ is a random variable depending only on ϵ. This means that the Δ_t^2-order convergence can be attained if the following inequality holds

$$\frac{C_\epsilon}{H+1-\epsilon} \Delta_I^{H-\epsilon} \leq C\Delta_t^2,$$

i.e., the condition $\Delta_I^{H-\epsilon} \leq C'(H+1-\epsilon)\Delta_t^2$, where $C' = C/C_\epsilon$, is necessary for Δ_t^2-order convergence (see also [38, 64, 94, 95]).

We can generate $B_H(t)$ with very small step size in order to have $I(B_H) := \int_0^\Delta B_H(s)ds$ with the desired order, however, solving large covariance matrix is time consuming, e.g., Cholesky decomposition requires n^3-order time for $n \times n$ matrix and it becomes $(10 \times n)^3$-order if we take $m = 10$ in (6.9). To avoid this large calculation, we generate first $B_H(t)$ by the above three methods and then generate intermediate points on each interval $[t_{i-1}, t_i]$ by the RMD method.

There is a different approach to avoid the calculation of the Riemann sums, i.e., (6.9). The idea is that we estimate the covariance matrix of fBm and its integral and calculate the square root of it. Then we generate $B_H(t)$ and its Riemann integral $I(B_H)$ simultaneously.

6.4.1 Covariance matrix of $B_H(t)$

In order to generate $B_H(t)$, firstly we generate the covariance matrix:

$$G_{11} = (\mathbb{E}[X_i\, X_j])_{i,j}, \tag{6.11}$$

where

$$(X_i, X_j) = (B_H(t_i) - B_H(t_{i-1}), B_H(t_j) - B_H(t_{j-1}))\,,$$

for i, $j = 1, \ldots, n$. For simplicity, we assume an equidistant partition on a given interval $[t_0, t_n]$ and $\Delta_t = t_i - t_{i-1}$ for $i = 1, \ldots, n$.

(1) $G_{11} = (\mathbb{E}[X_i\, X_j])_{i,j}$

$$\begin{aligned}
&\mathbb{E}[(B_H(t_i) - B_H(t_{i-1}))\,(B_H(t_j) - B_H(t_{j-1}))] \\
&= \mathbb{E}[B_H(t_i)B_H(t_j) - B_H(t_i)B_H(t_{j-1}) - B_H(t_{i-1})B_H(t_j) \\
&\qquad\qquad + B_H(t_{i-1})B_H(t_{j-1})] \\
&= \frac{1}{2}\Big((t_i^{2H} + t_j^{2H} - |t_i - t_j|^{2H}) - (t_i^{2H} + t_{j-1}^{2H} - |t_i - t_{j-1}|^{2H}) \\
&\qquad\qquad - (t_{i-1}^{2H} + t_j^{2H} - |t_{i-1} - t_j|^{2H}) + (t_{i-1}^{2H} + t_{j-1}^{2H} - |t_{i-1} - t_{j-1}|^{2H})\Big) \\
&= \frac{1}{2}(-\underbrace{|t_i - t_j|^{2H}}_{a} + \underbrace{|t_i - t_{j-1}|^{2H}}_{b} + \underbrace{|t_{i-1} - t_j|^{2H}}_{c} - \underbrace{|t_{i-1} - t_{j-1}|^{2H}}_{d}).
\end{aligned} \tag{6.12}$$

(i) Case $t_i = t_j$

The two terms a and d in (6.12) are canceled out and we have

$$(6.12) = (t_i - t_{i-1})^{2H} = \Delta_t^{2H}. \tag{6.13}$$

(ii) Case $t_i > t_j$

$$\begin{aligned}
(6.12) &= -\frac{1}{2}\left((t_i - t_j)^{2H} - (t_{i-1} - t_j)^{2H} - (t_i - t_{j-1})^{2H} + (t_{i-1} - t_{j-1})^{2H}\right) \\
&= \frac{1}{2}\Delta_t^{2H}\left(-2k^{2H} + (k-1)^{2H} + (k+1)^{2H}\right),
\end{aligned} \tag{6.14}$$

where $t_i - t_j = k\Delta_t$.

(iii) Case $t_i < t_j$

$$(6.12) = -\frac{1}{2}\left((t_j - t_i)^{2H} - (t_{j-1} - t_i)^{2H} - (t_j - t_{i-1})^{2H} + (t_{j-1} - t_{i-1})^{2H}\right)$$

$$= \frac{1}{2}\Delta_t^{2H}\left(-2k^{2H} + (k-1)^{2H} + (k+1)^{2H}\right), \tag{6.15}$$

where $t_j - t_i = k\Delta_t$.

The equations (6.13), (6.14) and (6.15) give the covariance matrix G_{11} as

$$G_{11} = \begin{pmatrix} \alpha_0 & \alpha_1 & \alpha_2 & \cdots & \alpha_{n-1} \\ \alpha_1 & \alpha_0 & \alpha_1 & \cdots & \alpha_{n-2} \\ \alpha_2 & \alpha_1 & \alpha_0 & \cdots & \alpha_{n-3} \\ \vdots & \vdots & \vdots & \ddots & \vdots \\ \alpha_{n-1} & \alpha_{n-2} & \alpha_{n-3} & \cdots & \alpha_0 \end{pmatrix}, \tag{6.16}$$

where α_0 is given by (6.13), α_i by (6.14).

The Cholesky method

The matrix (6.16) is always positive definite due to the local non-determinism of fBm [103]. Then it has a Cholesky decomposition and it is given as

$$G_{11} = L\Lambda L^T = (L\sqrt{\Lambda})\,(\sqrt{\Lambda}L^T) = (L\sqrt{\Lambda})\,(L\sqrt{\Lambda})^T = \tilde{L}\,\tilde{L}^T,$$

where L is a lower triangular matrix and Λ is a matrix of eigenvalues, i.e., $\Lambda = \mathrm{diag}(\lambda_0, \ldots, \lambda_{n-1})$ with eigenvalues λ_i for $i = 0, \ldots, n-1$ [61].

Suppose that the matrix $\tilde{L}$ is given by

$$\tilde{L} = \begin{pmatrix} l_{1,1} & 0 & \cdots & 0 \\ l_{2,1} & l_{2,2} & \cdots & 0 \\ \vdots & \vdots & \ddots & \vdots \\ l_{n,1} & l_{n,2} & \cdots & l_{n,n} \end{pmatrix}.$$

Prepare a vector $\mathbf{n} = (n_1, n_2, \ldots, n_n)$ which has independent and identically distributed (iid) $\mathcal{N}(0,1)$ components. The product of $\tilde{L}$ and $\mathbf{n}^T$:

$$\begin{pmatrix} l_{1,1} & 0 & \cdots & 0 \\ l_{2,1} & l_{2,2} & \cdots & 0 \\ \vdots & \vdots & \ddots & \vdots \\ l_{n,1} & l_{n,2} & \cdots & l_{n,n} \end{pmatrix} (n_1, n_2, \ldots, n_n)^T = \begin{pmatrix} l_{1,1}n_1 \\ \sum_{i=1}^{2} l_{2,i}n_i \\ \vdots \\ \sum_{i=1}^{n} l_{n,i}n_i \end{pmatrix} = \begin{pmatrix} X_1 \\ X_2 \\ \vdots \\ X_n \end{pmatrix}$$

gives the increments of fBm, i.e., $B_H(t_i) - B_H(t_{i-1})$ for $i = 1, \ldots, n$.

Now we take $B_H(t_0) = 0$ and

$$\begin{aligned} B_H(t_1) - B_H(t_0) &= X_1 \\ B_H(t_1) &= X_1. \end{aligned}$$

Similarly

$$\begin{aligned} B_H(t_2) - B_H(t_1) &= X_2 \\ B_H(t_2) &= X_2 + B_H(t_1) = \sum_{j=1}^{2} X_j. \end{aligned}$$

This means

$$B_H(t_m) = \sum_{j=1}^{m} X_j. \tag{6.17}$$

The fast Fourier transformation

The idea of using the FFT was firstly introduced by Davies & Harte [27] and later it was generalized by Dietrich & Newsam [30] and Wood & Chan [102]. Similar to Cholesky decomposition, the method estimate the square root of the covariance matrix G_{11}, however, it can be applied only to matrices of size $2^s \times 2^s$ where $s \in \mathbb{N}$. When $n < 2^s$ for some $s \in \mathbb{N}$, we need to embed G_{11} firstly in a Toeplitz matrix G_{11}^* of size $2^s \times 2^s$. Then G_{11}^* is embedded in a circulant matrix C_{11} of size 2^{s+1}.

For simplicity, we assume that $n = 2^s$ for some $s \in \mathbb{N}$, i.e., we do not have to consider about embedding G_{11} in G_{11}^*. The circulant matrix C_{11} of size $2n = 2^{s+1}$ can be obtained in the following manner:

$$C_{11} = \begin{pmatrix} \alpha_0 & \alpha_1 & \alpha_2 & \cdots & \alpha_{n-1} & \Phi & \alpha_{n-1} & \alpha_{n-2} & \cdots & \alpha_1 \\ \alpha_1 & \alpha_0 & \alpha_1 & \cdots & \alpha_{n-2} & \alpha_{n-1} & \Phi & \alpha_{n-1} & \cdots & \alpha_2 \\ \alpha_2 & \alpha_1 & \alpha_0 & \cdots & \alpha_{n-3} & \alpha_{n-2} & \alpha_{n-1} & \Phi & \cdots & \alpha_3 \\ \vdots & \vdots & \vdots & \ddots & \vdots & \vdots & \vdots & \vdots & \ddots & \vdots \\ \alpha_{n-1} & \alpha_{n-2} & \alpha_{n-3} & \cdots & \alpha_0 & \alpha_1 & \alpha_2 & \alpha_3 & \cdots & \Phi \\ \Phi & \alpha_{n-1} & \alpha_{n-2} & \cdots & \alpha_1 & \alpha_0 & \alpha_1 & \alpha_2 & \cdots & \alpha_{n-1} \\ \alpha_{n-1} & \Phi & \alpha_{n-1} & \cdots & \alpha_2 & \alpha_1 & \alpha_0 & \alpha_1 & \cdots & \alpha_{n-2} \\ \alpha_{n-2} & \alpha_{n-1} & \Phi & \cdots & \alpha_3 & \alpha_2 & \alpha_1 & \alpha_0 & \cdots & \alpha_{n-3} \\ \vdots & \vdots & \vdots & \ddots & \vdots & \vdots & \vdots & \vdots & \ddots & \vdots \\ \alpha_1 & \alpha_2 & \alpha_3 & \cdots & \Phi & \alpha_{n-1} & \alpha_{n-2} & \alpha_{n-3} & \cdots & \alpha_0 \end{pmatrix}, \tag{6.18}$$

where Φ is arbitrary. Then we generate a random vector $X \sim \mathcal{N}(0, G_{11})$ as follows (see details in [26, 29]).

Define $Y = Q\Lambda^{1/2}Q^*Z$ where $\Lambda^{1/2} = \operatorname{diag}\{\lambda_0^{1/2}, \ldots, \lambda_{2n-1}^{1/2}\}$ and $Z = (Z_0, \ldots, Z_{2n-1})^T$ is a vector of independent $\mathcal{N}(0,1)$ random variables. Then

$Y \sim \mathcal{N}(0, C_{11})$ because Q is unitary. If we take a subvector $X = (Y_0, \ldots, Y_{n-1})$, X has the desired property, i.e., $X \sim \mathcal{N}(0, G_{11})$.

Step 1.
The fast Fourier transform is performed to the elements of the first row of the matrix C_{11} in order to determine the eigenvalues Λ:

$$\lambda_k = \sum_{j=0}^{2n-1} \alpha_k \exp\left(-\frac{2\pi i j k}{2n}\right),$$

for $k = 0, \cdots, 2n-1$.

Step 2.
Generate random numbers $Z \sim \mathcal{N}(0, 1)$ and determine $W = \Lambda^{1/2} Q^* Z$. $Q^* Z$ can be generated in the following manner:

- Generate two standard normal random variables for $Q^* Z_0$ and $Q^* Z_n$, the first and n-th elements.
- For $1 \leq j < n$, generate two independent standard normal random variables $V_j^{(1)}$ and $V_j^{(2)}$ and calculate

$$\begin{aligned} Q^* Z_j &= \frac{1}{\sqrt{2}}\left(V_j^{(1)} + i V_j^{(2)}\right) \\ Q^* Z_{2n-j} &= \frac{1}{\sqrt{2}}\left(V_j^{(1)} - i V_j^{(2)}\right). \end{aligned}$$

Step 3.
Generate Y by the fast Fourier transform and X can be obtained by picking up n elements from the top of Y:

$$X\left(\frac{k}{n}\right) = \sum_{j=0}^{2n-1} \frac{1}{\sqrt{2n}} W_j \exp\left(-\frac{2\pi i j k}{2n}\right),$$

for $k = 0, \ldots, n-1$.

We sum up the generated Gaussian noise as we did in Cholesky decomposition case and the fBm at time t_m can be obtained as (6.17).

The random midpoint displacement method

The RMD method was first introduced by Fournier et al. as a method to generate fractal terrains [34]. The base idea of the RMD method is bisection and interpolation and it generates intermediate points keeping the original property of fBm on a given interval. The Figure 6.2 illustrates the first two steps of RMD method [86].

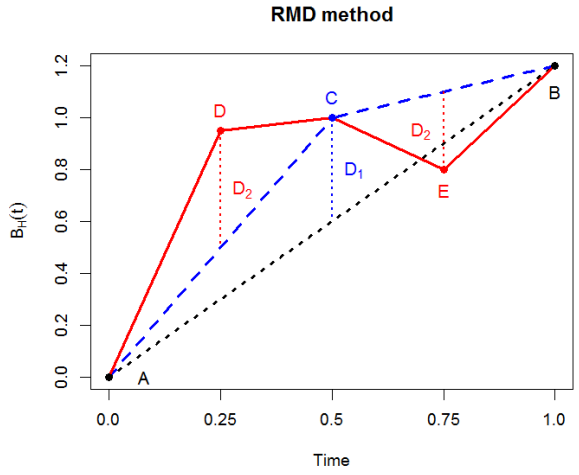

Figure 6.2: The first two steps of the RMD method.

Assume that A and B are points at $t = 0$ and 1 and denote their values by $X(0)$ and $X(1)$, respectively. The process is fBm and the increment has mean 0 and variance:

$$\mathbb{V}[X(t_2) - X(t_1)] = |t_2 - t_1|^{2H}\sigma^2, \tag{6.19}$$

for some $0 \leq t_1 \leq t_2 \leq 1$.

The point C is a midpoint between A and B and $t = 0.5$. $X(0.25)$ is then given as the sum of the average of $X(0)$ and $X(1)$ and a Gaussian random offset D_1 with mean 0 and variance Δ_1^2, i.e.,

$$X(0.5) = \frac{1}{2}(X(1) + X(0)) + D_1. \tag{6.20}$$

Now we subtract $X(0)$ from both sides of the equation (6.20) and take the variance:

$$\mathbb{V}\left[X(0.5) - X(0)\right] = \mathbb{V}\left[\frac{1}{2}(X(1) - X(0)) + D_1\right] = \frac{1}{4}\sigma^2 + \Delta_1^2. \tag{6.21}$$

By the equation (6.19), the left hand side of the equation (6.21) is $(1/2)^{2H}\sigma^2$ and this gives

$$\Delta_1^2 = \left(\left(\frac{1}{2}\right)^{2H} - \frac{1}{4}\right)\sigma^2.$$

The points D and E are midpoints between A and C and C and B and $t = 0.25$ and 0.75, respectively. $X(0.25)$ and $X(0.75)$ are then given in the

same manner as

$$X(0.25) = \frac{1}{2}(X(0.5) + X(0)) + D_2, \qquad X(0.75) = \frac{1}{2}(X(1) + X(0.5)) + D_2, \tag{6.22}$$

where D_2 is a Gaussian random offset with mean 0 and variance Δ_2^2. Subtracting $X(0)$ from the both sides of the first equation in (6.22) and taking variance give

$$\mathbb{V}\left[X(0.25) - X(0)\right] = \mathbb{V}\left[\frac{1}{2}(X(0.5) - X(0)) + D_2\right] = \frac{1}{4}\left(\frac{1}{2}\right)^{2H}\sigma^2 + \Delta_2^2. \tag{6.23}$$

The left hand side of the equation (6.23) is $(1/4)^{2H}\sigma^2$ and

$$\Delta_2^2 = \left(\left(\frac{1}{4}\right)^{2H} - \frac{1}{4}\left(\frac{1}{2}\right)^{2H}\right)\sigma^2.$$

This argument yields the variance of the midpoint displacement D_n at n-step as

$$\Delta_n^2 = \frac{1}{(2^n)^{2H}}\left(1 - 2^{2H-2}\right)\sigma^2.$$

After generating $B_H(t)$ by the Cholesky decomposition or the FFT, we generate enough intermediate points on each subinterval by the RMD method to have the desired resolution. In general, the RMD method requires n-order computational costs when n points are needed and combining Cholesky decomposition or the FFT with the RMD method is much faster than estimating the square root of the large covariance matrix and calculating the Riemann sums although the RMD method is not exact while the Cholesky decomposition and the FFT are.

6.4.2 $B_H(t)$ and $I(B_H)$ by the Cholesky method

In order to generate fBm, $B_H(t)$, and the Riemann integral of fBm, $I(B_H)$, simultaneously, firstly we generate the full covariance matrix:

$$G = \begin{pmatrix} G_{11} & G_{12} \\ G_{21} & G_{22} \end{pmatrix} = \begin{pmatrix} (\mathbb{E}[X_i\, X_j])_{i,j} & (\mathbb{E}[X_i\, Y_j])_{i,j} \\ (\mathbb{E}[Y_i\, X_j])_{i,j} & (\mathbb{E}[Y_i\, Y_j])_{i,j} \end{pmatrix}, \tag{6.24}$$

where

$$
\begin{aligned}
(X_i, X_j) &= (B_H(t_i) - B_H(t_{i-1}), B_H(t_j) - B_H(t_{j-1}))\,, \\
(X_i, Y_j) &= \left(B_H(t_i) - B_H(t_{i-1}), \int_{t_{j-1}}^{t_j} (B_H(t) - B_H(t_{j-1}))dt \right), \\
(Y_i, X_j) &= \left(\int_{t_{i-1}}^{t_i} (B_H(t) - B_H(t_{i-1}))dt, B_H(t_j) - B_H(t_{j-1}) \right), \\
(Y_i, Y_j) &= \left(\int_{t_{i-1}}^{t_i} (B_H(t) - B_H(t_{i-1}))dt, \int_{t_{j-1}}^{t_j} (B_H(t) - B_H(t_{j-1}))dt \right),
\end{aligned}
$$

for $i, j = 1, \cdots, n$. Then we estimate each covariance matrix and sum them up. For simplicity, we assume again an equidistant partition on a given interval $[t_0, t_n]$ and $\Delta_t = t_i - t_{i-1}$ for $i = 1, \ldots, n$.

(1) $G_{11} = (\mathbb{E}[X_i\, X_j])_{i,j}$

As we see in subsection 6.4.1, the covariance matrix G_{11} is given as (6.16).

(2) $G_{21} = (\mathbb{E}[Y_i\, X_j])_{i,j}$

$$
\begin{aligned}
&\int_{t_{i-1}}^{t_i} \mathbb{E}[(B_H(t) - B_H(t_{i-1}))\,(B_H(t_j) - B_H(t_{j-1}))]dt \\
&= \int_{t_{i-1}}^{t_i} \mathbb{E}[B_H(t)B_H(t_j) - B_H(t)B_H(t_{j-1}) - B_H(t_{i-1})B_H(t_j) \\
&\qquad\qquad + B_H(t_{i-1})B_H(t_{j-1})]dt \\
&= \frac{1}{2}\int_{t_{i-1}}^{t_i} \Big((t^{2H} + t_j^{2H} - |t - t_j|^{2H}) - (t^{2H} + t_{j-1}^{2H} - |t - t_{j-1}|^{2H}) \\
&\qquad -(t_{i-1}^{2H} + t_j^{2H} - |t_{i-1} - t_j|^{2H}) + (t_{i-1}^{2H} + t_{j-1}^{2H} - |t_{i-1} - t_{j-1}|^{2H}) \Big) dt \\
&= \frac{1}{2}\int_{t_{i-1}}^{t_i} (-\underbrace{|t - t_j|^{2H}}_{e} + \underbrace{|t - t_{j-1}|^{2H}}_{f} + \underbrace{|t_{i-1} - t_j|^{2H}}_{g} - \underbrace{|t_{i-1} - t_{j-1}|^{2H}}_{h})dt.
\end{aligned}
\tag{6.25}
$$

Compute terms e, f, g and h separately again.

(i) Case $t_i = t_j$: $t \in [t_{i-1}, t_i]$ gives $t - t_j \le 0$, $t - t_{j-1} \ge 0$, $t_{i-1} - t_j < 0$ and $t_{i-1} - t_{j-1} = 0$.

Term e:

$$\begin{aligned}\frac{1}{2}\int_{t_{i-1}}^{t_i}(-|t-t_j|^{2H})dt &= -\frac{1}{2}\int_{t_{i-1}}^{t_i}(t_i-t)^{2H}dt \\ &= -\frac{1}{2(2H+1)}(t_i-t_{i-1})^{2H+1}.\end{aligned}$$

Term f:

$$\frac{1}{2}\int_{t_{i-1}}^{t_i}|t-t_{j-1}|^{2H}dt = \frac{1}{2}\int_{t_{i-1}}^{t_i}(t-t_{i-1})^{2H}dt = \frac{1}{2(2H+1)}(t_i-t_{i-1})^{2H+1}.$$

Term g:

$$\frac{1}{2}\int_{t_{i-1}}^{t_i}|t_{i-1}-t_j|^{2H}dt = \frac{1}{2}\int_{t_{i-1}}^{t_i}(t_i-t_{i-1})^{2H}dt = \frac{1}{2}(t_i-t_{i-1})^{2H+1}.$$

Substituting e, f and g in (6.25) yields

$$(6.29) = \frac{1}{2}(t_i-t_{i-1})^{2H+1} = \frac{1}{2}\Delta_t^{2H+1}. \tag{6.26}$$

(ii) Case $t_i > t_j$: $t \in [t_{i-1}, t_i]$ gives $t - t_j \geq 0$, $t - t_{j-1} > 0$, $t_{i-1} - t_j \geq 0$ and $t_{i-1} - t_{j-1} > 0$.

Term e:

$$\begin{aligned}\frac{1}{2}\int_{t_{i-1}}^{t_i}(-|t-t_j|^{2H})dt &= -\frac{1}{2}\int_{t_{i-1}}^{t_i}(t-t_j)^{2H}dt \\ &= -\frac{1}{2(2H+1)}\left((t_i-t_j)^{2H+1}-(t_{i-1}-t_j)^{2H+1}\right).\end{aligned}$$

Term f:

$$\begin{aligned}\frac{1}{2}\int_{t_{i-1}}^{t_i}|t-t_{j-1}|^{2H}dt &= \frac{1}{2}\int_{t_{i-1}}^{t_i}(t-t_{j-1})^{2H}dt \\ &= \frac{1}{2(2H+1)}\left((t_i-t_{j-1})^{2H+1}-(t_{i-1}-t_{j-1})^{2H+1}\right).\end{aligned}$$

Term g:

$$\frac{1}{2}\int_{t_{i-1}}^{t_i}|t_{i-1}-t_j|^{2H}dt = \frac{1}{2}\int_{t_{i-1}}^{t_i}(t_{i-1}-t_j)^{2H}dt = \frac{1}{2}(t_i-t_{i-1})(t_{i-1}-t_j)^{2H}.$$

Term h:

$$\begin{aligned}\frac{1}{2}\int_{t_{i-1}}^{t_i}(-|t_{i-1}-t_{j-1}|^{2H})dt &= -\frac{1}{2}\int_{t_{i-1}}^{t_i}(t_{i-1}-t_{j-1})^{2H}dt \\ &= -\frac{1}{2}(t_i-t_{i-1})(t_{i-1}-t_{j-1})^{2H}.\end{aligned}$$

Substituting e, f, g and h in (6.25) gives

$$\begin{aligned}(6.25) &= -\frac{1}{2}\Big\{\frac{1}{2H+1}\Big((t_i-t_j)^{2H+1}-(t_{i-1}-t_j)^{2H+1} \\ &\qquad -(t_i-t_{j-1})^{2H+1}+(t_{i-1}-t_{j-1})^{2H+1}\Big) \\ &\qquad -(t_i-t_{i-1})(t_{i-1}-t_j)^{2H}+(t_i-t_{i-1})(t_{i-1}-t_{j-1})^{2H}\Big\} \\ &= -\frac{1}{2}\Delta_t^{2H+1}\Big(\frac{1}{2H+1}\left(2k^{2H+1}-(k-1)^{2H+1}-(k+1)^{2H+1}\right) \\ &\qquad -(k-1)^{2H}+k^{2H}\Big), \qquad (6.27)\end{aligned}$$

where $t_i - t_j = k\Delta_t$.

(iii) Case $t_i < t_j$: $t \in [t_{i-1}, t_i]$ gives $t - t_j < 0$, $t - t_{j-1} \leq 0$, $t_{i-1} - t_j < 0$ and $t_{i-1} - t_{j-1} < 0$.

The equation (6.25) can be estimated in the same manner with the case $t_i > t_j$ and

$$\begin{aligned}(6.25) &= \frac{1}{2}\Big\{\frac{1}{2H+1}\Big((t_j-t_i)^{2H+1}-(t_{j-1}-t_i)^{2H+1} \\ &\qquad -(t_j-t_{i-1})^{2H+1}+(t_{j-1}-t_{i-1})^{2H+1}\Big) \\ &\qquad +(t_i-t_{i-1})(t_j-t_{i-1})^{2H}-(t_i-t_{i-1})(t_{j-1}-t_{i-1})^{2H}\Big\} \\ &= \frac{1}{2}\Delta_t^{2H+1}\Big(\frac{1}{2H+1}\left(2k^{2H+1}-(k-1)^{2H+1}-(k+1)^{2H+1}\right) \\ &\qquad +(k+1)^{2H}-k^{2H}\Big), \qquad (6.28)\end{aligned}$$

where $t_j - t_i = k\Delta_t$.

(3) $G_{12} = (\mathbb{E}[X_i\, Y_j])_{i,j}$

The argument for G_{21} can be applied to $G_{12} = (\mathbb{E}[X_i\, Y_j])_{i,j}$.

$$\int_{t_{j-1}}^{t_j} \mathbb{E}[(B_H(t_i) - B_H(t_{i-1}))\,(B_H(s) - B_H(t_{j-1}))]ds$$

$$= \int_{t_{j-1}}^{t_j} \mathbb{E}[B_H(t_i)B_H(s) - B_H(t_i)B_H(t_{j-1}) - B_H(t_{i-1})B_H(s) + B_H(t_{i-1})B_H(t_{j-1})]ds$$

$$= \frac{1}{2}\int_{t_{j-1}}^{t_j} \Big((t_i^{2H} + s^{2H} - |t_i - s|^{2H}) - (t_i^{2H} + t_{j-1}^{2H} - |t_i - t_{j-1}|^{2H}) - (t_{i-1}^{2H} + s^{2H} - |t_{i-1} - s|^{2H}) + (t_{i-1}^{2H} + t_{j-1}^{2H} - |t_{i-1} - t_{j-1}|^{2H})\Big)ds$$

$$= \frac{1}{2}\int_{t_{j-1}}^{t_j} (-\underbrace{|t_i - s|^{2H}}_{i} + \underbrace{|t_i - t_{j-1}|^{2H}}_{j} + \underbrace{|t_{i-1} - s|^{2H}}_{k} - \underbrace{|t_{i-1} - t_{j-1}|^{2H}}_{l})ds. \tag{6.29}$$

(i) Case $t_i = t_j$

Obviously

$$(6.29) = \frac{1}{2}(t_i - t_{i-1})^{2H+1} = \frac{1}{2}\Delta_t^{2H+1}. \tag{6.30}$$

(ii) Case $t_i > t_j$

The equation (6.29) can be estimated in the same manner with (6.25) and

$$\begin{aligned}(6.29) &= \frac{1}{2}\Big\{\frac{1}{2H+1}\Big((t_i - t_j)^{2H+1} - (t_{i-1} - t_j)^{2H+1} - (t_i - t_{j-1})^{2H+1} + (t_{i-1} - t_{j-1})^{2H+1}\Big) \\ &\quad + (t_j - t_{j-1})(t_i - t_{j-1})^{2H} - (t_j - t_{j-1})(t_{i-1} - t_{j-1})^{2H}\Big\} \\ &= \frac{1}{2}\Delta_t^{2H+1}\Big(\frac{1}{2H+1}\left(2k^{2H+1} - (k-1)^{2H+1} - (k+1)^{2H+1}\right) \\ &\quad + (k+1)^{2H} - k^{2H}\Big),\end{aligned} \tag{6.31}$$

where $t_i - t_j = k\Delta_t$.

(iii) Case $t_i < t_j$

Similarly

$$
\begin{aligned}
(6.29) \quad &= -\frac{1}{2}\Big\{\frac{1}{2H+1}\Big((t_j-t_i)^{2H+1}-(t_{j-1}-t_i)^{2H+1} \\
&\qquad -(t_j-t_{i-1})^{2H+1}+(t_{j-1}-t_{i-1})^{2H+1}\Big) \\
&\qquad -(t_j-t_{j-1})(t_{j-1}-t_i)^{2H}+(t_j-t_{j-1})(t_{j-1}-t_{i-1})^{2H}\Big\} \\
&= -\frac{1}{2}\Delta_t^{2H+1}\Big(\frac{1}{2H+1}\left(2k^{2H+1}-(k-1)^{2H+1}-(k+1)^{2H+1}\right) \\
&\qquad -(k-1)^{2H}+k^{2H}\Big), \qquad (6.32)
\end{aligned}
$$

where $t_j - t_i = k\Delta_t$.

(4) $G_{22} = (\mathbb{E}[Y_i\, Y_j])_{i,j}$

$$
\begin{aligned}
&\int_{t_{i-1}}^{t_i}\int_{t_{j-1}}^{t_j}\mathbb{E}[(B_H(t)-B_H(t_{i-1}))\,(B_H(s)-B_H(t_{j-1}))]dsdt \\
&= \int_{t_{i-1}}^{t_i}\int_{t_{j-1}}^{t_j}\mathbb{E}[B_H(t)B_H(s)-B_H(t)B_H(t_{j-1})-B_H(t_{i-1})B_H(s) \\
&\qquad +B_H(t_{i-1})B_H(t_{j-1})]dsdt \\
&= \frac{1}{2}\int_{t_{i-1}}^{t_i}\int_{t_{j-1}}^{t_j}\Big((t^{2H}+s^{2H}-|t-s|^{2H})-(t^{2H}+t_{j-1}^{2H}-|t-t_{j-1}|^{2H}) \\
&\qquad -(t_{i-1}^{2H}+s^{2H}-|t_{i-1}-s|^{2H})+(t_{i-1}^{2H}+t_{j-1}^{2H}-|t_{i-1}-t_{j-1}|^{2H})\Big)dsdt \\
&= \frac{1}{2}\int_{t_{i-1}}^{t_i}\int_{t_{j-1}}^{t_j}(-\underbrace{|t-s|^{2H}}_{m}+\underbrace{|t-t_{j-1}|^{2H}}_{n}+\underbrace{|t_{i-1}-s|^{2H}}_{o}-\underbrace{|t_{i-1}-t_{j-1}|^{2H}}_{p})dsdt. \qquad (6.33)
\end{aligned}
$$

Compute m, n, o and p separately.

(i) Case $t_i = t_j$: $t,\ s \in [t_{i-1}, t_i]$ gives $t - t_{j-1} \geq 0$ and $t_{i-1} - s \leq 0$. In addition, $t_{i-1} - t_{j-1} = 0$.

Term m:

$$
\begin{aligned}
\frac{1}{2}\int_{t_{i-1}}^{t_i}\int_{t_{j-1}}^{t_j}(-|t-s|^{2H})dsdt &= -\frac{1}{2}\int_{t_{i-1}}^{t_i}\int_{t_{i-1}}^{t_i}|t-s|^{2H}dsdt \\
&= -\frac{1}{2}\int_{t_{i-1}}^{t_i}\left(\int_{t_{i-1}}^{t}(t-s)^{2H}ds+\int_{t}^{t_i}(s-t)^{2H}ds\right)dt
\end{aligned}
$$

$$= -\frac{1}{2(2H+1)} \int_{t_{i-1}}^{t_i} \left(\left[-(t-s)^{2H+1} \right]_{t_{i-1}}^{t} + \left[(s-t)^{2H+1} \right]_{t}^{t_i} \right) dt$$

$$= -\frac{1}{2(2H+1)} \int_{t_{i-1}}^{t_i} \left((t-t_{i-1})^{2H+1} + (t_i - t)^{2H+1} \right) dt$$

$$= -\frac{1}{2(2H+1)(2H+2)} \left[(t-t_{i-1})^{2H+2} - (t_i - t)^{2H+2} \right]_{t_{i-1}}^{t_i}$$

$$= -\frac{1}{(2H+1)(2H+2)} (t_i - t_{i-1})^{2H+2}.$$

Term n:

$$\begin{aligned} \frac{1}{2} \int_{t_{i-1}}^{t_i} \int_{t_{j-1}}^{t_j} |t - t_{j-1}|^{2H} ds dt &= \frac{1}{2} \int_{t_{i-1}}^{t_i} \int_{t_{i-1}}^{t_i} (t - t_{i-1})^{2H} ds dt \\ &= \frac{1}{2} (t_i - t_{i-1}) \int_{t_{i-1}}^{t_i} (t - t_{i-1})^{2H} dt \\ &= \frac{1}{2(2H+1)} (t_i - t_{i-1})^{2H+2}. \end{aligned}$$

Term o:

$$\begin{aligned} \frac{1}{2} \int_{t_{i-1}}^{t_i} \int_{t_{j-1}}^{t_j} |t_{i-1} - s|^{2H} ds dt &= \frac{1}{2} \int_{t_{i-1}}^{t_i} \int_{t_{i-1}}^{t_i} (s - t_{i-1})^{2H} ds dt \\ &= \frac{1}{2} \int_{t_{i-1}}^{t_i} \frac{1}{2H+1} (t_i - t_{i-1})^{2H+1} dt \\ &= \frac{1}{2(2H+1)} (t_i - t_{i-1})^{2H+2}. \end{aligned}$$

Substituting terms m, n and o in (6.33) gives

$$\begin{aligned} (6.33) &= -\frac{1}{(2H+1)(2H+2)} (t_i - t_{i-1})^{2H+2} + \frac{1}{(2H+1)} (t_i - t_{i-1})^{2H+2} \\ &= \frac{1}{2H+2} (t_i - t_{i-1})^{2H+2} \\ &= \frac{1}{2H+2} \Delta_t^{2H+2}. \end{aligned} \tag{6.34}$$

(ii) Case $t_i > t_j$: $t \in [t_{i-1}, t_i]$ and $s \in [t_{j-1}, t_j]$ yield $t - s \geq 0$, $t - t_{j-1} > 0$, $t_{i-1} - s \geq 0$ and $t_{i-1} - t_{j-1} > 0$.

Term m:

$$\begin{aligned}\frac{1}{2}\int_{t_{i-1}}^{t_i}\int_{t_{j-1}}^{t_j}(-|t-s|^{2H})dsdt &= -\frac{1}{2}\int_{t_{i-1}}^{t_i}\int_{t_{j-1}}^{t_j}(t-s)^{2H}dsdt \\ &= -\frac{1}{2}\int_{t_{i-1}}^{t_i}\left[-\frac{1}{2H+1}(t-s)^{2H+1}\right]_{t_{j-1}}^{t_j}dt \\ &= \frac{1}{2(2H+1)}\int_{t_{i-1}}^{t_i}\left((t-t_j)^{2H+1}-(t-t_{j-1})^{2H+1}\right)dt \\ &= \frac{1}{2(2H+1)(2H+2)}\Big((t_i-t_j)^{2H+2}-(t_{i-1}-t_j)^{2H+2} \\ &\qquad -(t_i-t_{j-1})^{2H+2}+(t_{i-1}-t_{j-1})^{2H+2}\Big).\end{aligned}$$

Term n:

$$\begin{aligned}\frac{1}{2}\int_{t_i}^{t_{i+1}}\int_{t_j}^{t_{j+1}}|t-t_j|^{2H}dsdt &= \frac{1}{2}\int_{t_i}^{t_{i+1}}\int_{t_j}^{t_{j+1}}(t-t_j)^{2H}dsdt \\ &= \frac{1}{2}(t_{j+1}-t_j)\int_{t_i}^{t_{i+1}}(t-t_j)^{2H}dt \\ &= \frac{1}{2(2H+1)}(t_{j+1}-t_j)\left((t_{i+1}-t_j)^{2H+1}-(t_i-t_j)^{2H+1}\right).\end{aligned}$$

Term o:

$$\begin{aligned}\frac{1}{2}\int_{t_{i-1}}^{t_i}\int_{t_{j-1}}^{t_j}|t_{i-1}-s|^{2H}dsdt &= \frac{1}{2}\int_{t_{i-1}}^{t_i}\int_{t_{j-1}}^{t_j}(t_{i-1}-s)^{2H}dsdt \\ &= \frac{1}{2}\int_{t_{i-1}}^{t_i}-\frac{1}{2H+1}\left((t_{i-1}-t_j)^{2H+1}-(t_{i-1}-t_{j-1})^{2H+1}\right)dt \\ &= -\frac{1}{2(2H+1)}(t_i-t_{i-1})\left((t_{i-1}-t_j)^{2H+1}-(t_{i-1}-t_{j-1})^{2H+1}\right).\end{aligned}$$

Term p:

$$\begin{aligned}\frac{1}{2}\int_{t_{i-1}}^{t_i}\int_{t_{j-1}}^{t_j}(-|t_{i-1}-t_{j-1}|^{2H})dsdt &= -\frac{1}{2}\int_{t_{i-1}}^{t_i}\int_{t_{j-1}}^{t_j}(t_{i-1}-t_{j-1})^{2H}dsdt \\ &= -\frac{1}{2}(t_i-t_{i-1})(t_j-t_{j-1})(t_{i-1}-t_{j-1})^{2H}.\end{aligned}$$

Substituting terms m, n, o and p in (6.33) gives

$$\begin{aligned}(6.33) \quad = \quad & \frac{1}{2(2H+1)(2H+2)}\Big((t_i-t_j)^{2H+2}-(t_{i-1}-t_j)^{2H+2} \\ & \qquad -(t_i-t_{j-1})^{2H+2}+(t_{i-1}-t_{j-1})^{2H+2}\Big) \\ & +\frac{1}{2(2H+1)}(t_j-t_{j-1})\left((t_i-t_{j-1})^{2H+1}-(t_{i-1}-t_{j-1})^{2H+1}\right) \\ & -\frac{1}{2(2H+1)}(t_i-t_{i-1})\left((t_{i-1}-t_j)^{2H+1}-(t_{i-1}-t_{j-1})^{2H+1}\right) \\ & -\frac{1}{2}(t_i-t_{i-1})(t_j-t_{j-1})(t_{i-1}-t_{j-1})^{2H}.\end{aligned}$$

Suppose that $t_i - t_j = k\Delta_t$. Then $t_{i-1} - t_j = (k-1)\Delta_t$ and $t_i - t_{j-1} = (k+1)\Delta_t$ and

$$\begin{aligned}(6.33) \quad = \quad & \frac{1}{2}\Delta_t^{2H+2}\Big(\frac{1}{2H+1}\left((k+1)^{2H+1}-(k-1)^{2H+1}\right)-k^{2H} \qquad (6.35) \\ & +\frac{1}{(2H+1)(2H+2)}\left(2k^{2H+2}-(k-1)^{2H+2}-(k+1)^{2H+2}\right)\Big).\end{aligned}$$

(iii) Case $t_i < t_j$: $t \in [t_{i-1}, t_i]$ and $s \in [t_{j-1}, t_j]$ give $t - s \leq 0$, $t - t_{j-1} \leq 0$, $t_{i-1} - s < 0$ and $t_{i-1} - t_{j-1} < 0$.

The terms m, n, o and p can be estimated in the same manner and

$$\begin{aligned}(6.33) \quad = \quad & \frac{1}{2(2H+1)(2H+2)}\Big((t_j-t_i)^{2H+2}-(t_{j-1}-t_i)^{2H+2} \\ & \qquad -(t_j-t_{i-1})^{2H+2}+(t_{j-1}-t_{i-1})^{2H+2}\Big) \\ & +\frac{1}{2(2H+1)}(t_i-t_{i-1})\left((t_j-t_{i-1})^{2H+1}-(t_{j-1}-t_{i-1})^{2H+1}\right) \\ & -\frac{1}{2(2H+1)}(t_j-t_{j-1})\left((t_{j-1}-t_i)^{2H+1}-(t_{j-1}-t_{i-1})^{2H+1}\right) \\ & -\frac{1}{2}(t_i-t_{i-1})(t_j-t_{j-1})(t_{j-1}-t_{i-1})^{2H}.\end{aligned}$$

Suppose that $t_j - t_i = k\Delta_t$. Then $t_{j-1} - t_i = (k-1)\Delta_t$ and $t_j - t_{i-1} = (k+1)\Delta_t$ and

$$\begin{aligned}(6.33) \quad = \quad & \frac{1}{2}\Delta_t^{2H+2}\Big(\frac{1}{2H+1}\left((k+1)^{2H+1}-(k-1)^{2H+1}\right)-k^{2H} \qquad (6.36) \\ & +\frac{1}{(2H+1)(2H+2)}\left(2k^{2H+2}-(k-1)^{2H+2}-(k+1)^{2H+2}\right)\Big),\end{aligned}$$

which is equal to (6.35).

For simplicity, denote

$$G_{11} = \begin{pmatrix} \alpha_0 & \alpha_1 & \alpha_2 & \cdots & \alpha_{n-1} \\ \alpha_1 & \alpha_0 & \alpha_1 & \cdots & \alpha_{n-2} \\ \alpha_2 & \alpha_1 & \alpha_0 & \cdots & \alpha_{n-3} \\ \vdots & \vdots & \vdots & \ddots & \vdots \\ \alpha_{n-1} & \alpha_{n-2} & \alpha_{n-3} & \cdots & \alpha_0 \end{pmatrix},$$

$$G_{12} = \begin{pmatrix} \beta_0 & \beta_1 & \beta_2 & \cdots & \beta_{n-1} \\ \gamma_1 & \beta_0 & \beta_1 & \cdots & \beta_{n-2} \\ \gamma_2 & \gamma_1 & \beta_0 & \cdots & \beta_{n-3} \\ \vdots & \vdots & \vdots & \ddots & \vdots \\ \gamma_{n-1} & \gamma_{n-1} & \gamma_{n-3} & \cdots & \beta_0 \end{pmatrix},$$

$$G_{21} = \begin{pmatrix} \beta_0 & \gamma_1 & \gamma_2 & \cdots & \gamma_{n-1} \\ \beta_1 & \beta_0 & \gamma_1 & \cdots & \gamma_{n-2} \\ \beta_2 & \beta_1 & \beta_0 & \cdots & \gamma_{n-3} \\ \vdots & \vdots & \vdots & \ddots & \vdots \\ \beta_{n-1} & \beta_{n-2} & \beta_{n-3} & \cdots & \beta_0 \end{pmatrix},$$

$$G_{22} = \begin{pmatrix} \delta_0 & \delta_1 & \delta_2 & \cdots & \delta_{n-1} \\ \delta_1 & \delta_0 & \delta_1 & \cdots & \delta_{n-2} \\ \delta_2 & \delta_1 & \delta_0 & \cdots & \delta_{n-3} \\ \vdots & \vdots & \vdots & \ddots & \vdots \\ \delta_{n-1} & \delta_{n-2} & \delta_{n-3} & \cdots & \delta_0 \end{pmatrix},$$

where α_0 is given by (6.13), α_i by (6.14), β_0 by (6.30), β_i by (6.31), γ_i by (6.32), δ_0 by (6.34) and δ_i by (6.35) for $i = 1, \cdots, n-1$. Obviously the covariance matrix G given by (6.24) is a symmetric matrix which elements are real numbers.

The same argument in subsubsection 6.4.1 gives the covariance matrix G has a Cholesky decomposition and it is given as $G = \tilde{L}\,\tilde{L}^T$. Suppose that the matrix $\tilde{L}$ is given by

$$\tilde{L} = \begin{pmatrix} l_{1,1} & 0 & \dots & 0 \\ l_{2,1} & l_{2,2} & \dots & 0 \\ \vdots & \vdots & \ddots & \vdots \\ l_{2n,1} & l_{2n,2} & \dots & l_{2n,2n} \end{pmatrix}.$$

Similarly prepare a vector $\mathbf{n} = (n_1, n_2, \dots, n_{2n})$ which has iid $\mathcal{N}(0,1)$ com-

ponents. Then,

$$\begin{pmatrix} l_{1,1} & 0 & \dots & 0 \\ l_{2,1} & l_{2,2} & \dots & 0 \\ \vdots & \vdots & \ddots & \vdots \\ l_{2n,1} & l_{2n,2} & \dots & l_{2n,2n} \end{pmatrix} (n_1, n_2, \dots, n_{2n})^T = \begin{pmatrix} l_{1,1}n_1 \\ \sum_{i=1}^{2} l_{2,i}n_i \\ \vdots \\ \sum_{i=1}^{2n} l_{2n,i}n_i \end{pmatrix} = \begin{pmatrix} X \\ Y \end{pmatrix},$$

where X and Y are given by

$$X = \begin{pmatrix} X_1 \\ X_2 \\ \vdots \\ X_n \end{pmatrix} = \begin{pmatrix} l_{1,1}n_1 \\ \sum_{i=1}^{2} l_{2,i}n_i \\ \vdots \\ \sum_{i=1}^{n} l_{n,i}n_i \end{pmatrix}, \qquad Y = \begin{pmatrix} Y_1 \\ Y_2 \\ \vdots \\ Y_n \end{pmatrix} = \begin{pmatrix} \sum_{i=1}^{n+1} l_{n+1,i}n_i \\ \sum_{i=1}^{n+2} l_{n+2,i}n_i \\ \vdots \\ \sum_{i=1}^{2n} l_{2n,i}n_i \end{pmatrix},$$

which correspond to the increments of fBm $B_H(t_i) - B_H(t_{i-1})$ and the integral $\int_{t_{i-1}}^{t_i} (B_H(s) - B_H(t_{i-1}))\, ds$.

Now we take $B_H(t_0) = 0$ and

$$\begin{aligned} B_H(t_1) - B_H(t_0) &= X_1 \\ B_H(t_1) &= X_1. \end{aligned}$$

Similarly

$$\begin{aligned} B_H(t_2) - B_H(t_1) &= X_2 \\ B_H(t_2) &= X_2 + B_H(t_1) = \sum_{i=1}^{2} X_i. \end{aligned}$$

This means

$$B_H(t_m) = \sum_{i=1}^{m} X_i.$$

The m-th element of Y is given by

$$Y_m = \int_{t_{m-1}}^{t_m} (B_H(s) - B_H(t_{m-1}))\, ds = \int_{t_{m-1}}^{t_m} B_H(s)\, ds - B_H(t_{m-1}) \int_{t_{m-1}}^{t_m} ds$$

and we obtain

$$\int_{t_{m-1}}^{t_m} B_H(s)\, ds = Y_m + B_H(t_{m-1})\Delta_t. \tag{6.37}$$

The equation (6.37) gives the Riemann integral of $B_H(t)$ on $[t_0, t_m]$ as

$$\begin{aligned}\int_{t_0}^{t_m} B_H(s)\,ds &= \int_{t_0}^{t_1} B_H(s)\,ds + \cdots + \int_{t_{m-1}}^{t_m} B_H(s)\,ds \\ &= (Y_1 + B_H(t_0)\Delta_t) + \cdots + (Y_m + B_H(t_{m-1})\Delta_t) \\ &= \sum_{i=1}^{m} (Y_i + B_H(t_{i-1})\Delta_t)\,.\end{aligned}$$

6.4.3 Comparison of computational costs

Here we compare the computational costs to generate $B_H(t)$ and $I(B_H)$ on $[0, 1]$ interval by the following methods:

1. Solving the full covariance matrix G by Cholesky decomposition and generating $B_H(t)$ and $I(B_H)$ simultaneously.

2. Solving G_{11} by Cholesky decomposition, generating intermediate points by the RMD method and taking the Riemann sums for $I(B_H)$.

3. Solving G_{11} by the FFT, generating intermediate points by the RMD method and taking the Riemann sums for $I(B_H)$.

4. Generating $B_H(t)$ with small step size by the RMD method and taking the Riemann sums for $I(B_H)$.

The step size for $B_H(t)$ are $\Delta_t = 2^{-4}$, 2^{-6}, 2^{-8} and 2^{-10} and the step size for $I(B_H)$ for the methods 2-4 are set to $\Delta_I = 2^{-8}$, 2^{-12}, 2^{-16} and 2^{-20}, i.e., $\Delta_I = \Delta_t^2$.

Computational costs to generate 1 sample path as well as 1000 paths by the above four methods with different step sizes Δ_t are listed on Tables 6.1 and 6.2 and also illustrated in Figure 6.3. We consider the simulation on the $[0, 1]$ interval and the number of subintervals in each column is given by $1/\Delta_t$.

Δ_t	2^{-4}	2^{-6}	2^{-8}	2^{-10}
Method 1	0.007063	0.020983	0.514968	23.880383
Method 2	0.004789	0.025458	0.225578	12.767898
Method 3	0.004829	0.009526	0.068878	0.851457
Method 4	0.004082	0.010707	0.034688	0.740504

Table 6.1: Computational costs to generate 1 sample path.

Δ_t	2^{-4}	2^{-6}	2^{-8}	2^{-10}
Method 1	1.149970	2.806160	18.66572	170.5010
Method 2	2.882757	9.091249	52.02268	693.3296
Method 3	3.587168	9.020846	51.34058	679.4948
Method 4	3.930499	10.310124	51.16574	655.2259

Table 6.2: Computational costs to generate 1000 sample path.

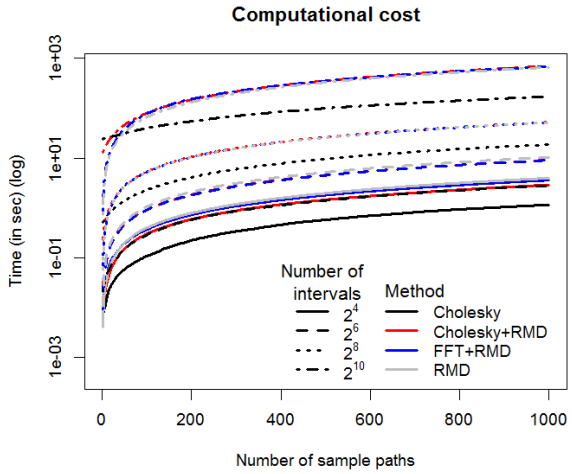

Figure 6.3: Comparison of computational costs to generate $B_H(t)$ and $I(B_H)$.

In general, the FFT and the RMD method require $\mathcal{O}(n\log(n))$ and $\mathcal{O}(n)$ computational costs, respectively, while Cholesky decomposition does $\mathcal{O}(n^3)$ [60, 61, 86]. In fact, Table 6.1 shows the FFT and the RMD method have a big advantage from computational point and they generate sample paths much faser than Cholesky decomposition. However, it is necessary to repeat the whole process by these two methods while in case of Cholesky decomposition, we can reuse the obtained square root of the covariance matrix and generate new sample paths by multiplying newly generated random numbers. We generate many sample paths in practice and if the number of sample paths to be generated is quite big, the total computational costs by Cholesky decomposition (the method 2) are almost the same with the FFT (the method 3) and the RMD method (method 4).

The computational costs to generate one sample path by the method 1 gets very large especially when the step size Δ_t gets smaller, i.e., the number of intervals gets larger. However, we can reuse the estimated square root of

the covariance matrix in the method 1 and Table 6.2 and Figure 6.3 show that it requires the least computational cost when the number of sample paths are big.

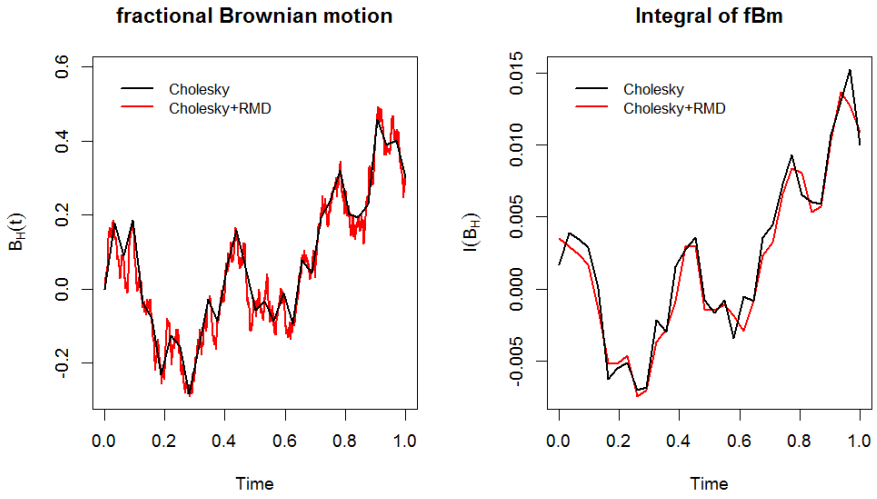

Figure 6.4: Sample paths by the method 1 and the method 2 with $H = 0.6$, $\Delta_t = 2^{-5}$ and $\Delta_I = \Delta_t^2$.

Figure 6.4 illustrates the sample paths of $B_H(t)$ and $I(B_H)$ generated by the method 1 and the method 2.

Chapter 7

Numerical examples

Analytical solutions are rarely obtained in practice and numerical simulation can give us useful information of the behavior of the systems. In addition, it can yield valuable insights into the problem of identifying which variables have big impacts on the systems and we can see their change in behavior under different conditions.

As we saw in previous chapters, we can control calculation error by step sizes, i.e., the approximation with small calculation error will be obtained for small step sizes. On the other hand, the computational costs get higher for such small step sizes and it is quite important to choose appropriate differential equation solvers and suitable step sizes. In particular, when the system is stiff, explicit schemes do not perform well and implicit schemes should be used because they are more stable.

Figure 7.1 is the simulation result of hepatitis C virus (HCV) kinetic model [6].

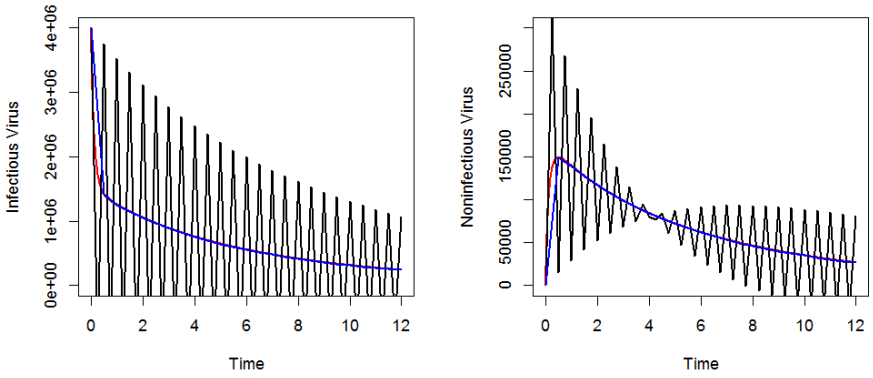

Figure 7.1 continued.

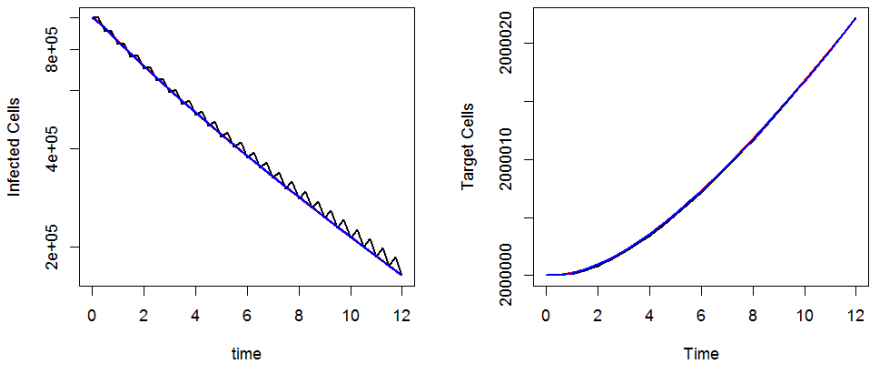

Figure 7.1: Simulation results of HCV model by different solvers.

The black line is approximated by explicit Euler scheme (3.18) and the blue and red lines by *lsoda* [46], an LMM which detects stiffness of the system and switches automatically between stiff and nonstiff methods. The step sizes are set to 0.25 for the black line, 0.5 for the blue line and 0.01 for the red line. The black line describes completely different trajectory even though its step size is smaller than the blue line, while the blue line coincides well with the red line, the "exact" solution.

There are various kinds of noisy scenario in practice and three different kinds of noise processes are introduced in section 7.1. Then, the numerical schemes derived in the previous chapters are applied to biological and medical models. Systems of RODEs are transformed into RODE-SODE pair in section 7.2 to section 7.5 and RODE parts of the systems are solved by the numerical schemes introduced in chapter 3. Only numerical schemes for RODEs are developed in previous chapters, but in general, many systems are much more complicated and they depend not only on time, but also on space, i.e., we need to solve random partial differential equations (RPDEs). One approach is method of lines. RPDEs are discretized by method of lines with respect to spatial parameter and they are transformed into a system of RODEs so that the derived schemes can be applied to the system. In section 7.6 and section 7.7, RPDEs are discretized in space and RODE-Taylor schemes as well as SLMMs are applied to the systems. A model with affine structure is introduced in section 7.8 and the affine-RODE schemes in chapter 4 are used. In the last section, 7.9, a simple system of RODEs with different kinds of noisy scenario are investigated and their trajectories are compared here.

In order to see the performance of the numerical schemes, trajectories of

solutions and computational costs are illustrated in section 7.2, section 7.3 and section 7.9 and the error vs step sizes as well as their computational costs are compared among them in the rest of the sections.

7.1 Noise process

Biological systems such as human body can be considered as random environment. They vary randomly with respect to time, but they are assumed to be continuous and essentially bounded.

One simple example to obtain bounded noise processes is implementing a Wiener process $Y(t)$ in *cosine* function, i.e.,

$$c(Y(t)) := c_0(1 - 2\nu\cos(Y(t))), \tag{7.1}$$

where ν is a positive parameter. A typical example of sample paths and the histogram of the values are illustrated in Figure 7.2. The process $c(Y(t))$ has values on the interval $[c_0 - \nu, c_0 + \nu]$, especially more values near its boundaries $c_0 - \nu$ and $c_0 + \nu$.

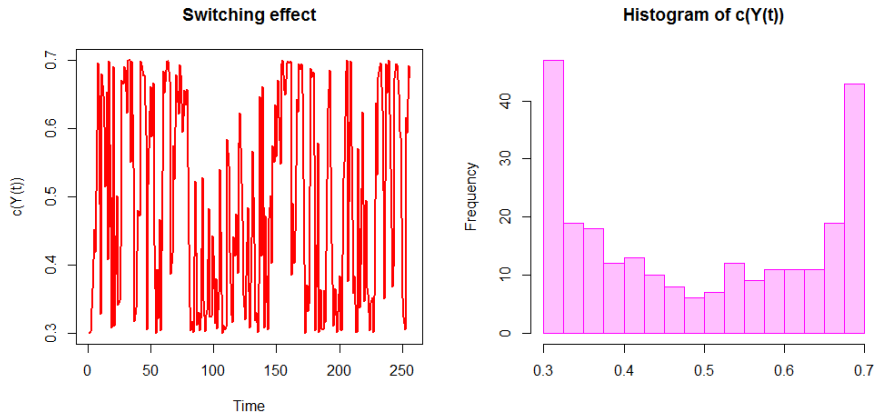

Figure 7.2: An example of the switching noise (7.1). The parameter is set to $c_0 = 0.5$ and $\nu = 0.2$.

Second example also gives noisy switching effect. Here a positive parameter k is replaced by the stochastic process

$$k(Y(t)) := k_0\left(1 - 2\nu\frac{Y(t)}{1 + Y(t)^2}\right), \tag{7.2}$$

where k_0 and ν are positive constants with $\nu \in (0, 1]$. The noise process $k(Y(t))$ tends to peak around $k_0(1 \pm \nu)$, and is thus suitable for a noisy switching scenario.

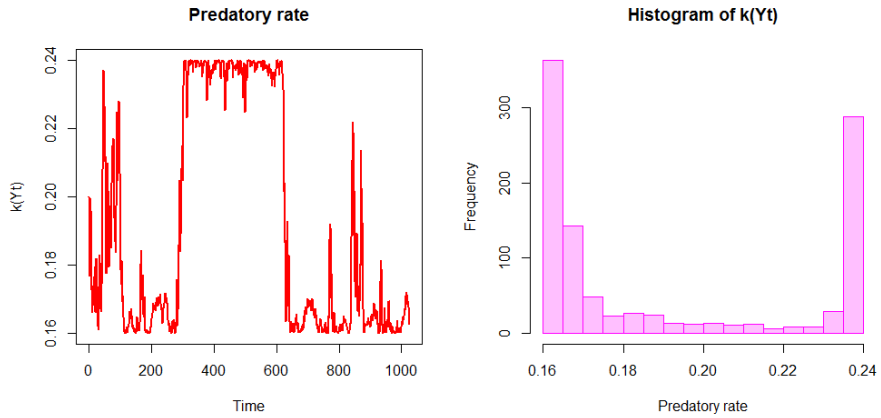

Figure 7.3: An example of the switching noise (7.2). A Wiener process is implemented in this example and the parameters are set to $k_0 = 0.2$ and $\nu = 0.2$.

In the last example, a positive parameter δ will be replaced by the stochastic process

$$\delta(Y(t)) := \delta_0 \left(1 - \frac{2\nu}{\pi} \arctan Y(t)\right), \tag{7.3}$$

where δ_0 and ν are positive constants with $\nu \in (0, 1]$. This process takes values in the interval $\delta_0(1 \pm \nu)$ and is centered on δ_0.

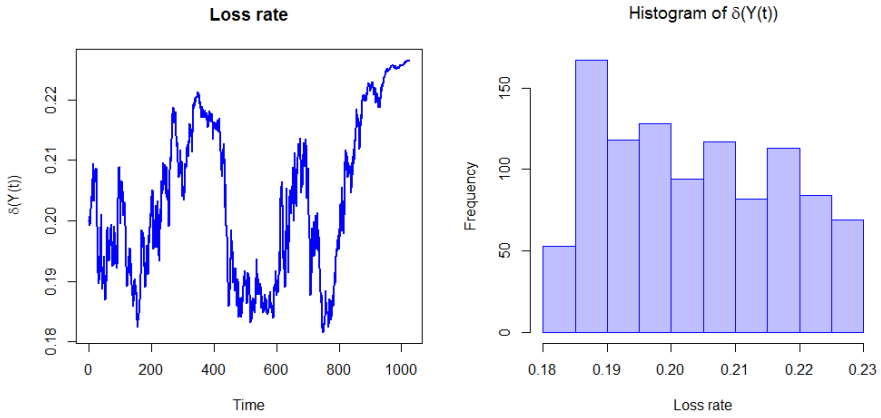

Figure 7.4: An example of (7.3). An OU process is implemented in this example and the parameters are set to $\delta_0 = 0.2$ and $\nu = 0.15$.

7.2 Tumor growth model

As an example of non-stiff system, we consider the cancer model from Wodarz & Komarova [100], page 154, in which angiogenesis inhibition prevents tumor cell division, namely

$$\begin{aligned}
\frac{dC(t)}{dt} &= \left(\frac{rC(t)}{\epsilon C(t)+1}\right)\left(\frac{P(t)}{I(t)+1}\right) - \delta C(t),\\
\frac{dP(t)}{dt} &= a_P C(t) - b_P P(t),\\
\frac{dI(t)}{dt} &= \zeta + a_I C(t) - b_I I(t),
\end{aligned}$$

where C is the population of cancer cells, P promoters of cancer cell growth and I inhibitors. The parameters are all positive except the inhibitor input ζ which may be zero. Note that the coefficient functions and their partial derivatives satisfy global Lipschitz bounds on the biologically relevant region $\mathbb{R}^3_+$.

Replacing ζ by the bounded random process $\zeta(Y(t))$:

$$\zeta(Y(t)) := \zeta_0\left(1 - 2\nu\frac{Y(t)}{1+Y(t)^2}\right),$$

we obtain a system of RODEs:

$$\begin{aligned}
\frac{dC(t)}{dt} &= \left(\frac{rC(t)}{\epsilon C(t)+1}\right)\left(\frac{P(t)}{I(t)+1}\right) - \delta C(t),\\
\frac{dP(t)}{dt} &= a_P C(t) - b_P P(t),\\
\frac{dI(t)}{dt} &= \zeta(Y(t)) + a_I C(t) - b_I I(t),
\end{aligned}$$

or the equivalent vector Itô SODE, i.e., a RODE-SODE pair:

$$d\begin{pmatrix} C(t)\\ P(t)\\ I(t)\\ Y(t)\end{pmatrix} = \begin{pmatrix} \left(\frac{rC(t)}{\epsilon C(t)+1}\right)\left(\frac{P(t)}{I(t)+1}\right) - \delta C(t)\\ a_P C(t) - b_P P(t)\\ \zeta(Y(t)) + a_I C(t) - b_I I(t)\\ 0\end{pmatrix} dt + \begin{pmatrix} 0\\ 0\\ 0\\ 1\end{pmatrix} dW(t). \quad (7.4)$$

In the following simulation example, the step size is fixed to $\Delta_a = 0.2$ for the EAES (2.35) and $\Delta_t = \Delta_a^2$ for other schemes. The parameters are set to $r = 1$, $\delta = 0.1$, $a_P = 4.5$, $b_P = 0.11$, $a_I = 0.2$, $b_I = 0.01$, $\epsilon = 0.34$, $\zeta_0 = 4$ and the initial population of cancer cells $C_0 = 35$. The other initial

values are obtained by the quasistationary approach and the initial value of promoters P_0 and one of inhibitors I_0 are given by $P_0 = a_P/b_P\, C_0$ and $I_0 = (\zeta_0 + a_I C_0)/b_I$. Moreover, the spread of the noise ν is fixed to 1.

Solutions of the system (7.4) are approximated by the explicit Euler scheme (3.18), the derivative-free explicit 1.5 order scheme (3.24), the Adams-Bashforth scheme (3.37) and the EAES (2.35).

Figures 7.5 and 7.6 illustrate a typical sample path. The black line, the red line and the light green line are the population of the cancer cells, the promoters and the inhibitors, respectively. The black line, the dark blue line, the red line and the light green line on the left figure of Figure 7.7 are the solutions by the explicit Euler scheme (3.18), the derivative-free explicit 1.5 order scheme (3.24), the Adams-Bashforth scheme (3.37) and the EAES (2.35). The histogram shows the sum of 100 times simulation time by each scheme.

All solution curves look very similar, however, the computational cost for the EAES (2.35) is much smaller than the ones by other three schemes.

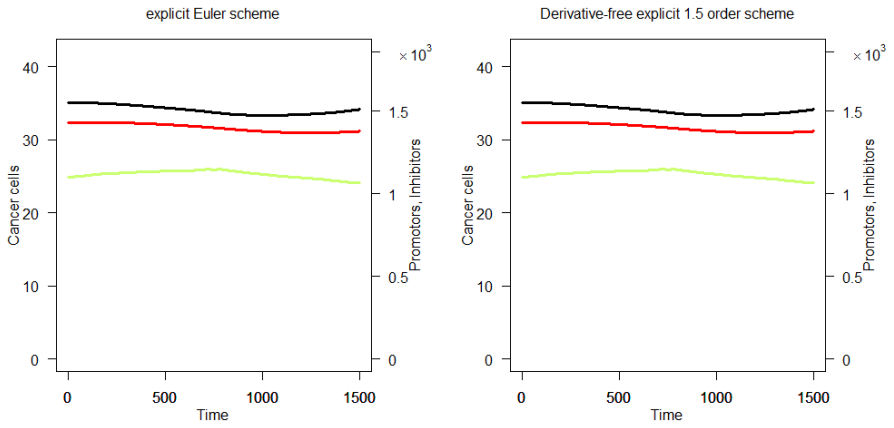

Figure 7.5: The approximation by the explicit Euler scheme (3.18) and the derivative-free explicit 1.5-order scheme (3.24). The step sizes are $\Delta_a = 0.2$ for the EAES (2.35) and $\Delta_t = \Delta_a^2$ for the other schemes. The parameters are set to $r = 1$, $\delta = 0.1$, $a_P = 4.5$, $b_P = 0.11$, $a_I = 0.2$, $b_I = 0.01$, $\epsilon = 0.34$ and $\zeta_0 = 4$ with initial value $C_0 = 35$, $P_0 = a_P/b_P\, C_0$ and $I_0 = (\zeta_0 + a_I C_0)/b_I$. The black line: the population of the cancer cells, the red line: the population of the promoters and the light green line: the population of the inhibitors.

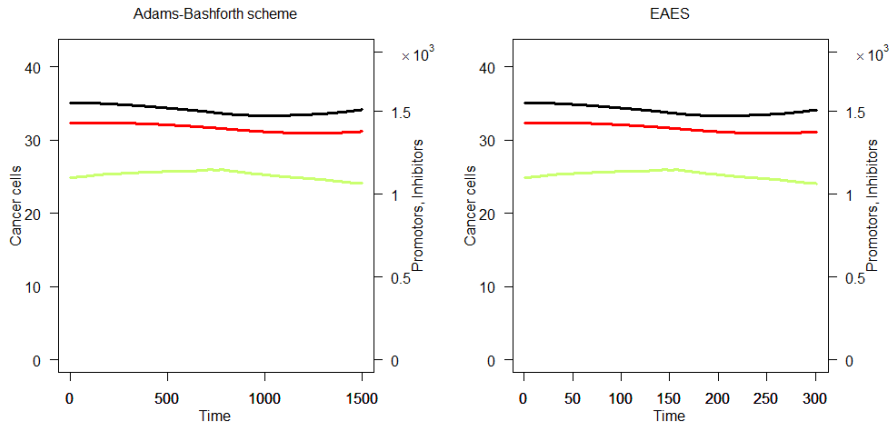

Figure 7.6: The approximation by the Adams-Bashforth scheme (3.37) and the EAES (2.35). The step sizes are $\Delta_a = 0.2$ for the EAES (2.35) and $\Delta_t = \Delta_a^2$ for the other schemes. The parameter values and the line colors are the same with Figure 7.5.

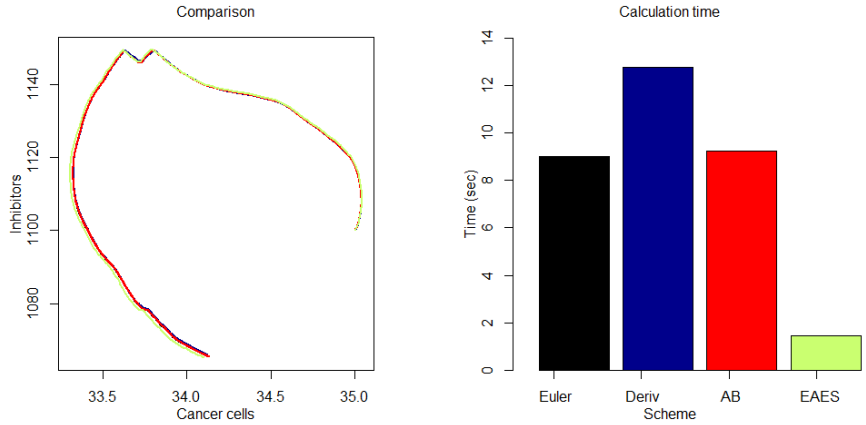

Figure 7.7: The comparison of the trajectories and the calculation costs by the explicit Euler scheme (3.18), the derivative-free explicit 1.5-order scheme (3.24), Adams-Bashforth scheme (3.37) and the EAES (2.35). The parameter values and the line colors are the same with Figure 7.5.

7.3 HCV kinetic model

As an example of stiff system, we consider the epidemiological model in [7]. The three compartment HCV kinetics model given by

$$\frac{dV(t)}{dt} = (1-\epsilon)pI(t) - cV(t),$$

$$\frac{dI(t)}{dt} = \beta T(t)V(t) + p_I\left(1 - \frac{T(t)+I(t)}{T_{max}}\right)I(t) - \delta I(t),$$

$$\frac{dT(t)}{dt} = \gamma\left(1 - \frac{T(t)+I(t)}{T_{max}}\right),$$

where V is a compartment for viruses, I for infected cells and T for target cells. The parameters of the model are the effect of interferon ϵ, the production rate of new virus p, the clearance rate of virus c, the de-novo infection rate β, the proliferation rate of infected cells p_I, the death rate of infected cells δ, the regeneration rate of target cells γ and the maximum number of cells T_{max}.

We replace the parameter δ by the bounded noise process $\delta(Y(t))$ given as (7.3) to obtain a stiff system of RODEs:

$$\begin{aligned}
\frac{dV(t)}{dt} &= (1-\epsilon)pI(t) - cV(t), \\
\frac{dI(t)}{dt} &= \beta T(t)V(t) + p_I\left(1 - \frac{T(t)+I(t)}{T_{max}}\right)I(t) - \delta(Y(t))I, \\
\frac{dT(t)}{dt} &= \gamma\left(1 - \frac{T(t)+I(t)}{T_{max}}\right).
\end{aligned}$$

This can be reformulated as a vector Itô SODE or a RODE-SODE pair:

$$d\begin{pmatrix} V(t) \\ I(t) \\ T(t) \\ Y(t) \end{pmatrix} = \begin{pmatrix} (1-\epsilon)pI(t) - cV(t) \\ \beta T(t)V(t) + \left\{p_I\left(1 - \frac{T(t)+I(t)}{T_{max}}\right) - \delta(Y(t))\right\}I(t) \\ \gamma\left(1 - \frac{T(t)+I(t)}{T_{max}}\right) \\ \theta_1 - \theta_2 Y(t) \end{pmatrix} dt + \begin{pmatrix} 0 \\ 0 \\ 0 \\ \theta_3 \end{pmatrix} dW(t), \tag{7.5}$$

where, to be specific, we have taken $Y(t)$ to be an OU process solution of the Itô SODE:

$$dY(t) = (\theta_1 - \theta_2 Y(t))\, dt + \theta_3\, dW(t), \tag{7.6}$$

with θ_1 non-negative and θ_2, θ_3 positive. This has the explicit solution

$$Y(t) = \frac{\theta_1}{\theta_2} + \left(Y_0 - \frac{\theta_1}{\theta_2}\right)e^{-\theta_2 t} + \theta_3 \int_0^t e^{-\theta_2(t-s)} dW(s).$$

In this simulation example, the step size is fixed to $\Delta_a = 0.1$ for the IAES (2.36) and $\Delta_t = \Delta_a^2$ for other schemes. The parameters are set to $\epsilon = 0.3$, $c = 6$, $p_I = 0.2$, $\delta_0 = 0.42$, $\gamma = 1 \times 10^5$, $T_{max} = 3 \times 10^6$ and the initial population of the viruses $V_0 = 1 \times 10^7$, the infected cells $I_0 = 1.9 \times 10^6$ and the target cells $T_0 = 1.1 \times 10^6$. p and β are given by $p = cV_0/I_0$ and $\beta =$

$\delta_0 I_0/(T_0\, V_0)$ from the quasistationary approach. The spread of the noise ν is fixed to 1 in this model.

Solutions of the system (7.5) will be approximated by the implicit Euler scheme (3.22), the derivative-free implicit 1.5-order scheme (3.26), the Adams-Moulton scheme (3.38) and the IAES (2.36).

An example of sample paths is given on Figures 7.8 and 7.9. Here the black line, the red line and the light green line are the population of the viruses, the infected cells and the target cells, respectively. The black line, the dark blue line, the red line and the light green line on the left figure of Figure 7.10 are the solutions by the implicit Euler scheme (3.22), the derivative-free implicit 1.5 order scheme (3.26), the Adams-Moulton scheme (3.38) and the IAES (2.36). The histogram shows the sum of 100 times simulation time by each scheme.

All schemes are implicit schemes and the trajectories on Figure 7.10 coincide well. The step size is set to $\Delta_a = 0.1$ for the IAES (2.36) and $\Delta_t = \Delta_a^2 = 0.01$ for the other schemes and the difference in the calculation time is quite obvious.

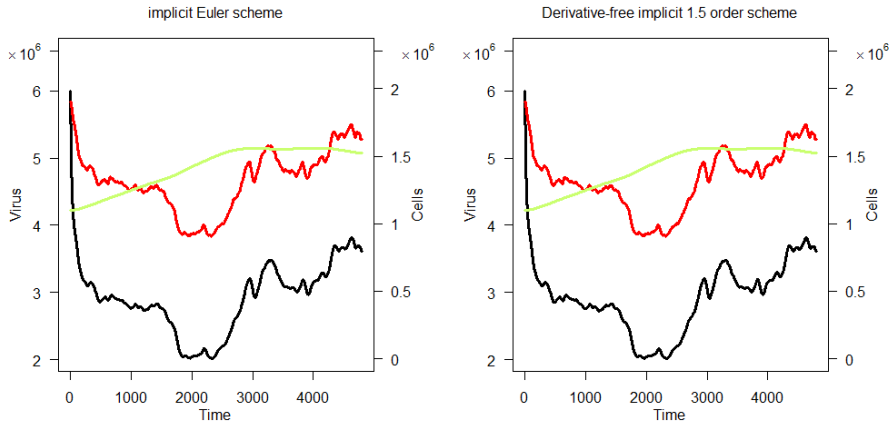

Figure 7.8: The approximation by the implicit Euler scheme (3.22) and the derivative-free implicit 1.5-order scheme (3.26). The step sizes are $\Delta_a = 0.1$ for the IAES (2.36) and $\Delta_t = \Delta_a^2$ for the other schemes. The parameters are set to $\epsilon = 0.3$, $c = 6$, $p_I = 0.2$, $\delta_0 = 0.42$, $\gamma = 1 \times 10^5$, $T_{max} = 3 \times 10^6$ and the initial values $V_0 = 1 \times 10^7$, $I_0 = 1.9 \times 10^6$ and $T_0 = 1.1 \times 10^6$. The black line: the virus compartment, the red line: the infected cells compartment and the light green line: the target cells compartment.

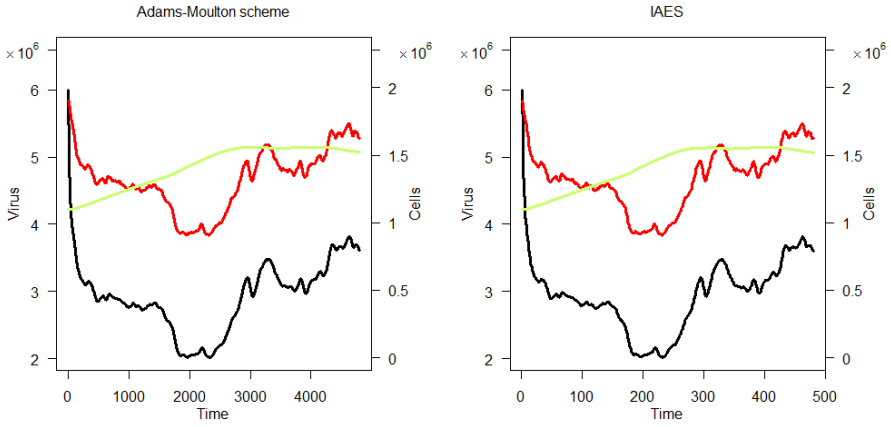

Figure 7.9: The approximation by the Adams-Moulton scheme (3.38) and the IAES (2.36). The step sizes are $\Delta_a = 0.1$ for the IAES (2.36) and $\Delta_t = \Delta_a^2$ for the other schemes. The parameter values and the line colors are the same with Figure 7.8.

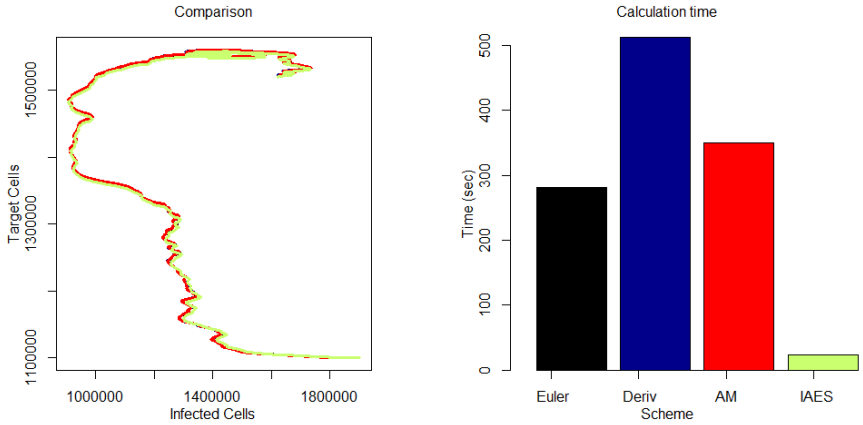

Figure 7.10: The comparison of the trajectories and the calculation costs by the implicit Euler scheme (3.22), the derivative-free implicit 1.5-order scheme (3.26), Adams-Moulton scheme (3.38) and the IAES (2.36). The parameter values and the line colors are the same with Figure 7.8.

7.4 Population dynamics

The next example is a non-stiff nonlinear scalar RODE originating in population dynamics [45] and given by

$$\frac{dX(t)}{dt} = rX(t)(k - X(t))\cos(Y(t)), \tag{7.7}$$

where $Y(t)$ is an OU process satisfying (7.6).

The 1.0, 1.5 and 2.0-order RODE-Taylor schemes (3.18), (3.19) and (3.20) are applied here. In addition, explicit SLMMs of order 1.0, 1.5 and 2.0 to be applied are as follows

$$\text{(Ex1.0) } X_n = X_{n-1} + \frac{1}{2}\Delta_t \left(f_{n-1} + f_{n-2}\right), \tag{7.8}$$

$$\begin{aligned}\text{(Ex1.5) } X_n &= X_{n-1} + \Delta_t f_{n-2} + L^1 f_{n-1} I_{(1,0),t_{n-1}} + L^1 f_{n-2} I_{(1),t_{n-2}} \Delta_t \\ &\quad + L^0 f_{n-1} I_{(0,0),t_{n-1}} + L^0 f_{n-2} I_{(0),t_{n-2}} \Delta_t,\end{aligned} \tag{7.9}$$

$$\begin{aligned}\text{(Ex2.0) } X_n &= \frac{1}{2} X_{n-1} + \frac{1}{2} X_{n-2} + \Delta_t \left(f_{n-1} + \frac{1}{2} f_{n-2}\right) \\ &\quad + L^1 f_{n-1} I_{(1,0),t_{n-1}} + \frac{1}{2} L^1 f_{n-2} I_{(1,0),t_{n-2}} \\ &\quad + L^0 f_{n-1} I_{(0,0),t_{n-1}} + \frac{1}{2} L^0 f_{n-2} I_{(0,0),t_{n-2}} \\ &\quad + L^1 L^1 f_{n-1} I_{(1,1,0),t_{n-1}} + \frac{1}{2} L^1 L^1 f_{n-2} I_{(1,1,0),t_{n-2}},\end{aligned} \tag{7.10}$$

as well as the Adams-Bashforth scheme (3.37), which has order 1.0 convergence.

In the following simulations, the initial condition and the parameters are fixed to $X_0 = 0.5$, $r = 5$, $K = 3$, $\theta_1 = 0$, $\theta_2 = 4$ and $\theta_3 = 0.1$. For comparison, the solution of the 2.0-order Itô-Taylor scheme (3.20) with the step size $\Delta_t = 2^{-12}$ is used as the "exact" solution and compared to the other schemes with step sizes $\Delta_t = 2^{-10}$, 2^{-9}, 2^{-8}, 2^{-7}, 2^{-6} and 2^{-5}.

The step size versus mean error and the computational costs for 100 times simulation are shown on Figure 7.11. The solid thick lines on the first figure are the error by 1-step schemes and the dashed lines by multi-step schemes. The solid thin lines are for reference and they have slopes of orders 1.0, 1.5 and 2.0.

The error by 1.5-order Itô-Taylor scheme (3.19) (solid cyan) coincides closely with the 2.0-order Itô-Taylor scheme (3.20) (solid dark red) and is not visible here. The Adams-Bashforth scheme (3.37) (dashed gray) has order 1.0 convergence, but its consistency conditions satisfy $C^*_{\alpha,j} = 0$ for $\alpha = (1,0)$ and $(0,0)$. Moreover, $Y(t)$ oscillates around 0, which gives $L^1 f \approx 0$ and the remainder term of 1.0-order convergence schemes is also close to 0, so the Adams-Bashforth scheme (3.37) in fact shows higher order convergence, while the other 1.0-order SLMM (7.8) (dashed light brown) does not.

No big difference in computational costs can be observed here.

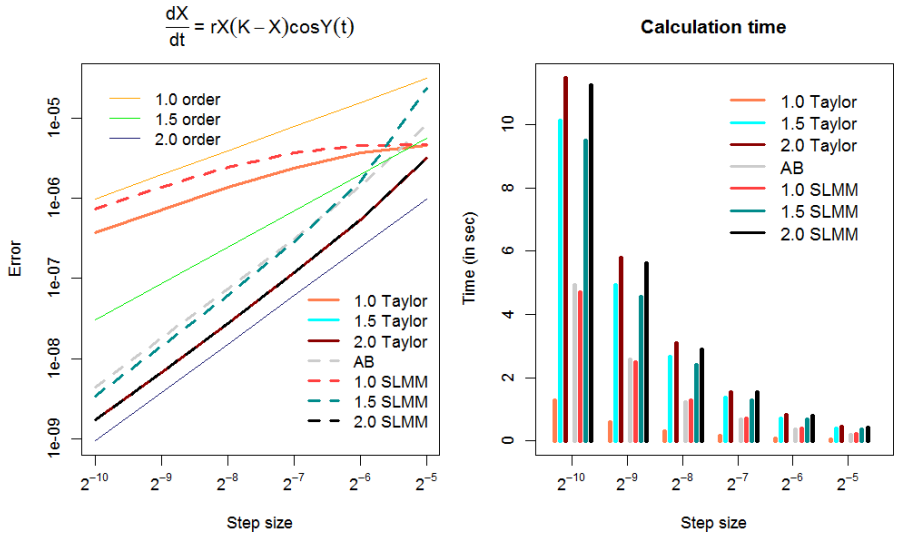

Figure 7.11: The comparison of accuracy and calculation time for (7.7)

7.5 Lotka-Volterra model

Multi-species Lotka-Volterra model in [96] has a form:

$$\begin{aligned}
\frac{dA(t)}{dt} &= (\epsilon_A - k_A C(t))\, A(t), \\
\frac{dB(t)}{dt} &= (\epsilon_B - k_B C(t))\, B(t), \\
\frac{dC(t)}{dt} &= (-\epsilon_C + k_A A(t) + k_B B(t))\, C(t),
\end{aligned}$$

where A, B and C are the population of two kinds of preys and predators, respectively, k_A and k_B the predatory rates of A and B, ϵ_A and ϵ_B the birth rate of A and B and ϵ_C the death rate of C.

In [96], a switching scenario was considered and the predatory rates k_A and k_B were replaced by suitable functions:

$$k_A(A,B) = \frac{a}{1+(B/A)^n}, \qquad k_B(A,B) = \frac{b}{1+(A/B)^n},$$

for some constants a and b.

Instead of using three compartment model, a switching noise process is implemented in two compartment model, i.e., one predator species and one

prey species, and the corresponding RODE-SODE pair is given by

$$d\begin{pmatrix} A^*(t) \\ C^*(t) \\ Y(t) \end{pmatrix} = \begin{pmatrix} (\epsilon_{A^*} - k(Y(t))C^*(t))\, A^*(t) \\ (-\epsilon_{C^*} + k(Y(t))A^*(t))\, C^*(t) \\ \theta_1 - \theta_2 Y(t) \end{pmatrix} dt + \begin{pmatrix} 0 \\ 0 \\ \theta_3 \end{pmatrix} dW(t), \tag{7.11}$$

where A^* and C^* are prey and predator compartments, ϵ_{A^*} the birth rate of A^* and ϵ_{C^*} the death rate of C^*. The predatory rate $k(Y(t))$ is given by the equation (7.2) with $Y(t)$ an OU process.

Explicit SLMMs of order 1.0, 1.5 and 2.0 to be applied are as follows

$$\text{(Ex1.0) } X_n = X_{n-1} + \frac{1}{2}\Delta_t \left(f_{n-1} + f_{n-2}\right), \tag{7.12}$$

$$\begin{aligned} \text{(Ex1.5) } X_n &= X_{n-1} + \frac{1}{2}\Delta_t \left(f_{n-1} + f_{n-2}\right) \\ &\quad + L^1 f_{n-1} I_{(1,0),t_{n-1}} + \frac{1}{2} L^1 f_{n-2} I_{(1),t_{n-2}} \Delta_t \\ &\quad + L^0 f_{n-1} I_{(0,0),t_{n-1}} + \frac{1}{2} L^0 f_{n-2} I_{(0),t_{n-2}} \Delta_t, \end{aligned} \tag{7.13}$$

$$\begin{aligned} \text{(Ex2.0) } X_n &= X_{n-1} + \frac{1}{2}\Delta_t \left(f_{n-1} + f_{n-2}\right) \\ &\quad + L^1 f_{n-1} I_{(1,0),t_{n-1}} + \frac{1}{2} L^1 f_{n-2} I_{(1),t_{n-2}} \Delta_t \\ &\quad + L^0 f_{n-1} I_{(0,0),t_{n-1}} + \frac{1}{2} L^0 f_{n-2} I_{(0),t_{n-2}} \Delta_t, \\ &\quad + L^1 L^1 f_{n-1} I_{(1,1,0),t_{n-1}} + \frac{1}{2} L^1 L^1 f_{n-2} I_{(1,1),t_{n-2}} \Delta_t. \end{aligned} \tag{7.14}$$

In addition, the EAES (2.35), 1.0, 1.5 and 2.0-order Itô-Taylor schemes (3.18), (3.19) and (3.20) are applied.

The initial conditions and the parameters are fixed to $A_0^* = 100$, $C_0^* = 10$, $k_0 = 0.2$, $\epsilon_{A^*} = 1$, $\epsilon_{C^*} = 1.2$, $\theta_1 = 0$, $\theta_2 = 5$ and $\theta_3 = 0.1$. For comparison, the solution of the 2.0-order Itô-Taylor scheme (3.20) with the step size $\Delta_t = 2^{-12}$ is used as the "exact" solution and compared to the other schemes with step sizes $\Delta_t = 2^{-11}$, 2^{-10}, 2^{-9}, $2^{-8}$and 2^{-7}.

Figure 7.12 shows the results of 100 times simulation. The EAES (2.35) shows 1.0-order convergence while the accuracy is relatively low comparing to higher order schemes. $L^1L^1 f$ term in the 2.0-order schemes are very small and 1.5-order schemes show 2.0-order decay. No big difference in computational cost is observed between Itô-Taylor schemes and SLMMs.

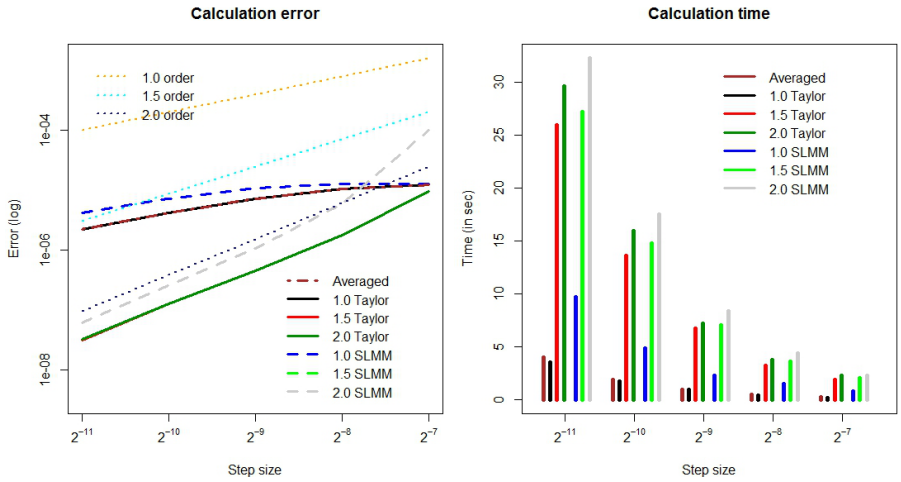

Figure 7.12: The comparison of accuracy and calculation time for (7.11).

7.6 Pattern formation

Consider a system of RPDEs:

$$\begin{aligned} \frac{\partial a(t,x)}{\partial t} &= s\left(\frac{a(t,x)^2}{b(t,x)} + b_a\right) - r_a a(t,x) + D_a \frac{\partial^2 a(t,x)}{\partial x^2}, \\ \frac{\partial b(t,x)}{\partial t} &= s\, a(t,x)^2 - r_b b(t,x) + D_b \frac{\partial^2 b(t,x)}{\partial x^2} + b_b, \end{aligned} \tag{7.15}$$

on a spatial domain given by the bounded interval $0 \leq x \leq x_f$ with Neumann boundary conditions. This system describes an interaction between the activator $a(t,x)$ and the inhibitor $b(t,x)$ in pattern formation of sea shells [75]. Here D_a and D_b are the diffusion coefficients, r_a and r_b the decay rates of a and b, b_a and b_b the basic activator and inhibitor production and s is the ability of the cells to perform the autocatalysis. The parameter s is given by random fluctuations around r_a through the noise process (7.3), where $\nu = 0.01$ and $Y(t)$ a Wiener process.

The system of RPDEs (7.15) is discretized with respect to space by the method of lines [89] using a uniform partition of the interval $[0, x_f]$ with grid size $\Delta_x = x_f/M$. In particular, the second order derivatives in (7.15) are approximated by central finite difference quotients:

$$\begin{aligned} \frac{\partial^2 a(t,x_j)}{\partial x^2} &= \frac{a(t,x_{j+1}) - 2a(t,x_j) + a(t,x_{j-1})}{\Delta_x^2} + \mathcal{O}(\Delta_x^2), \\ \frac{\partial^2 b(t,x_j)}{\partial x^2} &= \frac{b(t,x_{j+1}) - 2b(t,x_j) + b(t,x_{j-1})}{\Delta_x^2} + \mathcal{O}(\Delta_x^2), \end{aligned}$$

where $a(t, x_j)$ and $b(t, x_j)$ are the values of a and b at j-th grid in space. Then $a(t, x_j)$ and $b(t, x_j)$ are replaced by $a_j^*(t)$ and $b_j^*(t)$ for $i = 0, 1, \cdots, M$ and the local discretization error is discarded. This results in a $2(M+1)$-dimensional system of RODEs for which the core blocks are

$$\begin{aligned}
\frac{da_j^*(t)}{dt} &= s(Y(t))\left(\frac{a_j^{*2}(t)}{b_j^*(t)} + b_a\right) - r_a a_j^*(t) + D_a \frac{a_{j+1}^*(t) - 2a_j^*(t) + a_{j-1}^*(t)}{\Delta_x^2} \\
\frac{db_j^*(t)}{dt} &= s(Y(t))\, a_j^{*2}(t) - r_b b_j^*(t) + D_b \frac{b_{j+1}^*(t) - 2b_j^*(t) + b_{j-1}^*(t)}{\Delta_x^2} + b_b
\end{aligned}$$

with initial conditions:

$$\begin{aligned}
a_j^*(t=0) &= a(t=0, x=x_j), \\
b_j^*(t=0) &= b(t=0, x=x_j),
\end{aligned}$$

for $j = 0, 1, \ldots, M$. The boundary blocks need to be modified to take into account the Neumann boundary conditions:

$$\begin{aligned}
\frac{\partial a^*(t, x=0)}{\partial x} &= \frac{\partial a^*(t, x=x_f)}{\partial x} = 0, \\
\frac{\partial b^*(t, x=0)}{\partial x} &= \frac{\partial b^*(t, x=x_f)}{\partial x} = 0.
\end{aligned}$$

The system is stiff, so the IAES (2.36), 1.0 and 1.5-order implicit Itô-Taylor schemes (3.22) and (3.23) as well as implicit SLMMs:

$$\text{(Imp1.0) } X_n = X_{n-1} + \frac{1}{4}\Delta_t \left(2f_n + f_{n-1} + f_{n-2}\right), \tag{7.16}$$

$$\begin{aligned}
\text{(Imp1.5) } X_n &= X_{n-1} + \frac{1}{12}\Delta_t \left(5f_n + 8f_{n-1} - f_{n-2}\right) \\
&\quad + L^1 f_{n-1} I_{(1,0),t_{n-1}} - \frac{5}{12} L^1 f_{n-1} I_{(1),t_{n-1}} \Delta_t - \frac{1}{12} L^1 f_{n-2} I_{(1),t_{n-2}} \Delta_t \\
&\quad + L^0 f_{n-1} I_{(0,0),t_{n-1}} - \frac{5}{12} L^0 f_{n-1} I_{(0),t_{n-1}} \Delta_t - \frac{1}{12} L^0 f_{n-2} I_{(0),t_{n-2}} \Delta_t,
\end{aligned} \tag{7.17}$$

are applied to the model. The first implicit SLMM (7.16) has order 1.0 convergence and the second (7.17) order 1.5.

In the simulation, the parameters are set to $D_a = 0.01$, $D_b = 0.4$, $r_a = 0.05$, $r_b = 0.08$, $b_a = 0.05$ and $b_b = 0$ [75] with the initial values $a_0 = 0.2$ and $b_0 = 0.1$. Moreover, $x_0 = 0$ and $x_f = 5$ with $\Delta_x = 2^{-2}$, which gives a 42-dimensional system of RODEs. The "exact" solution is obtained by 1.5-order implicit Itô-Taylor scheme (3.23) with the step size $\Delta_t = 2^{-11}$ and compare with approximations by 1.0 and 1.5-order implicit Itô-Taylor

schemes (3.22) and (3.23), the implicit SLMMs (7.16) and (7.17) and the IAES (2.36) with different step sizes $\Delta_t = 2^{-9}$, 2^{-8}, 2^{-7}, 2^{-6} and 2^{-5}. For the latter initial conditions at time t_1 were calculated using 1-step schemes of the same orders.

Figures 7.13 and 7.14 illustrate the step size versus mean error and computational costs for 25 times simulation by the above schemes. The solid thick lines are the error by 1-step schemes and the dashed lines by multi-step schemes. The solid thin lines are for reference and have slopes of order 1.0, 1.5 and 2.0.

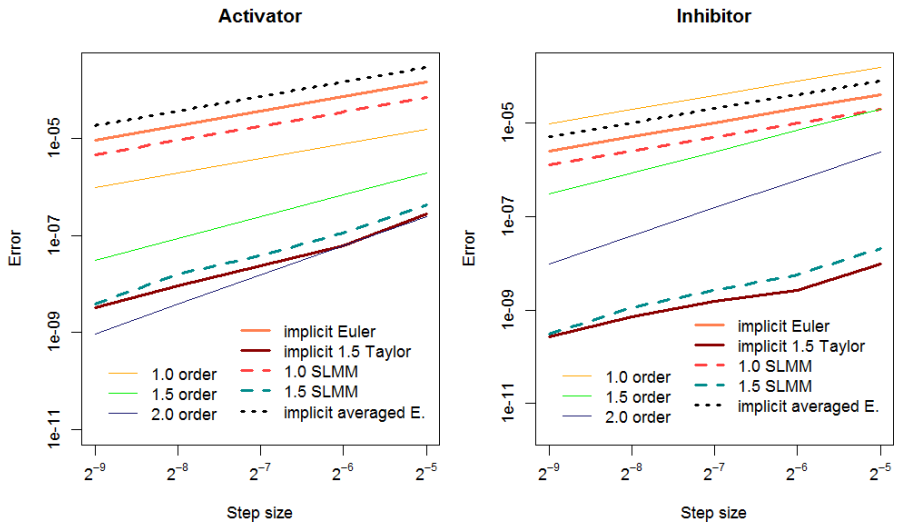

Figure 7.13: The comparison of accuracy for (7.15)

The difference between the 1.5-order and 2.0-order schemes comes from L^1L^1f terms and it depends deeply on the value of a in the inhibitor compartment. In particular a is small when time is small and this makes the 1.5-order schemes show roughly 2.0-order convergence decay.

The system is now of relatively high dimension and a difference in computational costs, especially between 1.5-order Itô-Taylor scheme (3.23) and the SLMM (7.17), is quite apparent.

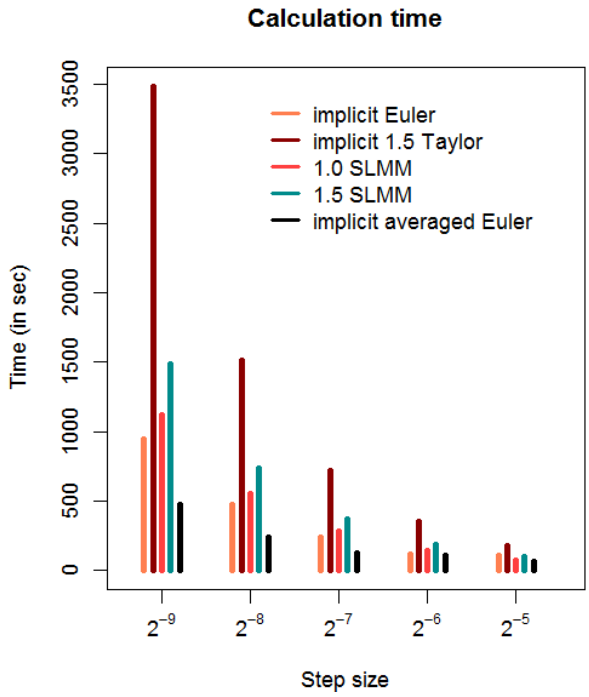

Figure 7.14: The comparison of calculation time for (7.15)

7.7 HBV with spatial dependence

Hepatitis B virus (HBV) with spatial dependence model can be given by

$$\begin{aligned}
\frac{\partial T(t,x)}{\partial t} &= s - \beta T(t,x)V(t,x) - mT(t,x),\\
\frac{\partial I(t,x)}{\partial t} &= \beta T(t,x)V(t,x) - \delta I(t,x),\\
\frac{\partial V(t,x)}{\partial t} &= d\Delta V(t,x) + pI(t,x) - cV(t,x),
\end{aligned} \tag{7.18}$$

where T, I and V are the compartments of target cells, infected cells and free viruses, respectively [98]. The parameters here are the production rate of the target cells s, the de-novo infection rate β, the loss rate of the target cells m, the loss rate of infected cells δ, the diffusion coefficient d, the production rate of the new virus p and the loss rate of the virus c. Δ in V compartment is Laplacian and it is given by $\Delta V = \sum_{l=1}^{n} \partial^2 V/\partial x_l^2$, $n = 1$, 2 or 3.

We investigate the model when $n = 2$, i.e., $\mathbb{R}^2$ spatial domain in this section. Similar to the pattern formation example in section 7.6, firstly the RPDEs (7.18) are discretized with respect to space by method of lines. We

assume an equidistant partition in space and denote the spatial interval by Δ_x and we set $\Delta_x = 1$ for simplicity. Suppose that the system is given on the spatial domain $[0, 20] \times [0, 20]$.

The second order derivative $\sum_{l=1}^{2} \partial^2 V/\partial x_l^2$ are

$$\begin{aligned}\Delta V(t, x_{i,j}) &= \frac{\partial^2 V(t, x_{i,j})}{\partial x_1^2} + \frac{\partial^2 V(t, x_{i,j})}{\partial x_2^2} \\ &= \frac{V(t, x_{i+1,j}) - 2V(t, x_{i,j}) + V(t, x_{i-1,j})}{\Delta_x^2} \\ &\quad + \frac{V(t, x_{i,j+1}) - 2V(t, x_{i,j}) + V(t, x_{i,j-1})}{\Delta_x^2} + \mathcal{O}(\Delta_x^2),\end{aligned}$$

where $V(t, x_{i,j})$ is a value of V in i-th and j-th grid with respect to x_1 and x_2 respectively.

Now ignore the local discretization error $\mathcal{O}(\Delta_x^2)$ and replace $V(t, x_{i,j})$ by $V_{i,j}^*(t)$. Denote $T_{i,j}^*(t)$ and $I_{i,j}^*(t)$ as the values of T and I in i-th and j-th grid respectively. δ is replace by (7.3) with $Y(t)$ a Wiener process and the core blocks of the corresponding system of RODEs are obtained:

$$\begin{aligned}\frac{dT_{i,j}^*(t)}{dt} &= s_{i,j} - \beta V_{i,j}^*(t) T_{i,j}^*(t) - m T_{i,j}^*(t), \\ \frac{dI_{i,j}^*(t)}{dt} &= \beta T_{i,j}^*(t) V_{i,j}^*(t) - \delta(Y(t)) I_{i,j}^*(t), \\ \frac{dV_{i,j}^*(t)}{dt} &= \frac{d}{\Delta_x^2}\Big((V_{i+1,j}^*(t) - 2V_{ij}^*(t) + V_{i-1,j}^*(t)) \\ &\qquad + (V_{i,j+1}^*(t) - 2V_{i,j}^*(t) + V_{i,j-1}^*(t))\Big) + p I_{i,j}^*(t) - c V_{i,j}^*(t),\end{aligned}$$

for i, $j = 1, \ldots, 19$. The initial conditions are given as

$$\begin{aligned}T_{i,j}^*(t=0) &= T(t=0, x=x_{i,j}), \\ I_{i,j}^*(t=0) &= I(t=0, x=x_{i,j}), \\ V_{i,j}^*(t=0) &= V(t=0, x=x_{i,j}),\end{aligned}$$

for i, $j = 0, 1, \ldots, 20$ and the boundary blocks are now modified to take into account the Neumann boundary conditions:

$$\frac{\partial T^*(t, x=x_{i,j})}{\partial x} = \frac{\partial I^*(t, x=x_{i,j})}{\partial x} = \frac{\partial V^*(t, x=x_{i,j})}{\partial x} = 0,$$

for i, $j = 0$ or 20.

The system is stiff, so the IAES (2.36), 1.0 and 1.5-order implicit Itô-Taylor schemes (3.22) and (3.23) as well as implicit SLMMs:

$$\text{(Imp1.0) } X_n = X_{n-1} + \frac{1}{4}\Delta_t \left(2f_n + f_{n-1} + f_{n-2}\right), \tag{7.19}$$

$$\begin{aligned}\text{(Imp1.5) } X_n &= X_{n-1} + \frac{1}{12}\Delta_t \left(5f_n + 8f_{n-1} - f_{n-2}\right) \\ &+L^1 f_{n-1} I_{(1,0),t_{n-1}} - \frac{5}{12} L^1 f_{n-1} I_{(1),t_{n-1}} \Delta_t - \frac{1}{12} L^1 f_{n-2} I_{(1),t_{n-2}} \Delta_t \\ &+L^0 f_{n-1} I_{(0,0),t_{n-1}} - \frac{5}{12} L^0 f_{n-1} I_{(0),t_{n-1}} \Delta_t - \frac{1}{12} L^0 f_{n-2} I_{(0),t_{n-2}} \Delta_t,\end{aligned} \tag{7.20}$$

are applied to the model.

The parameters are set to $s_{i,j} = 1 \times 10^7/(21 \times 21)$, $\beta = 5 \times 10^{-10}$, $m = 0.1$, $d = 0.002$, $p = 15$ and $c = 5$. The initial values are randomly assigned in $[0, 20] \times [0, 20]$ grids in each simulation, but the their sums are fixed to $T_0 = 2 \times 10^5$, $I_0 = 1 \times 10^5$ and $V_0 = 1 \times 10^6$. In addition, $\delta_0 = 0.1$ and $\nu = 0.1$ for $\delta(Y(t))$. The "exact" solution is obtained by 1.5-order implicit Itô-Taylor scheme (3.23) with the step size $\Delta_t = 2^{-7}$ and compare with approximations by the IAES (2.36), 1.0 and 1.5-order implicit Itô-Taylor schemes (3.22) and (3.23) and the implicit SLMMs (7.19) and (7.20) with different step sizes $\Delta_t = 2^{-6}$, 2^{-5}, 2^{-4} and 2^{-3}. For the latter initial conditions at time t_1 were calculated using 1-step schemes of the same orders.

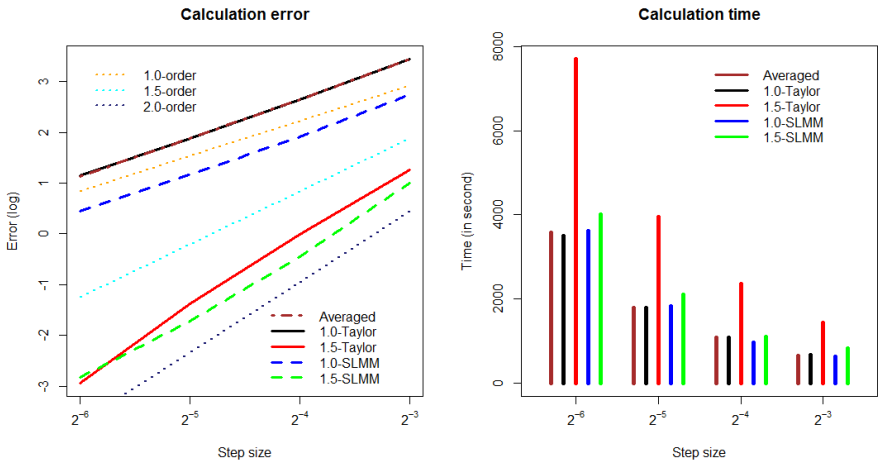

Figure 7.15: The comparison of calculation time for (7.18).

Figure 7.15 illustrates the 25 times simulation of HBV kinetic model. Each compartment was discretized into 21×21 grids, i.e. $i, j = 0, 1, \ldots, 20$. $L^1 L^1 f$ term in the 2.0-order schemes are very small and 1.5-order schemes

show 2.0-order decay. Now the system is of high dimension due to the spatial discretization and the difference in computational costs, especially between 1.5-order Itô-Taylor scheme (3.23) and the SLMM (7.20), is quite apparent.

7.8 Toggle-switch model

A simple toggle switch model with time-dependent parameters appeared in [97] is investigated in this section. The authors consider two interacting genes X and Y and the concentrations of the corresponding protein products are labeled x and y. Then the model is formulated as

$$\begin{aligned} \frac{dx(t)}{dt} &= \left(\alpha_x + \frac{x(t)^4}{a^4 + x(t)^4}\right)\left(\frac{b^4}{b^4 + y(t)^4}\right) - \lambda_x x(t), \\ \frac{dy(t)}{dt} &= \left(\alpha_y + \frac{y(t)^4}{c^4 + y(t)^4}\right)\left(\frac{d^4}{d^4 + x(t)^4}\right) - \lambda_y y(t), \end{aligned} \tag{7.21}$$

where parameters α_x and α_y represent the external activation on genes X and Y, a and c determine auto-activation thresholds, b and d thresholds for mutual repression and λ_x and λ_y protein decay rates. For the simulations here we assume α_x and α_y are given by two compound Poisson processes (6.6).

First to third order affine-RODE-Taylor schemes (4.14), (4.15) and (4.16) and LMM:

$$\text{(Ex1.0) } X_n^k = X_{n-1}^k + \frac{1}{2}(f_{n-1}^{0,k} + f_{n-2}^{0,k})\Delta_t + \sum_{j=1}^{m} f_{n-1}^{j,k} I_{(j),t_{n-1}}, \tag{7.22}$$

$$\begin{aligned} \text{(Ex2.0) } X_n^k &= X_{n-1}^k + \frac{1}{2}(3f_{n-1}^{0,k} + f_{n-2}^{0,k})\Delta_t + \sum_{j=1}^{m} f_{n-1}^{j,k} I_{(j),t_{n-1}}, \\ &\quad + \sum_{\substack{j_1,j_2=0 \\ j_1+j_2\neq 0}}^{m} L^{j_1} f_{n-1}^{j_2,k} I_{(j_1,j_2),t_{n-1}} - \frac{1}{2}\sum_{j=1}^{m} L^j f_{n-2}^{0,k} I_{(j),t_{n-2}}\Delta_t, \end{aligned} \tag{7.23}$$

as well as 1- and 2-order RODE-Taylor schemes [57, 64] are applied to the model.

In the simulation, the parameters are set to $a = c = 0.25$, $b = d = 0.4$ and $\lambda_x = \lambda_y = 1.25$ with the initial values $x_0 = y_0 = 10$. The jump magnitudes of two compound Poisson processes follow a uniform distribution on $[0, 0.5]$ and the parameter λ for (6.5) is fixed to 5 in both cases. The "exact" solution is obtained by 3-order affine-RODE-Taylor scheme (4.16) with the step size $\Delta_t = 2^{-9}$ and compare with approximations by (4.14), (4.15), (4.16), (7.22), (7.23), 1-order and 2-order RODE-Taylor schemes with different step sizes

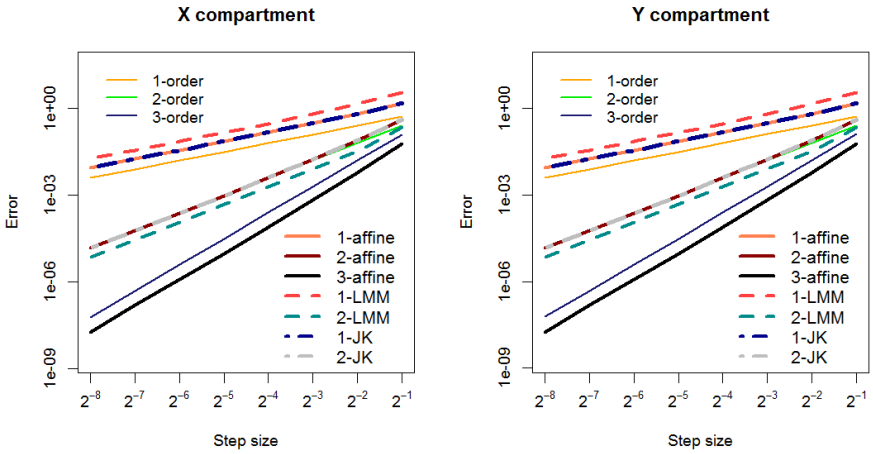

Figure 7.16: Plots for error vs step sizes for (7.21).

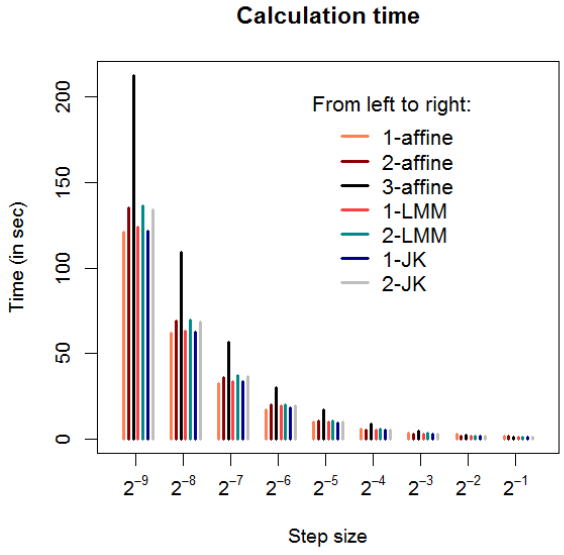

Figure 7.17: The histogram for the computational costs for (7.21).

$\Delta_t = 2^{-8}, 2^{-7}, 2^{-6}, 2^{-5}, 2^{-4}, 2^{-3}, 2^{-2}, 2^{-1}$. The values at time t_1 for LMMs were calculated by the same order affine-RODE-Taylor schemes.

The step size versus mean error and the computational costs for 100 times simulations are shown on Figures 7.16 and 7.17. The solid thick lines on Figure 7.16 are the errors by affine-RODE-Taylor schemes, the dashed

lines by LMMs and the dashed and dotted lines by RODE-Taylor schemes. The solid thin lines are for reference and have 1-, 2- and 3-order slopes.

Both of the 1- and 2-order RODE-Taylor schemes (dashed and dotted lines) coincide closely with the 1- and 2-order affine-RODE-Taylor schemes (4.14) and (4.15) (solid lines), respectively. No big difference in computational costs can be observed among the affine-RODE-Taylor schemes, LMMs and RODE-Taylor schemes.

7.9 Virus kinetic model

One of the simplest models for human immunodeficiency virus (HIV) or HCV kinetics with three compartments is given by

$$\begin{aligned}
\frac{dH(t)}{dt} &= s - \beta H(t)V(t) - dH(t),\\
\frac{dI(t)}{dt} &= \beta H(t)V(t) - \delta I(t),\\
\frac{dV(t)}{dt} &= (1-\epsilon)pI(t) - cV(t),
\end{aligned}$$

where H is the compartment for the healthy cells, I for the infected cells and V for the free viruses [80, 87]. This already displays some of the complications that arise in higher dimensional models, in particular different interaction rates and time scales [1, 79]. The parameters here are the production rate of the healthy cells s, the de-novo infection rate β, the loss rate of the healthy cells d, the loss rate of infected cells δ, the production rate of the new virus p, the loss rate of the virus c and the effect of treatment ϵ.

The parameter δ has a strong impact on the outcome. Here, it will be considered to vary randomly, but to remain bounded, so δ is replaced by (7.3), where $Y(t)$ is a Wiener process. This gives the RODE:

$$\begin{aligned}
\frac{dH(t)}{dt} &= s - \beta H(t)V(t) - dH(t),\\
\frac{dI(t)}{dt} &= \beta H(t)V(t) - \delta_0\left(1 - \nu\frac{2}{\pi}\arctan Y(t)\right)I(t),\\
\frac{dV(t)}{dt} &= (1-\epsilon)pI(t) - cV(t).
\end{aligned} \tag{7.24}$$

The time step size is set to $\Delta_t = \Delta_a^2$ for the explicit Euler scheme (3.18) and Δ_a for the averaged schemes. The other parameters are fixed to $c = 8$, $\delta_0 = 0.4$, $s = 1.3 \times 10^6$, $d = 0.5$ and $\epsilon = 0.1$ with initial values $H_0 = 1.6 \times 10^6$, $I_0 = 1.2 \times 10^6$ and $V_0 = 1 \times 10^7$. Moreover, p and β are given by $p = cV_0/I_0$ and $\beta = \delta_0 I_0/(H_0 V_0)$.

Solutions of the system (7.24) are approximated by the explicit Euler scheme (3.18), the EAES (2.35), the IAES (2.36) and the IAMS (2.37).

Typical sample paths are illustrated on Figures 7.18 to 7.26. The black line, the blue line and the red line on the first four graphs for each step size are the virus, the infected cell and the healthy cell values, respectively. The black line, the blue line, the red line and the green line on the graph for comparison are the solutions for the explicit Euler scheme (3.18), the EAES (2.35), the IAES (2.36) and the IAMS (2.37), respectively. The spread of the noise ν is fixed to 1 in these examples. The histograms show the sum of 100 times simulation time by each scheme. In Figure 7.18, with step size Δ_a = 0.2, the solution of the EAES (2.35) oscillates unstably, which makes this scheme unsuitable with such step size. A difference between the solutions of the explicit Euler scheme (3.18) and the EAES (2.35) is still apparent for step size $\Delta_a = 0.1$ (Figure 7.21), while all solution curves look very similar when the step size Δ_a is 0.05 (Figure 7.26). The implicit schemes return a good approximation even for large step sizes such as $\Delta_a = 0.2$ (Figure 7.19). At the same time, the computational costs by these schemes are mostly smaller than one by the explicit Euler scheme (3.18), in particular for small step sizes (Figure 7.26).

Figures 7.27–7.35 are simulation results under different amplitude ν. The step size is fixed to 0.1 and ν is changed from 0.3 to 0.8. The results by both implicit schemes are similar to ones by the explicit Euler scheme (3.18) even for large ν (Figure 7.35).

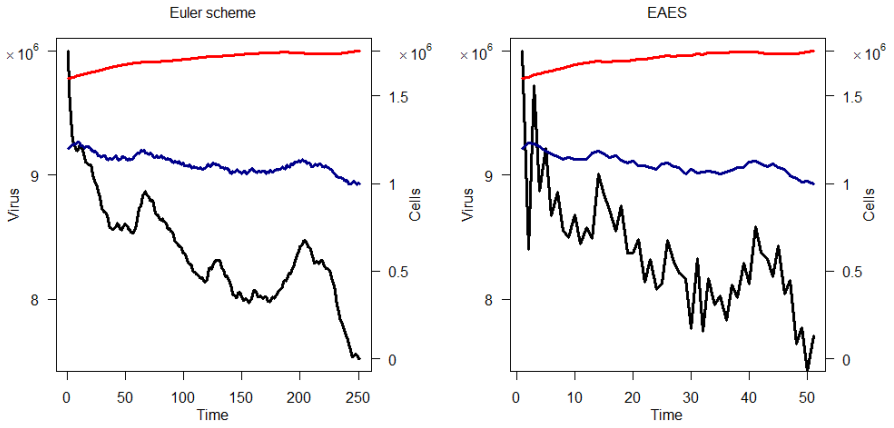

Figure 7.18: The approximation by the explicit Euler scheme (3.18) and the EAES (2.35). The step sizes are $\Delta_a = 0.2$ for the averaged schemes and $\Delta_t = \Delta_a^2$ for the explicit Euler scheme (3.18). The parameters are set to $c = 8$, $\delta_0 = 0.4$, $s = 1.3 \times 10^6$, $d = 0.5$ and $\epsilon = 0.1$ with initial values $H_0 = 1.6 \times 10^6$, $I_0 = 1.2 \times 10^6$ and $V_0 = 1 \times 10^7$. The black line: the virus compartment, the blue line: the infected cells compartment and the red line: the healthy cells compartment.

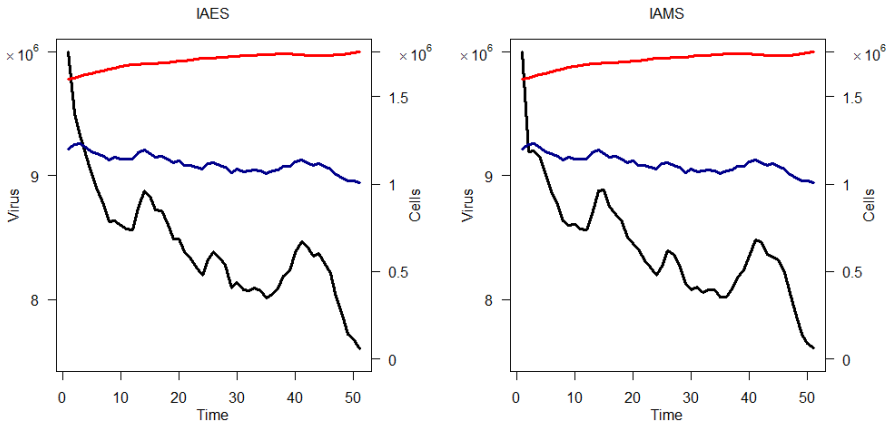

Figure 7.19: The approximation by the IAES (2.36) and the IAMS (2.37). The step sizes are $\Delta_a = 0.2$ for the averaged schemes and $\Delta_t = \Delta_a^2$ for the explicit Euler scheme (3.18). The parameter values and the line colors are the same with Figure 7.18.

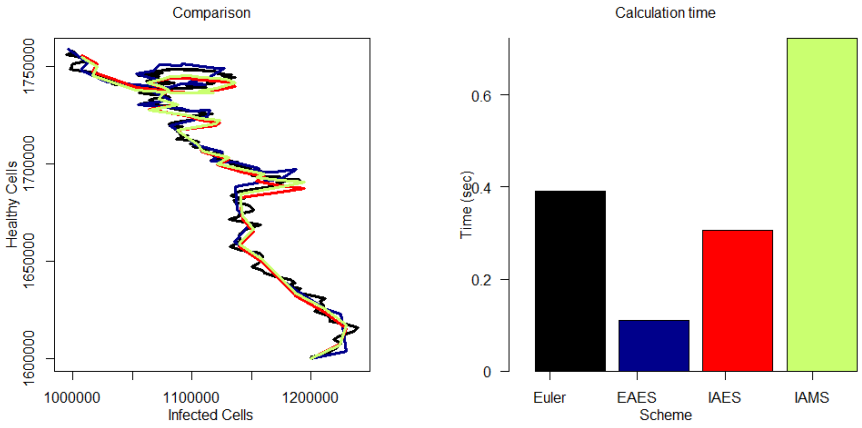

Figure 7.20: The comparison of the trajectories and the calculation costs by the explicit Euler scheme (3.18), the EAES (2.35), the IAES (2.36) and the IAMS (2.37). The step sizes are $\Delta_a = 0.2$ for the averaged schemes and $\Delta_t = \Delta_a^2$ for the explicit Euler scheme (3.18). The parameter values and the line colors are the same with Figure 7.18.

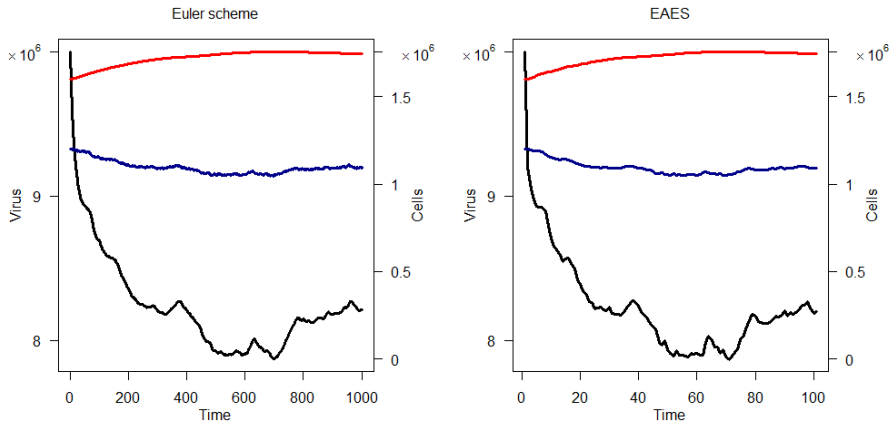

Figure 7.21: The approximation by the explicit Euler scheme (3.18) and the EAES (2.35). The step sizes are $\Delta_a = 0.1$ for the averaged schemes and $\Delta_t = \Delta_a^2$ for the explicit Euler scheme (3.18). The parameter values and the line colors are the same with Figure 7.18.

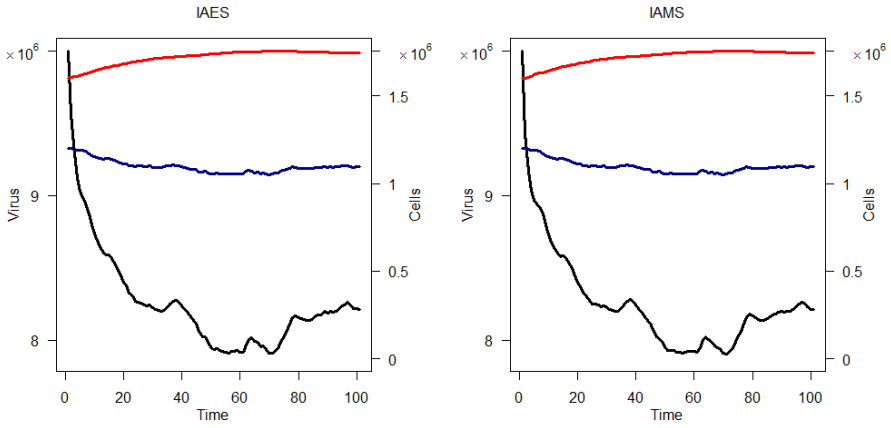

Figure 7.22: The approximation by the IAES (2.36) and the IAMS (2.37). The step sizes are $\Delta_a = 0.1$ for the averaged schemes and $\Delta_t = \Delta_a^2$ for the explicit Euler scheme (3.18). The parameter values and the line colors are the same with Figure 7.18.

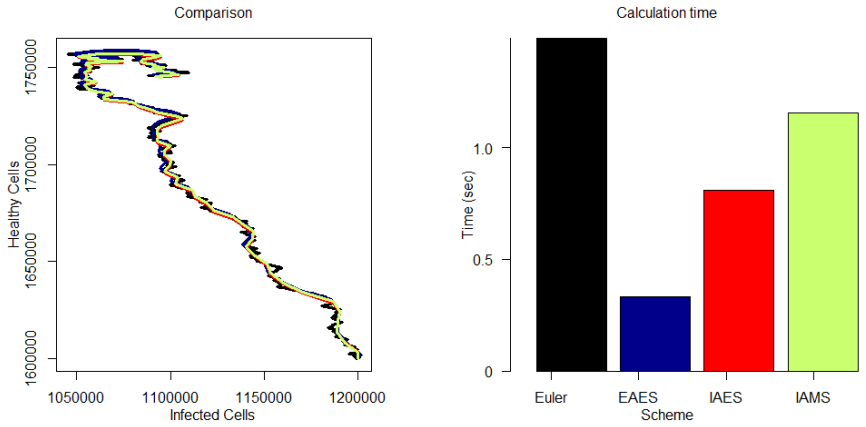

Figure 7.23: The comparison of the trajectories and the calculation costs by the explicit Euler scheme (3.18), the EAES (2.35), the IAES (2.36) and the IAMS (2.37). The step sizes are $\Delta_a = 0.1$ for the averaged schemes and $\Delta_t = \Delta_a^2$ for the explicit Euler scheme (3.18). The parameter values and the line colors are the same with Figure 7.18.

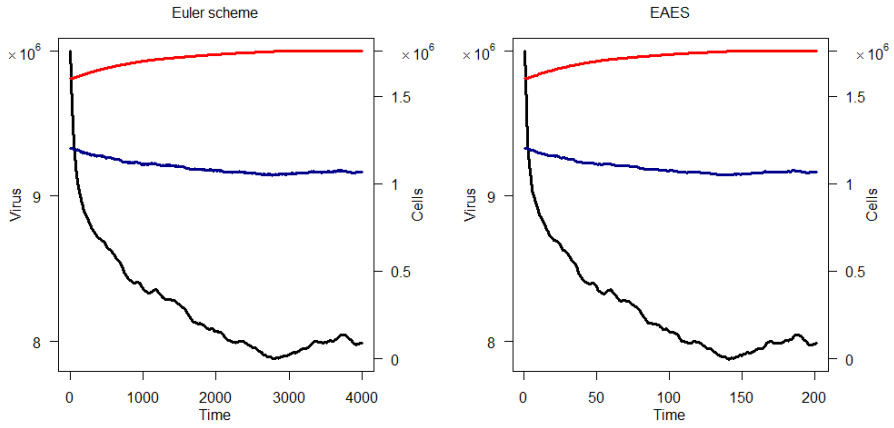

Figure 7.24: The approximation by the explicit Euler scheme (3.18) and the EAES (2.35). The step sizes are $\Delta_a = 0.05$ for the averaged schemes and $\Delta_t = \Delta_a^2$ for the explicit Euler scheme (3.18). The parameter values and the line colors are the same with Figure 7.18.

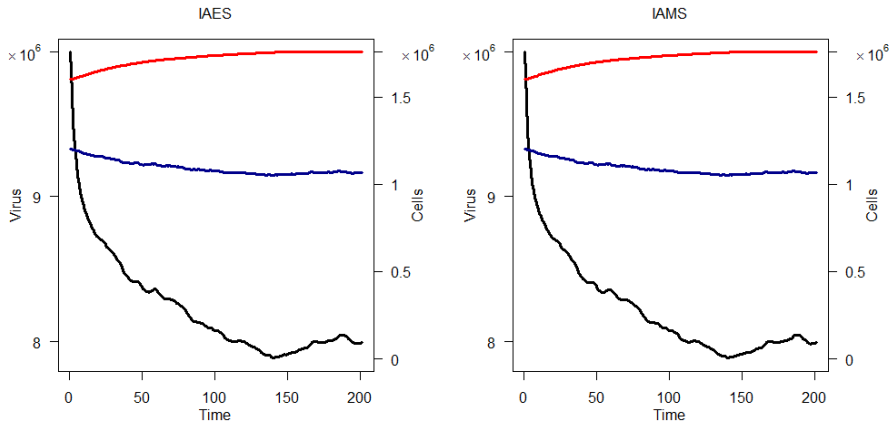

Figure 7.25: The approximation by the IAES (2.36) and the IAMS (2.37). The step sizes are $\Delta_a = 0.05$ for the averaged schemes and $\Delta_t = \Delta_a^2$ for the explicit Euler scheme (3.18). The parameter values and the line colors are the same with Figure 7.18.

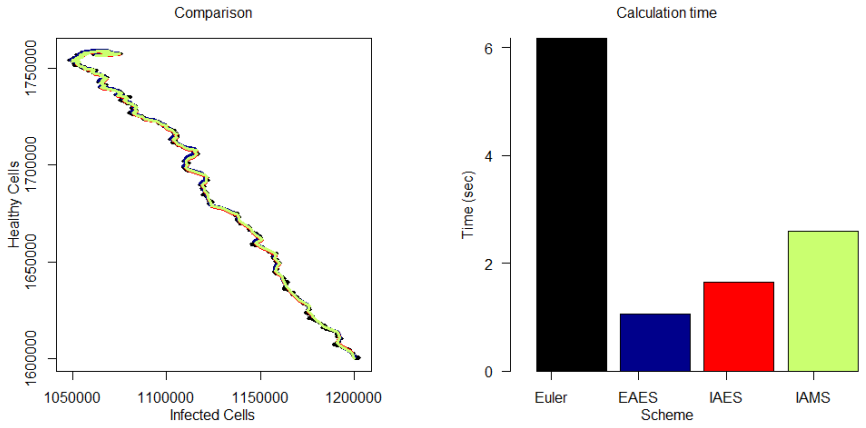

Figure 7.26: The comparison of the trajectories and the calculation costs by the explicit Euler scheme (3.18), the EAES (2.35), the IAES (2.36) and the IAMS (2.37). The step sizes are $\Delta_a = 0.05$ for the averaged schemes and $\Delta_t = \Delta_a^2$ for the explicit Euler scheme (3.18). The parameter values and the line colors are the same with Figure 7.18.

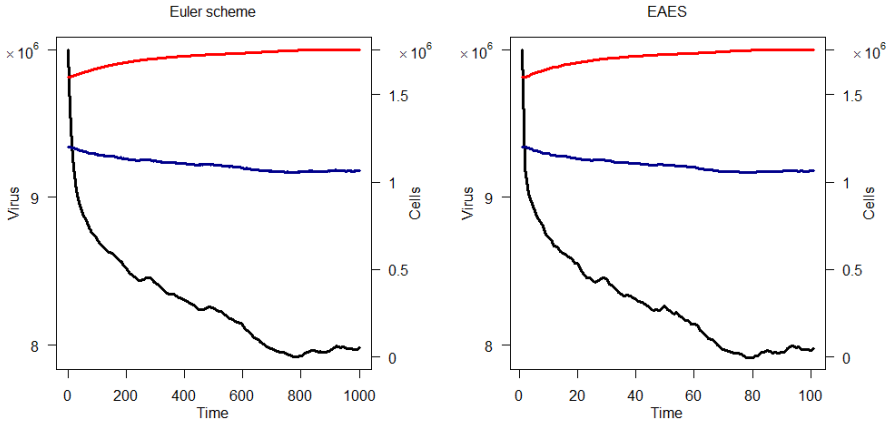

Figure 7.27: The approximation by the explicit Euler scheme (3.18) and the EAES (2.35). The step sizes are $\Delta_a = 0.1$ for the averaged schemes and $\Delta_t = \Delta_a^2$ for the explicit Euler scheme (3.18) and $\nu = 0.3$. The parameter values and the line colors are the same with Figure 7.18.

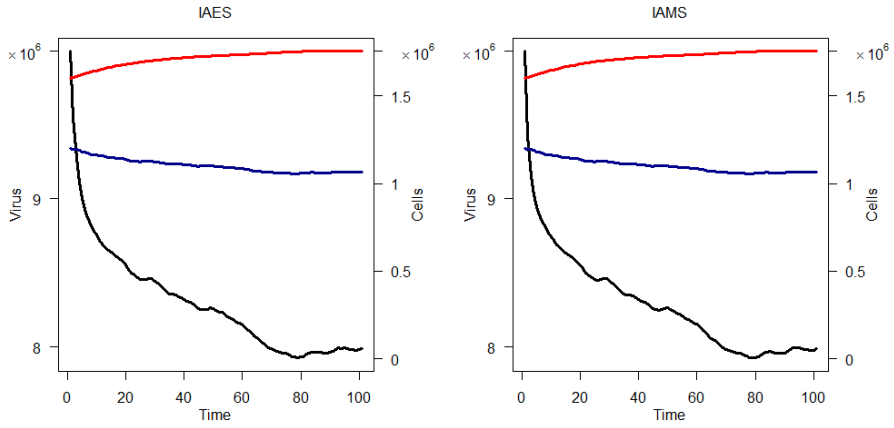

Figure 7.28: The approximation by the IAES (2.36) and the IAMS (2.37). The step sizes are $\Delta_a = 0.1$ for the averaged schemes and $\Delta_t = \Delta_a^2$ for the explicit Euler scheme (3.18) and $\nu = 0.3$. The parameter values and the line colors are the same with Figure 7.18.

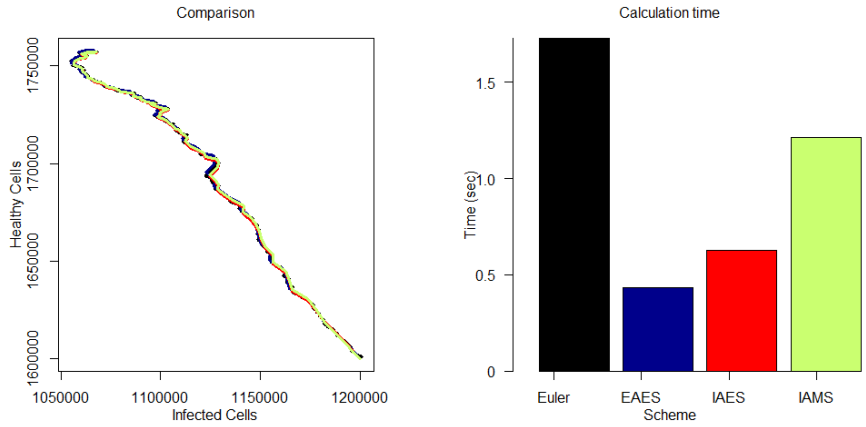

Figure 7.29: The comparison of the trajectories and the calculation costs by the explicit Euler scheme (3.18), the EAES (2.35), the IAES (2.36) and the IAMS (2.37). The step sizes are $\Delta_a = 0.1$ for the averaged schemes and $\Delta_t = \Delta_a^2$ for the explicit Euler scheme (3.18) and $\nu = 0.3$. The parameter values and the line colors are the same with Figure 7.18.

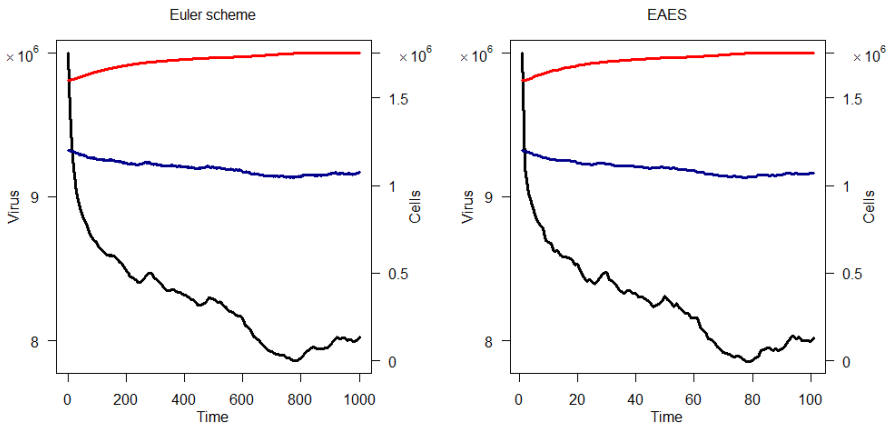

Figure 7.30: The approximation by the explicit Euler scheme (3.18) and the EAES (2.35). The step sizes are $\Delta_a = 0.1$ for the averaged schemes and $\Delta_t = \Delta_a^2$ for the explicit Euler scheme (3.18) and $\nu = 0.5$. The parameter values and the line colors are the same with Figure 7.18.

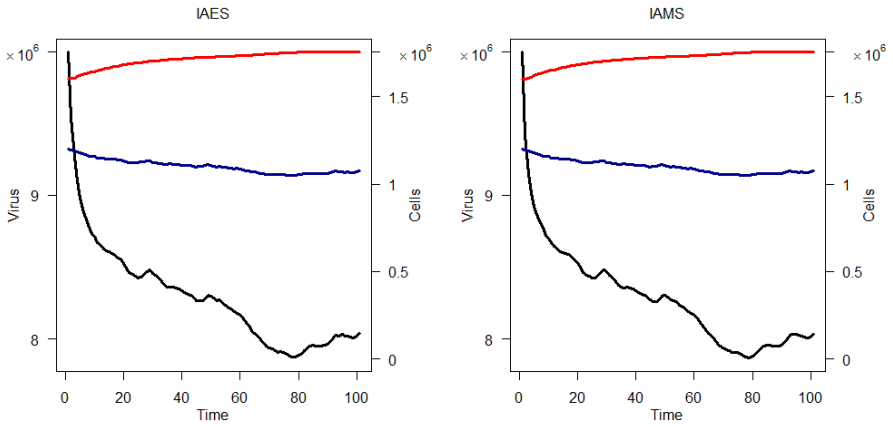

Figure 7.31: The approximation by the IAES (2.36) and the IAMS (2.37). The step sizes are $\Delta_a = 0.1$ for the averaged schemes and $\Delta_t = \Delta_a^2$ for the explicit Euler scheme (3.18) and $\nu = 0.5$. The parameter values and the line colors are the same with Figure 7.18.

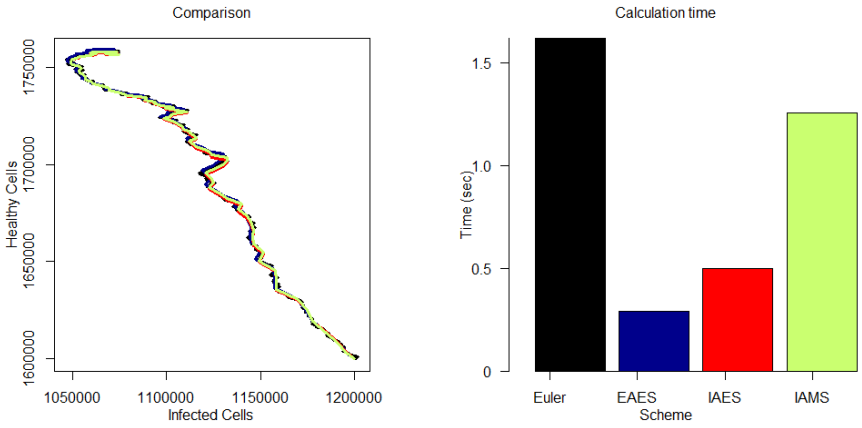

Figure 7.32: The comparison of the trajectories and the calculation costs by the explicit Euler scheme (3.18), the EAES (2.35), the IAES (2.36) and the IAMS (2.37). The step sizes are $\Delta_a = 0.1$ for the averaged schemes and $\Delta_t = \Delta_a^2$ for the explicit Euler scheme (3.18) and $\nu = 0.5$. The parameter values and the line colors are the same with Figure 7.18.

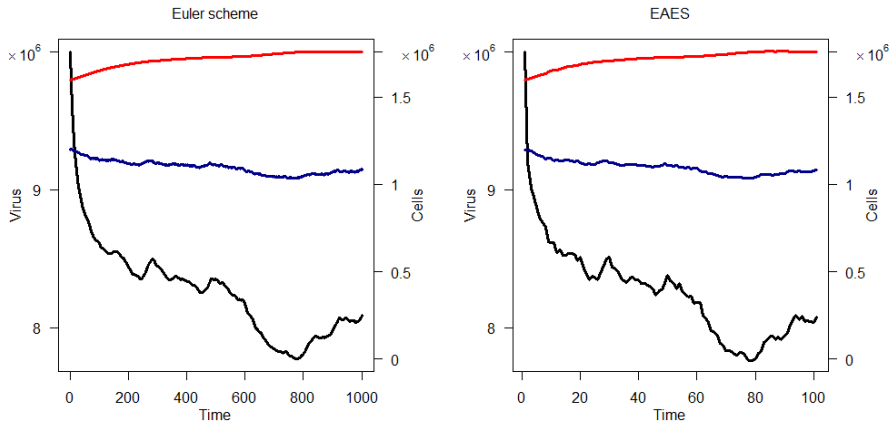

Figure 7.33: The approximation by the explicit Euler scheme (3.18) and the EAES (2.35). The step sizes are $\Delta_a = 0.1$ for the averaged schemes and $\Delta_t = \Delta_a^2$ for the explicit Euler scheme (3.18) and $\nu = 0.8$. The parameter values and the line colors are the same with Figure 7.18.

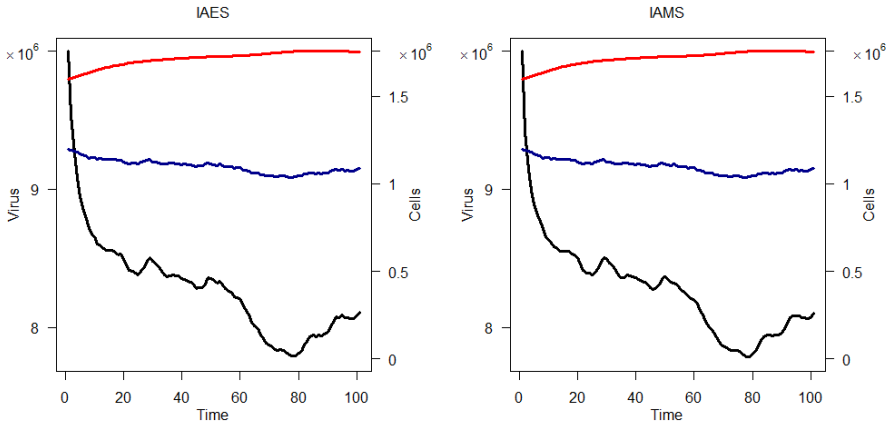

Figure 7.34: The approximation by the IAES (2.36) and the IAMS (2.37). The step sizes are $\Delta_a = 0.1$ for the averaged schemes and $\Delta_t = \Delta_a^2$ for the explicit Euler scheme (3.18) and $\nu = 0.8$. The parameter values and the line colors are the same with Figure 7.18.

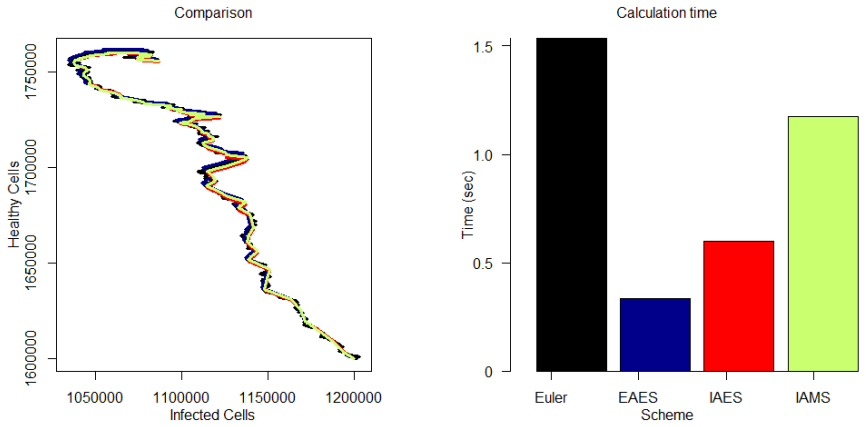

Figure 7.35: The comparison of the trajectories and the calculation costs by the explicit Euler scheme (3.18), the EAES (2.35), the IAES (2.36) and the IAMS (2.37). The step sizes are $\Delta_a = 0.1$ for the averaged schemes and $\Delta_t = \Delta_a^2$ for the explicit Euler scheme (3.18) and $\nu = 0.8$. The parameter values and the line colors are the same with Figure 7.18.

Bibliography

[1] Adiwijaya B.S., Herrmann E., Hare B., Kieffer T., Lin C., Kwong A.D., Garg V., Randle J.C.R., Sarrazin C., Zuezem S. and Caron P.R., A multi-variant, rival dynamic model of genotype 1 HCV to assess the in vivo evolution of protease inhibitor resistant variants, *PLoS Computational Biology*, 6 (4) (2010), 1–13.

[2] Allen E., *Modeling with Itô Stochastic Differential Equations*, Springer, Netherlands, 2007.

[3] Allen E. and Allen L.J.S., Construction of equivalent stochastic differential equation models, *Stoch. Anal. Applns.*, **26** (2008) 274–297.

[4] Arnold L., *Stochastic Differential Equations: Theory and Applications*, John Wiley & Sons, Inc., 1974.

[5] Arnold L., *Random Dynamical Systems*, Springer-Verlag, Berlin, 1997.

[6] Asai Y., *Building a Graphical User Interface to simulate treatment effect of combination therapy of chronic hepatitis C*, Master thesis, Institute of Biostatistics and Mathematical Modeling, Department of Medicine, Johann Wolfgang Goethe-University Frankfurt am Main, 2012.

[7] Asai Y., Herrmann E. and Kloeden P.E., Stable integration of stiff random ordinary differential equations, *Stoch. Anal. Appl.*, **31** (2013) 293–313.

[8] Asai Y. and Kloeden P.E., Numerical schemes for random ODEs via stochastic differential equations, *Commun. Appl. Anal.*, (2013) **17** no.3 & 4, 511–528.

[9] Asai Y. and Kloeden P.E., Multi-step methods for random ODEs driven by Itô diffusions, *J. Comput. Appl. Math.*, **294** (2016) 210–224.

[10] Asai Y. and Kloeden P.E., Numerical schemes for random ODEs with affine noise, *Numer. Algor.*, (2016) 72:155–171.

[11] Bachelier L., Théorie de la spéculation, *Annales scientifiques de l'É.N.S. 3e série*, tome 17 (1900), 21–86.

[12] Bobrowski D., Wstęp do losowych równań różniczkowych zwyczajnych, Państwowe Wydawnictwo Naukowe, Warszawa 1987.

[13] Buckwar E. and Winkler R., Multi-step methods for SODEs and their application to problems with small noise, *SIAM J. Numer. Anal.*, **44** (2006), no. 2. 779–803.

[14] Buckwar E. and Winkler R., Improved linear multi-step methods for stochastic ordinary differential equations, *J. Comput. Appl. Math.*, **205** (2007), 912–922.

[15] Bunke H., *Gewöhnliche Differentialgleichungen mit zufälligen Parametern*, Akademie-Verlag, Berlin, 1972.

[16] Burrage K., Burrage P.M. and Tian T., Numerical methods for strong solutions of stochastic differential equations: An overview, *Proc. R. Soc. Lond., Ser. A, Math. Phys. Eng. Sci.*, **460** 2004, 373–402.

[17] Butcher J.C., A stability property of implicit Runge-Kutta methods, *BIT* **15** (1975), 358–361.

[18] Butcher J.C., *Numerical Methods for Ordinary Differential Equations*, John Wiley & Sons, Ltd, Chichester, 2003.

[19] Butcher J.C., Thirty years of G-stability, *BIT Numerical Mathematics*, **46** (2006), 479–489.

[20] Caraballo T. and Kloeden P.E., The persistence synchronization under environmental noise, *Proc. Roy. Soc. London*, **A461** (2005), 2257–2267.

[21] Carbonell F., Jimenez J.C., Biscay R.J. and de la Cruz H., The local linearization methods for numerical integration of random differential equations, *BIT*, **45** (2005), 1–14.

[22] Charpentier É., Lesne A. and Nikolski N.K., *Kolmogorov's Heritage in Mathematics*, Springer-Verlag Berlin, 2007.

[23] Chandrasekhar S., Kac M. and Smoluchowski R., *Marian Smoluchowski His Life and Scientific Work*, Polish Scientific Publishers PWN, Warszawa 1999.

[24] Coffey W.T., Kalmykov Yu.P. and Waldron J.T., *The Langevin Equations with Applications to Stochastic Problems in physics, Chemistry and Electrical Engineering, Second Edition*, World Scientific, Singapore, 2004.

[25] Cont R. and Tankov P., *Financial Modelling with Jump Processes*, Chapman & Hall/CRC Financial Mathematics Series, Boca Raton, 2004.

[26] Couerjolly J.-F., Simulation and identification of the fractional Brownian motion: a bibliographical and comparative study, *Journal of Statistical Software*, Vol.5, 2000.

[27] Davies R.B. and Harte D.S., Tests for Hurst effect, *Biometrika*, **74** (1987), 95–102.

[28] Deuflhard P. and Bornemann F., *Numerische Mathematik II*, de Gruyter Lehrbuch, Berlin, 2002.

[29] Dieker T., Simulation of fractional Brownian motion, (2004) *http://www2.isye.gatech.edu/ adieker3/index.html.*

[30] Dietrich C.R. and Newsam G.N., Fast and exact simulation of stationary Gaussian processes through circulant embedding of the covariance matrix, *SIAM J. Sci. Comput.*, Vol. 18, No. 4, 1088–1107, July 1997.

[31] d'Onofrio A., *Bounded Noises in Physics, Biology, and Engineering*, Birkhäuser, Springer Science+Business Media New York, 2013.

[32] Doss H., Liens entre équations différentielles stochastiques et ordinaires, *Ann. Inst. Henri Poincaré, Nouv. Sér., Sect. B*, **13** 1977, 99–125.

[33] Einstein A., *Investigations on the Theory of the Brownian Movement*, BN Publishing, 2011.

[34] Fournier A., Fussel D., and Carpenter L., Computer rendering of stochastic models, *Communications of the ACM*, **25** (1982) 371–384.

[35] Gard T.C., *Introduction to Stochastic Differential Equations*, Marcel Dekker, New York, 1988.

[36] Griffiths D.F. and Higham D.J., *Numerical Methods for Ordinary Differential Equations Initial Value Problems*, Springer, 2010.

[37] Grüne L. and Kloeden P.E., Higher order numerical schemes for affinely controlled nonlinear systems, *Numer. Math.*, **89** (2001) 669–690.

[38] Grüne L. and Kloeden P.E., Pathwise approximation of random ordinary differential equations, *BIT* **41** (4) (2001), 711–721.

[39] Günther M. and Jüngel A., *Finanzderivate mit MATLAB Mathematische Modellierung und numerische Simulation 2. Auflage*, Vieweg+Teubner Verlag, Wiesbaden, 2003.

[40] Gyöngy I., A note on Euler's approximations, *Potential Anal.*, **8** (1998), 205–216.

[41] Hairer E. and Wanner G., *Solving Ordinary Differential Equations I*, Springer-Verlag, Heidelberg, 1991.

[42] Hairer E. and Wanner G., *Solving Ordinary Differential Equations II*, Springer-Verlag, Heidelberg, 1991.

[43] Hanson F.B., *Applied Stochastic Processes and Control for Jump-Diffusions Modeling, Analysis, and Computation*, SIAM, Philadelphia, 2007.

[44] Higham D.J., Mean-square and asymptotic stability of the stochastic theta method, *SIAM J. Numer. Anal.*, **38** (2000), no. 3. 753–769.

[45] Higham D.J., An algorithmic introduction to numerical simulation of stochastic differential equations, *SIAM J. Numer. Anal.*, **43** (2001), no. 3. 525-546.

[46] Hindmarsh A.C., A systematized collection of ODE solvers, *Lawrence Livermore National Laboratory*, August, 1982.

[47] Hutzenthaler M., Jentzen A. and Kloeden P.E., Strong and weak divergence in finite time Euler's method for SDEs with non-globally Lipschitz coefficients, *Proc. Roy. Soc. London A*, **A467** (2011), no. 2130, 1563–1576.

[48] Hutzenthaler M., Jentzen A. and Kloeden P.E., Strong convergence of an explicit numerical method for SDEs with non-globally Lipschitz continuous coefficients, *Annals Appl. Probability*, **22** (2012), 1611–1641.

[49] Imkeller P. and Lederer C., On the cohomology of flows of stochastic and random differential equations, *Probab. Theory & Related Fields*, **120**, 2001, 209–235.

[50] Imkeller P. and Schmalfuß B., The conjugacy of stochastic and random differential equations and the existence of global attractors, *J. Dyn. Diff. Eqns.*, **13** (2001), 215–249.

[51] Imkeller P. and Lederer C., The cohomology of stochastic and random differential equations, and local linearization of stochastic flows, *Stoch. Dyn.*, **2**, 2002, 131–159.

[52] Itô K., *Kakuritsu Katei*, Iwanami Shoten, Tokyo, 2007.
(確率過程　伊藤清著　岩波書店)

[53] Itô K., *Kakuritsuron to Watashi*, Iwanami Shoten, Tokyo, 2010.
(確率論と私　伊藤清著　岩波書店)

[54] Ikeda N. and Watanabe S., *Stochastic Differential Equations and Diffusion Processes*, Kodansha Ltd Tokyo, 1981.

[55] Jentzen A., *Numerische Verfahren hoher Ordnung für zufällige Differentialgleichungen*, Diplomarbeit, J.W. Goethe-Universität, Frankfurt am Main, February 2007.

[56] Jentzen A. and Kloeden P.E., Pathwise Taylor schemes for random ordinary differential equations, *BIT* **49** (1) (2009), 113–140.

[57] Jentzen A. and Kloeden P.E., *Taylor Approximations of Stochastic Partial Differential Equations*, CMS Lecture series, SIAM, Philadelphia, 2011.

[58] Jentzen A., Kloeden P.E. and Neuenkirch A., Pathwise approximation of stochastic differential equations on domains: higher order convergence rates without global Lipschitz coefficients, *Numerische Mathematik*, **112** (2009) (1), 41–64.

[59] Jentzen A., Kloeden P.E. and Neuenkirch A., Pathwise convergence of numerical schemes for random and stochastic differential equations, in *Foundations of Computational Mathematics: Hong Kong 2008*, Editors: F. Cucker, A. Pinkus & M. Todd, Cambridge University Press, 2009, 140–161.

[60] Jeong H.-D.J., McNickle D. and Pawlikowski K., A Search for Computationally Efficient Generators of Synthetic Self-similar Teletraffic, *Proc. Australasian Computer Science Conference ASCS'99, Auckland*, **21** Springer-Verlag Singapore, 1999, 75–86

[61] Kloeden P.E., *Script for the lectures on "Numerical Methods for Differential Equations"*, Institut für Computerorientierte Mathematik, Johann Wolfgang Goethe-Universität, 2008.

[62] Kloeden P.E., *Script for the lectures on "Numerical Linear Algebra" Einführung in die numerische Mathematik*, Institut für Mathematik Johann Wolfgang Goethe Universität (2008).

[63] Kloeden P.E., *Skript zur Vorlesung: "Numerik stochastischer Differentialgleichungen"*, Fachbereich Mathematik, Johann Wolfgang Goethe-Universität, 2010.

[64] Kloeden P.E. and Jentzen A., Pathwise convergent higher order numerical schemes for random ordinary differential equations, *Proc. R. Soc. A*, **463** (2007), 2929–2944.

[65] Kloeden P.E. and Neuenkirch A., The pathwise convergence of approximation schemes for stochastic differential equations, *LMS J. Comput. & Math.*, **10** (2007), 235–253.

[66] Kloeden P.E. and Platen E., *Numerical Solution of Stochastic Differential Equations*, Springer-Verlag, Heidelberg, 1992.

[67] Kloeden P.E. and Platen E., Higher-order implicit strong numerical schemes for stochastic differential equations, *J. Statistical Physics*, **66** (1992), 283–314.

[68] Kloeden P.E. and Pöetzsche C., *Nonautonomous Dynamical Systems in the Life Sciences*, Springer, Heidelberg, 2013.

[69] Kloeden P.E. and Rößler A., Runge-Kutta methods for affinely controlled nonlinear systems, *Journal of Computational and Applied Mathematics*, **205** (2007) 957–968.

[70] Kloeden P.E., Sonner S. and Surulescu C., A nonlocal sample dependence SDE-PDE system modeling proton dynamics in a tumor. (to appear)

[71] Kolmogorov A.N., Über die analitischen Methoden in der Warscheinlichkeitsrechnung, *Math. Ann.*, 1931, **104**, 415–458.

[72] Kolmogorov A.N., *Grundbegriffe der Wahrscheinlichkeistsrechnung*, Springer, Berlin, 1933.

[73] Langevin P., Sur la théorie du mouvement brownien, *C. R. Acad. Sci. (Paris)*, **146**, (1908), 530–533.

[74] Mandelbrot B.B. and Van Ness J.W., Fractional Brownian motions, fractional noises and applications, *SIAM Review* **10** 4, 1968.

[75] Meinhardt H., *The Algorithmic Beauty of Sea Shells, Fourth Edition*, Springer-Verlag, Heidelberg, 2009.

[76] Milstein G.N., *Numerical Integration of Stochastic Differential Equations*, Kluwer Academic Publishers, Dordrecht, 1995.

[77] Milstein G.N. and Tretjakov M.V., *Stochastic Numerics for Mathematical Physics*, Springer, Berlin, 2004.

[78] Mitsui T., Koto T., Saito Y., *Bibunhôteishiki ni yoru keisan kagaku nyûmon*, Kyôritsu shuppan kabushikigaisha, Tokyo, 2004.
(微分方程式による計算科学入門　三井斌友　小藤俊幸　斎藤善弘著　共立出版株式会社)

[79] Murphy A.A., Herrmann E., Osinusi A.O., Wu L., Sachau W., Lempicki R.A., Yang J., Chung T.L., Wood B.J., Haagmans B.L., Kottilil S. and Polis M.A., Twice-weekly pegylated interefon-α-2a and ribavirin results in superior viral kinetics in HIV/hepatitis C virus co-infected patients compared to standard therapy, *AIDS*, **25** (2011), 1179–1187.

[80] Neumann A.U., Lam N.P., Dahari H., Gretch D.R., Wiley T.E., Layden T.J. and Perelson A.S., Hepatitis C viral dynamics in vivo and the antiviral efficacy of interferon-α therapy, *Science*, **282** (1998), 103–107.

[81] Neckel T. and Rupp F., *Random Differential Equations in Scientific Computing*, Versita / De Gutyer Publishing, 2013.

[82] Nelson E., *Dynamical Theories of Brownian Motion*, Princeton, New Jersey, Princeton University Press, Princeton, 1967.

[83] Norros I., Mannersalo P. and Wang J.L., Simulation of fractional Brownian motion with conditionalized random midpoint displacement, *Advances in Performance Analysis*, **2** (1999), 77–101.

[84] Nualart D., Kolmogorov and probability theory, *Arbor CLXXVIII*, **704**, (Agosto 2004), 607–619.

[85] Øksendal B., *Stochastic Differential Equations An Introduction with Applications Sixth Edition*, Springer-Verlag, Heidelberg, 2003.

[86] Peitgen H.-O. and Saupe D., *The Science of Fractal Images*, Springer-Verlag New York Inc., 1988.

[87] Perelson A.S. and Ribeiro R.M., Modeling the within-host dynamics of HIV infection, *BMC Biology*, **11** (2013) 96.

[88] Platen E., An introduction to numerical methods for stochastic differential equations, *Acta Numerica*, (1999), 197–246.

[89] Schiesser W.E. and Griffiths G.W., *A Compendium of Partial Differential Equation Models Method of Lines Analysis with Matlab*, Cambridge University Press, Cambridge, 2009.

[90] Sobczyk K., *Stochastic Differential Equations with Applications to Physics and Engineering*, Kluwer, Dordrecht, 1991.

[91] Stuart A.M. and Humphries A.R., *Dynamical Systems and Numerical Analysis*, Cambridge University Press, Cambridge, 1996.

[92] Soong T.T., *Random Differential Equations in Science and Engineering*, Academic Press, New York, 1973.

[93] Sussmann H.J., On the gap between deterministic and stochastic differential equations, *Ann. Probab.* **6**, 1978, 19–41.

[94] Talay D., Efficient numerical schemes for the approximation of expectations of functionals of the solution of a SDE and applications, *Filtering and Control of Random Processes, Lecture Notes in Control and Inform. Sci.*, Springer-Verlag, Berlin, 1984, 294–313.

[95] Talay D., Disctirisation d'une équation différentielle stochastique et calcul approché d'espérances de fonctionnelles de la solution, *RAIRO Modél. Math. Anal. Numér.* **20**, 1986, 141–179.

[96] Tansky N., Switching effect in prey-predator system, *J. theor. Biol.*, (1978) **70**, 263–271.

[97] Verd B., Crombach A. and Jaeger J., Classification of transient behaviors in a time-dependent toggle switch model, *BMC Systems Biology*, (2014), **8**:43 1–19.

[98] Wang K. and Wang W., Propagation of HBV with spatial dependence, *Mathematical Biosciences*, 210, (2007), 78–95.

[99] Watanabe S. and Shigekawa I., *Kakuritsuron handbook*, Maruzen Publishing, Tokyo, 2012.
(確率論ハンドブック　渡辺信三　重川一郎著　丸善出版)

[100] Wodarz D. and Komarova N.L., *Computational Biology of Cancer*, World Scientific Publishing, Singapore, 2005.

[101] Wong W. and Zakai M., On the relation between ordinary and stochastic differential equations, *Internat. J. Engineering Sci.*, **3** 1965, 213–229.

[102] Wood A.T.A. and Chan G., Simulation of stationary Gaussian processes in $[0,1]^d$, *J. Comput. Graph. Stat.*, **3**, 4 (1994) 409–432.

[103] Xiao Y., Properties of local-nondeterminism of Gaussian and stable random fields and their applications, (2005)
http://130.120.83.239/Archive-LSP/Autosim05/download/xiao.pdf.

[104] Yosida K., *Butsuri sûgaku gairon*, Nihon hyôronsha, Tokyo, 1949.
(物理数学概論　吉田耕作著　日本評論社)

Deutsche Zusammenfassung

Zufällige gewöhnliche Differentialgleichungen (englisch: Random Ordinary Differential Equations, Akronym: RODEs) sind gewöhnliche Differentialgleichungen (englisch: Ordinary Differential Equations, Akronym: ODEs), die einen stochastischen Prozess in ihrer Vektorfeld-Funktion haben. RODEs werden in einer Vielzahl von Anwendungen, z.B. in der Biologie, Medizin, Populationsdynamik und der Technik eingesetzt [15, 70, 81, 90, 92] und spielen eine wichtige Rolle in der Theorie der zufälligen dynamischen Systeme [5]. Lange jedoch standen sie im Schatten von stochastischen Differentialgleichungen (englisch: Stochastic Differential Equations, Akronym: SDEs).

Allgemein werden RODEs auf $\mathbb{R}^{d_1}$ in der Form:

$$\frac{dx}{dt} = f(x, Y(t)), \tag{1}$$

geschrieben, wobei $Y(t)$ ein stochastischer Prozess [57] ist. Typischerweise hat der Antriebsstochastische Prozess $Y(t)$ höchstens Hölder-stetige Pfade. Das resultierende Vektorfeld $(t, x) \mapsto f(x, y(t))$ ist somit höchstens Hölder-stetig in der Zeit, egal wie glatt die Vektorfunktion in der Originalvariablen ist, so dass die Pfade der Lösung von (1) sicherlich stetig differenzierbar, aber ihre Ableitungen zumindest Hölder-stetig in der Zeit sind. Somit können die klassischen numerischen Verfahren für ODEs pfadweise als RODEs angewendet werden, aber ihre traditionellen Ordnungen werden dabei nicht erreicht werden können.

Neuerdings haben Grüne & Kloeden dabei explizite gemittelte Euler-Verfahren abgeleitet, indem sie den Mittelwert des Rauschens innerhalb des Vektorfeldes verwendet haben. Darüber hinaus wurden von Jentzen & Kloeden für RODEs neue Formen Taylor-artiger Verfahren systematisch abgeleitet. Trotzdem ist es wichtig, numerische Verfahren höherer Ordnung weniger rechnenintensiv und numerisch stabil zu konstruieren. Das ist die Motivation dieser Arbeit. Die Verfahren in [56, 64] sind sehr allgemein gehalten. Hier werden RODEs mit spezieller Struktur, d.h. RODEs mit Itô-Rauschen und RODEs mit affiner Struktur fokussiert und es werden numerische Verfahren genutzt, die diese speziellen Strukturen untersuchen.

Taylor-Entwicklungen

Taylor-Entwicklungen sind das Rückgrat der Entwicklung von numerischen Verfahren für die deterministischen ODEs und Taylor-Verfahren beliebig hoher Ordnung können durch vernachlässigen der entsprechende Restglieder erhalten werden. Zusätzlich zu den Taylor-Verfahren werden verschiedene Klassen von numerischen Methoden wie das Runge-Kutta-Verfahren und das lineare Mehrschrittverfahren (englisch: Linear Multi-step Methods, Akronym: LMMs) entwickelt und auf verschiedene Arten von Problemen angewendet [18, 36, 41, 42, 61].

Ähnlich zu der deterministischen Numerik, sind die Itô-Taylor-Entwicklungen die wichtigsten Werkzeuge, um numerische Verfahren für SDEs abzuleiten. Nehmen wir an, $Y(t)$ sei ein Itô stochastisches ODE (englisch: Stochastic ODE, Akronym: SODE) auf $\mathbb{R}^{d_2}$, d.h.

$$dY(t) = a(Y(t))\,dt + \sum_{j=1}^{m} b_j(Y(t))\,dW^j(t), \tag{2}$$

mit m unabhängigen skalaren Wiener Prozessen $W^1(t)$, $W^2(t)$, ..., $W^m(t)$. Dann wird die k-te Komponente von $Y(t)$ durch ein starkes Itô-Taylor-Verfahren der Ordnung γ approximiert als

$$Y_n^k = \sum_{\alpha\in\Lambda_\gamma} L^\alpha id_{\mathbf{Y}}^k(t_{n-1}, Y_{n-1})\, I_{\alpha,t_{n-1}}, \tag{3}$$

mit einem linearen Differentialoperator L:

$$L^0 = \frac{\partial}{\partial t} + \sum_{k=1}^{d_2} a^k \frac{\partial}{\partial y_k} + \frac{1}{2}\sum_{k,l=1}^{d_2}\sum_{j=1}^{m} b_j^k b_j^l \frac{\partial^2}{\partial y_k \partial y_l}, \quad L^j = \sum_{k-1}^{d_2} b_j^k \frac{\partial}{\partial y_k},$$

und einer hierarchischen Menge von Multiindizes Λ_γ:

$$\Lambda_\gamma = \left\{\alpha \in \mathcal{M}_m : l(\alpha) + n(\alpha) \le 2\gamma \quad \text{oder} \quad l(\alpha) = n(\alpha) = \gamma + \frac{1}{2}\right\},$$

$n(\alpha)$ sei die Menge von Komponenten von α gleich 0 ist und $l(\alpha)$ die Länge α ist. Zusätzlich notieren wir die Menge aller Multiindizes $\mathcal{M}_m$ als

$$\mathcal{M}_m = \Big\{\alpha = (j_1, \ldots, j_l) \in \{0, 1, 2, \ldots, m\}^l : l \in \mathbb{N}\Big\} \cup \{\emptyset\},$$

wobei $\emptyset$ die leere Menge ist mit der Länge $l(\alpha) = 0$. Außerdem gilt für die Multiindizes $\alpha = (j_1, \ldots, j_l)$ mit $l \ge 1$, dass die multiplen Integrale $I_{\alpha,t_{n-1}}$ und die iterierten Operatoren L^α definiert werden als

$$I_{\alpha,t_{n-1}} := \int_{t_{n-1}}^{t_n} \cdots \int_{t_{n-1}}^{s_2} dW^{j_1}(s_1)\cdots dW^{j_l}(s_l), \quad L^\alpha := L^{j_1}\cdots L^{j_l},$$

wobei $I_{\emptyset,t_{n-1}} = 1$ und $L^\emptyset = id$.

Die stochastischen Runge-Kutta-Verfahren und die stochastischen LMMs (englisch: Stochastic LMMs, Akronym: SLMMs) sind ebenfalls systematisch aufgebaut und ihre Konvergenz, sowie ihre starke, schwache und pfadweise Konvergenz und ihre Stabilitätseigenschaften sind in der Literatur [35, 45, 54, 57, 63, 65, 66, 76, 88] ausführlich diskutiert.

Gekoppeltes RODE-SODE System

Wenn das Rauschen regelmäßig ist, so gibt es in der Tat eine enge Verbindung

zwischen RODEs und SDEs. Dabei können RODEs in der Form von SODEs und umgekehrt geschrieben werden.

Angenommen, der Rauschprozess $Y(t)$ ist wie in (2) beschrieben gegeben. Dann kann ein gekoppeltes RODE-SODE System für das RODE aus (1) durch die folgende Gleichung gegeben werden:

$$d\begin{pmatrix} X(t) \\ Y(t) \end{pmatrix} = \begin{pmatrix} f(X(t), Y(t)) \\ a(Y(t)) \end{pmatrix} dt + \sum_{j=1}^{m} \begin{pmatrix} 0 \\ b_j(Y(t)) \end{pmatrix} dW^j(t). \tag{4}$$

Der Diffusionskoeffizient aus RODE Teil (4), d.h. die Komponente X, ist 0 und wegen dieser speziellen Struktur können die Verfahren aus (3) als RODE-Taylor-Darstellung in komponentenweiser Form reduziert werden:

$$X_n^k = \sum_{\alpha \in \Lambda_\gamma^0} L^\alpha id_{\mathbf{X}}^k(X_{n-1}, Y_{n-1})\, I_{\alpha, t_{n-1}}, \quad k = 1, \ldots, d_1. \tag{5}$$

Dabei ist Λ_γ^0 eine Teilmenge von Λ_γ:

$$\Lambda_\gamma^0 = \{\alpha \in \Lambda_\gamma : \alpha = \emptyset \text{ oder } l(\alpha) \geq 1 \text{ mit letzte Komponent } j_l = 0\}.$$

Es ist bekannt, dass die starken Itô-Taylor-Approximationen der Ordnung γ eine starke Konvergenz der Ordnung γ zeigen, falls die Koeffizienten den Standardannahmen [67, 76] genügen, d.h. die Koeffizientenfunktionen gehören zu dem Raum $C_b^{2\gamma+1}$ der $(2\gamma+1)$-mal stetig differenzierbaren Funktionen mit gleichmäßig beschränkten partiellen Ableitungen. Daraus folgt, durch ein Ergebnis der Arbeit von Kloeden & Neuenkirch [65], dass die Verfahren pfadweise Konvergenz der Ordnung $(\gamma - \epsilon)$ und die entsprechenden Verfahren für RODEs auch eine pfadweise Konvergenz der Ordnung $(\gamma - \epsilon)$ haben.

Andererseits ist die Bedingung, in der Tat, zu stark für die pfadweise Konvergenz der RODE-Taylor-Verfahren (5), da sie viele interessante Anwendungen ausschließt. In dieser Arbeit wird gezeigt, dass das Ergebnis der pfadweisen Konvergenz auch für $f \in C^{2\gamma+1}$ gilt, wobei die partiellen Ableitungen von f in der x-Variable nicht gleichmäßig beschränkt werden muss, obwohl sie es in den y-Variablen sind. Der Beweis basiert auf einem Lokalisierungs-Argument ähnlich dem von Satz 1 in [56], der wiederum, in einem anderen Kontext, Ideen von [40] nutzt. Es kommt nicht auf die spezifische Struktur von starken Itô-Taylor-Verfahrenen an, nur auf die Tatsache, dass sie pfadweise konvergieren unter der Standardannahme, die durch ein Borel-Cantelli Argument folgt, wenn alle Fehler Momente gegen die gleiche Ordnung γ konvergieren.

Die RODE-Taylor-Verfahren (5) der Ordnung γ enthalten die Ableitungen der Koeffizientenfunktionen. Sie sind schwer in höherdimensionalen Beispielen zu bestimmen. Durch den Austausch solcher Ableitungen mit

geeigneten Finite-Differenzen-Quotienten können die ableitungfreien Verfahren entwickelt werden. LMMs haben große Vorteile im Rechenaufwand und es können willkürliche SLMMs höherer Ordnung abgeleitet werden:

$$\sum_{j=0}^{s} C_{\emptyset,j} X_{n-j} = \Delta_t \sum_{j=0}^{s} C_{(0),j} f(X_{n-j}, \bar{Y}_{n-j}) \tag{6}$$
$$+ \sum_{j=1}^{s} \sum_{\alpha \in \Lambda_\gamma^0 \setminus \{\emptyset,(0)\}} L^\alpha id_{\mathbf{X}}^1(X_{n-j}, \bar{Y}_{n-j}) \left(C_{\alpha,j} I_{\alpha,t_{n-j}} + C^*_{\alpha,j} I_{\alpha-,t_{n-j}} \Delta_t \right),$$

wobei s die Anzahl der Schritte ist, Δ_t die Schrittgröße, $\alpha-$ die Komponenten des α ohne das letzte Element und C sind die Konstanten die die korrespondierenden Konsistenzbedingungen erfüllen. $\bar{Y}_{n-j}$ ist der Rauschanteil, der genau erzeugt oder unabhängig angenähert wird durch numerische Verfahren ausreichend höherer Ordnung. Das Verfahren reduziert sich auf ein explizites Verfahren, wenn $C_{(0),0} = 0$ gilt. Im Folgenden wird die pfadweise Konvergenz von SLMMs untersucht.

RODEs mit affiner Struktur

Ein d-dimensionales RODE mit m-dimensionalen affinen Rauschen hat die Form:

$$\frac{dx}{dt} = f^0(t,x) + \sum_{j=1}^{m} f^j(t,x)\, \zeta_t^j,$$

wobei $x = (x^1, \ldots, x^d) \in \mathbb{R}^d$ und der Rauschprozess $\zeta_t = (\zeta_t^1, \ldots, \zeta_t^m)$ Werte in $\mathbb{R}^m$ ausnimmt. Für die Probenpfade von ζ_t wird angenommen, dass sie mindestens Lebesgue-messbar und fast sicher begrenzt sind, so dass die Differentialgleichung im Sinne von Carathéodory ausgelegt werden kann.

Die numerischen Verfahren für RODEs mit einer affinen Struktur sind mit einem ähnlichen Ansatz aufgebaut wie Grüne & Kloeden benutzt haben, um numerische Verfahren systematisch höherer Ordnung für deterministische affine Steuerungssysteme zu entwickeln [37]. Sie basieren auf Stratonovich-Taylor-Entwicklungen und der hierarchischen Menge in [66], da hier die deterministischen Ketten-Regeln und die Stratonovich-Kalküle analog sind.

Nach der Herleitung der Taylor-Entwicklung für affine-RODEs werden nun affine-RODE-Taylor-Verfahren und LMMs auf deren Basis entwickelt.

B-Stabilität

Es gibt oft steife Systeme in der Praxis und die Stabilitätseigenschaften der numerischen Verfahren sind dabei ein wichtiges Thema, sobald wir solche Systeme numerisch lösen wollen. Es ist aus der Theorie der klassischen Runge-Kutta-Verfahren bekannt, dass implizite Verfahren erforderlich sind für die stabile Integration von einem steifen ODE.

Im Falle der RODEs müssen wir in Betracht ziehen, dass die Effekte von Nichtlinearität in den Gleichungen eine viel größere Rolle in RODEs

spielen als im deterministischen Fall. Es ist auch nicht klar, welche Klasse von linearen Testfunktionen für RODE oder SODE geeignet ist. Zusätzlich enthält eine einfache lineare RODE ein Rauschterm in der Matrix, und es macht das System pfadweise nichtautonom. Daher kann man nicht einfach die Dahlquist-Theorie verallgemeinern, da es Lyapunov-Exponenten anstelle von Eigenwerten enthält und diese sind sehr schwer zu berechnen. Um diese Probleme zu umgehen wird in der Dissertation die B-Stabilität fokussiert.

In der Tat sind B-stabile implizite Verfahren noch besser [28, 42], d.h. die Erhaltung der nicht-expansiven Struktur von Trajektorien von ODEs mit einer dissipativen einseitigen Lipschitz-Bedingung, d.h.

$$\|X_i - X_i'\| \leq \|X_{i-1} - X_{i-1}'\|,$$

für $i = 1, 2, \ldots, n$, wobei X_i und X_i' zwei Lösungen sind.

B-Stabilität der gemittelten Verfahren, nämlich das implizit gemittelte Euler-Verfahren und das implizit gemittelte Mittelpunktverfahren, sowie die B-Stabilität der impliziten SLMMs (6) beliebig höherer Ordnung werden im Folgenden gezeigt und ihre entsprechenden Bedingungen für die Dissipativitätskonstante und die Schrittweite entwickelt.

Integrale von stochastischen Prozessen

Die numerischen Verfahren dieser Dissertation setzen die Simulation von Rauschprozessen ζ_t und folgende Integrale voraus:

$$I_{(j_1,\ldots,j_l),t_{n-1}} = \int_{t_{n-1}}^{t_n} \cdots \int_{t_{n-1}}^{s_{l-1}} \zeta_{s_l}^{j_l} \cdots \zeta_{s_1}^{j_1} \, ds_l \cdots ds_1,$$

auf jedem diskreten Teilintervall $[t_{n-1}, t_n]$.

In der Regel können für Prozesse mit stetigen oder stückweise stetigen Pfaden die Integrale mit Riemann-Summen für viel feinere Teilungen der Diskretisierung in Teilintervallen berechnet werden, so dass der Fehler durch die lokale Diskretisierungsfehler der Verfahren selbst dominiert wird.

Auf der anderen Seite können wir einige Integrale direkt simulieren, wenn die Verteilungen von ζ_t^j bekannt sind. Zum Beispiel, wenn der Rauschprozess ζ_t ein Wiener-Prozess oder ein Ornstein-Uhlenbeck (OU)-Prozess ist, können die Integrale von Probenpfaden direkt berechnet werden.

Vier Arten von Rauschprozessen, d.h. ein Wiener-Prozess, ein OU-Prozess, ein zusammengesetzte Poisson-Prozess und eine gebrochene Brownsche Bewegung, werden vorgestellt und die zugehörigen Prozesse sowie deren Riemann-Integrale ausgewertet.

Numerische Beispiele

Biologische Modelle z.B. menschliche Körper können als zufällige Umgebung berücksichtigt werden. Sie unterscheiden sich nach dem Zufallsprinzip in Bezug auf die Zeit, wobei angenommen wird, dass sie stetig und wesentlich

beschränkt ist. Es gibt verschiedene Arten von noisy-Szenarien. Das gleichmäßig verteilte beschränkte Rauschen und das Schaltrauschen werden zunächst eingeführt.

Dann werden die entwickelten numerischen Verfahren auf mehrere mathematische Modelle in der Biologie und Medizin angewendet. In der Dissertation werden lediglich numerische Verfahren für RODEs konstruiert. Im Allgemeinen gibt es aber viele komplizierte Systeme, die nicht nur von der Zeit, sondern auch vom Raum abhängen, d.h. dazu müssen wir mit zufälligen partiellen Differentialgleichungen (englisch: Random Partial Differential Equations, Akronym: RPDEs) umgehen. Eine Idee dazu ist die Linienmethode [89], bei der RPDEs durch die Linienmethode auf räumliche Parameter diskretisiert werden. D.h. sie werden in einem System von RODEs transformiert, so dass die abgeleitete Verfahren auf das System angewendet werden können.

Um die Leistungsfähigkeit der numerischen Verfahren zu untersuchen, sind Trajektorien von Lösungen dargestellt. Zusätzlich werden die Fehler versus der Schrittgrößen sowie der Rechnenaufwand bei den neu entwickelten Verfahren und den Methoden in der Literatur verglichen [38, 56, 57].

Summary

Random ordinary differential equations (RODEs) are ordinary differential equations (ODEs) which have a stochastic process in their vector field functions. RODEs have been used in a wide range of applications such as biology, medicine, population dynamics and engineering [15, 70, 81, 90, 92] and play an important role in the theory of random dynamical systems [5], however, they have been long overshadowed by stochastic differential equations (SDEs).

In general, RODEs on $\mathbb{R}^{d_1}$ can be written in the form:

$$\frac{dx}{dt} = f(x, Y(t)), \tag{1}$$

where $Y(t)$ is a stochastic process [57]. Typically, the driving stochastic process $Y(t)$ has at most Hölder continuous sample paths and the resulting vector field $(t, x) \mapsto f(x, y(t))$ is, thus, at most Hölder continuous in time, no matter how smooth the vector function is in its original variables, so the sample paths of the solution of (1) are certainly continuously differentiable, but their derivatives are at most Hölder continuous in time. Consequently, although the classical numerical schemes for ODEs can be applied pathwise to RODEs, they do not achieve their traditional orders.

Recently, Grüne & Kloeden derived the explicit averaged Euler scheme by taking the average of the noise within the vector field [38]. In addition, new forms of higher order Taylor-like schemes for RODEs are derived systematically by Jentzen & Kloeden [56, 64]. However, it is still important to build higher order numerical schemes and computationally less expensive schemes as well as numerically stable schemes and this is the motivation of this thesis. The schemes in [56, 64] are very general, so RODEs with special structure, i.e., RODEs with Itô noise and RODEs with affine structure, are focused and numerical schemes which exploit these special structures are investigated.

Taylor expansions
Taylor expansions are the backbone of developing numerical schemes for the deterministic ODEs and arbitrary higher order Taylor schemes can be obtained by discarding the respective remainder terms appropriately. In addition to the Taylor schemes, different classes of numerical methods such as Runge-Kutta schemes and linear multi-step methods (LMMs) have been developed and applied to various kinds of problems [18, 36, 41, 42, 61].

Similar to the deterministic numerics, the stochastic Itô-Taylor expansions are the fundamental tools in the derivation of numerical methods for SDEs. When $Y(t)$ satisfies an Itô stochastic ODE (SODE) on $\mathbb{R}^{d_2}$, i.e.,

$$dY(t) = a(Y(t))\, dt + \sum_{j=1}^{m} b_j(Y(t))\, dW^j(t), \tag{2}$$

with m independent scalar Wiener processes $W^1(t)$, $W^2(t)$, ..., $W^m(t)$, the k-th component of $Y(t)$ is approximated by γ-order strong Itô-Taylor scheme as

$$Y_n^k = \sum_{\alpha\in\Lambda_\gamma} L^\alpha id_{\mathbf{Y}}^k(t_{n-1}, Y_{n-1})\, I_{\alpha,t_{n-1}}, \tag{3}$$

where L is the differential operator given by

$$L^0 = \frac{\partial}{\partial t} + \sum_{k=1}^{d_2} a^k \frac{\partial}{\partial y_k} + \frac{1}{2}\sum_{k,l=1}^{d_2}\sum_{j=1}^{m} b_j^k b_j^l \frac{\partial^2}{\partial y_k \partial y_l}, \quad L^j = \sum_{k-1}^{d_2} b_j^k \frac{\partial}{\partial y_k},$$

and Λ_γ is the hierarchical set of multi-indices given by

$$\Lambda_\gamma = \left\{\alpha \in \mathcal{M}_m : l(\alpha) + n(\alpha) \le 2\gamma \quad \text{or} \quad l(\alpha) = n(\alpha) = \gamma + \frac{1}{2}\right\},$$

with $n(\alpha)$ is the number of components of α that are equal to 0 and $l(\alpha)$ is the length of α. In addition, $\mathcal{M}_m$ is given as

$$\mathcal{M}_m = \left\{\alpha = (j_1, \ldots, j_l) \in \{0, 1, 2, \ldots, m\}^l : l \in \mathbb{N}\right\} \cup \{\emptyset\},$$

with $\emptyset$ being the empty index of length $l(\alpha) = 0$. Moreover, for a multi-index $\alpha = (j_1, \ldots, j_l)$ with $l \ge 1$, the multiple integrals $I_{\alpha,t_{n-1}}$ and iterated operators L^α are defined by

$$I_{\alpha,t_{n-1}} := \int_{t_{n-1}}^{t_n} \cdots \int_{t_{n-1}}^{s_2} dW^{j_1}(s_1) \cdots dW^{j_l}(s_l), \quad L^\alpha := L^{j_1} \cdots L^{j_l},$$

with $I_{\emptyset,t_{n-1}} = 1$ and $L^\emptyset = id$.

The stochastic Runge-Kutta schemes and the stochastic LMMs (SLMMs) have been also constructed systematically and their convergence such as strong, weak and pathwise convergence as well as their stability properties have been discussed in literature [35, 45, 54, 57, 63, 65, 66, 76, 88].

Coupled RODE-SODE system

When the noise is regular noise, there is, in fact, a close connection between RODEs and SDEs and RODEs can be written in the form of SODEs and vice versa.

Suppose that the noise process $Y(t)$ is given as (2). Then, a coupled RODE-SODE system for the RODE (1) can be given as

$$d\begin{pmatrix} X(t) \\ Y(t) \end{pmatrix} = \begin{pmatrix} f(X(t), Y(t)) \\ a(Y(t)) \end{pmatrix} dt + \sum_{j=1}^{m} \begin{pmatrix} 0 \\ b_j(Y(t)) \end{pmatrix} dW^j(t). \tag{4}$$

The diffusion coefficient in RODE part of (4), i.e., the X-component, is 0 and because of this special structure, the numerical scheme (3) can be reduced to RODE-Taylor scheme in componentwise form:

$$X_n^k = \sum_{\alpha\in\Lambda_\gamma^0} L^\alpha id_{\mathbf{X}}^k(X_{n-1}, Y_{n-1})\, I_{\alpha,t_{n-1}}, \quad k = 1, \ldots, d_1, \tag{5}$$

with Λ_γ^0, a subset of Λ_γ, given by

$$\Lambda_\gamma^0 = \{\alpha \in \Lambda_\gamma : \alpha = \emptyset \text{ or } l(\alpha) \geq 1 \text{ with last component } j_l = 0\}.$$

It is well-known that the order γ strong Itô-Taylor scheme has order γ strong convergence if the coefficients satisfy the standard assumptions [67, 76], i.e., the coefficient functions belong to the space $C_b^{2\gamma+1}$ of $(2\gamma+1)$ time continuously differentiable functions with uniformly bounded partial derivatives. It follows by a result of Kloeden & Neuenkirch [65] that the scheme has order $(\gamma-\epsilon)$ pathwise convergence and the corresponding scheme for RODE also has order $(\gamma-\epsilon)$ pathwise convergence.

On the other hand, the assumptions are, in fact, too strong just for the pathwise convergence of the RODE-Taylor scheme (5) and it excludes many interesting applications. In this thesis, it is shown that the result of pathwise convergence also holds in case $f \in C^{2\gamma+1}$, where the partial derivatives of f in the x-variable need not be uniformly bounded, although those in the y-variables are. The proof is based on a localization argument similar to that of Theorem 1 in [56] in a different context, which in turn uses ideas from [40]. It does not depend on the specific structure of the strong Itô-Taylor schemes, just the fact that they converge pathwise under the standard assumptions, which follows by a Borel-Cantelli argument when all of the error moments converge with the same order γ.

The order γ RODE-Taylor schemes (5) contain derivatives of the coefficients functions and they may be difficult to determine in higher dimensional examples. By replacing such derivatives with appropriate finite difference quotients, the derivative-free schemes can be developed. LMMs have big advantages in computational costs and arbitrary higher order SLMMs are also derived:

$$\begin{aligned}\sum_{j=0}^{s} C_{\emptyset,j} X_{n-j} = \Delta_t \sum_{j=0}^{s} C_{(0),j} f(X_{n-j}, \bar{Y}_{n-j}) \\ + \sum_{j=1}^{s} \sum_{\alpha \in \Lambda_\gamma^0 \setminus \{\emptyset,(0)\}} L^\alpha id_{\mathbf{X}}^1(X_{n-j}, \bar{Y}_{n-j}) \left(C_{\alpha,j} I_{\alpha,t_{n-j}} + C_{\alpha,j}^* I_{\alpha-,t_{n-j}} \Delta_t\right),\end{aligned} \tag{6}$$

where s is the number of steps, Δ_t is the step size, $\alpha-$ is the components of α without the last element and Cs are the constants satisfying the corresponding consistency conditions. $\bar{Y}_{n-j}$ is the noise term, which is exactly generated or independently approximated by enough higher order numerical schemes. The method reduces to an explicit scheme when $C_{(0),0} = 0$. Furthermore, the pathwise convergence of SLMMs are investigated.

RODEs with affine structure

A d-dimensional RODE with m-dimensional affine noise has the form:

$$\frac{dx}{dt} = f^0(t,x) + \sum_{j=1}^{m} f^j(t,x)\,\zeta_t^j,$$

where $x = (x^1, \ldots, x^d) \in \mathbb{R}^d$ and the noise process $\zeta_t = (\zeta_t^1, \ldots, \zeta_t^m)$ takes values in $\mathbb{R}^m$. The sample paths of ζ_t are assumed to be at least Lebesgue measurable and almost surely bounded, so the differential equation can be interpreted in the sense of Carathéodory.

The numerical schemes for RODEs with an affine structure are constructed with a similar approach that were used by Grüne & Kloeden [37] to systematically derive higher order numerical schemes for deterministic affine control systems. These are based on stochastic Stratonovich-Taylor expansion and the hierarchical sets in [66], which is possible since the chain rules of deterministic and Stratonovich stochastic calculi are analogous.

After deriving the Taylor expansions for affine-RODEs, both of the affine-RODE-Taylor schemes and LMMs are developed based on them.

B-stability

We often encounter stiff systems in practice and the stability property of numerical schemes is a crucial issue when we solve such systems numerically. It is known from the theory of classical Runge-Kutta schemes for ODEs that an implicit scheme is required for the stable integration of a stiff ODE.

In case of RODEs, we need to take into account of the effects of nonlinearlity in the equations, which play a much more significant role in RODEs than deterministic ones. It is also not clear in RODE or SODE what class of linear test functions is suitable. In addition, even a simple linear RODE contains a noise term in its matrix and it makes the system pathwise nonautonomous, so it is not easy to generalize the Dahlquist theory since it involves Lyapunov exponents instead of eigenvalues and they are very hard to calculate. In order to circumvent these problems, B-stability is focused in the thesis.

In fact, B-stable implicit schemes are even better [28, 42], i.e., preserve the non-expansive structure of trajectories of ODEs with a dissipative one-sided Lipschitz condition, i.e.,

$$\|X_i - X_i'\| \leq \|X_{i-1} - X_{i-1}'\|,$$

for $i = 1, 2, \ldots, n$, where X_i and X_i' are two solutions of the scheme.

B-stability of the averaged schemes, namely the implicit averaged Euler scheme and the implicit averaged midpoint scheme, as well as B-stability of the arbitrary higher order implicit SLMMs (6) are shown and the corresponding conditions for dissipativity constant and the step size are obtained.

Integrals of stochastic processes

The numerical schemes derived in this thesis require the simulation of noise process ζ_t and their integral

$$I_{(j_1,\ldots,j_l),t_{n-1}} = \int_{t_{n-1}}^{t_n} \cdots \int_{t_{n-1}}^{s_{l-1}} \zeta_{s_l}^{j_l} \cdots \zeta_{s_1}^{j_1} \, ds_l \cdots ds_1,$$

on each discretized subinterval $[t_{n-1}, t_n]$.

In general, for processes with continuous or piecewise continuous sample paths, the integrals can be calculated using Riemann sums on much finer partition of the discretization subinterval so that the error is dominated by the local discretization error of the scheme itself.

On the other hand, some integrals can be simulated directly if the distributions of ζ_t^j are known. For example, if the noise process ζ_t is a Wiener process or an Ornstein-Uhlenbeck (OU) process, the sample paths of the integrals can be calculated directly.

Four kinds of noise processes, i.e., a Wiener process, an OU process, a compound Poisson process and a fractional Brownian motion, are introduced and the processes as well as their Riemann integrals are evaluated.

Numerical examples

Biological models such as human body can be considered as random environment. They vary randomly with respect to time, but they are assumed to be continuous and essentially bounded. There are various kinds of noisy scenario and uniformly distributed bounded noise and switching noise are firstly introduced here.

Then the developed numerical schemes are applied to several mathematical models in biology and medicine. Only numerical schemes for RODEs are constructed in the thesis, however, in general, many systems are much more complicated and they depend not only on time, but also on space, i.e., we need to deal with random partial differential equations (RPDEs). One idea is method of lines [89] and RPDEs are discretized by method of lines with respect to spatial parameter and they are transformed into a system of RODEs so that the derived schemes can be applied to the system.

In order to see the performance of the numerical schemes, trajectories of solutions are illustrated. In addition, the error vs. step sizes as well as the computational costs are compared among newly developed schemes and the schemes in literature [38, 56, 57].

要約

ランダム常微分方程式 (Random Ordinary Differential Equations，以下，RODEs) は，そのベクトル場をなす関数に確率過程を伴った常微分方程式 (Ordinary Differential Equations，以下，ODEs) である．RODEs は，生物学，医学，人口動態および工学といった様々な分野 [15, 70, 81, 90, 92] で応用され，さらにランダムな力学系の理論において重要な役割を果たしてきたが [5]，長い間，確率微分方程式 (Stochastic Differential Equations，以下，SDEs) の影に隠れる存在であった．

一般に，$\mathbb{R}^{d_1}$ において，RODEs は

$$\frac{dx}{dt} = f(x, Y(t)), \tag{1}$$

の形で表現することができる．ここで，$Y(t)$ は確率過程とする [57]．概して，確率過程 $Y(t)$ はせいぜい Hölder 連続な見本路を持ち，結果として得られるベクトル場 $(t, x) \mapsto f(x, y(t))$ は，いかにその関数が元の変数について滑らかであっても，時間についてはせいぜい Hölder 連続である．そのため，(1) の解の見本路は，連続微分可能であるが，その導関数は時間についてせいぜい Hölder 連続である．その結果，ODEs の従来の数値計算法はパスごとに RODEs に適用可能であるが，元の収束次数を満たすことはない．

近年，Grüne と Kloeden が，ベクトル場内のノイズの平均を取ることにより，陽的平均化 Euler 法を導出した [38]．さらに，新しい形の高次の Taylor 法に似た方法が Jentzen と Kloeden により導き出された [56, 64]．しかしながら，高次の数値計算法や計算量の少ない方法，そして数値計算の面でより安定した方法を作ることは，いまだに重要であり，これが本論文の動機である．Jentzen と Kloeden は，一般的な RODEs に対する数値計算法を開発したが，ここでは，伊藤の SDEs で与えられるノイズを伴う RODEs とアファイン構造を持つ RODEs という二つの特別な形を持った RODEs に焦点をあて，それらの構造を利用した数値計算法を考えた．

Taylor 展開

Taylor 展開は，決定論における ODEs の数値計算法を作っていく上で重要な要素であり，任意の高次の Taylor 法は，その剰余項を適切に省くことで得られる．Taylor 法以外にも，Runge-Kutta 法や線形多段階法 (Linear Multi-step Methods，以下，LMMs) といった異なった形の数値計算法が導かれ，様々な問題に応用されてきた [18, 36, 41, 42, 61]．

決定論における数値計算法と同様に，伊藤-Taylor 展開が SDEs に対する数値計算法の導出における重要な要素となる．ここで，$Y(t)$ が $\mathbb{R}^{d_2}$ 上

の確率常微分方程式 (Stochastic Ordinary Differential Equations，以下，SODEs)

$$dY(t) = a(Y(t))\,dt + \sum_{j=1}^{m} b_j(Y(t))\,dW^j(t), \tag{2}$$

で与えられるとする．ただし，$W^1(t), W^2(t), \ldots, W^m(t)$ は，m 個の独立なスカラー Wiener 過程とする．そのとき，$Y(t)$ の k 番目の要素は，γ-次の強伊藤-Taylor 法によって

$$Y_n^k = \sum_{\alpha\in\Lambda_\gamma} L^\alpha id_{\mathbf{Y}}^k(t_{n-1}, Y_{n-1})\, I_{\alpha,t_{n-1}}, \tag{3}$$

と近似される．ただし，微分作用素 L は

$$L^0 = \frac{\partial}{\partial t} + \sum_{k=1}^{d_2} a^k \frac{\partial}{\partial y_k} + \frac{1}{2}\sum_{k,l=1}^{d_2}\sum_{j=1}^{m} b_j^k b_j^l \frac{\partial^2}{\partial y_k \partial y_l}, \quad L^j = \sum_{k-1}^{d_2} b_j^k \frac{\partial}{\partial y_k},$$

Λ_γ は多重指数からなる階層集合で

$$\Lambda_\gamma = \left\{\alpha \in \mathcal{M}_m : l(\alpha) + n(\alpha) \le 2\gamma \text{ もしくは } l(\alpha) = n(\alpha) = \gamma + \frac{1}{2}\right\},$$

で与えられる．$n(\alpha)$ は α の要素で 0 に等しいものの数，$l(\alpha)$ は α の長さとする．さらに，$\mathcal{M}_m$ は

$$\mathcal{M}_m = \left\{\alpha = (j_1, \ldots, j_l) \in \{0, 1, 2, \ldots, m\}^l : l \in \mathbb{N}\right\} \cup \{\emptyset\},$$

で与えられ，$\emptyset$ は，その長さが $l(\alpha) = 0$ となる空な要素である．また，$l \ge 1$ である多重指数 $\alpha = (j_1, \ldots, j_l)$ に対し，多重積分 $I_{\alpha,t_{n-1}}$，また反復作用素 L^α は

$$I_{\alpha,t_{n-1}} := \int_{t_{n-1}}^{t_n} \cdots \int_{t_{n-1}}^{s_2} dW^{j_1}(s_1)\cdots dW^{j_l}(s_l), \quad L^\alpha := L^{j_1}\cdots L^{j_l},$$

で定義される．ここで，$I_{\emptyset,t_{n-1}} = 1$ および $L^\emptyset = id$ である．

SDEs に対する Runge-Kutta 法や LMMs (Stochastic LMMs，以下，SLMMs) も同様に導かれ，強い収束，弱い収束，パスごとの収束 (pathwise convergence) といった収束性や，それらの安定性についても多く議論されてきた [35, 45, 54, 57, 63, 65, 66, 76, 88].

RODE-SODE システム

ノイズが一般的なノイズのとき，RODEs と SDEs の間には密接な関係があり，RODEs は SODEs の形で表現することができ，また逆もまた同様に可能である．

確率過程 $Y(t)$ が (2) で与えられたとする．そのとき，(1) に対して，RODE-SODE システムは

$$d\begin{pmatrix} X(t) \\ Y(t) \end{pmatrix} = \begin{pmatrix} f(X(t), Y(t)) \\ a(Y(t)) \end{pmatrix} dt + \sum_{j=1}^{m} \begin{pmatrix} 0 \\ b_j(Y(t)) \end{pmatrix} dW^j(t), \quad (4)$$

で与えられる．(4) の RODE 項，すなわち X 項の拡散係数は 0 であり，この特別な構造により，(3) は，以下の RODE-Taylor 法

$$X_n^k = \sum_{\alpha \in \Lambda_\gamma^0} L^\alpha id_{\mathbf{X}}^k(X_{n-1}, Y_{n-1})\, I_{\alpha, t_{n-1}}, \quad k = 1, \ldots, d_1, \quad (5)$$

に変形される．ただし，Λ_γ^0 は Λ_γ の部分集合で

$$\Lambda_\gamma^0 = \{\alpha \in \Lambda_\gamma : \alpha = \emptyset \text{ もしくは } l(\alpha) \geq 1 \text{ で最後の要素 } j_l = 0\},$$

で与えられる．

係数が標準仮定 (standard assumptions) [67, 76]，すなわちその関数が $(2\gamma+1)$ 回連続微分可能な関数でその偏導関数が一様に有界な空間，$C_b^{2\gamma+1}$ に属するとき，γ-次の強伊藤-Taylor 法は，γ-次の強い収束を満たすことがよく知られている．Kloeden と Neuenkirch の結果 [65] により，その数値計算法は $(\gamma - \epsilon)$-次のパスごとの収束を示し，ここから，それに対応する RODE-Taylor 法も同じく $(\gamma - \epsilon)$-次のパスごとの収束を示すことがわかる．

一方で，この標準仮定は，RODE-Taylor 法 (5) のパスごとの収束のためには強すぎ，この仮定のために多くの興味深い問題が除外されてしまう．そのため，本論文では，$f \in C^{2\gamma+1}$，すなわち，その偏導関数が y については一様に有界でも，x についてはそうではない場合にも，このパスごとの収束性が満たされることを示した．その証明は，[56] の定理 1 で用いられた局所化の議論に似た議論に基づいているが，異なったコンテクスト，つまり，[40] のアイディアを用いて示されている．これは，強伊藤-Taylor 法の特定の構造によるわけではなく，全てのエラーモーメントが同じ次数 γ で収束するとき，Borel-Cantelli の議論によって標準仮定の下，その数値計算法がパスごとに収束するということである．

γ-次の RODE-Taylor 法 (5) は，係数関数の導関数を含んでおり，高次元の場合においては，それらを求めるのは難しいことがある．それらの導関数を適当な有限差分商で置き換えることにより，導関数項を持たない数値計算法を導出することが可能である．また，LMMs はコンピューターコストの面で非常にメリットがあることが知られており，任意の高次の

SLMMs

$$\sum_{j=0}^{s} C_{\emptyset,j} X_{n-j} = \Delta_t \sum_{j=0}^{s} C_{(0),j} f(X_{n-j}, \bar{Y}_{n-j}) \tag{6}$$
$$+ \sum_{j=1}^{s} \sum_{\alpha \in \Lambda_\gamma^0 \setminus \{\emptyset,(0)\}} L^\alpha id_{\mathbf{X}}^1(X_{n-j}, \bar{Y}_{n-j}) \left(C_{\alpha,j} I_{\alpha,t_{n-j}} + C^*_{\alpha,j} I_{\alpha-,t_{n-j}} \Delta_t \right).$$

を導いた．ただし，s はステップ数であり，Δ_t はステップ幅，$\alpha-$ は α の要素で最後の要素を除いたもの，そして C は適合条件式 (consistency conditions) を満たす係数である．$\bar{Y}_{n-j}$ はノイズ項で，これは正確に生成されるか，もしくは十分高次の数値計算法により独立に近似されるものとする．ここで，(6) は $C_{(0),0} = 0$ のときに陽的となる．さらに，本論文では，(6) がパスごとに収束することも示された．

アファイン構造を持つ RODEs

m-次のアファインノイズを持つ d-次元 RODE は，次の形

$$\frac{dx}{dt} = f^0(t,x) + \sum_{j=1}^{m} f^j(t,x)\, \zeta_t^j,$$

で与えられる．ただし，$x = (x^1, \ldots, x^d) \in \mathbb{R}^d$ であり，ノイズ過程 $\zeta_t = (\zeta_t^1, \ldots, \zeta_t^m)$ は $\mathbb{R}^m$ に値を持つものとする．ζ_t の見本路を，少なくとも Lebesgue 可測でほとんど確実に有界であると想定すると，その微分方程式は Carathéodory の意味で解釈されうる．

アファイン構造を持つ RODEs の数値計算法は，決定論におけるアファインコントロールシステムに対する，Grüne と Kloeden による高次の数値計算法の導出方法に似たアプローチで導かれる．これは，決定論における連鎖律と Stratonovich の意味での確率計算が同類であることから可能であり，その導出方法は，Stratonovich-Taylor 展開と [66] の階層集合に基づいている．

ここでは，affine-RODEs に対する Taylor 展開を導いた後，それに基づいて，affine-RODE-Taylor 法および LMMs を導出した．

B-stability

実用においては，硬い系に遭遇することがしばしばある．そのような問題を数値解析的に解こうとすると，数値計算法の安定性が非常に大きな問題となる．ODEs に対する古典的 Runge-Kutta 法の理論により，硬い系を安定して積分するには，陰的方法が必要であることが知られている．

RODEs では，決定論における議論よりもさらに重要な役割を果たす，式の非線形性の効果を考慮に入れる必要がある．同時に，RODE や SODE においては，どのようなクラスの線形テスト関数が適しているかがはっき

りしていない．さらに，シンプルな線形 RODE でさえ，その中にノイズ項を含むため，システムがパスごとに非自励系となる．そのため，固有値のかわりに Lyapunov 指数が含まれ，それらを計算することは難しく，Dahlquist の理論を一般化することは困難である．これらの問題を回避するため，ここでは B-stability に焦点を当てた．

実際，B-stable な陰的方法はさらによい性質を持ち，散逸的な片側 Lipschitz 条件を持つ ODEs の軌道の非拡張構造を保存する [28, 42]．すなわち X_i と X_i' を 2 つの解としたとき，$i = 1, 2, \ldots, n$ に対し，

$$\|X_i - X_i'\| \leq \|X_{i-1} - X_{i-1}'\|$$

が成り立つ．

陰的平均化 Euler 法および陰的平均化中点法の B-stability，また，任意の高次の陰的 SLMMs (6) の B-stability が示され，対応する散逸性定数とステップ幅の条件が得られた．

確率過程の積分

導出された数値計算法を用いるには，各離散区間 $[t_{n-1}, t_n]$ における確率過程 ζ_t とその積分

$$I_{(j_1,\ldots,j_l),t_{n-1}} = \int_{t_{n-1}}^{t_n} \cdots \int_{t_{n-1}}^{s_{l-1}} \zeta_{s_l}^{j_l} \cdots \zeta_{s_1}^{j_1} \, ds_l \cdots ds_1,$$

が必要となる．

一般に，連続かもしくは区分的に連続な見本路を持つ過程については，各区間をさらに細かい区間に分け，その Riemann 和を取ることで積分値を評価することができる．このとき，その誤差は数値計算法自体が持つ局所離散化誤差に支配される．

一方で，確率過程 ζ_t^j の分布が既知の場合，その積分値は直接評価することができる．例えば，ζ_t が Wiener 過程や Ornstein-Uhlenbeck (以下，OU) 過程で与えられるとき，その積分の見本路は直接計算可能である．

本論文では，Wiener 過程，OU 過程，複合 Poisson 過程および非整数 Brown 運動の 4 つの確率過程について，その過程とそれらの Riemann 積分を評価した．

数値解析例

人体といった生物モデルはノイズの入った環境とみなすことができる．それらは，時間についてランダムに変化するが，連続で，本質的に有界と想定することが可能である．様々な形のノイズが考えられるが，ここでは，一様に分布する有界なノイズとスイッチ状の役割を果たすノイズを紹介する．

また，本論文で導出された数値計算法を，生物学，医学に現れる数理モデルに適用した．RODEs に対する数値計算法のみを本論文では扱ったが，現実の多くのモデルはより複雑であり，それらは時間だけでなく，空間にもよる構造をしている．そのような場合，ランダム偏微分方程式 (Random Partial Differential Equations，以下，RPDEs) を考える必要がある．これらの問題を扱う方法の一つとして，線の方法 (method of lines) [89] がある．これを用いて，RPDEs を空間について離散化することで，RPDEs を RODEs からなる系に書き直すことができ，導出した数値計算法が適用可能となる．

数値計算法の性能を見るため，解の軌道を例示した．同時に，新しく得られた数値計算法と既存の方法 [38, 56, 57] を比較するために，誤差とステップ幅およびコンピューターコストのグラフを作成した．

Curiculumn Vitae

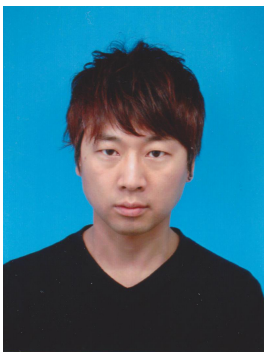

Name: Yusuke Asai

Birthday: 07/02/1978

Place of birth: Tokyo, Japan

School:

04/1984 ∼ 03/1986	Yokokawa Primary School, Hachioji, Tokyo
04/1986 ∼ 03/1990	Kunitachi Daisan Primary School, Kunitachi, Tokyo
04/1990 ∼ 03/1993	Kunitachi Daiichi Junior High School, Kunitachi, Tokyo
04/1993 ∼ 03/1996	Waseda University Senior High School, Tokyo

University:

04/1996 ∼ 03/2000	Department of Mathematical Sciences, School of Science and Engineering, Waseda University, Tokyo, Japan (Bachelor in Mathematical Sciences, Prof. Dr. Y. Shibata)
04/2000 ∼ 03/2002	Department of Mathematics, Graduate School of Science and Engineering, Waseda University, Tokyo, Japan (Master in Mathematics, Prof. Dr. Y. Shibata)
04/2009 ∼ 03/2012	Department of Physics (Computational Science Program), Johann Wolfgang Goethe-Universität (Master in Computational Science, Prof. Dr. E. Herrmann)
10/2012 ∼ present	Institut für Mathematik, Johann Wolfgang Goethe-Universität (Ph.D. study, Prof. Dr. P.E. Kloeden)

Visiting experience:

10/2001 ∼ 09/2003	Institute of Applied Mathematics, Department of Mathematics, Informatics and Mechanics, Warsaw University, Warsaw, Poland
12/2014 09/2015 ∼ 10/2015	Department of Global Health Policy, Graduate School of Medicine, The University of Tokyo, Tokyo, Japan

03/2015 ∼ 04/2015	South African Centre for Epidemiological Modelling and Analysis (SACEMA), Stellenbosch, South Africa
09/2015	Institute of Mathematics, Huazhong University of Science and Technology, Wuhan, China

Working experience:

04/2004 ∼ 07/2008	Clinical Development Department, Terumo Corporation, Japan
12/2008 ∼ 09/2009 01/2010 ∼ 12/2013 10/2014 ∼ 09/2015	Clinical and Medical Development Department, Terumo Europe N.V., Leuven, Belgium
04/2009 ∼ 03/2010	Japanisches Institut Frankfurt am Main (Japanese Primary and Junior High School in Frankfurt)
05/2010 ∼ 09/2010	Institut für Biostatistik und Mathematische Modellierung, Klinikum und Fachbereich Medizin, Johann Wolfgang Goethe-Universität (Studentische Hilfskraft)
10/2010 ∼ 12/2011 04/2012 ∼ 03/2016	Institut für Biostatistik und Mathematische Modellierung, Klinikum und Fachbereich Medizin, Johann Wolfgang Goethe-Universität (Research assistant)
10/2012, 2013, 2014	Institut für Mathematik, Johann Wolfgang Goethe-Universität (Teaching assistant)
04/2016 ∼ present	Department of Hygiene, Graduate School of Medicine, Hokkaido University, Japan (Assistant professor)

Awards:

10/2001 ∼ 09/2003	Scholarship from Polish Government (Stypendium rządu polskiego)
10/2010 ∼ 12/2011	Scholarship from German Research Foundation (Deutsche Forschungsgemeinschaft)